Microglia phenotypes in CNS plasticity and regeneration

Olah, Marta

Microglia phenotypes

in CNS plasticity and regeneration

Printing of this thesis was financially supported by

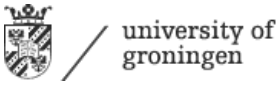

Rijksuniversiteit Groningen

Universitair Medisch Centrum Groningen

School of Behavioral and Cognitive Neurosciences

Stichting MS Research

Printing Ipskamp Drukkers B.V.
Cover and layout Marta Olah

ISBN 978-90-367-4782-0

RIJKSUNIVERSITEIT GRONINGEN

Microglia phenotypes

in CNS plasticity and regeneration

Proefschrift

ter verkrijging van het doctoraat in de
Medische Wetenschappen
aan de Rijksuniversiteit Groningen op
gezag van de
Rector Magnificus, dr. F. Zwarts,
in het openbaar te verdedigen op
woensdag 23 februari 2011
om 16.15 uur

door

Marta Olah

geboren op 7 januari 1979
te Szeged, Hongarije

Promotor:	Prof. dr. H.W.G.M. Boddeke
Beoordelingscommissie:	Prof. dr. C.D. Dijkstra
	Prof. dr. P.G.M. Luiten
	Prof. dr. T. Harkany

TABLE OF CONTENTS

General introduction

Microglia phenotype diversity

Marta Olah[1], Knut P.H. Biber[1,2], Jonathan Vinet[1], Hendrikus W.G.M. Boddeke[1]

[1] Department of Neuroscience, Section Medical Physiology, University Medical Center Groningen, The Netherlands

[2] Department of Psychiatry and Psychotherapy, Section Molecular Psychiatry, University Medical Center Freiburg, Germany

Available as Epub ahead of print CNS & Neurological Disorders - Drug Targets, 2011, Vol. 10, No. 1

ABSTRACT

Microglia, the tissue macrophages of the brain, have under healthy conditions a resting phenotype that is characterised by a ramified morphology. With their fine processes microglia are continuously scanning their environment. Upon any homeostatic disturbance microglia rapidly change their phenotype and contribute to processes including inflammation, tissue remodeling, and neurogenesis. In this review we will address functional phenotypes of microglia in diverse brain regions and phenotypes associated with neuroinflammation, neurogenesis, brain tumor homeostasis and aging.

REGIONAL DIFFERENCES OF MICROGLIA PHENOTYPES IN THE CENTRAL NERVOUS SYSTEM

In addition to their apparent structural complexity, the phenotype diversity of microglia cells was recognised already at the dawn of microglia research. Images produced by classical silver impregnation clarified that microglia not only exhibit considerable phenotype plasticity over the course of cellular activation during pathologies, but already exist in a variety of distinct morphological states in the healthy brain. With the camera lucida drawings of his seminal work in 1932, Rio-Hortega (del Rio-Hortega, 1932) demonstrated a variety of microglial morphologies in different brain regions, and under diverse pathological conditions.

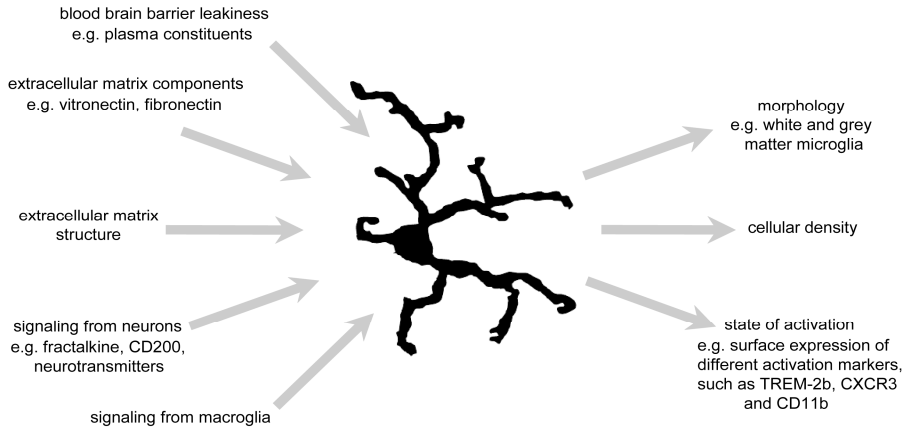

Figure 1. Regional differences of microglia phenotypes in the CNS. Microglia regional phenotype diversity is manifested in their cellular density and state of activation. A multitude of factors has been suggested to possess potential to influence the phenotype of microglia under physiological conditions (such as structure of the blood-brain barrier, extracellular matrix components and signaling from other CNS cells). The causal connection, however, between these factors and the observed regional phenotype diversity of microglia *in vivo* has not been tested yet. (For references see the text. For the acronyms see List of abbreviations).

However, despite the development of various histochemical, biochemical, and genetic tools, the physiological relevance of regional microglial diversity in the central nervous system (CNS) has largely remained obscure. Still, this diversity likely reflects diverse functional phenotypes (Figure 1), adapted to the very needs and circumstances of the various CNS niches in which microglia reside (Ransohoff & Perry, 2009; Kraft et al., 2009; Carson et al., 2007; Hanisch & Kettenmann, 2007).

Differences in regional density

Whereas microglia are known to occupy all brain areas, differences in their cellular density between different brain regions under physiological conditions can be as high as five-fold in mouse (Lawson et al., 1990), and ten-fold in human (Mittelbronn et al., 2001). Considering only the gross anatomical regions, microglia are most numerous in the telencephalon, followed by diencephalon, mesencephalon and rhombencephalon, which contains the lowest number microglia (Savchenko et al., 2000; Lawson et al., 1990). Furthermore, within one anatomical region differences between microglia in white and grey matter parts exist. Myelinated parts are known to contain a higher density of microglia as compared to non-myelinated tissue of the same anatomical region (Mittelbronn et al., 2001; Lawson et al., 1990). Not surprisingly, these significant differences in microglia density are not without functional consequences. It has been shown that the extent of lipopolysaccharide (LPS)-induced neurodegeneration is positively correlated with microglia cell density (Ji et al., 2008; Kim et al., 2000), and thus differs in different brain regions.

Differences in microglia responsiveness

Microglia responsiveness to perturbations in CNS homeostasis per se also shows regional differences irrespective of the presence of neurodegeneration. After administration of 1-methyl-4-phenyl-1,2,3,6-

tetrahydropyridine, a compound used to induce experimental Parkinson's disease in laboratory animals, microglia activation was observed in brain regions that were unrelated to neuronal cell death (Hurley et al., 2003). Also after transient global cer ebral ischemia, microglia activation and proliferation was not restricted to the vulnerable CA1 region of the hippocampus, but it was present also in the hilus and cortex, where no neurodegeneration occurs (Soltys et al., 2005). Furthermore, interferon gamma (IFN-γ) injection in the brain induces significantly higher levels of microglial major histocompatibility complex II (MHC II) molecules in brainstem as compared to hippocampus (Philips et al. 1999). The difference in microglial responsiveness in various brain regions in diverse experimental animal models might be attributed to the diversity of their immediate microenvironment. Nevertheless, some of the region-specific traits of microglia seem to be inherent to these cells. That microglia isolated from mixed glial cultures prepared from different brain regions display different inflammatory profiles under basal conditions (expression of the transcripts for interleukin-6 (IL-6), tumor necrosis factor alpha (TNF-α), Fc gamma receptor) (Xie et al., 2003; Ren et al., 1999), or upon LPS stimulation (IL-6, TNF-α, IL-1α, IL-1β, inducible nitric oxide synthase) (Xie et al., 2003; Guo et al., 2001), support this idea. Moreover, acutely isolated microglia from the cortex, hippocampus, cerebellum, striatum, and spinal cord show differences in surface expression of multiple immune-regulatory proteins, such as cluster of differentiation protein 11b (CD11b), CD40, CD45, CD80, CD86, F4/80, triggering receptor expressed on myeloid cells 2 b, CXCR3, and CCR9 (De Haas et al., 2008).

Microglia differences within anatomical regions

Despite the somewhat sparse knowledge regarding the causes and the functional consequence of regional diversity of microglia, the above data might create the impression that microglia within one region constitute a single homogeneous population. Most likely, however, this

is not the case. Phenotype heterogeneity between microglia can readily be observed within one anatomical region. Microglia associated with different layers of the olfactory bulb show differences in lectin labeling, and expression of inflammatory markers such as complement receptor 3, MHCI, ED1 (cell surface marker CD68), ED2 (macrophage surface marker), and LCA (leukocyte common antigens) (Wu et al., 1997). Moreover, microglia in the rat pineal gland also show heterogeneous expression of complement receptor 3, MHCII, and ED2 (Jiang-Shieh et al., 2003). Furthermore, physiological activation of a specific brain region can reveal the inherent diversity of the resident microglia population. In the hypothalamic supraoptic nucleus, systemic dehydration causes an increase in the morphological diversity of resident microglia (Ayoub et al., 2003). Increased physical activity in the running wheel model results in an increase in microglial proliferation in certain cortical regions, in a layerspecific manner (Ehninger & Kempermann, 2003). These differences between microglia within one region can also be detected in different lesion models. In the facial nerve axotomy model, a diversification of microglia responses within the facial nucleus could be seen (MHCII, CD4, LCA) (Streit & Gaeber, 1993). In the entorhinal cortex lesion model, only a subpopulation of microglia becomes CD34-positive, and highly proliferative in the perforant path projection area of the hippocampus (Ladeby et al., 2005).

Factors involved in regional differences in microglia

Although our recent understanding of regional differences in microglia phenotypes is derived mainly from circumstantial evidence, the existence of inter- and intra-regional diversity of microglial cells in the CNS is a widely accepted concept in neurobiology (Ransohoff & Perry, 2009; Carson et al., 2007; Hanisch & Kettenmann, 2007). Due to lack of pertinent experimental data, however, the causes and the consequences of this diversity largely remain the subject of speculation. Factors that mediate microglial phenotype adaptation to their

microenvironment are believed to be of physical and chemical nature. Undeniably, the cytoarchitecture of a brain region determines to a great extent the morphology of the microglia residing in the given anatomical structure. The most apparent example of this is the difference in cell morphology between grey and white matter microglia, the latter having a bipolar arborisation, in contrast to the radially extending processes of the former (Lawson et al., 1990). Apart from the ultrastructure of a given brain area, the extracellular matrix represents the direct physical environment of a cell. Although some extracellular matrix components such as fibronectin and vitronectin (Ribes et al., 2010; Milner & Campbell, 2003) are known to influence microglial activation *in vitro*, little is known about regional differences in the composition of the extracellular matrix, which could account for differences in microglial phenotypes. Regional differences in permeability of the blood-brain barrier and their relation to the activation state of microglia are somewhat better understood. In line with the *in vitro* observation that plasma constituents readily activate microglia (Zhao et al., 2009; Si et al., 2000), microglia in brain regions where the blood-brain barrier is incomplete or absent, such as the median eminence, pituitary stalk and neurohypophysis, display a higher level of basal activation (Mander et al., 1995). Signaling from surrounding other cell types most likely plays an essential part in determining microglial phenotypes. Neurons are known to influence microglial activation through so-called 'on' and 'off' signals (Biber et al., 2007). These signals involve multiple systems (CX3CL1-CX3CR1, CD200-CD200 receptor, CD47-CD172a) with variable modes of action, and provide the CNS with the means to actively manipulate local immune responses. These neuronal signaling molecules and their receptors on microglia have an established role in certain animal models (Deckert et al., 2006; Cardona et al., 2006), but their potential contribution to shape the microglial phenotype under physiological conditions still has to be firmly established. Since microglia are known to express functional neurotransmitter receptors (Pocock &

Kettenmann, 2007), and since different neurotransmitters have a distinct effect on microglial cells (Farber et al., 2005a), it is also possible that region-specific release of neurotransmitters by neurons also influences regional phenotype diversity of microglia. Moreover, other glial cells including oligodendrocytes and astrocytes show regional differences in the CNS (Olsen et al., 2007; Du et al., 2003). The fact that microglial phenotype is influenced by microglia-macroglia cross-talk as well, adds an additional level of complexity to the regulatory network that shapes microglia phenotype in the CNS.

MICROGLIA PHENOTYPES ASSOCIATED WITH INFLAMMATION

In the adult healthy brain microglia are characterised by a ramified morphology. By moving their thin, highly branched processes microglia continuously survey their microenvironment for potential threats, making these cells the first line of defense in the CNS. Any type of brain injury inevitably activates microglia, which is characterised by a stereotypic morphological reaction (Hanisch & Kettenmann, 2007; Van Rossum & Hanisch, 2004; Streit, 2002; Kreutzberg, 1996). Based on morphological changes, microglial activation was originally defined as a stereotypic and graded process (Streit, 2002; Kreutzberg, 1996). This concept has been recently challenged (Ransohoff & Perry, 2009; Hanisch & Kettenmann, 2007). It is now clear that microglia respond with a variety of different reactions by integrating multifarious input signals (Ransohoff & Perry, 2009; Hanisch & Kettenmann, 2007; Van Rossum & Hanisch, 2004; Streit, 2002; Kreutzberg, 1996). In line with this, microglia responses are not inevitably neurotoxic. Various neuroprotective effects of activated microglia have been demonstrated recently *in vivo*. Microglial activation turned out to prove beneficial in a model of nitric oxide-dependent excitotoxicity (Turrin & Rivest, 2006), and in stroke (Lalancette-Hebert et al., 2007). Moreover, protective microglial activity has been described in mouse models of amyotrophic

lateral sclerosis (ALS) (Boillee et al., 2006) and Alzheimer's disease (AD) (El Khoury et al., 1998). Conversely, neurotoxicity might occur in case of overshooting, as a result of uncontrolled stimulation of microglia [30, 36], or when microglial functions are impaired (Neumann & Takahashi, 2007; Boillee et al., 2006; Streit, 2006). Not only is pro-inflammatory microglial activity important in neurodegenerative and neuroinflammatory diseases, but there is accumulating evidence that immune malfunction is also involved in psychiatric diseases like schizophrenia and mood disorders. Microglial activity has thus recently attracted interest in biological psychiatry. Indeed, recent findings suggest a role of microglia-driven brain inflammation also in psychiatry (see for review: Bernstein et al., 2009; Muller & Schwarz, 2007). Thus, microglial activity is currently considered to be involved in a wide range of brain diseases.

M1 versus M2 activation of microglia

Due to their myeloid lineage microglia belong to the innate arm of the immune system, with its inherent and pre-programmed responses. Peripheral macrophages show at least two distinct activation patterns, i.e. M1 (classical, induced by IFN-γ and LPS) and M2 (alternative, induced by IL-4 or IL-13) activation, in parallel to the classification of T cell responses into Th1 and Th2. Various lines of evidence, however, suggest that this is a simplification, as indeed it is for T cells, and that at least one additional macrophage activation state exists. However, universal agreement on the nomenclature of the different macrophage activation states beyond the M1 versus M2 concept has yet to be reached (Martinez et al., 2009; Gordon, 2008; Mantovani, 2008; Mosser & Edwards, 2008). There is clear evidence that cultured microglia can acquire a classical activation pattern (M1) when activated by LPS and IFN-γ (reviewed in Colton, 2009). However, compared to peripheral tissue macrophages, much less is currently known about alternatively (M2) activated microglia *in vitro* and *in vivo*. There are various reports

on the effects of IL-4 or IL-13 stimulation in microglia. These reports, however, show little consistency. For example it has been noted that IL-4 stimulation of cultured microglia up-regulates MHCII and CD11c expression, leading to a dendritic cell-like, neuroprotective microglial phenotype (Butovsky et al., 2007). In contrast, injection of IL-4 into brains of CD11c-enhanced yellow fluorescent protein (eYFP) mice reportedly did not induce expression of MHCII and CD11c *in vivo* (Gottfried-Blackmore et al., 2009). In another study, stimulation with IL-4 and IL-10 induced expression of various mRNAs like arginase I, mannose receptor, found in inflammatory zone I, and chitinase 3-like protein 3 (YMI), indicating a cytokine induced alternative activation state of microglia (Colton et al., 2009). In an animal model for multiple sclerosis, experimental autoimmune encephalomyelitis (EAE) it was found that cells of the myeloid lineage are positive for YMI, indicating their alternative activation which was dependent on IL-4 (Ponomarev et al., 2007). However, it should be noted that YMI expression in this study was restricted to CD45high cells, characteristic for infiltrated macrophages rather than endogenous microglia (Remington et al., 2007; De Haas et al., 2007; Sedgwick et al, 1998). Similarly, in a model of uncontrolled cerebral cryptococcosis infection, IL-4/IL-13-dependent alternative activation was only found in peripheral macrophages that infiltrated the infected brain, but not in endogenous microglia (Stenzel et al., 2009). Together, these data do not yet offer a consistent view on the possible role of IL-4/IL-13 during alternative activation of microglia.

The presence of endogenous dendritic cells in the brain in response to inflammation

Dendritic cells (DC), the professional antigen presenting cells (APC) of the peripheral immune system, are essential for antigen processing, antigen transport to lymphoid organs, and subsequent antigen-specific activation of naïve T cells. DC therefore bridge innate and adaptive immunity (Steinman & Banchereau, 2007). Differentiated DC typically

express CD11c and MHCII both of which can be further induced upon activation and subsequent maturation of the cells. In the non-challenged CNS parenchyma, both markers are undetectable by immunhistochemical methods. Since CD11c and MHCII-positive cells in the brain are restricted to perivascular spaces and the choroid plexus, it has been widely assumed that a healthy brain is free of DCs (for review see Ransohoff & Perry, 2009; Colton, 2009). This is in contrast to pathological circumstances, where DCs (CD11c positive cells) have been be found in brain parenchyma during experimental allergic encephalomyelitis (Matyszak & Perry, 1996), toxoplasmic encephalitis (Fischer & Reichmann, 2001; Fischer et al., 2000), and stroke (Reichmann et al., 2002). Whether or not these DC are derived from endogenous microglia, or infiltrate the inflamed brain from the periphery is currently debated (Ransohoff & Perry, 2009; Colton, 2009). Recent findings using a CD11c/EYFP transgenic mouse model have provided evidence for a CD11c-positive population of cells with ramified, microglia-like morphology (Bulloch et al., 2008). Stroke experiments in bone-marrow chimeras of CD11c/EYFP transgenic and wild-type animals have shown that CD11c-positive cells in the core of the stroke lesion were derived from peripheral sources, and that the border region contained CD11c-positive cells derived from endogenous brain cells (Felger et al., 2009). These studies suggest that the brain indeed hosts an endogenous source of potential DC, designated brain DC (Gottfried-Blackmore et al., 2009; Felger et al., 2009; Bulloch et al., 2008). The notion that endogenous DC exist in the brain has been further strengthened by the finding that intracerebral injection of IFN-γ induces the differentiation of DC into effective APC, with the ability to activate even naïve T cells (Gottfried-Blackmore et al., 2009). However, intracerebroventricular (i.c.v.) application of IFN-γ did not have such an effect, neither were microglia found to differentiate into DC or APC-like cells in response to i.c.v. application of granulocyte macrophage-colony stimulating factor (Mausberg et al., 2009), a stimulus that induces

differentiation of microglia into dendritic cells *in vitro* (Fischer & Reichmann, 2001; Santambrogio et al, 2001). Taken together, whether or not the brain hosts an endogenous population of DC, and whether or not DC with APC capacity in the brain are actually derived from microglia, remain open issues.

MICROGLIA PHENOTYPES ASSOCIATED WITH SPECIALISED NICHES IN THE CNS

Microglia as part of the neurogenic niche

In the mainly post-mitotic mammalian CNS there are two exceptional sites where neurogenesis continues even during adulthood, i.e. the hippocampal dentate gyrus and the subventricular zone (Suh et al., 2009; Gould, 2007; Kempermann et al., 2004; Gross, 2000). Considering that microglia are likely adapted to the requirements of their local micro-environment, a unique microglial phenotype is likely associated with the adult neurogenic niche. Initially, evidence for microglial involvement in adult neurogenesis was indirect, based on the observation that during damage to the CNS, recruitment of neural stem cells to the site of insult and their subsequent differentiation coincides with the presence of activated microglia (Chang et al., 2008; Aarum et al., 2003) (reviewed in Das & Basu, 2008; Simard & Rivest, 2004). However, apparently contradictory results were reported as well (Olah et al., 2009; Cacci et al., 2008; Battista et al., 2006; Wachs et al., 2006; Ziv et al., 2006; Walton et al., 2006). It is therefore likely, that any role of microglia in the self-renewing capacity of the CNS, and in the differentiation of neural stem cells is to a large extent context dependent (Figure 2). At present, the generally accepted idea is that a given microglia phenotype can be classified, based on its functional influence on (adult) neurogenesis, as detrimental, permissive or beneficial (Ekdahl et al., 2009; Whitney et al., 2009). Whether microglia will exert a beneficial or detrimental effect on multiple aspects of

neurogenesis, greatly depends on the mode of activation. *In vitro* studies have pointed out that substances like LPS, IFN-γ and amyloid β-peptide, which induce a microglial phenotype (CD11b+/CD11c-/MHCII-) characterised by TNF-α expression, are unfavorable for neurogenesis. Conversely, IL-4 and low levels of IFN-γ endow microglia with an insulin-like growth factor-1 (IGF-1) producing phenotype (CD11b+/CD11c+/MHCII+), hence rendering them supportive of neurogenesis (Balasubramaniam et al., 2009; Butovsky et al., 2006a; Butovsky et al., 2006b; Liu et al., 2005; Cacci et al., 2005). Acutely activated microglia reduce neuronal cell differentiation and increase cell death through the expression of IL-1α, IL-1β, inducible nitric oxide synthase, IL-6, and TNF-α, while chronically activated microglia become permissive for neurogenesis due to the upregulation of IL-10 and prostaglandin E2 (Cacci et al., 2008). Moreover, conditioned medium from microglia activated with two different fragments of the tenascin-R molecule promotes neuronal cell differentiation of neural stem cells through transforming growth factor-β1 (TGF-β1), nerve growth factor, and brain-derived growth factor (Liao et al., 2008). Microglia-conditioned medium itself seems to have a beneficial influence on the survival (Cacci et al., 2005), proliferation (Cacci et al., 2008), and migration (Aarum et al., 2003) of neural precursors *in vitro* and their differentiation towards neuronal (Walton et al., 2006) and astrocytic (Cacci et al., 2008; Zhu et al., 2008; Nakanishi et al., 2007) lineages. *In vivo*, both acute and chronic activation of microglia, for example by means of intra-hippocampal LPS injection, or induction of epilepsy or transient cerebral ischemia, have been documented to be either advantageous (Kim et al., 2009; Choi et al., 2008; Jakubs et al., 2008; Spulber et al., 2008; Bonde et al., 2006) or disadvantageous (Ekdahl et al., 2003; Monje et al., 2003) with respect to adult neurogenesis. Under pathological

conditions, which are associated with increased numbers of apoptotic cells microglia acquire a phenotype that promotes adult hippocampal neurogenesis through the
production of TGF-β1 (Battista et al., 2006). However, determination of the exact microglial phenotype that is instrumental in the maintenance of the neurogenic niches in the adult brain under physiological conditions seems a challenge. Various lines of evidence do support the idea that even in health, microglia residing in the adult neurogenic niches bear a special phenotype. It has been shown that microglia associated with the subventricular zone exist at a higher basal level of activation, based on the expression levels of CD45, CD11b, and IB4 (Goings et al., 2006). Moreover, subventricular zone-derived microglia seem to possess a greater capacity for *in vitro* expansion than microglia isolated from other brain regions (Marshall et al., 2008). Upon ischemic insult, microglia in the subventricular zone acquired a pro-neurogenic phenotype [expression of IGF-1], which is concomitant with persistent neurogenesis in the striatum after stroke (Thored et al., 2009). Concerning the microglia phenotype that supports adult hippocampal neurogenesis under physiological conditions, mainly indirect evidence exists. The experiments done in this context point to an involvement of the complement system (Rahpeymai et al., 2006), SPARC (secreted protein acidic and rich in cysteine) (Vincent et al., 2008), microglial cyclooxygenase-2 (Goncalves et al., 2010), and stromal cell derived factor-1 (SDF-1)(Choi et al., 2008). A unified hypothesis however, is still missing. It has been suggested that an increase in hippocampal neurogenesis is associated with the presence of IL-4-producing T helper 2 cells in the brain parenchyma, which could instruct resident microglia towards an IGF-1 expressing phenotype, supportive of neurogenesis (Ziv et al., 2006). However, the presence of T cells in healthy brain parenchyma continues to be disputed. Furthermore, elevated levels of adult hippocampal neurogenesis appear to also occur in the absence of either T cells or MHC II-expressing microglia (Olah et al., 2009).

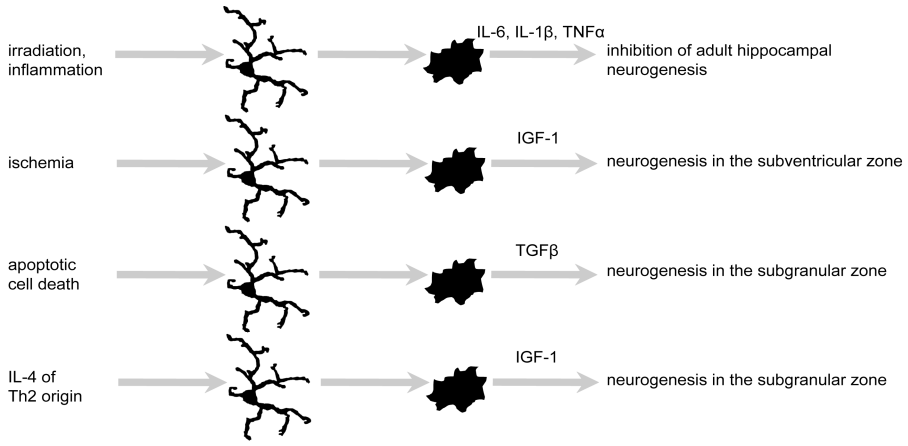

Figure 2. Microglia as part of the neurogenic niche. Microglia are believed to exert either beneficial or detrimental effect, on adult neurogenesis depending on their mode of activation. The pro-neurogenic microglia phenotype is characterised by the expression of IGF-1 and TGFβ1 and it arises under certain conditions (as a result of apoptotic cell death or ischemia) in brain areas such as the hippocampal dentate gyrus or the subventricular zone. References can be found in the text. (For references see the text. For the acronyms see List of abbreviations).

The phenotype differences of microglia residing in the white and grey matter of the CNS

Increasing evidence suggests that white and grey matter in the CNS harbor phenotypically distinct microglia populations. Based on the observation that corpus callosum microglia in mice have a constitutively higher level of expression of costimulatory molecules such as B7.2 (CD86) than their cortical counterparts, it has been postulated that microglia residing in white matter exist with a higher basal level of activation under physiological conditions, when compared to microglia located in non or less myelinated regions of the CNS (Carson et al., 2007). Supporting this idea, it has been shown that the number of HLA-DR (major histocompatibility complex, cell surface receptor)/MHC II-positive microglia, or the cellular expression level of this molecule in humans, monkeys, dogs and rats under physiological conditions, is higher in white matter (corpus callosum, capsula interna) than in the cerebral cortex (Sheffield and Berman, 1998; Alldinger et al. 1996; Ong et al., 1995; Ogura et al., 1994; Gehrmann et al., 1993; Sasaki et al.,

1992; Styren et al., 1990). Furthermore, Tim-3, a membrane protein involved in the regulation of macrophage and T-cell responses, was recently found to be expressed specifically on corpus callosal microglia in the non-inflamed human brain (Anderson et al., 2007). Moreover, microglia residing in forebrain and spinal cord white matter are affected more profoundly by the age related increase in the basal level of activation than their grey matter counterparts (Kullberg et al., 2001; Sheffield & Berman, 1998; Ogura et al., 1994). Furthermore, in an experimental model of chronic cerebral hypoperfusion in the rat, microglia activation was mainly observed in the white matter (Wakita et al., 1998; Wakita et al., 1995; Wakita et al., 1994). Multiple sclerosis is another pathological condition of the CNS, during which intriguing differences between white and grey matter microglia manifest themselves. Grey matter lesions in multiple sclerosis display less pronounced inflammation, microglia activation and complement deposition, as compared to white matter lesions (Bo, 2009; Brink et al., 2005) providing further support to the above mentioned idea. However, the actual extent and the functional consequences of the phenotype differences between white and grey matter microglia remain to be fully clarified.

MICROGLIA IN BRAIN TUMORS

Whereas microglia are generally considered as the primary cells involved in “CNS defense”, the persistent malignant behavior of astrocytic gliomas suggests that the immune functions of microglia are suppressed in a glioma environment (Figure 3). There is abundant evidence that microglial behavior is controlled by tumor cells, resulting in secretion of cytokines and growth factors that may contribute to immune evasion, growth, and invasion of brain neoplasms. In this section we will describe the “immunosuppressed” phenotype of

microglia in gliomas and the factors in glioma tissue that mediate this phenotype.

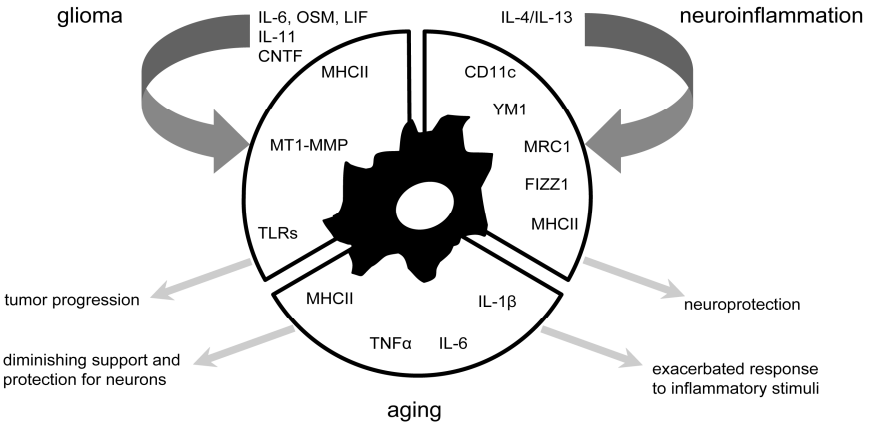

Figure 3. Certain microglia phenotypes associated with neuroinflammation, aging and gliomas. Presently it is not well understood whether the microglia phenotypes present in the CNS under different inflammatory conditions can be indeed classified as M1 or M2, as in the case of peripheral macrophages. Some studies have shown M2-like activation of microglia could point towards their neuroprotective function. Microglia associated with gliomas is generally considered to have attained an "immuno-suppressed" phenotype, being unable to present antigen, due to lack of expression of co-stimulatory molecules. On the other hand tumor-associated microglia have been shown to express molecules involved in tissue remodelling, hence they might contribute to glioma progression. The phenotype of microglia in the aging brain is contradictory. Microglia acutely isolated from the aged brain displayed higher basal expression levels of pro-inflammatory cytokines and increased response to LPS challenge, supporting the hypothesis that microglia in the aged brain are hyperactive. However, in certain studies microglia were found to be dystrophic rather than hyperactive in the aged brain. Whether these two phenotypes are mutually exclusive or their occurrence shows species specificity is still matter of debate. They both might, however, contribute to decreased support for neurons from the side of microglia. (For references see the text. For the acronyms see List of abbreviations).

The microglia phenotype in gliomas

Many human gliomas show prominent infiltration of microglia/macrophages. In addition, a correlation exists between abundance of microglia/macrophages and the grade of malignancy. Thus, the number of microglia/macrophages in grade IV glioblastomas is higher than in grade II or III gliomas, and is closely correlated with

vascular density in the tumors (Nishie et al., 2001; Nishie et al., 1999). Based on membrane markers distinctive for resident microglia (CD11b+/CD45low) and macrophages (CD11b+/CD45high), the presence of both cell types in gliomas has been confirmed in mice. A comparable identification of distinct CD45low and CD45high subpopulations has been reported for human glioma tissue (Watters et al., 2005). However, the presence of these specific subpopulations appears to be less obvious in human gliomas (Hussain et al., 2006). Infiltrating microglia/macrophages may account for up to 30% of the tumor mass (Giometto et al., 1996). The morphology of microglia changes with tumor progression. Thus, diffuse low-grade astrocytomas still contain highly ramified microglia. However, in high-grade astrocytomas microglia have shorter and thicker processes, and often are amoeboid (Graeber et al., 2002). Furthermore, the immunophenotype of microglial cells in astrocytic gliomas correlates with tumor grade. Despite their activated morphology, microglia in high-grade astrocytomas express lower levels of immune markers such as MHCII antigens as compared to less activated microglia in low-grade astrocytomas. Although human tumor-associated microglia express surface MHCII, they lack expression of the costimulatory molecules CD86, CD80, and CD40, critical for T-cell activation. In addition, microglia/macrophages in human astrocytomas express considerable levels of Toll-like receptors (TLRs), but do not respond to TLR stimulation in tems of cytokine secretion (Hussain et al., 2006). Furthermore, while LPS binds TLR4, it does not induce microglia/macrophage-mediated T-cell proliferation (Nishie et al., 1999). In contrast, soluble factors in murine gliomas do stimulate microglial TLRs, as evidenced by microglial membrane type 1 metalloprotease induction via the TLR downstream signaling molecules MyD88 and p38 mitogen-activated protein kinase. In turn, membrane type 1 metalloprotease expression and activity in these immune cells promotes glioma cell invasion and tumor expansion (Markovic et al., 2009).

Antigen Presentation Capacity of Microglia in Tumors

Evidence for antigen presentation activity of microglia in brain tumors is limited. Several reports have described expression of MHCII, B7-1 and B7-2 costimulatory molecules by microglia in human gliomas. This would suggest that microglia may be capable of presenting antigens *in vivo* (Tran et al., 1998; Graeber et al., 1994). Furthermore, it has been observed that the expression of MHC II and co-stimulatory B7 molecules correlated directly with both tumor immunogenicity and the extent of lymphocyte infiltration into tumors (Badie et al., 2002). Microglia and macrophages associated with immunogenic C6 and 9L tumor models have higher expression levels of both MHC II and B7.1 molecules as compared to non-immunogenic RG-2 gliomas (Badie et al., 2002).

Tumor-induced effects on microglia

Gliomas synthesise and secrete multiple factors that are capable of inhibiting T-cell responsiveness as well as microglia activation. These include the IL-6 type cytokines IL-11, ciliary neurotrophic factor (CNTF), cardiotrophin-1, leukemia inhibitory factor (LIF), and oncostatin M (Repovic et al., 2003; Hao et al., 2002; Halfter et al., 1998a,b; Murphy et al., 1995). Thus, abundant IL-6, CNTF, LIF, IL-11, and oncostatin M are produced by glioblastoma tumors and glioblastoma cell lines such as U87MG and U373MG (Repovic et al., 2003; Goswami et al., 1998; Van Meir et al. 1990). Whereas IL-6 and LIF enhance pro-inflammatory microglia stimulation, CNTF suppresses microglia activation and IL-11 represses expression of co-stimulatory molecules in microglia (Krady et al., 2008; Holmberg and Patterson, 2006, Wei and Jonakait, 1999). All members of the immune suppressive TGF-β cytokine family are also expressed in human glioblastomas (Hao et al., 2002; Constam et al., 1992, Olofsson et al., 1992). TGF- β1 and -2 inhibit pro-inflammatory activity of microglia (Qian et al., 2008; Schluter et al., 1998). [140,141]. The expression of IL-10 mRNA increases significantly with tumor grade. Thus, 87% of grade III–IV astrocytomas express IL-10 mRNA. In contrast,

only 4% of grade II astrocytomas express IL-10 mRNA (Huettner et al., 1997). Gliomas exhibiting a high degree of brain invasiveness express IL-10 at higher levels than more localised gliomas. The anti-inflammatory effect of IL-10 on microglia (Marques et al., 2004; Ledeboer et al., 2000) fits the immune suppressive environment in glioblastoma tissue. Microglia/macrophages in tumors release many factors, including extracellular matrix proteases, cytokines and chemokines, which may influence tumor migration/invasiveness (Watters et al., 2005, Platten et al., 2003, Rao, 2003). Glioma cell migration is stimulated by the presence of macrophages/microglia, or macrophage/microglia-conditioned medium (Bettinger et al., 2002). Furthermore, in organotypic brain cultures the invasive potential of glioblastoma was lower in microglia-depleted slices (Markovic et al., 2005). These findings suggest that microglia/macrophages in human gliomas may promote and support the invasive phenotype of these tumors. Some studies have also indicated that gliomas are able to secrete chemokines that attract and support the growth of microglia/macrophages in brain tumors (Kielian et al., 2002; Galasso et al., 2000; Alterman and Stanley, 1994). Macrophage chemoattractive protein-1 is secreted by a variety of glioma cell lines and is expressed in glioblastomas (Jordan et al., 2008; Brown et al., 2007; Desbaillets et al., 1994; Takeshima et al., 1994). Macrophage chemoattractive protein -1 is believed to be a major contributor to microglia/macrophage recruitment to gliomas (Platten et al., 2003; Leung et al.,1997). Whereas the immune suppressed and permissive microglia phenotype associated with brain tumors is now largely characterised, it will be of great interest to identify tumor-related factors that induce this immune suppression.

THE MICROGLIA PHENOTYPE IN THE AGING CNS

Microglia support neuronal cells during their whole life span. They provide trophic and other supportive factors to protect neurons during

adverse conditions, and eliminate dying neurons that might injure their neighbors. In order to perform their supportive function, microglia may undergo an activation process and proliferative state several times. This intense activity over the life span of the brain will result in microglia senescence, associated with a change of microglia phenotype and possibly a decrease in supportive function (Figure 3). Age-related neurodegenerative diseases are often accompanied by protein aggregation and neuronal cell death, thus increasing the demand for removal of cell debris and aggregates by microglia. It is therefore important to determine how the functionality of these cells is affected by the process of aging. Two theories have been proposed: (i) microglia become hyperactive and develop a proinflammatory phenotype; (ii) microglia undergo replicative senescence and become dystrophic, making them unable to perform their protective support.

The phenotype of aging microglia

Many reports indicate that microglia acquire activated morphology during normal aging. More precisely, process shortening and thickening have been observed in microglia in aged mice (Sierra et al., 2007), rats (Kullberg et al., 2001; Perry et al., 1993; Vaughan and Peters, 1974) monkeys (Peters and Sethares, 2002; Sloane et al., 1999; Sheffield and Berman, 1998; Peters et al., 1991) as well as in humans (Sheng et al., 1998; DiPatre and Gelman, 1997). Interestingly, this change in microglia morphology from a typical resting state to an activated phenotype during aging is associated with an increased production of proinflammatory mediators. Acutely isolated microglia derived from aging mice show increased basal levels of TNF-α, IL-1β, and IL-6 (Sierra et al., 2007). When these aged animals where challenged by injection with LPS, microglial expression of TNF-α, IL-1β, and IL-6 were rapidly up-regulated along with IL-10, whereas a down-regulation of TGF-β1 was observed. These results reflect a pre-conditioned state of microglia. Upon aging, they show increased responsiveness to a pro-inflammatory

stimulus. These results corroborate data obtained earlier in total brain extracts (Godbout et al., 2005), and in cultured microglia derived from old brains (Xie et al., 2003; Ye & Johnson, 1999). All these observations have led to the idea that in the aging brain microglia acquire a hypersensitive, primed state. This phenotype causes a more rapid and pronounced activation upon any insult, and it will thus generate an increased inflammatory environment that will lead to increased bystander injury. How this phenotype is acquired is still unclear, but it seems to be associated with increased expression of TLRs (Letiembre et al., 2007), as well as increased expression of MHC II (Sloane et al., 1999; Ong et al., 1995; Perry et al., 1993). On the other hand, microglia in the aging CNS have been described with aberrant features in their morphology, including deramification, shortening, twisting and fragmentation of their processes (Streit et al., 2004). These changes in morphology were clearly different from those characterising microglial activation, suggesting that microglia become dystrophic during aging. Dystrophic microglia also display strong ferritin staining (Lopes et al., 2008), hypertrophy of the peri-nuclear cytoplasm (Conde & Streit, 2006), and the presence of numerous autophagic vacuoles in the cytoplasm. These observations have led to the hypothesis that microglia become senescent with aging. This senescent phenotype may well imply that microglia are less able to repair or help during neuronal cell damage, and that the CNS consequently becomes more susceptible to the development of neurodegenerative diseases. According to this idea, microglia secrete reduced levels of neurotrophic factors, and have lower phagocytic activity (Streit et al., 2008). In the context of neurodegenerative diseases, where phagocytic function and autophagy are necessary for the clearance of toxic protein aggregates and cell debris, dystrophic microglia would have a major negative impact. Indeed, if microglia would be less efficient in clearance, combined with a decreased production of neurosupportive factors, this would promote the accumulation of stressed neurons, and neuronal cell death (Streit et

al., 2008). This, in turn, would lead to activation of neighboring microglia, increased secretion of inflammatory mediators and bystander neuronal cell death, thus creating a vicious loop that would aggravate disease severity. It is likely that both phenotypes, hyperactive and senescent, may occur under different circumstances during aging, thus conveying an increased risk for neurodegenerative diseases and lack of trophic support. However, it is important to note that the senescent phenotype has been observed primarily in human postmortem brains, and thus might reflect a major difference between rodents and humans. In fact, it is well known that rodent cells have longer telomeres (see below) than their primate counterparts, which might prevent rodent microglia from developing replicative senescence.

The mechanism of microglia aging

The mechanism of microglial aging is still under investigation. One possible factor is that microglia suffer from DNA damage caused by lifelong exposure to reactive oxygen species (Streit et al., 2008). Another more plausible cause for microglia senescence is a decrease of replicative property. During their life span, microglia will undergo replication through mitosis when they become activated (Lawson et al., 1992). This process of activation/replication may lead to replicative senescence, caused by telomere attrition, DNA damage, and chromatin perturbation. Ultimately, cellular senescence leads to the inability to proliferate and altered gene expression that will affect the phenotype and function of microglia. Interestingly, telomere shortening has been observed in microglia derived from rat brain (Miller & Streit, 2007). Thus, microglia cultured without proliferative agents reportedly enter a state of proliferative arrest when their telomeres reached a critical length below 14 kb. Interestingly, microglia stimulated with granulocyte macrophage-colony stimulating factor, a potent microglial mitogen, did not undergo such replicative senescence. Instead, they demonstrated reduced viability and mitotic activity suggesting that they were subject

to telomere independent cellular senescence. These data suggest that, when submitted to a stressful situation, aged microglia may still be able to divide, but to a lower extent. Nevertheless, since they are more fragile they will probably die. Another study has documented a decline in telomere length with increasing age in rats, confirming that cellular senescence might indeed occur *in vivo* (Flanary & Streit, 2003). Finally, the idea has been put forward that microglia would become deficient in their lysosomal activity due to alterations in cathepsin activity. This would lead to a decrease in autophagic activity, and to a lower turnover of mitochondria. Compromised mitochondria would then produce less ATP and more reactive oxygen species, leading to energy deficit and oxidative stress (Ralay Ranaivo et al., 2006). It is important to note that this idea is based on observations made in several cell types of the aging brain and thus may apply to microglia.

Microglia in age-related neurodegenerative disease

In neurodegenerative diseases, enhanced production of mutated proteins and protein misfolding will lead to protein aggregation in neurons. It has been suggested that microglia become activated either by stress signals produced by affected neurons or by encounter with the aggregate itself once the neuron is dead (Hanisch & Kettenmann, 2007). This activation may lead to secondary neuronal degeneration via release of microglia-derived neurotoxic factors. Thus, microglia are thought to be responsible for the massive neuronal death occurring in Parkinson's disease, AD (Ralay Ranaivo et al., 2006), and ALS (Boillee et al., 2006). While this has inspired the testing of anti-inflammatory drugs in neurodegenerative disorders, many of the attempts have so far failed to produce beneficial effects, and some have even led to worsening of the symptoms (McGeer et al., 2006). For example, ablation of microglia does not affect motoneuron degeneration in ALS (Gowing et al., 2008), or amyloid β-peptide plaque formation in AD models (Grathwohl et al., 2009). These data emphasise that the functions of microglia in

neurodegenerative disease are complex, and probably involve intricate balances between diverse immune-regulatory functions, complicated by age-related changes.

Outline of the thesis

The aim of this thesis was to investigate the role and characteristics of microglia phenotypes associated with different aspects of maintenance of tissue homeostasis in the central nervous system. In **Chapter 1** we have provided a detailed overview of the available literature regarding the phenotype diversity of microglia and discussed the functional relevance of the different microglia phenotypes and the future perspectives in the field. In our experimental work we focused on the regional phenotype differences of microglia under physiological conditions and the microglia phenotypes associated with plasticity and regeneration. The techniques applied range from genome wide gene expression analysis to functional *in vitro* cellular assays. Furthermore, we extended our scope of investigations from mouse to human, by setting up a protocol for rapid isolation of human microglia from post mortem brain samples.

Chapter 2 concerns the role of microglia in the regulation of adult neurogenesis. It was long believed that in the adult central nervous system proliferation is restricted to the glial cells. Moreover, it has been assumed that the brain, in view of its synaptic connectivity, is hard-wired and that after infancy no new neuronal elements are produced and added to the system. The discovery of neurogenesis in specialised niches of the adult brain from birds to humans in the course of the last decade of the 20th century has proven this dogma to be wrong. Consequently, the role of adult neurogenesis in plasticity and regeneration in the CNS has been established. Microglia cells are considered a part of the neurogenic niche, and they have been documented to contribute to the regulation of adult neurogenesis under certain pathological conditions. However, the nature of the microglia phenotype that contributes to the neurogenic niche in the healthy brain was not firmly established yet. In order to investigate the role of microglia in the regulation of adult neurogenesis under physiological

conditions, we used the mouse running wheel model, in which voluntary physical exercise beneficially influences multiple aspects of adult hippocampal neurogenesis (proliferation and survival of the neural precursors and their differentiation into dentate gyrus granule cells). In the study described in **Chapter 2** we investigated the microglia phenotype associated with basal and physiologically elevated level of adult hippocampal neurogenesis in the dentate gyrus.

Chapter 3 addresses the regional differences in microglia phenotypes in the central nervous system under physiological conditions. The morphological heterogeneity of the microglia populations associated with different anatomical sites in the brain and the spinal cord was early recognised and has been suggested to reflect differences in their state of activation. Consequently, it has been proposed that the regional differences in microglia phenotype might contribute to the dissimilar susceptibility of different brain regions to certain pathophysiological processes. Several lines of evidence suggest that the cerebral white and the grey matter constitute the two most distinct inflammatory environments in the brain parenchyma (e.g. the inflammatory profile of cortical versus white matter MS lesions; susceptibility to aging, hypoxia and viral infections). Thus, we intended to investigate the phenotype differences of microglia resident in the corpus callosum and cerebral cortex, respectively. We examined and compared the phenotype of white and grey matter microglia at multiple levels: morphology, gene expression, surface expression of marker molecules and functionality in the healthy brain. Furthermore, we examined the differences in their responsiveness to inflammatory challenge in a mouse model of endotoxemia.

In **Chapter 4** we aimed at characterising the microglia phenotypes that are associated with central nervous system de- and remyelination. It is now well recognised that inflammation has a multifaceted role in regenerative processes, including remyelination in the CNS. Microglia, as the resident immune cells of the brain, play a central role in the

outcome of any inflammatory (and regenerative) event. Determining the exact microglia phenotype that is supportive of remyelination is of importance due to its potential therapeutic relevance. We used the cuprizone model of primary demyelination in mice, where spontaneous remyelination occurs upon cessation of cuprizone treatment. In this model, the recruitment of systemic immune cells to the local microglia/macrophage population is negligible. To determine the characteristics of the microglia phenotype associated with de- and remyelination we applied genome wide gene expression analysis and subsequently confirmed our findings at the protein level.

In **Chapter 5** a rapid and highly efficient protocol is described for the isolation of microglia from human post mortem (and biopsy) brain samples. Earlier protocols for isolation of adult human microglia made use of the dissimilar attachment properties of the different glial cell subtypes. These protocols involved extended time in culture (sometimes weeks, during which cells were exposed to, among others, recombinant growth factors) to obtain reasonable microglia purity and yield. In the procedure described in this chapter we tested multiple elements of the already existing protocols and combined them in the most efficient way, to attain a fast and proficient (in terms of yield and purity) method. This protocol enables the investigation of the phenotype and functionality of microglia cells acutely isolated from the CNS tissue.

Chapter 6 provides a general overview and discussion of the results obtained in the course of the PhD project.

LIST OF ABBREVIATIONS

AD	Alzheimer's disease
ALS	amyotrophic lateral sclerosis
APC	antigen presenting cell
CD11b	integrin alpha-M
CD11c	integrin alpha-X
CNS	central nervous system
CNTF	ciliary neurotrophic factor
CXCR3	C-X-C chemokine receptor type 3
DC	dendritic cells
EYFP	enhanced yellow fluorescent protein
FIZZ1	resistin-like alpha
i.c.v	intracerebroventricular
IFN-γ	interferon-γ
IGF-1	insulin-like growth factor-1
IL-11	interleukin-11
IL-13	interleukin-13
IL-1β	interleukin-1 beta
IL-4	interleukin-4
IL-6	interleukin-6
IL-6	interleukin-6
LIF	leukemia inhibitory factor
LPS	lipopolysaccharide
MHCII	major histocompatibility complex class II
MRC1	macrophage mannose receptor 1
MT1-MMP	membrane type 1 metalloprotease
OSM	oncostatin-M
TGF-β1	transforming growth factor-β1
Th2	T helper 2 cell
TLR	Toll-like receptor
TNF-α	tumor necrosis factor- α
TREM-2b	triggering receptor expressed on myeloid cells 2
YM1	chitinase-3-like protein 3

LIST OF REFERENCES

Aarum J, Sandberg K, Haeberlein SL, Persson MA. 2003. Migration and differentiation of neural precursor cells can be directed by microglia. Proc Natl Acad Sci U S A 100:15983-15988.

Alldinger S, Wunschmann A, Baumgartner W, Voss C, Kremmer E. 1996. Up-regulation of major histocompatibility complex class II antigen expression in the central nervous system of dogs with spontaneous canine distemper virus encephalitis. Acta Neuropathol 92:273-280.

Alterman RL, Stanley ER. 1994. Colony stimulating factor-1 expression in human glioma. Mol Chem Neuropathol 21:177-188.

Anderson AC, Anderson DE, Bregoli L, Hastings WD, Kassam N, Lei C, Chandwaskar R, Karman J, Su EW, Hirashima M, Bruce JN, Kane LP, Kuchroo VK, Hafler DA. 2007. Promotion of tissue inflammation by the immune receptor Tim-3 expressed on innate immune cells. Science 318:1141-1143.

Ayoub AE, Salm AK. 2003. Increased morphological diversity of microglia in the activated hypothalamic supraoptic nucleus. J Neurosci 23:7759-7766.

Badie B, Bartley B, Schartner J. 2002. Differential expression of MHC class II and B7 costimulatory molecules by microglia in rodent gliomas. J Neuroimmunol 133:39-45.

Balasubramaniam B, Carter DA, Mayer EJ, Dick AD. 2009. Microglia derived IL-6 suppresses neurosphere generation from adult human retinal cell suspensions. Exp Eye Res 89:757-766.

Battista D, Ferrari CC, Gage FH, Pitossi FJ. 2006. Neurogenic niche modulation by activated microglia: transforming growth factor beta increases neurogenesis in the adult dentate gyrus. Eur J Neurosci 23:83-93.

Bernstein HG, Steiner J, Bogerts B. 2009. Glial cells in schizophrenia: pathophysiological significance and possible consequences for therapy. Expert Rev Neurother 9:1059-1071.

Bettinger I, Thanos S, Paulus W. 2002. Microglia promote glioma migration. Acta Neuropathol 103:351-355.

Biber K, Neumann H, Inoue K, Boddeke HW. 2007. Neuronal 'On' and 'Off' signals control microglia. Trends Neurosci 30:596-602.

Bo L. 2009. The histopathology of grey matter demyelination in multiple sclerosis. Acta Neurol Scand Suppl51-57.

Boillee S, Vande VC, Cleveland DW. 2006. ALS: a disease of motor neurons and their nonneuronal neighbors. Neuron 52:39-59.

Bonde S, Ekdahl CT, Lindvall O. 2006. Long-term neuronal replacement in adult rat hippocampus after status epilepticus despite chronic inflammation. Eur J Neurosci 23:965-974.

Brink BP, Veerhuis R, Breij EC, van d, V, Dijkstra CD, Bo L. 2005. The pathology of multiple sclerosis is location-dependent: no significant complement activation is detected in purely cortical lesions. J Neuropathol Exp Neurol 64:147-155.

Brown CE, Vishwanath RP, Aguilar B, Starr R, Najbauer J, Aboody KS, Jensen MC. 2007. Tumor-derived chemokine MCP-1/CCL2 is sufficient for mediating tumor tropism of adoptively transferred T cells. J Immunol 179:3332-3341.

Bulloch K, Miller MM, Gal-Toth J, Milner TA, Gottfried-Blackmore A, Waters EM, Kaunzner UW, Liu K, Lindquist R, Nussenzweig MC, Steinman RM, McEwen BS. 2008. CD11c/EYFP transgene illuminates a discrete network of dendritic cells within the embryonic, neonatal, adult, and injured mouse brain. J Comp Neurol 508:687-710.

Butovsky O, Ziv Y, Schwartz A, Landa G, Talpalar AE, Pluchino S, Martino G, Schwartz M. 2006. Microglia activated by IL-4 or IFN-gamma differentially induce neurogenesis and oligodendrogenesis from adult stem/progenitor cells. Mol Cell Neurosci 31:149-160.

Butovsky O, Landa G, Kunis G, Ziv Y, Avidan H, Greenberg N, Schwartz A, Smirnov I, Pollack A, Jung S, Schwartz M. 2006. Induction and blockage of oligodendrogenesis by differently activated microglia in an animal model of multiple sclerosis. J Clin Invest 116:905-915.

Butovsky O, Bukshpan S, Kunis G, Jung S, Schwartz M. 2007. Microglia can be induced by IFN-gamma or IL-4 to express neural or dendritic-like markers. Mol Cell Neurosci 35:490-500.

Cacci E, Claasen JH, Kokaia Z. 2005. Microglia-derived tumor necrosis factor-alpha exaggerates death of newborn hippocampal progenitor cells *in vitro*. J Neurosci Res 80:789-797.

Cacci E, jmone-Cat MA, Anelli T, Biagioni S, Minghetti L. 2008. *In vitro* neuronal and glial differentiation from embryonic or adult neural precursor cells are differently affected by chronic or acute activation of microglia. Glia 56:412-425.

Cardona AE, Pioro EP, Sasse ME, Kostenko V, Cardona SM, Dijkstra IM, Huang D, Kidd G, Dombrowski S, Dutta R, Lee JC, Cook DN, Jung S, Lira SA, Littman DR, Ransohoff RM. 2006. Control of microglial neurotoxicity by the fractalkine receptor. Nat Neurosci 9:917-924.

Carson MJ, Bilousova TV, Puntambekar SS, Melchior B, Doose JM, Ethell IM. 2007. A rose by any other name? The potential consequences of microglial heterogeneity during CNS health and disease. Neurotherapeutics 4:571-579.

Chang A, Smith MC, Yin X, Fox RJ, Staugaitis SM, Trapp BD. 2008. Neurogenesis in the chronic lesions of multiple sclerosis. Brain 131:2366-2375.

Choi SH, Veeraraghavalu K, Lazarov O, Marler S, Ransohoff RM, Ramirez JM, Sisodia SS. 2008. Non-cell-autonomous effects of presenilin 1 variants on enrichment-mediated hippocampal progenitor cell proliferation and differentiation. Neuron 59:568-580.

Colton CA. 2009. Heterogeneity of microglial activation in the innate immune response in the brain. J Neuroimmune Pharmacol 4:399-418.

Conde JR, Streit WJ. 2006. Microglia in the aging brain. J Neuropathol Exp Neurol 65:199-203.

Constam DB, Philipp J, Malipiero UV, ten Dijke P, Schachner M, Fontana A. 1992. Differential expression of transforming growth factor-beta 1, -beta 2, and -beta 3 by glioblastoma cells, astrocytes, and microglia. J Immunol 148:1404-1410.

Das S, Basu A. 2008. Inflammation: a new candidate in modulating adult neurogenesis. J Neurosci Res 86:1199-1208.

De Haas AH, Boddeke HW, Brouwer N, Biber K. 2007. Optimized isolation enables *ex vivo* analysis of microglia from various central nervous system regions. Glia 55:1374-1384.

De Haas AH, Boddeke HW, Biber K. 2008. Region-specific expression of immunoregulatory proteins on microglia in the healthy CNS. Glia 56:888-894.

Deckert M, Sedgwick JD, Fischer E, Schluter D. 2006. Regulation of microglial cell responses in murine Toxoplasma encephalitis by CD200/CD200 receptor interaction. Acta Neuropathol 111:548-558.

del Rio-Hortega P. 1932. Microglia. In: Penfield W, editor. Cytology and Cellular Pathology of the Nervous System. New York: Paul B. Hoeber. p 482-534.

Desbaillets I, Tada M, de Tribolet N, Diserens AC, Hamou MF, Van Meir EG. 1994. Human astrocytomas and glioblastomas express monocyte chemoattractant protein-1 (MCP-1) *in vivo* and *in vitro*. Int J Cancer 58:240-247.

DiPatre PL, Gelman BB. 1997. Microglial cell activation in aging and Alzheimer disease: partial linkage with neurofibrillary tangle burden in the hippocampus. J Neuropathol Exp Neurol 56:143-149.

Du Y, Fischer TZ, Lee LN, Lercher LD, Dreyfus CF. 2003. Regionally specific effects of BDNF on oligodendrocytes. Dev Neurosci 25:116-126.

Ehninger D, Kempermann G. 2003. Regional effects of wheel running and environmental enrichment on cell genesis and microglia proliferation in the adult murine neocortex. Cereb Cortex 13:845-851.

Ekdahl CT, Claasen JH, Bonde S, Kokaia Z, Lindvall O. 2003. Inflammation is detrimental for neurogenesis in adult brain. Proc Natl Acad Sci U S A 100:13632-13637.

Ekdahl CT, Kokaia Z, Lindvall O. 2009. Brain inflammation and adult neurogenesis: the dual role of microglia. Neuroscience 158:1021-1029.

El Khoury J, Hickman SE, Thomas CA, Loike JD, Silverstein SC. 1998. Microglia, scavenger receptors, and the pathogenesis of Alzheimer's disease. Neurobiol Aging 19:S81-S84.

Farber K, Pannasch U, Kettenmann H. 2005. Dopamine and noradrenaline control distinct functions in rodent microglial cells. Mol Cell Neurosci 29:128-138.

Felger JC, Abe T, Kaunzner UW, Gottfried-Blackmore A, Gal-Toth J, McEwen BS, Iadecola C, Bulloch K. 2010. Brain dendritic cells in ischemic stroke: time course, activation state, and origin. Brain Behav Immun 24:724-737.

Fischer HG, Bonifas U, Reichmann G. 2000. Phenotype and functions of brain dendritic cells emerging during chronic infection of mice with Toxoplasma gondii. J Immunol 164:4826-4834.

Fischer HG, Reichmann G. 2001. Brain dendritic cells and macrophages/microglia in central nervous system inflammation. J Immunol 166:2717-2726.

Flanary BE, Streit WJ. 2003. Telomeres shorten with age in rat cerebellum and cortex *in vivo*. J Anti Aging Med 6:299-308.

Galasso JM, Stegman LD, Blaivas M, Harrison JK, Ross BD, Silverstein FS. 2000. Experimental gliosarcoma induces chemokine receptor expression in rat brain. Exp Neurol 161:85-95.

Gehrmann J, Banati RB, Kreutzberg GW. 1993. Microglia in the immune surveillance of the brain: human microglia constitutively express HLA-DR molecules. J Neuroimmunol 48:189-198.

Giometto B, Bozza F, Faresin F, Alessio L, Mingrino S, Tavolato B. 1996. Immune infiltrates and cytokines in gliomas. Acta Neurochir (Wien) 138:50-56.

Godbout JP, Chen J, Abraham J, Richwine AF, Berg BM, Kelley KW, Johnson RW. 2005. Exaggerated neuroinflammation and sickness behavior in aged mice following activation of the peripheral innate immune system. FASEB J 19:1329-1331.

Goings GE, Kozlowski DA, Szele FG. 2006. Differential activation of microglia in neurogenic versus non-neurogenic regions of the forebrain. Glia 54:329-342.

Goncalves MB, Williams EJ, Yip P, Yanez-Munoz RJ, Williams G, Doherty P. 2010. The COX-2 inhibitors, meloxicam and nimesulide, suppress neurogenesis in the adult mouse brain. Br J Pharmacol.

Gordon S. 2008. Elie Metchnikoff: father of natural immunity. Eur J Immunol 38:3257-3264.

Goswami S, Gupta A, Sharma SK. 1998. Interleukin-6-mediated autocrine growth promotion in human glioblastoma multiforme cell line U87MG. J Neurochem 71:1837-1845.

Gottfried-Blackmore A, Kaunzner UW, Idoyaga J, Felger JC, McEwen BS, Bulloch K. 2009. Acute *in vivo* exposure to interferon-gamma enables resident brain dendritic cells to become effective antigen presenting cells. Proc Natl Acad Sci U S A 106:20918-20923.

Gould E. 2007. How widespread is adult neurogenesis in mammals? Nat Rev Neurosci 8:481-488.

Gowing G, Philips T, Van WB, Audet JN, Dewil M, Van Den BL, Billiau AD, Robberecht W, Julien JP. 2008. Ablation of proliferating microglia does not affect motor neuron degeneration in amyotrophic lateral sclerosis caused by mutant superoxide dismutase. J Neurosci 28:10234-10244.

Graeber MB, Bise K, Mehraein P. 1994. CR3/43, a marker for activated human microglia: application to diagnostic neuropathology. Neuropathol Appl Neurobiol 20:406-408.

Graeber MB, Scheithauer BW, Kreutzberg GW. 2002. Microglia in brain tumors. Glia 40:252-259.

Grathwohl SA, Kalin RE, Bolmont T, Prokop S, Winkelmann G, Kaeser SA, Odenthal J, Radde R, Eldh T, Gandy S, Aguzzi A, Staufenbiel M, Mathews PM, Wolburg H, Heppner FL, Jucker M. 2009. Formation and maintenance of Alzheimer's disease beta-amyloid plaques in the absence of microglia. Nat Neurosci 12:1361-1363.

Gross CG. 2000. Neurogenesis in the adult brain: death of a dogma. Nat Rev Neurosci 1:67-73.

Guo L, Sawkar A, Zasadzki M, Watterson DM, Van Eldik LJ. 2001. Similar activation of glial cultures from different rat brain regions by neuroinflammatory stimuli and downregulation of the activation by a new class of small molecule ligands. Neurobiol Aging 22:975-981.

Halfter H, Lotfi R, Westermann R, Young P, Ringelstein EB, Stogbauer FT. 1998. Inhibition of growth and induction of differentiation of glioma cell lines by oncostatin M (OSM). Growth Factors 15:135-147.

Halfter H, Kremerskothen J, Weber J, Hacker-Klom U, Barnekow A, Ringelstein EB, Stogbauer F. 1998. Growth inhibition of newly established human glioma cell lines by leukemia inhibitory factor. J Neurooncol 39:1-18.

Hanisch UK, Kettenmann H. 2007. Microglia: active sensor and versatile effector cells in the normal and pathologic brain. Nat Neurosci 10:1387-1394.

Hao C, Parney IF, Roa WH, Turner J, Petruk KC, Ramsay DA. 2002. Cytokine and cytokine receptor mRNA expression in human glioblastomas: evidence of Th1, Th2 and Th3 cytokine dysregulation. Acta Neuropathol 103:171-178.

Holmberg KH, Patterson PH. 2006. Leukemia inhibitory factor is a key regulator of astrocytic, microglial and neuronal responses in a low-dose pilocarpine injury model. Brain Res 1075:26-35.

Huettner C, Czub S, Kerkau S, Roggendorf W, Tonn JC. 1997. Interleukin 10 is expressed in human gliomas *in vivo* and increases glioma cell proliferation and motility *in vitro*. Anticancer Res 17:3217-3224.

Hurley SD, O'Banion MK, Song DD, Arana FS, Olschowka JA, Haber SN. 2003. Microglial response is poorly correlated with neurodegeneration following chronic, low-dose MPTP administration in monkeys. Exp Neurol 184:659-668.

Hussain SF, Yang D, Suki D, Aldape K, Grimm E, Heimberger AB. 2006. The role of human glioma-infiltrating microglia/macrophages in mediating antitumor immune responses. Neuro Oncol 8:261-279.

Jakubs K, Bonde S, Iosif RE, Ekdahl CT, Kokaia Z, Kokaia M, Lindvall O. 2008. Inflammation regulates functional integration of neurons born in adult brain. J Neurosci 28:12477-12488.

Ji KA, Eu MY, Kang SH, Gwag BJ, Jou I, Joe EH. 2008. Differential neutrophil infiltration contributes to regional differences in brain inflammation in the substantia nigra pars compacta and cortex. Glia 56:1039-1047.

Jiang-Shieh YF, Wu CH, Chang ML, Shieh JY, Wen CY. 2003. Regional heterogeneity in immunoreactive macrophages/microglia in the rat pineal gland. J Pineal Res 35:45-53.

Jordan JT, Sun W, Hussain SF, DeAngulo G, Prabhu SS, Heimberger AB. 2008. Preferential migration of regulatory T cells mediated by glioma-secreted chemokines can be blocked with chemotherapy. Cancer Immunol Immunother 57:123-131.

Kempermann G, Jessberger S, Steiner B, Kronenberg G. 2004. Milestones of neuronal development in the adult hippocampus. Trends Neurosci 27:447-452.

Kielian T, van Rooijen N, Hickey WF. 2002. MCP-1 expression in CNS-1 astrocytoma cells: implications for macrophage infiltration into tumors *in vivo*. J Neurooncol 56:1-12.

Kim BJ, Kim MJ, Park JM, Lee SH, Kim YJ, Ryu S, Kim YH, Yoon BW. 2009. Reduced neurogenesis after suppressed inflammation by minocycline in transient cerebral ischemia in rat. J Neurol Sci 279:70-75.

Kim WG, Mohney RP, Wilson B, Jeohn GH, Liu B, Hong JS. 2000. Regional difference in susceptibility to lipopolysaccharide-induced neurotoxicity in the rat brain: role of microglia. J Neurosci 20:6309-6316.

Krady JK, Lin HW, Liberto CM, Basu A, Kremlev SG, Levison SW. 2008. Ciliary neurotrophic factor and interleukin-6 differentially activate microglia. J Neurosci Res 86:1538-1547.

Kraft AD, McPherson CA, Harry GJ. 2009. Heterogeneity of microglia and TNF signaling as determinants for neuronal death or survival. Neurotoxicology 30:785-793.

Kreutzberg GW. 1996. Microglia: a sensor for pathological events in the CNS. Trends Neurosci 19:312-318.

Kullberg S, Aldskogius H, Ulfhake B. 2001. Microglial activation, emergence of ED1-expressing cells and clusterin upregulation in the aging rat CNS, with special reference to the spinal cord. Brain Res 899:169-186.

Ladeby R, Wirenfeldt M, Dalmau I, Gregersen R, Garcia-Ovejero D, Babcock A, Owens T, Finsen B. 2005. Proliferating resident microglia express the stem cell antigen CD34 in response to acute neural injury. Glia 50:121-131.

Lalancette-Hebert M, Gowing G, Simard A, Weng YC, Kriz J. 2007. Selective ablation of proliferating microglial cells exacerbates ischemic injury in the brain. J Neurosci 27:2596-2605.

Lawson LJ, Perry VH, Dri P, Gordon S. 1990. Heterogeneity in the distribution and morphology of microglia in the normal adult mouse brain. Neuroscience 39:151-170.

Lawson LJ, Perry VH, Gordon S. 1992. Turnover of resident microglia in the normal adult mouse brain. Neuroscience 48:405-415.

Ledeboer A, Breve JJ, Poole S, Tilders FJ, Van Dam AM. 2000. Interleukin-10, interleukin-4, and transforming growth factor-beta differentially regulate lipopolysaccharide-induced production of pro-inflammatory cytokines and nitric oxide in co-cultures of rat astroglial and microglial cells. Glia 30:134-142.

Letiembre M, Hao W, Liu Y, Walter S, Mihaljevic I, Rivest S, Hartmann T, Fassbender K. 2007. Innate immune receptor expression in normal brain aging. Neuroscience 146:248-254.

Leung SY, Wong MP, Chung LP, Chan AS, Yuen ST. 1997. Monocyte chemoattractant protein-1 expression and macrophage infiltration in gliomas. Acta Neuropathol 93:518-527.

Liao H, Huang W, Niu R, Sun L, Zhang L. 2008. Cross-talk between the epidermal growth factor-like repeats/fibronectin 6-8 repeats domains of Tenascin-R and microglia modulates neural stem/progenitor cell proliferation and differentiation. J Neurosci Res 86:27-34.

Liu YP, Lin HI, Tzeng SF. 2005. Tumor necrosis factor-alpha and interleukin-18 modulate neuronal cell fate in embryonic neural progenitor culture. Brain Res 1054:152-158.

Lopes KO, Sparks DL, Streit WJ. 2008. Microglial dystrophy in the aged and Alzheimer's disease brain is associated with ferritin immunoreactivity. Glia 56:1048-1060.

Mander TH, Morris JF. 1995. Immunophenotypic evidence for distinct populations of microglia in the rat hypothalamo-neurohypophysial system. Cell Tissue Res 280:665-673.

Mantovani A. 2008. From phagocyte diversity and activation to probiotics: back to Metchnikoff. Eur J Immunol 38:3269-3273.

Markovic DS, Glass R, Synowitz M, Rooijen N, Kettenmann H. 2005. Microglia stimulate the invasiveness of glioma cells by increasing the activity of metalloprotease-2. J Neuropathol Exp Neurol 64:754-762.

Markovic DS, Vinnakota K, Chirasani S, Synowitz M, Raguet H, Stock K, Sliwa M, Lehmann S, Kalin R, van Rooijen N, Holmbeck K, Heppner FL, Kiwit J, Matyash V, Lehnardt S, Kaminska B, Glass R, Kettenmann H. 2009. Gliomas induce and exploit microglial MT1-MMP expression for tumor expansion. Proc Natl Acad Sci U S A 106:12530-12535.

Marques CP, Hu S, Sheng W, Cheeran MC, Cox D, Lokensgard JR. 2004. Interleukin-10 attenuates production of HSV-induced inflammatory mediators by human microglia. Glia 47:358-366.

Marshall GP, Demir M, Steindler DA, Laywell ED. 2008. Subventricular zone microglia possess a unique capacity for massive *in vitro* expansion. Glia 56:1799-1808.

Martinez FO, Helming L, Gordon S. 2009. Alternative activation of macrophages: an immunologic functional perspective. Annu Rev Immunol 27:451-483.

Matyszak MK, Perry VH. 1996. The potential role of dendritic cells in immune-mediated inflammatory diseases in the central nervous system. Neuroscience 74:599-608.

Mausberg AK, Jander S, Reichmann G. 2009. Intracerebral granulocyte-macrophage colony-stimulating factor induces functionally competent dendritic cells in the mouse brain. Glia 57:1341-1350.

McGeer PL, Rogers J, McGeer EG. 2006. Inflammation, anti-inflammatory agents and Alzheimer disease: the last 12 years. J Alzheimers Dis 9:271-276.

Miller KR, Streit WJ. 2007. The effects of aging, injury and disease on microglial function: a case for cellular senescence. Neuron Glia Biol 3:245-253.

Milner R, Campbell IL. 2003. The extracellular matrix and cytokines regulate microglial integrin expression and activation. J Immunol 170:3850-3858.

Mittelbronn M, Dietz K, Schluesener HJ, Meyermann R. 2001. Local distribution of microglia in the normal adult human central nervous system differs by up to one order of magnitude. Acta Neuropathol 101:249-255.

Monje ML, Toda H, Palmer TD. 2003. Inflammatory blockade restores adult hippocampal neurogenesis. Science 302:1760-1765.

Mosser DM, Edwards JP. 2008. Exploring the full spectrum of macrophage activation. Nat Rev Immunol 8:958-969.

Muller N, Schwarz MJ. 2007. [Immunological aspects of depressive disorders]. Nervenarzt 78:1261-1273.

Murphy GM, Jr., Bitting L, Majewska A, Schmidt K, Song Y, Wood CR. 1995. Expression of interleukin-11 and its encoding mRNA by glioblastoma cells. Neurosci Lett 196:153-156.

Nakanishi M, Niidome T, Matsuda S, Akaike A, Kihara T, Sugimoto H. 2007. Microglia-derived interleukin-6 and leukaemia inhibitory factor promote astrocytic differentiation of neural stem/progenitor cells. Eur J Neurosci 25:649-658.

Neumann H, Takahashi K. 2007. Essential role of the microglial triggering receptor expressed on myeloid cells-2 (TREM2) for central nervous tissue immune homeostasis. J Neuroimmunol 184:92-99.

Nishie A, Ono M, Shono T, Fukushi J, Otsubo M, Onoue H, Ito Y, Inamura T, Ikezaki K, Fukui M, Iwaki T, Kuwano M. 1999. Macrophage infiltration and heme oxygenase-1 expression correlate with angiogenesis in human gliomas. Clin Cancer Res 5:1107-1113.

Nishie A, Masuda K, Otsubo M, Migita T, Tsuneyoshi M, Kohno K, Shuin T, Naito S, Ono M, Kuwano M. 2001. High expression of the Cap43 gene in infiltrating macrophages of human renal cell carcinomas. Clin Cancer Res 7:2145-2151.

Ogura K, Ogawa M, Yoshida M. 1994. Effects of aging on microglia in the normal rat brain: immunohistochemical observations. Neuroreport 5:1224-1226.

Olah M, Ping G, De Haas AH, Brouwer N, Meerlo P, Van Der Zee EA, Biber K, Boddeke HW. 2009. Enhanced hippocampal neurogenesis in the absence of microglia T cell interaction and microglia activation in the murine running wheel model. Glia 57:1046-1061.

Olofsson A, Miyazono K, Kanzaki T, Colosetti P, Engstrom U, Heldin CH. 1992. Transforming growth factor-beta 1, -beta 2, and -beta 3 secreted by a human glioblastoma cell line. Identification of small and different forms of large latent complexes. J Biol Chem 267:19482-19488.

Olsen ML, Campbell SL, Sontheimer H. 2007. Differential distribution of Kir4.1 in spinal cord astrocytes suggests regional differences in K+ homeostasis. J Neurophysiol 98:786-793.

Ong WY, Leong SK, Garey LJ, Tan KK, Zhang HF. 1995. A light and electron microscopic study of HLA-DR positive cells in the human cerebral cortex and subcortical white matter. J Hirnforsch 36:553-563.

Perry VH, Matyszak MK, Fearn S. 1993. Altered antigen expression of microglia in the aged rodent CNS. Glia 7:60-67.

Peters A, Josephson K, Vincent SL. 1991. Effects of aging on the neuroglial cells and pericytes within area 17 of the rhesus monkey cerebral cortex. Anat Rec 229:384-398.

Peters A, Sethares C. 2002. The effects of age on the cells in layer 1 of primate cerebral cortex. Cereb Cortex 12:27-36.

Phillips LM, Simon PJ, Lampson LA. 1999. Site-specific immune regulation in the brain: differential modulation of major histocompatibility complex (MHC) proteins in brainstem vs. hippocampus. J Comp Neurol 405:322-333.

Platten M, Kretz A, Naumann U, Aulwurm S, Egashira K, Isenmann S, Weller M. 2003. Monocyte chemoattractant protein-1 increases microglial infiltration and aggressiveness of gliomas. Ann Neurol 54:388-392.

Platten M, Kretz A, Naumann U, Aulwurm S, Egashira K, Isenmann S, Weller M. 2003. Monocyte chemoattractant protein-1 increases microglial infiltration and aggressiveness of gliomas. Ann Neurol 54:388-392.

Pocock JM, Kettenmann H. 2007. Neurotransmitter receptors on microglia. Trends Neurosci 30:527-535.

Ponomarev ED, Maresz K, Tan Y, Dittel BN. 2007. CNS-derived interleukin-4 is essential for the regulation of autoimmune inflammation and induces a state of alternative activation in microglial cells. J Neurosci 27:10714-10721.

Qian L, Wei SJ, Zhang D, Hu X, Xu Z, Wilson B, El Benna J, Hong JS, Flood PM. 2008. Potent anti-inflammatory and neuroprotective effects of TGF-beta1 are mediated through the inhibition of ERK and p47phox-Ser345 phosphorylation and translocation in microglia. J Immunol 181:660-668.

Rahpeymai Y, Hietala MA, Wilhelmsson U, Fotheringham A, Davies I, Nilsson AK, Zwirner J, Wetsel RA, Gerard C, Pekny M, Pekna M. 2006. Complement: a novel factor in basal and ischemia-induced neurogenesis. EMBO J 25:1364-1374.

Ralay RH, Craft JM, Hu W, Guo L, Wing LK, Van Eldik LJ, Watterson DM. 2006. Glia as a therapeutic target: selective suppression of human amyloid-beta-induced upregulation of brain proinflammatory cytokine production attenuates neurodegeneration. J Neurosci 26:662-670.

Ransohoff RM, Perry VH. 2009. Microglial physiology: unique stimuli, specialized responses. Annu Rev Immunol 27:119-145.
Rao JS. 2003. Molecular mechanisms of glioma invasiveness: the role of proteases. Nat Rev Cancer 3:489-501.

Reichmann G, Schroeter M, Jander S, Fischer HG. 2002. Dendritic cells and dendritic-like microglia in focal cortical ischemia of the mouse brain. J Neuroimmunol 129:125-132.

Remington LT, Babcock AA, Zehntner SP, Owens T. 2007. Microglial recruitment, activation, and proliferation in response to primary demyelination. Am J Pathol 170:1713-1724.

Ren L, Lubrich B, Biber K, Gebicke-Haerter PJ. 1999. Differential expression of inflammatory mediators in rat microglia cultured from different brain regions. Brain Res Mol Brain Res 65:198-205.

Repovic P, Fears CY, Gladson CL, Benveniste EN. 2003. Oncostatin-M induction of vascular endothelial growth factor expression in astroglioma cells. Oncogene 22:8117-8124.

Ribes S, Ebert S, Regen T, Czesnik D, Scheffel J, Zeug A, Bunkowski S, Eiffert H, Hanisch UK, Hammerschmidt S, Nau R. 2010. Fibronectin stimulates Escherichia coli phagocytosis by microglial cells. Glia 58:367-376.

Santambrogio L, Belyanskaya SL, Fischer FR, Cipriani B, Brosnan CF, Ricciardi-Castagnoli P, Stern LJ, Strominger JL, Riese R. 2001. Developmental plasticity of CNS microglia. Proc Natl Acad Sci U S A 98:6295-6300.

Sasaki A, Nakazato Y. 1992. The identity of cells expressing MHC class II antigens in normal and pathological human brain. Neuropathol Appl Neurobiol 18:13-26.

Savchenko VL, McKanna JA, Nikonenko IR, Skibo GG. 2000. Microglia and astrocytes in the adult rat brain: comparative immunocytochemical analysis demonstrates the efficacy of lipocortin 1 immunoreactivity. Neuroscience 96:195-203.

Schluter D, Bertsch D, Frei K, Hubers SB, Wiestler OD, Hof H, Fontana A, Deckert-Schluter M. 1998. Interferon-gamma antagonizes transforming growth factor-beta2-mediated immunosuppression in murine Toxoplasma encephalitis. J Neuroimmunol 81:38-48.

Sedgwick JD, Ford AL, Foulcher E, Airriess R. 1998. Central nervous system microglial cell activation and proliferation follows direct interaction with tissue-infiltrating T cell blasts. J Immunol 160:5320-5330.

Sheffield LG, Berman NE. 1998. Microglial expression of MHC class II increases in normal aging of nonhuman primates. Neurobiol Aging 19:47-55.

Sheng JG, Mrak RE, Griffin WS. 1998. Enlarged and phagocytic, but not primed, interleukin-1 alpha-immunoreactive microglia increase with age in normal human brain. Acta Neuropathol 95:229-234.

Si Q, Nakamura Y, Kataoka K. 2000. A serum factor enhances production of nitric oxide and tumor necrosis factor-alpha from cultured microglia. Exp Neurol 162:89-97.

Sierra A, Gottfried-Blackmore AC, McEwen BS, Bulloch K. 2007. Microglia derived from aging mice exhibit an altered inflammatory profile. Glia 55:412-424.

Simard AR, Rivest S. 2004. Role of inflammation in the neurobiology of stem cells. Neuroreport 15:2305-2310.

Sloane JA, Hollander W, Moss MB, Rosene DL, Abraham CR. 1999. Increased microglial activation and protein nitration in white matter of the aging monkey. Neurobiol Aging 20:395-405.

Soltys Z, Orzylowska-Sliwinska O, Zaremba M, Orlowski D, Piechota M, Fiedorowicz A, Janeczko K, Oderfeld-Nowak B. 2005. Quantitative morphological study of microglial cells in the ischemic rat brain using principal component analysis. J Neurosci Methods 146:50-60.

Spulber S, Oprica M, Bartfai T, Winblad B, Schultzberg M. 2008. Blunted neurogenesis and gliosis due to transgenic overexpression of human soluble IL-1ra in the mouse. Eur J Neurosci 27:549-558.

Steinman RM, Banchereau J. 2007. Taking dendritic cells into medicine. Nature 449:419-426.

Stenzel W, Muller U, Kohler G, Heppner FL, Blessing M, McKenzie AN, Brombacher F, Alber G. 2009. IL-4/IL-13-dependent alternative activation of macrophages but not microglial cells is associated with uncontrolled cerebral cryptococcosis. Am J Pathol 174:486-496.

Streit WJ, Graeber MB. 1993. Heterogeneity of microglial and perivascular cell populations: insights gained from the facial nucleus paradigm. Glia 7:68-74.

Streit WJ. 2002. Microglia as neuroprotective, immunocompetent cells of the CNS. Glia 40:133-139.

Streit WJ, Sammons NW, Kuhns AJ, Sparks DL. 2004. Dystrophic microglia in the aging human brain. Glia 45:208-212.

Streit WJ. 2006. Microglial senescence: does the brain's immune system have an expiration date? Trends Neurosci 29:506-510.

Streit WJ, Miller KR, Lopes KO, Njie E. 2008. Microglial degeneration in the aging brain--bad news for neurons? Front Biosci 13:3423-3438.

Styren SD, Civin WH, Rogers J. 1990. Molecular, cellular, and pathologic characterization of HLA-DR immunoreactivity in normal elderly and Alzheimer's disease brain. Exp Neurol 110:93-104.

Suh H, Deng W, Gage FH. 2009. Signaling in adult neurogenesis. Annu Rev Cell Dev Biol 25:253-275.

Takeshima H, Kuratsu J, Takeya M, Yoshimura T, Ushio Y. 1994. Expression and localization of messenger RNA and protein for monocyte chemoattractant protein-1 in human malignant glioma. J Neurosurg 80:1056-1062.

Thored P, Heldmann U, Gomes-Leal W, Gisler R, Darsalia V, Taneera J, Nygren JM, Jacobsen SE, Ekdahl CT, Kokaia Z, Lindvall O. 2009. Long-term accumulation of microglia with proneurogenic phenotype concomitant with persistent neurogenesis in adult subventricular zone after stroke. Glia 57:835-849.

Tran CT, Wolz P, Egensperger R, Kosel S, Imai Y, Bise K, Kohsaka S, Mehraein P, Graeber MB. 1998. Differential expression of MHC class II molecules by microglia and neoplastic astroglia: relevance for the escape of astrocytoma cells from immune surveillance. Neuropathol Appl Neurobiol 24:293-301.

Turrin NP, Rivest S. 2006. Molecular and cellular immune mediators of neuroprotection. Mol Neurobiol 34:221-242.

Van Meir E, Sawamura Y, Diserens AC, Hamou MF, de Tribolet N. 1990. Human glioblastoma cells release interleukin 6 *in vivo* and *in vitro*. Cancer Res 50:6683-6688.

van Rossum D, Hanisch UK. 2004. Microglia. Metab Brain Dis 19:393-411.

Vaughan DW, Peters A. 1974. Neuroglial cells in the cerebral cortex of rats from young adulthood to old age: an electron microscope study. J Neurocytol 3:405-429.

Vincent AJ, Lau PW, Roskams AJ. 2008. SPARC is expressed by macroglia and microglia in the developing and mature nervous system. Dev Dyn 237:1449-1462.

Wachs FP, Winner B, Couillard-Despres S, Schiller T, Aigner R, Winkler J, Bogdahn U, Aigner L. 2006. Transforming growth factor-beta1 is a negative modulator of adult neurogenesis. J Neuropathol Exp Neurol 65:358-370.

Wakita H, Tomimoto H, Akiguchi I, Kimura J. 1994. Glial activation and white matter changes in the rat brain induced by chronic cerebral hypoperfusion: an immunohistochemical study. Acta Neuropathol 87:484-492.

Wakita H, Tomimoto H, Akiguchi I, Kimura J. 1995. Protective effect of cyclosporin A on white matter changes in the rat brain after chronic cerebral hypoperfusion. Stroke 26:1415-1422.

Wakita H, Tomimoto H, Akiguchi I, Kimura J. 1998. Dose-dependent, protective effect of FK506 against white matter changes in the rat brain after chronic cerebral ischemia. Brain Res 792:105-113.

Walton NM, Sutter BM, Laywell ED, Levkoff LH, Kearns SM, Marshall GP, Scheffler B, Steindler DA. 2006. Microglia instruct subventricular zone neurogenesis. Glia 54:815-825.

Watters JJ, Schartner JM, Badie B. 2005. Microglia function in brain tumors. J Neurosci Res 81:447-455.

Wei R, Jonakait GM. 1999. Neurotrophins and the anti-inflammatory agents interleukin-4 (IL-4), IL-10, IL-11 and transforming growth factor-beta1 (TGF-beta1) down-regulate T cell costimulatory molecules B7 and CD40 on cultured rat microglia. J Neuroimmunol 95:8-18.

Whitney NP, Eidem TM, Peng H, Huang Y, Zheng JC. 2009. Inflammation mediates varying effects in neurogenesis: relevance to the pathogenesis of brain injury and neurodegenerative disorders. J Neurochem 108:1343-1359.

Wu CH, Chien HF, Chang CY, Ling EA. 1997. Heterogeneity of antigen expression and lectin labeling on microglial cells in the olfactory bulb of adult rats. Neurosci Res 28:67-75.

Xie Z, Morgan TE, Rozovsky I, Finch CE. 2003. Aging and glial responses to lipopolysaccharide *in vitro*: greater induction of IL-1 and IL-6, but smaller induction of neurotoxicity. Exp Neurol 182:135-141.

Ye SM, Johnson RW. 1999. Increased interleukin-6 expression by microglia from brain of aged mice. J Neuroimmunol 93:139-148.

Zhao TZ, Xia YZ, Li L, Li J, Zhu G, Chen S, Feng H, Lin JK. 2009. Bovine serum albumin promotes IL-1beta and TNF-alpha secretion by N9 microglial cells. Neurol Sci 30:379-383.

Zhu P, Hata R, Cao F, Gu F, Hanakawa Y, Hashimoto K, Sakanaka M. 2008. Ramified microglial cells promote astrogliogenesis and maintenance of neural stem cells through activation of Stat3 function. FASEB J 22:3866-3877.

Ziv Y, Ron N, Butovsky O, Landa G, Sudai E, Greenberg N, Cohen H, Kipnis J, Schwartz M. 2006. Immune cells contribute to the maintenance of neurogenesis and spatial learning abilities in adulthood. Nat Neurosci 9:268-275.

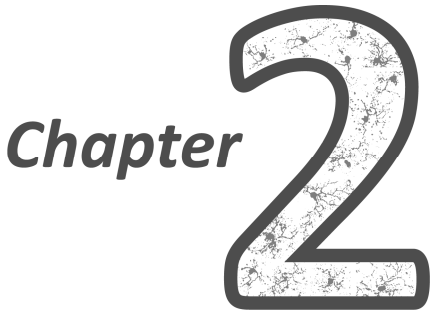

Enhanced hippocampal neurogenesis in the absence of microglia T cell interaction and microglia activation in the murine running wheel model

Marta Olah[1], Gao Ping[1], Alexander H. De Haas[1], Nieske Brouwer[1], Peter Meerlo[2], Eddy A. Van der Zee[2], Knut P.H. Biber[1] and Hendrikus W.G.M. Boddeke[1]

[1]Department of Medical Physiology, University Medical Center Groningen, University of Groningen, Groningen, The Netherlands
[2]Department of Molecular Neurobiology, University of Groningen, Haren, The Netherlands

Published in Glia 2009;57(10):1046-61

ABSTRACT

Recently, activated microglia have been shown to be involved in the regulation of several aspects of neurogenesis under experimental conditions both *in vitro* and *in vivo*. A neurogenesis supportive microglia phenotype has been suggested to arise from the interaction of microglia with homing encephalitogenic T cells. However, a unified hypothesis regarding the exact nature of microglia activity that is supportive of neurogenesis is yet missing. Our aim was to investigate the connection between microglia activity and adult hippocampal neurogenesis under physiological conditions. To address this question we compared the level of microglia activation in the hippocampus of mice that had access to a running wheel for ten days and that of sedentary controls. Suprisingly, despite elevated levels of proliferation of neural precursors and survival of newborn neurons in the dentate gyrus microglia remained in a 'resting' state morphologically, antigenically and at the transcriptional level. Moreover, neither T cells nor MHCII expressing microglia were present in the hippocampal brain parenchyma. Though microglia in the dentate gyrus of the runners proliferated at a higher level than in the sedentary controls, this difference was also present in non-neurogenic sites. Therefore, our findings suggest that classical signs of microglia activation and microglia activation arising from interaction with T cells in particular are not a prerequisite for the activity-induced increase in adult hippocampal neurogenesis in C57Bl/6 mice. Thus, our results draw attention on the species and model differences that might exist regarding the regulation of adult hippocampal neurogenesis.

INTRODUCTION

The presence of neural stem or progenitor cells in the adult central nervous system (CNS) and adult neurogenesis has obtained considerable attention not only because its discovery refuted a century old dogma, but also because its existence implies therapeutic possibilities (Colucci-D'Amato & di Porzio, 2008; Jagasia et al., 2006). Neural stem cells are considered to be of multipotent nature, hence there is a possibility that they might serve as an autologous source for cell replacement therapies in case of stroke, neurodegenerative disorders and injury to the CNS (Okano et al., 2007). Accordingly, understanding the exact mechanisms that underlie the regulation of multiple aspects of adult neurogenesis (activation and proliferation of the neural stem cells, survival, differentiation and integration of the newborn neurons in the existing circuitry), has been a major aim in the research of the past few years. In the mammalian central nervous system there are two brain regions that display constitutive neurogenesis in the adulthood: the subventricular zone, which lines the lateral ventricles and the subgranular zone of the dentate gyrus (Taupin, 2006; Zhao et al., 2008). Neurogenesis taking place in the hippocampal dentate gyrus is the most widely used *in vivo* model of neurogenesis-studies, since its level can be experimentally manipulated. Several environmental, cellular and molecular factors have been identified as the modulators of adult hippocampal neurogenesis (Ming & Song, 2005).

Recently, it has been suggested that microglia are involved in the regulation of the migration, proliferation and differentiation of neural stem/progenitor cells *in vitro* (Aarum et al., 2003; Butovsky et al., 2006; Morgan et al., 2004; Nakanishi et al., 2007; Walton et al., 2006). Microglia have also been suggested to play a role in the regulation of adult hippocampal neurogenesis under pathological conditions (Battista et al., 2006; Ekdahl et al., 2003; Monje et al., 2003). Depending on the type of activation (acute or chronic), activated microglia have been

reported to be either detrimental or supportive regarding neurogenesis from neural precursors *in vitro* (Cacci et al., 2008) or *in vivo* after status epilepticus, stroke and ischemia (Bonde et al., 2006; reviewed in Das and Basu, 2008; Ekdahl et al., 2008). Adding to the complexity of the picture, it has also been reported that non-neurogenic regions display higher levels of injury-induced microglia activation than the neurogenic dentate gyrus (Goings et al., 2006).

In addition, another cell type of the immune system, the neuro-antigenic specific T cell, has recently been suggested to support the maintenance of the adult hippocampal neurogenesis under physiological conditions (Ziv et al., 2006). Homing encephalitogenic T cells have been suggested to exert their beneficial effect on hippocampal neurogenesis partially through interaction with resident hippocampal microglial cells (Ziv et al., 2006; Ziv and Schwartz, 2008). Upon this interaction microglia would adopt a neurosupportive activated phenotype, which would manifest in surface expression of MHCII and secretion of cytokines, such as IGF-1 (Butovsky et al., 2006; Ziv et al., 2006).

The research done in this field has outlined that acutely activated microglia have detrimental, chronically activated microglia have permissive (Bonde et al., 2006; Cacci et al., 2008) and differentially activated microglia (Butovsky et al., 2006; Ziv et al., 2006) have supportive effect on neurogenesis. The question, whether microglia activation is indispensable for neurogenesis in the adult, however remains open. Our objective was thus, to investigate to what extent microglia activation and neurogenesis are interdependent phenomena under physiological conditions. For this purpose we have chosen a mouse model of voluntary physical exercise, the running wheel model, which is known to robustly elevate the level of both proliferation of the progenitors and differentiation/survival of the newborn neurons in the dentate gyrus of the hippocampus (van der Borght et al., 2006; van Praag, 2008). Though under certain conditions physical exercise can be

stressful (Stranahan et al., 2008), evidence exists, that the short-term model applied in our experiments does not lead to HPA axis activation (Koehl et al., 2008) and can be actually anxiolytic (Salam et al., 2008). Therefore, this physiological and acute (van der Borght et al., 2006) model of increased hippocampal neurogenesis enabled us to gain insight in the possible involvement of microglia in the regulation of both aspects of adult hippocampal neurogenesis (proliferation and survival/differentiation) without the occurrence of factors, which accompany increased neurogenesis in other models (e.g. extensive cell death, angiogenesis), and can influence the activation state of resident microglial cells.

Our experimental setup included two groups of animals – one group had access to a running wheel for ten days, the other group consisted of the sedentary control animals. We here investigated the relationship between several aspects of microglia activation and neurogenesis by the means of immunohistochemistry, flow cytometry and real time quantitative PCR (RT-qPCR) analysis.

MATERIALS AND METHODS

Housing, animal care and voluntary physical exercise

The experiments have been approved by the Animal Welfare Committee (DEC) of the University of Groningen, The Netherlands.

The experiments were conducted in young adult (8 week old) male C57Bl/6 mice, purchased from Harlan, The Netherlands. Following a week of acclimatisation, all animals were individually housed and randomly assigned to one of the two experimental groups. The 'runners' had access to a running wheel for ten days. The control group consisted of sedentary animals. Every running wheel was equipped with an electronic counter connected to a PC to record physical activity. The animal's welfare, the running wheels and the level of physical activity on the previous night were checked daily.

The animals were kept in a 12:12 hour light - dark regime, with lights on at 8 a.m. The animals received standard chow and tap water ad libitum.

Six independent experiments were performed: an initial experiment (sedentary control group) N = 8, (runners) N = 8), three follow up experiments ((sedentary control group) N = 4, (runners) N = 8 in each experiment), which included the flow cytometric analysis of the rapidly isolated microglia from the hippocampus, and two additional experiments ((sedentary control group) N = 5, (runners) N = 5 in both experiments), in which microglial gene expression was investigated with qPCR. A total number of 72 animals were used in the experiments.

BrdU labeling and sacrifice

During the last night of the experiment, at the middle of the active phase, all animals received an intraperitoneal injection of (+)-5-Bromo-2'-deoxyuridine (BrdU; Sigma Aldrich) dissolved in physiological saline solution. Since our aim was to label all the proliferating precursors we used a single BrdU pulse at a saturating dose (300mg/kg), as suggested by Mandyam and colleagues (Mandyam et al., 2007). As reviewed in

Taupin (2007), a single dose of 300 mg/kg has no physiological side effects or apparent toxic effect on the dividing cells in the dentate gyrus in the used administration scheme (single intraperitoneal injection). On the morning of the next day, between 9 and 10 a.m. the animals were deeply anesthetised with pentobarbital and transcardially perfused either with 50 ml PBS followed by 150 ml of 4% paraformaldehyde (PFA; Sigma Aldrich) in the case of the initial experiment, or with 50 ml of physiological saline solution alone, in the case of the follow up experiments. After perfusion the brains were removed from the skull. In the first experiment all brains were put in 4% PFA for post-fixation overnight at 4°C. For the follow up experiments, the right brain half was processed for flow cytometric analysis of rapidly isolated microglia from the hippocampus, the left brain half was immersion fixed in 4% PFA for five days at 4°C.

Tissue processing

After fixation or post-fixation, brains were equilibrated in 30% sucrose at 4°C until they sank. One-in-eight series of 30 micrometer thick coronal sections through the entire rostrocaudal extent of the hippocampus were cut on a Leica CM3050s cryostat. Each series contained approximately 12 sections. The sections were collected in PBS and immediately submitted to immunohistochemistry or stored in a cryoprotective solution (containing 25% glycerol (VWR International) and 25% ethylene glycol (Merck) in PBS) on -20°C until further processing.

Immunohistochemistry

For all immunohistochemical stainings one-in-eight series (twelve sections) of hippocampal brain slices from at least two of the four independent experiments were stained in a free-floating staining protocol. Thus, a total number of at least 288 hippocampal brain sections were stained and analysed for the particular

immunohistochemical stainings. To determine the total numbers of BrdU, doublecortin, Iba1 and Iba1/BrdU positive cells for the whole hippocampus per animal, after counting the above mentioned parameters in twelve sections from each animal the obtained values were multiplied by either the section periodicity (8) alone (in the case of the initial experiment), or by the section periodicity and by 2 (in the case of the follow up experiments, where only one brain halve was used for immunohistochemistry).

During the immunohistochemical procedure all washing steps were performed with phosphate buffered saline (PBS). For blocking and incubation steps involving antibodies 0,3% Triton X-100 (Merck) in PBS was used, except for the staining against major histocompatibility complex class II (MHCII) and CD3, where we used 0,1% Triton X-100 in PBS. Blocking of unspecific binding sites was achieved by incubating the slices at room temperature for 45 minutes in either 0,3% or 0,1% Triton X-100 in PBS containing 5% fetal calf serum (FCS; Gibco) and 2% bovine serum albumin (BSA; Gibco). The primary antibodies were diluted in either 0,3% or 0,1% TritonX in PBS containing 1% FCS and 1% BSA. Incubation in primary antibody solution lasted 72 hours at 4°C. Incubation in secondary antibody solution lasted 90 minutes at room temperature.

For detection of proliferation in the hippocampus immunohistochemistry against the incorporated BrdU was performed on the hippocampal slices. Briefly, DNA denaturation was achieved by treatment with 2N HCl for 20 minutes at 37°C, followed by neutralisation with 0,1M boric acid for 10 minutes. Endogenous peroxidase activity was blocked with 0,3% H_2O_2. Following the blocking step sections were incubated in mouse anti-BrdU monoclonal antibody (1:500; Sigma). On the fourth day sections were incubated with horse anti-mouse biotinylated secondary antibody (1:500; Vector Laboratories). Sections were then immersed in ABC solution (Vectastain Elite Kit; Vector Laboratories) and allowed for the avidin-biotin-horse-

radish peroxidase complex to develop for 2 hours on room temperature. The staining was finally visualised with 3,3'-diaminobenzidine-tetrahydrochloride (Sigma) in 0,05M Tris-HCl (Tris base purchased from MP North America). The reaction was initiated with 1,5% H_2O_2. The sections were mounted on gelatin (Merck) - poly-L-lysine (Sigma) double coated glass slides, air-dried, dehydrated through ethanol (VWR International) series, defatted in xylene (Biosolve) and coverslipped with DEPEX (VWR International).

The above mentioned protocol (except for the DNA denaturation step) was used to visualise microglia by means of rabbit anti Iba-1 antibody (1:1500; Wako) and immature neurons with rabbit anti-doublecortin (1:750; abcam) antibody. The secondary antibody used was goat anti-rabbit biotinylated antibody (1:500; Vector Laboratories).

The antibodies used for fluorescent double-labeling studies were the following: rabbit anti-Iba1 (1:1500; Wako), rat anti-mouse MHCII (1:100; eBioscience), rat anti-mouse CD4 (1:100; eBioscience), mouse anti-BrdU (1:500; Sigma). The secondary antibodies used were: goat anti-rabbit Cy3 (1:500, JacksonImmunoResearch), goat anti-rabbit FITC (1:250; Chemicon), goat anti-mouse Cy3 (1:500; JacksonImmunoResearch), goat anti-rat FITC (1:250; Southern Biotech). Following the staining protocol, sections were counterstained with Hoechst (1:1000; Sigma) mounted and coverslipped with Mowiol (Calbiochem).

For the immunohistochemical staining against MHCII and CD3, positive tissue controls were used. Brain sections of cuprizone fed mice and mice in which EAE was induced served as positive controls. The cuprizone diet is a model of CNS demyelination and remyelination (Matsushima and Morell, 2001), with extensive death of oligodendrocytes and microglia activation in the corpus callosum (Chen and Guilarte, 2006). Experimental autoimmune encephalomyelitis is a well established model of some aspects of multiple sclerosis. It is induced by priming the immune system with CNS derived antigens. The histopathological features of EAE in general include perivascular lymphocytic infiltrates in

both grey and white matter and microglia hyperplasia (Baxter, 2007). In both cases the animals belonged to the same mouse strain (C57Bl/6) as our experimental animals. Our experimental sections and the positive tissue control sections did not differ in tissue handling (fixation, storage) and were submitted to immunohistochemical stainings simultaneously.

Proliferation in the subgranular zone of the hippocampus and survival of the newborn neurons

BrdU incorporation and survival of newborn neurons was assessed at 40 times magnification. BrdU labeled cell nuclei were counted along the subgranular zone of the dentate gyrus and one cell body width deviating from it. Survival of newborn neurons was determined by counting those doublecortin positive dendrites that extended the whole width of the granule cell layer of the dentate gyrus. The total numbers of these parameters per hippocampus per animal were determined as described above.

Total number of microglia in the dentate gyrus of the hippocampus

The number of microglia was counted in the different subregions of the dentate gyrus in twelve sections per animal under a light microscope. The examined regions of the dentate gyrus included: the granule cell layer (GCL), the hilus (HIL) and the molecular layer (MOL). All microglia (either on the molecular layer side or the hilar side of the granule cell layer), that had at least of one of their main processes in the granule cell layer (Figure 2A, dashed dotted line), and their cell body not further away from the granule cell layer than the width of one cell body, were counted as belonging to the granule cell layer. The hilus was determined as the region between the two blades of the granule cell layer closed down by an imaginary line (Figure 2A, solid line) that connects the lateral ends of the two blades of the GCL. The molecular layer was determined as the region between the granule cell layer and the fissura hippocampi on the dorsal side, and the granule cell layer and the third

ventricle on the ventral side (Figure 2A, dotted line). The CA3 region was not included in this investigation. On average the total number of Iba1 positive microglial cells counted in one brain (12 sections) amounted to 1400, 1000, 1800 cells in the GCL, hilus and molecular layer subregions respectively.

Microglia morphology and activation

Microglia morphology was assessed with light microscopy at 20 times magnification in the granule cell layer of the dentate gyrus. The criteria for activated microglia were based on previous studies (Battista at al., 2006; Kreutzberg, 1996). Resting microglia were characterised by small somata and highly ramified dendritic arborisations. Stage two and three activated microglia had thicker and shorter processes. Stage four microglia, displaying amoboid morphology with vacuoles in the cytoplasm were not present in the dentate gyrus of our experimental animals. All microglia that displayed non-resting morphology (thus stage two and three activated microglia) were counted as activated. All microglia in the granule cell layer, together with the microglia in the molecular and hilus subregions, that had their processes in the granule cell layer but their cell bodies were not further from the granule cell layer, than the width of one cell body, were included in this analysis. Approximately 48.000 Iba1 positive cells (around 700 microglia per brain half) were examined in the granule cell layer of the dentate gyrus to assess morphological changes of the microglial cells. For each animal the level of microglia activation in the granule cell layer was expressed as the percentage of activated microglia in the total number of microglia.

Analysis of the fluorescent stainings

Fluorescent stainings were analysed with a fluorescent microscope (Zeiss, Axioskope 2) equipped with a mercury lamp (HBO 100) at 20 and 40 times magnification. Pictures were made with the help of Leica Application Suite software. Brightness and contrast were adjusted and

overlay of the different channels was done in Adobe Photoshop 7.0 software.

Microglia proliferation in the hippocampus

The number of proliferating microglia was determined by counting the BrdU/Iba1 double positive cells in the dentate gyrus and the cornu ammonis region (CA1-CA3) of the hippocampus. In the dentate gyrus most proliferating microglia cells were located in the molecular layer and the hilus. The percentage of the BrdU positive nuclei in the subgranular zone that belonged to an Iba1 positive cell was on average less than 0,5% (data not shown).

All countings (the total number of BrdU positive nuclei, total number of DCX positive dendrites, total number of microglia, total number of BrdU/Iba1 double positive cells) and the assessment of the level of microglia activation in the dentate gyrus were carried out in a blinded fashion.

Flow cytometric analysis of rapidly isolated microglia from the hippocampus

In each experiment microglia isolated from the brains of the runners (N = 8) and the sedentary control animals (N = 4), respectively, were pooled. Before the flow cytometric measurement, the cell suspension of microglia isolated from the runners was divided into two. As a result in each independent experiment we performed two independent flow cytometric measurements for the runner group (N = 2 x 4) and one independent measurement for the sedentary control group (N = 4).

Microglia were isolated based on the protocol published by De Haas and colleagues (De Haas et al., 2007). Briefly, the density separation of microglia was achieved by a Percoll (GE Healthcare) gradient. Single cell suspension of isolated CNS cells was resuspended in 75% and overlaid with 25% Percoll followed by a layer of PBS and centrifuged at 800 rcf for 25 minutes. After centrifugation microglia were collected from the

25%/75% Percoll interface. Subsequently microglia cell suspension was extensively washed and counted. Unspecific binding of the fluorochrome conjugated antibodies and Fc receptor binding were blocked with 10% normal rat serum (Invitrogen) and rat anti-mouse CD16/32 antibody (1:100; eBioscience), respectively. After the blocking step the cells were resuspended in PBS containing the antibodies for flow cytometry. Microglia were subsequently washed, pelleted by centrifugation and resuspended in 300 µl of PBS. About 10 minutes before the flow cytometric measurement the cells were incubated in 1:1500 dilution of DRAQ5 (Biostatus Limited). Cells were analysed with a 488 nm laser FACS Calibur (Becton Dickinson).

Antibodies used for flow cytometric analysis of microglial cells were phycoerythrin (PE) conjugated rat anti-mouse CD11b (1:160), fluorescein isothiocyanate (FITC) conjugated rat anti-mouse CD45 (1:200), FITC conjugated rat anti-mouse MHC class II (1:400), PE conjugated rat anti-mouse CD3ε (1:20). The isotype control preimmune antibodies used were: FITC conjugated rat IgG2a, FITC conjugated rat IgG2bκ, PE conjugated rat IgG2bκ. The isotype controls were used in the same concentration as the corresponding primary antibodies. All antibodies were purchased from eBioscience, except for the antibody against CD3ε, which was from Southern Biotech.

For the analysis of flow cytometric measurements WinMDI 2.8 software was used. At least four thousand cells were analysed for each immunocytochemical staining.

The microglial population was determined based on their characteristic expression pattern of CD11b and CD45 surface antigens (Figure 5C) and a positive viability staining with DRAQ5 (Figure 5B). Since the CD11b high/CD45 low population of living cells formed a well distinguishable group on the size and granularity plot (forward scatter (FSC)/side scatter (SSC) plot; Figure 5A), we used gating on the population within R1 (depicted on Figure 5A) to identify the microglial cells in the different stainings. Mean fluorescent intensity (MFI) of the R1 population was

determined using WinMDI 2.8 software for each staining. The difference in the surface expression of different markers on microglia isolated from runners and sedentary controls was calculated according to the following formula: $\Delta MFI = MFI_{runners} - MFI_{sedentary\ controls}$. The ΔMFIs of three independent experiments was averaged and is shown in Table 1. The means of the ΔMFIs for a given immunocytochemical staining of the microglial cells isolated from the runners and the sedentary controls were compared by paired sample T test. P value in Table 1. represents the one tailed probability value of the test. T cells were identified as CD3 positive living cells (Figure 6B). The percentage of the CD3 positive T cells (R2; Figure 6B) among living cells (R1; Figure 6A) was determined on a plot of fluorescent intensity *versus* side scatter (R3; Figure 6C).
Freshly isolated mouse spleen cells from C57Bl/6 mice served as positive control for the immunocytochemical staining against MHC class II and CD3. Mouse spleen was dissociated in 2-4 ml of RPMI containing 10% FCS in a Petri dish with the help of surgical blades. A single cell suspension was made with flamed Pasteur pipettes of decreasing diameter. The cell suspension was centrifuged at 1400 rpm for 5 minutes at 4°C. The pellet was resuspended in HBSS and centrifuged again at 1400 rpm for 5 minutes at 4°C. The cell suspension was incubated in red blood cell lysis buffer for 10 minutes at room temperature, diluted in PBS and centrifuged at 1400 rpm for 5 minutes at 4°C. The pellet was resuspended in blocking solution, washed, centrifuged, stained and submitted to flow cytometric analysis parallel with the hippocampal microglia, as described above. The analysis of the flow cytometric measurements was performed as described above.

Analysis of expression levels of different microglial genes by RT-qPCR
In a follow up experiment we investigated the expression levels of certain growth factors and cytokines in hippocampal microglia of runners and sedentary controls, that had been shown to be involved (either in a supportive or in an antagonistic way) in the regulation of

adult hippocampal neurogenesis. The factors in this study included insuline-like growth factor (IGF-1; Butovsky et al., 2006; Ziv et al., 2006) and interleukin-4 (IL-4; Butovsky et al., 2006; Ziv et al., 2006), transforming growth factor-beta1 (TGF-β1; Battista et al., 2006; Wachs et al., 2006), brain derived nerve growth factor (BDNF; Bergami et al., 2008), interferon gamma (IFN-γ; Baron et al., 2008), galectin-1 (Gal-1; Ishibashi et al., 2007; Sakaguchi et al., 2006), leukemia inhibitory factor (LIF; Bauer & Patterson, 2006), neurotrophin-3 (NT-3; Shimazu et al., 2006), interleukin-6 (IL-6; Nakanishi et al., 2007), inducible nitric oxide synthase (iNOS; Cárdenas et al., 2005), interleukin-1beta (IL-1β; Koo & Duman, 2008), tumor necrosis factor alpha (TNF-α; Bernardino, 2008; Iosif et al., 2006) and CD74, the invariant chain of the MHCII molecule (Ziv et al., 2006). The follow up experiment consisted of two independent experiments. Each independent experiment included ten animals in total - five of which had access to a running wheel for ten days, and five that were housed in cages without a running wheel. The animals were sacrificed and microglia was isolated from the hippocampus as described earlier (see Materials and methods corresponding sections and paragragphs). Total RNA was isolated using a Quiagen RNeasy Micro kit according to the manufacturer's protocol. The RNA was reverse transcribed into cDNA using random hexameres (Fermentas) on a MiniCycler™ thermal cycler (BIORAD). The reaction mixture also contained the RevertAid™ M-MuLV Reverse Transcriptase and RiboLock™ RNase Inhibitor (both from Fermentas). cDNA was subjected to RT-qPCR reaction using iQ™ SYBR® Green Supermix (Biorad) in a 384 well plate (Applied Biosystems) on an ABI7900HT machine (Applied Biosystems). Table 1 contains the sequences of the primers used for the analysis. All primers were designed using PRIMER DESIGNER v3.0 software for Windows and were ordered from Isogen. All primer efficiencies were tested on cDNA prepared from isolated total brain microglia as well as on different positive control tissues of male C57Bl/6 mice (the positive tissue controls used were: spleen (for TGF-

β1, IL-4, Gal1, IL-1β and CD74); lymph node (for IFN-γ, LIF and IL-6); brain of P2 pup (for BDNF and NT-3); liver (for IGF-1) and heart (for iNOS)). In the qPCR analysis scheme next to the samples of microglia from the runners and the sedentary controls positive control wells (containing cDNA from the corresponding positive tissue control) and negative control wells (containing no cDNA) were included. For each gene each measurement was performed in triplicate in both independent experiments. The specificity of the qPCR products was determined by the analysis of the dissociation curves. Four houskeeping genes were tested (Table 1; GAPDH, HPRT1, HMBS and β-actin). For normalisation purposes the HMBS gene was used, because its expression level was the most similar to the expression levels of the investigated genes of interest and it showed a stable expression across the samples (data not shown). Hippocampal microglia expressed all the investigated factors at a detectable level. The expression levels (expressed as cycle treshold, Ct) of the genes of interest (GOI) and the housekeeping gene (HKG) were corrected with the corresponding primer efficiencies (Eff). Subsequently, the corrected expression levels of genes of interest were normalised with the corrected expression level of the housekeeping gene (Eff(GOI)xCt(GOI)/Eff(HKG)xCt(HKG)). The primer efficiencies used in the above mentioned equation were determined by a qPCR analysis of a dilution series of cDNA prepared from freshly isolated adult total brain microglia (data not shown). Data were analayzed with the help of SDS v2.3 software (Applied Biosystems). Figure 7 shows the expression levels of the selected genes of interest in microglia cells isolated from the runners and the sedentary controls. Expression levels have been corrected for the differences in the primer efficiencies and normalised to the expression level of the houskeeping gene.

Statistics

Statistical analysis was done using SPSS 12.0.1 software. Student t-test was used to compare means in the case of immunohistochemical data. Paired sample t-test was used for the analysis of the flow cytometric measurements.

RESULTS

The effect of voluntary physical activity on hippocampal neurogenesis

The effect of voluntary physical activity on hippocampal neurogenesis was assessed by performing immunohistochemistry against incorporated BrdU, which marked the proliferating cells, and doublecortin, which is a marker for immature neurons.

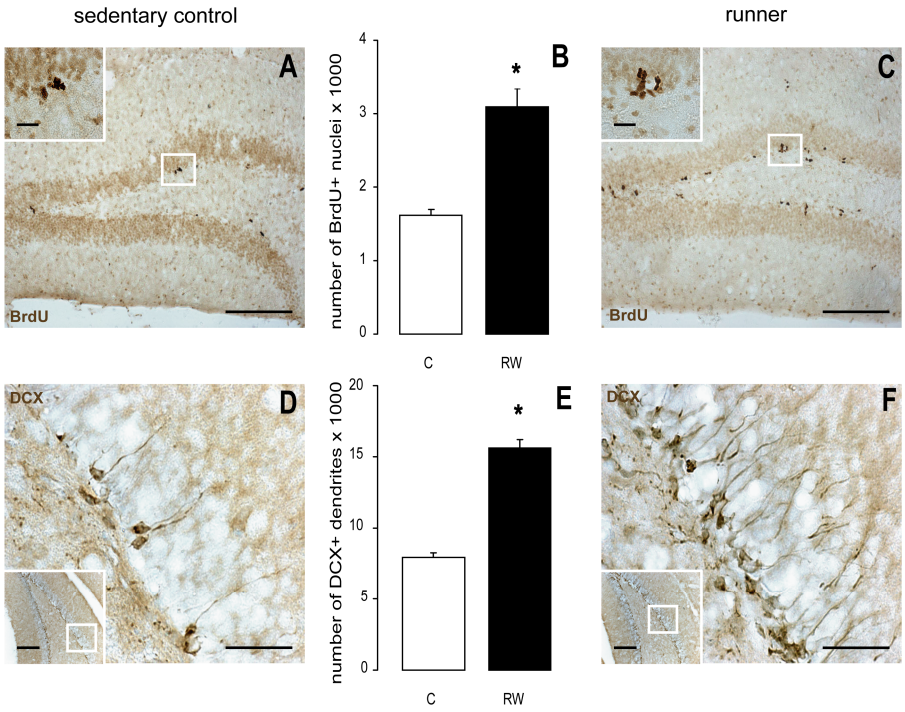

Figure 1. The effect of voluntary physical activity on hippocampal neurogenesis. Ten days of voluntary physical activity significantly elevated the level of neurogenesis in the dentate gyrus (DG) of the hippocampus. The level of proliferation of the neural precursors was assessed by counting BrdU positive nuclei in the subgranular zone (SGZ) of the DG. There were significantly more BrdU positive nuclei in the SGZ of the runners then of the sedentary controls (**A**-**C**; in **B** * $p < 0{,}001$; N(C) = 4, N(RW) = 8; C - sedentary controls, RW - runners). The survival of the newborn neurons was determined by counting the number of dendrites that were positive for the immature neuronal marker, doublecortin (DCX) in the granule cell layer (GCL) of the DG. The number of DCX positive dendrites in the GCL of the DG was also significantly higher in the runners then in the sedentary controls (**D**-**F**; in **E** * $p < 0{,}001$; N(C) = 4, N(RW) = 8). Panel **B** and **E** represent the total number of BrdU positive nuclei in the SGZ per animal, and the total number of DCX positive dendrites in the GCL per animal,

respectively. **A, C** and **D, F** are representative photomicrographs of immunohistochemical staining against BrdU and doublecortin, respectively, in the dentate gyrus of sedentary control animals (**A** & **D**) and runners (**C** & **F**). Scale bars represent 200 micrometers for the main pictures in **A**, **C** and the inserts in **D** and **F**, and 20 micrometers for **D**, **F** and the inserts in **A** and **C**. In graph **B** and **E** data are represented as mean (column bars) + standard error of the mean (error bars). All graphs represent the data of one out of three independent experiments. Similar results were obtained in the other two independent experiments.

Counting BrdU positive nuclei in the subgranular zone (SGZ) of the dentate gyrus (DG) revealed a significant increase in the number of proliferating cells in the SGZ of the runners, when compared to sedentary controls (Figure 1B). In the sedentary controls there were on average 1600 BrdU positive nuclei in the subgranular zone of the dentate gyrus, while in the runners this number was 2600 (three independent experiments: p = 0,005; p = 0,0002; p = 0,007). Therefore, voluntary running resulted on average in a 62% increase in the number of proliferating cells in the SGZ in the runners when compared to sedentary controls.

Doublecortin positive dendrites were counted in the granule cell layer (GCL) in order to assess the level of survival and differentiation of the newborn neurons in the DG. Running wheel activity significantly increased the number of doublecortin positive dendrites in the GCL (Figure 1E). The number of doublecortin positive dendrites that extended the whole width of the granule cell layer was on average 10.600 and 17.200 in the sedentary controls and the runners, respectively (three independent experiments: p = 0,0015; p = 1,2E-07; p = 0,024). Thus, the level of survival and differentiation of newborn neurons was elevated on average by 62,5% in the runners compared to the sedentary controls.

Thus, as described by earlier studies (van Praag et al., 2008; van der Borght et al., 2006), ten days of voluntary physical activity in a running wheel significantly increased both aspects of adult hippocampal neurogenesis: proliferation of neural precursor cells and survival of newborn neurons.

Classical signs of microglia activation

To assess the possible involvement of microglia in the regulation of adult hippocampal neurogenesis classical signs of microglia activation, such as proliferation and morphological changes, have been determined.

The number of microglia cells in the different subregions of the dentate gyrus was assessed in two independent experiments by counting Iba1 positive cells in three different subregions of the dentate gyrus: the molecular layer (MOL), the hilus (HIL) and the granule cell layer (GCL). The number of counted Iba1 positive cells per dentate gyrus subregion per animal (12 sections) was on average 1400, 1000 and 1800 for the GCL, hilus and molecular layer, respectively (two independent experiments). The number of Iba1 positive cells did not differ significantly between the runners and the sedentary controls in either of the above mentioned DG subregions (Figure 2A and 2B). The level of microglia proliferation was determined by counting BrdU/Iba1 double labeled cells (Figure 2C and 2D) in the hippocampus. There were significantly more proliferating microglia in the dentate gyrus and the cornu ammonis region of the hippocampus of the runners compared to the corresponding hippocampal subregions of the sedentary controls (Figure 2E). In the dentate gyrus there were on average 150 (2% of the total microglia number in the dentate gyrus) proliferating microglia in the sedentary controls, while this number for the runners was on average 380 (5% of the total microglia number in the dentate gyrus). Therefore, physical activity on the last night of our experiment increased the proliferation of microglia in the dentate gyrus and the cornu ammonis regions on average by 153% and 98%, respectively (two independent experiments: $p = 0,003$ in both experiments for the DG; $p = 0,004$ for the CA region).

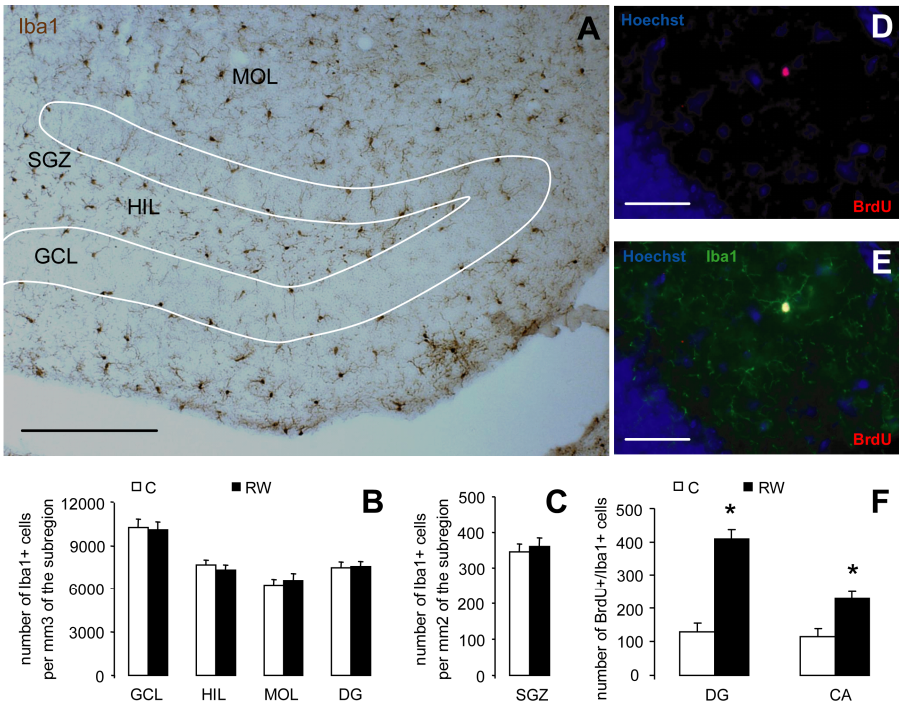

Figure 2. Classical signs of microglia activation. Total number of microglia and state of activation was not different in the runners (RW) when compared to sedentary controls (C). The total number of microglia is expressed as the number of Iba1 positive cells (**B**) of the granule cell layer (GCL), hilus (HIL) and molecular layer (MOL) of the dentate gyrus (DG). In **A** the spatial distribution of Iba1 stained microglia in the dentate gyrus is depicted. Ten days of voluntary physical activity significantly increased the number proliferating microglia both in the dentate gyrus (DG; **E**) and the cornu ammonis region (CA; **E**). **C**, **D** are representative photomicrographs showing BrdU/Iba1 double labeled proliferating microglia (BrdU - red, Iba1 - green, co-localisation - yellow, Hoechst - blue). Microglia proliferation is expressed in **E** as the total number of BrdU/Iba1 double labeled microglia in the given hippocampal subregion (* p = 0,003 for DG, * p = 0,004 for CA) per animal. Calibration bars represent 200 µm in **A** and 50 µm in **C** and **D**. In panels **B** and **E** data are represented as mean (column bars) + standard error of the mean (error bars). In all graphs C stands for sedentary controls and RW stand for runners. All graphs represent the data of one out of two independent experiments (N(C) = 8; N(RW) = 8). Similar results were obtained in the other independent experiment.

In order to gain insight in the activation state of the dentate gyrus microglia, their morphology was determined by visual examination. Microglia were classified into four different categories based on their morphology, as described elsewhere (see Materials and methods). The

morphology of in total more than 40.000 microglial cells was examined and characterised as either resting or activated.

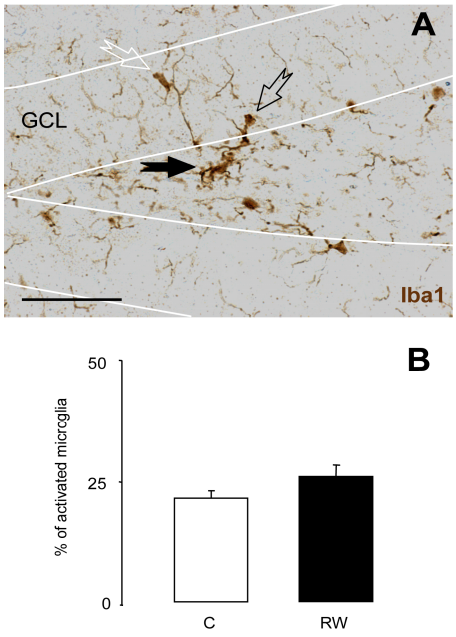

Figure 3. Classical signs of microglia activation. Microglial state of activation was not different in the runners (RW) when compared to sedentary controls (C). On average 25% of microglia associated with the granule cell layer (GCL) displayed non-resting morphology. In **A** a resting (white open arrow), a stage two activated microglia (black open arrow) and a stage three activated microglia (black filled arrow) are depicted in the granule cell layer. In **B** microglia activation is expressed as the percentage of the total number of microglia in the granule cell layer (GCL) that displayed stage two and stage three morphology. In panel **B** data are represented as mean (column bars) + standard error of the mean (error bars) (N(C) = 4; N(RW) = 8). In **B** C stands for sedentary controls and RW stands for runners. Panel **B** represents the data of one out of three independent experiments. We obtained the same results from the other two independent experiments as well.

Counting granule cell layer associated activated microglia (Figure 3A) revealed no difference in the activation status of the microglial cells in the dentate gyrus of runners compared to sedentary controls (Figure 3B). On average 25,65% of granule cell layer associated microglia displayed non-resting morphology (three independent experiments: p = 0,24; p = 0,06; p = 0,08).

Signs of microglia – T cell interaction in the dentate gyrus of the hippocampus

We next investigated whether signs of interaction between microglia and T cells were present in the dentate gyrus of our experimental animals. Microglia are generally believed to interact with T cells through the expression of major histocompatibility complex (MHC) molecules. To

determine whether or not microglia in the dentate gyrus were engaged in crosstalk with T cells, we performed immunohistochemical staining against MHC class II and Iba1, and counted the double-labeled cells. The antibody against MHCII (eBioscience; catalog number 14-5321) is specified to recognise the H-2^b haplotype of the MHCII molecule, which was described to be present in the C57Bl/6 strain (http://imgt.cines.fr/textes/IMGTrepertoireMHC/Polymorphism/haplotypes/mouse/MHC/Mu_haplotypes.html#n9). In all the animals investigated (52 animals, in total 624 hippocampal sections were examined) not more than a dozen of parenchymal Iba1 positive microglia in the dentate gyrus were also positive for MHCII (Figure 4A and 4B). The expression level of MHCII on these cells was rather low. Some ependymal (data not shown) and perivascular macrophages (Figure 4C and 4D) expressed higher levels of MHCII. In both positive tissue controls (brain sections from cuprizone and EAE mice) microglia in the corpus callosum displayed high levels of MHCII (Figure 4E-F and 4G). The presence of T cells in the dentate gyrus parenchyma was investigated by immunohistochemical staining against the pan T cell marker CD3 and the T helper 2 cell marker CD4 (a total number of 624 hippocampal sections examined for each). In our experiments neither T helper type 2 cells, nor T cells in general were present in the dentate gyrus or in the surrounding CNS parenchyma.

Sections from the EAE mice showed CD4 positive T helper 2 cell infiltrates in the corpus callosum below the longitudinal fissure (Figure 4H), while CD3 positive T cells were present dispersed in the brain parenchyma (data not shown).

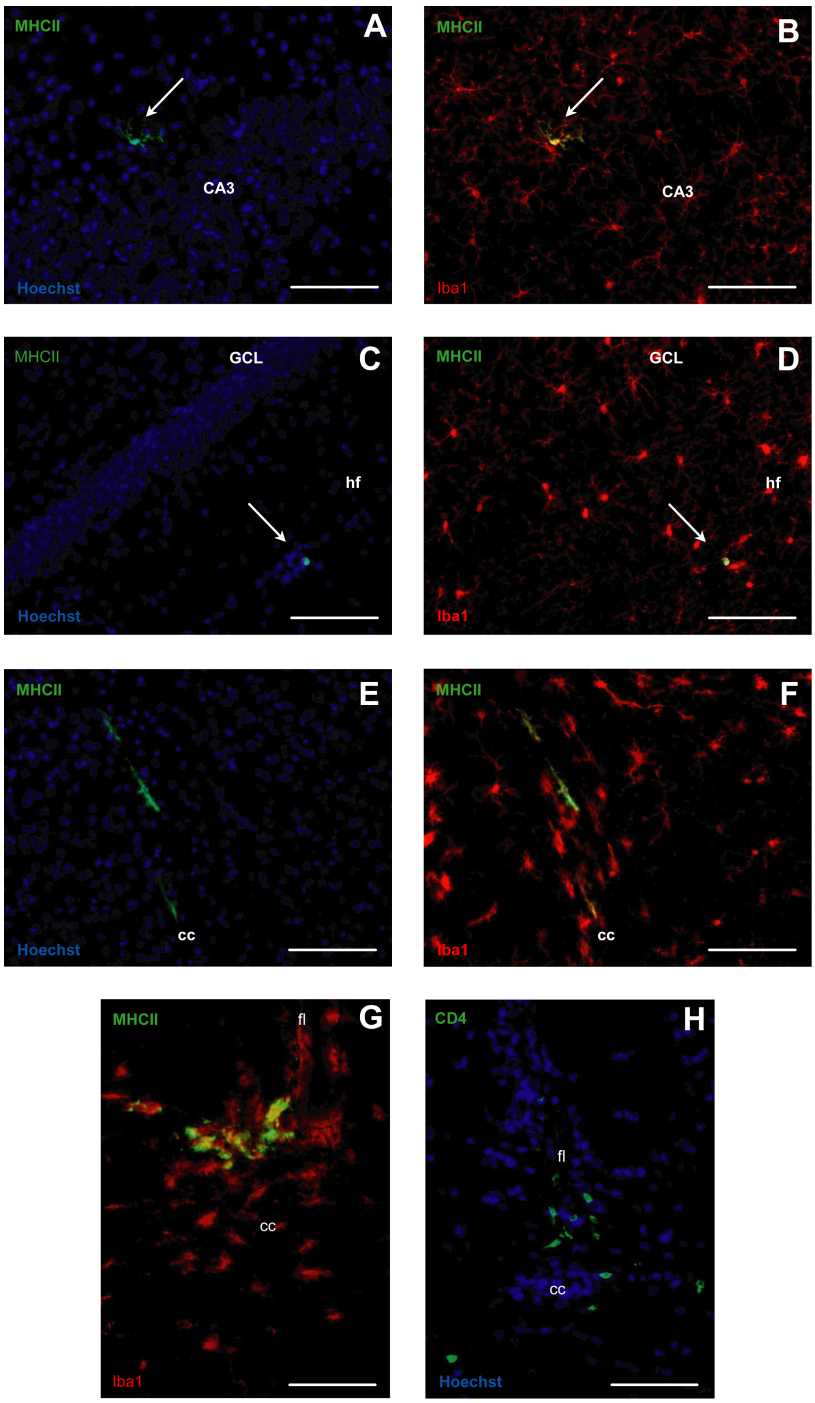

Figure 4. MHCII class II molecule expression on microglial cells and T cells were absent from the dentate gyrus of the hippocampus in both sedentary controls and

runners. MHCII expression was obvious in some ependymal and perivascular (**C** & **D**, arrow) macrophages. In **A** and **B** the arrow points to one of the few parenchymal microglia that were positive for MHCII. Positive controls for the immunostainings against MHCII (**E**, **F** and **G**) and CD4 (**H**) were brain slices from cuprizone fed (**E**, **F**) and EAE mice (**G**, **H**). (in **A**-**G** MHCII is green; in **H** CD4 is green; in **B**, **D**, **F** and **G** Iba1 is red; in **A**, **C**, **E** and **H** Hoechst is blue; in **B**, **D**, **F** and **G** co-localisation of Iba1 and MHCII is yellow; CA3 cornu ammonis region 3 of the hippocampus, hf hippocampal fissure, cc corpus callosum, fl fissura longitudinalis).

Flow cytometric analysis of rapidly isolated hippocampal microglia

In addition, flow cytometry as a more sensitive method, was used to study possible microglia – T cell interaction. We subjected rapidly isolated hippocampal microglia to flow cytometric analysis of surface markers as described recently (De Haas et al., 2007). The microglia population was identified by CD11b high/CD45 low expression profile and a positive viability staining with DRAQ5 (Figure 5A-C).

Immunocytochemical stainings were performed for MHCII, CD11b, CD45, F4/80 on the hippocampal microglia (Figure 5D-F). Concentration matched isotype controls were used for each staining (dotted line in Figure 5D-F and 5G). As a positive cell control for the staining against MHCII and CD3, freshly isolated mouse spleen cells were used (Figure 5G and 6E). The antibody against MHCII (eBioscience; catalog number 11-5321) is specified to recognise the H-2^b haplotype of MHCII molecule, which is described to be present in the C57Bl/6. Surface expression of MHCII was absent in hippocampal microglia isolated either from runners or sedentary controls. In both cases the mean fluorescence levels were not different from the background staining (Figure 5D; Table 2). Microglia isolated from the hippocampus showed high expression levels of CD11b and low expression levels of F4/80 (Figure 5E and 5F). Upon activation, CD11b and F4/80 are also known to be upregulated on microglial cells. However, there was no significant difference in the expression levels of these two markers between hippocampal microglia isolated from sedentary controls and runners (Table 1).

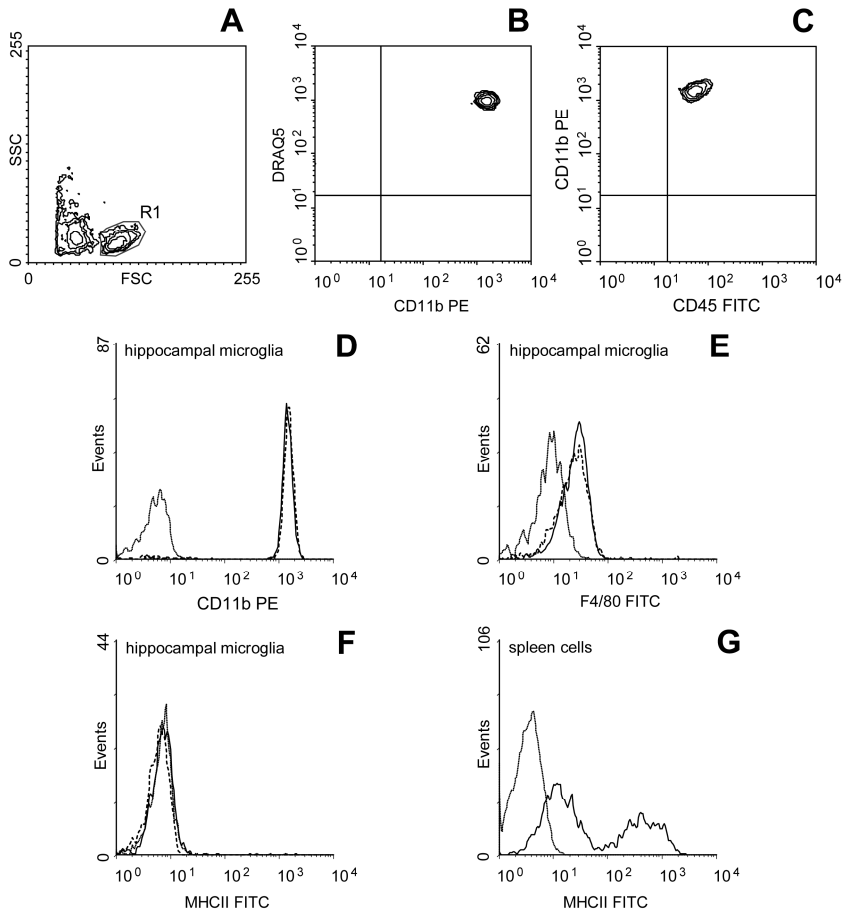

Figure 5. Flowcytometric analysis of rapidly isolated microglia from the hippocampus revealed no differences between runners and sedentary controls neither in MHCII expression (**F**), nor in the expression level of other microglial activity markers, such as CD11b (**D**) and F4/80 (**E**). Microglia cells were identified based on size (forward scatter, FSC) and granularity (side scatter, SSC) (**A**), a positive viability staining, (DRAQ5; **B**) and a characteristic CD11b high/CD45 low expression profile (**C**). In histograms **D**-**G** mean fluorescence intensity is plotted against the number of events. In each histogram dotted lines, dashed lines and solid lines represents the isotype control measurements, the sedentary controls and the runners, respectively. Freshly isolated spleen cells were used as positive control for the immunocytochemical staining against MHCII (**G**). All histograms represent the measurement of one out of three independent experiments. In each experiment every measurement was done in duplos. In every experiment similar results were obtained.

	CD11b	CD45	MHCII	F4/80
ΔMFI ± SD	30,17 ± 145,15	5,12 ± 0,66	-0,27 ± 0,54	2,6 ± 3,85
p value	0,38	0,03	0,24	0,26

Table 1. Surface expression of activity markers on freshly isolated hippocampal microglia. shows the average difference between the measured mean fluorescent intensities (ΔMFI) of the microglia isolated from the runners and the sedentary controls, and stained for different microglia markers and microglia activation markers (N(RW) = 2 x 4; N(C) = 4; three independent experiments). No significant difference was observed between microglia isolated from the hippocampus of the runners and the sedentary controls regarding the surface expression of CD11b, MHCII and F4/80 molecules. Statistical comparison was done by paired sample T test. P value represents the one tailed probability value of the test.

The 75%/25% Percoll interface in our isolation protocol, next to the hippocampal microglia, contained a small population of cells with CD11b-/CD45high expression profile, which are likely to be lymphocytes, macrophages and granulocytes (De Haas et al., 2007). Therefore we were able to address with our isolation protocol the question whether T cells are more numerous in the hippocampus of the runners than of the sedentary controls. For this purpose we stained the hippocampal mononuclear fraction with an antibody against the pan T cell marker, CD3. Flow cytometric analysis revealed no difference between runners and sedentary controls regarding the percentage of CD3 positive cells within the viable cell population (average difference between runners and sedentary controls in the three independent experiments was 2,52 %; SD = 2,3 %; p = 0,24 (paired sample t-test; one tailed)).

In both cases the average percentage of CD3 positive cells in our preparation was approximately 10 % (Figure 6C; three independent experiments). The expression level of CD3 did not differ either between runners and sedentary controls (ΔMFI ± SD = 4,13 ± 1,7; p = 0,09; two independent measurements for the runners (N = 2 x 4) and one measurement for the sedentary controls (N = 4) in each of the three independent experiments).

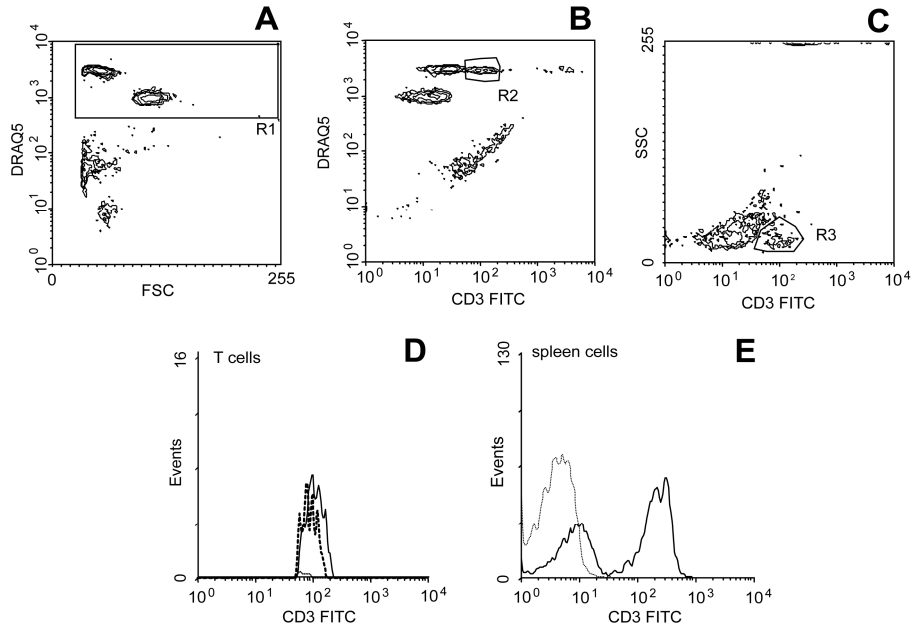

Figure 6. On average 10% of the living cells (**R1** in **A**) in our preparation were identifiable as T cells, based on their surface expression of the pan T cell marker, CD3 (**B**, **C**) and their size and granularity relative to the microglial cells (data not shown). The CD3 positive T cells were clearly distinguishable from the microglia population (**R2** in **B**, **R3** in **C**). The percentage of CD3 positive T cells present in our preparation was not different between runners and sedentary controls (see Results). The mean fluorescent intensity of the staining against CD3 in the T cell population was not significantly different between runners and controls (see Table 2). In the isotype control measurement **R2** region of interest (**B**) did not contain cells (data not shown).

The flow cytometric analysis of our positive cell controls revealed two subpopulations of spleen cells for both MHCII and CD3: one with high, and another one with moderate expression levels of these two markers, which clearly differed from the background fluorescent signal of the isotype control staining (Figure 5G and Figure 6E).

Analysis of expression levels of different microglial genes by RT-qPCR

In order to gain more insight in the activation state of hippocampal microglia of runners and sedentary controls, we performed qPCR analysis of gene expression. The expression level of a set of selected genes, that reportedly can have an effect on neurogenesis (see

Materials and methods section) has been investigated. Figure 7 shows the outcome of the quantitative PCR analysis of hippocampal microglia gene expression in runners (RW) and sedentary controls (C).

Different expression levels of the investigated genes could be detected (most abundant transcripts were that of TGF-β1, and the least abundant were that of IFNγ; Fig.7). Nonetheless, the expression level of the given genes did not differ between microglia isolated from the hippocampus of the runners and of the sedentary controls. Only, the transcript level of the inducible nitric oxide (iNOS) gene showed a tendency to be higher in the microglia isolated from the runners than from the sedentary controls.

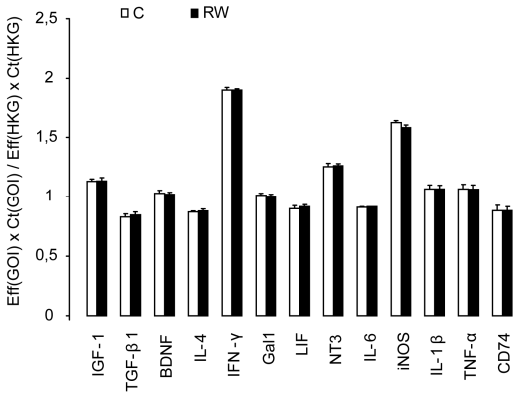

Figure 7. RT-qPCR analysis of microglial expression levels of some of the genes reported to be involved in the regulation of adult hippocampal neurogenesis (mean of two independent experiments). The genes selected for qPCR analysis were IGF-1, TGF-β1, BDNF, IL-4, IFN-γ, Gal-1, LIF, NT-3, IL-6, iNOS, IL-1β, TNF-α and CD74 (For the acronyms please see List of abbreviations). Gene expression levels have been corrected with the corresponding primer efficiencies (Eff(GOI) and Eff(HKG)), and normalised with the expression level of the housekeeping gene. (Ct(GOI) cycle tresholds of the genes of interest; Ct(HKG) cycle tresholds of the housekeeping genes; GOI – genes of interest; HKG - housekeeping genes). Please note that higher values on Y axis reflect lower expression level of a certain gene of interest when compared to the housekeeping gene.

	qPCR primers	
	forward	backward
GOI		
IGF-1	5'-AGGCTATGGCTCCAGCATTC-3'	5'-GGCACAGTACATCTCCAGTC-3'
TGF-β1	5'-TACGCCTGAGTGGCTGTCTT-3'	5'-AGAGCAGTGAGCGCTGAATC-3'
BDNF	5'-GGACTCTGGAGAGCGTGAAT-3'	5'-GTCCTCATCCAGCAGCTCTT-3'
IL-4	5'-CGGCACAGAGCTATTGATGG-3'	5'-CATCCGTGGATATGGCTCCT-3'
IFN-γ	5'-TTAACAGCAGGCCAGACAGC-3'	5'-GGAAGCACCAGGTGTCAAGT-3'
Gal1	5'-GCTGCCAGACGGACATGAAT-3'	5'-GGCCACGCACTTAATCTTGA-3'
LIF	5'-ATGTGCGCCTAACATGACAG-3'	5'-TATGCGACCATCCGATACAG-3'
NT3	5'-GAGACTGAATGACCGAACTC-3'	5'-CTGTAAGATCGTGGCAGAAG-3'
IL-6	5'-CCTTCCTACCCCAATTTCCAAT-3'	5'-GCCACTCCTTCTGTGACTCCAG-3'
iNOS	5'-AAGGCCACATCGGATTTCAC-3'	5'-GATGGACCCCAAGCAAGACTT-3'
IL-1β	5'-GGCAGGCAGTATCACTCATT-3'	5'-AAGGTGCTCATGTCCTCATC-3'
TNF-α	5'-GACGTGGAACTGGCAGAAGA-3'	5'-GCCACAAGCAGAATGAGAA-3'
CD74	5'-CCGCCTAGACAAGCTGACCA-3'	5'-GGAGTAGCCATCCGCATCTG-3'
HKG		
GAPDH	5'-ATGGCCTTCCGTGTTCCTAC-3'	5'-GCCTGCTTCACCACCTTCTT-3'
HPRT1	5'-GACTTGCTCGAGATGTCA-3'	5'-TGTAATCCAGCAGGTCAG-3'
β-actin	5'-AGACCTCTATGCCAACACAG-3'	5'-TAGGAGCCAGAGCAGTAATC-3'
HMBS	5'-CCGAGCCAAGGACCAGGATA-3'	5'-CTCCTTCCAGGTGCCTCAGA-3'

Table 2. Sequences of the primers used for gene expression analysis of microglia. (GOI – genes of interest; HKG - housekeeping genes; for the other acronyms please see List of abbreviations)

DISCUSSION

Our view of microglia has dramatically changed in the last few years. From cells simply being brain macrophages, microglia are now recognised as a multifaceted cell type with a variety of functions not only under pathological conditions but in the healthy central nervous system (CNS) as well (Hanisch and Kettenmann, 2007). In line with this, microglia have recently been suggested to be involved in the maintenance of both aspects of adult neurogenesis: proliferation of neural precursors and their differentiation into neurons (Battista et al., 2006; Ziv et al., 2006).

Microglia were found to contribute to the neurogenic niche in two different experimental animal models of adult hippocampal neurogenesis in rats: following adrenalectomy (ADX) and in an enriched environment (Battista et al., 2006; Ziv et al., 2006). However, it is not yet clear whether microglia activity is required for adult neurogenesis under all circumstances. Moreover, although it has been suggested that a special microglia phenotype, which results from the interaction of microglia by T helper 2 cells (Ziv et al., 2006), is instrumental in adult neurogenesis, very little is yet known about the mechanisms through which microglia are able to exert their effect on adult neurogenesis. In order to investigate the involvement of microglia in adult neurogenesis in detail, we have used the model of voluntary physical activity in C57Bl/6 mice, which reportedly elevates the level of adult hippocampal neurogenesis (van Praag, 2008).

Here we describe that classical microglia activation, and in particular microglia activation arising from interaction with T helper cells, is not an essential prerequisite for acute increase in the proliferation of neural precursors and for the increase in the survival of newborn neurons on the short term caused by voluntary physical activity in C57Bl/6 mice. Our conclusions are based on the following findings. Ten days of increased voluntary physical activity in a running wheel significantly

elevated the level of neural precursor cell proliferation and the survival of the newborn neurons in the dentate gyrus. Despite the significant increase in the level of neurogenesis and in the number of proliferating microglial cells, microglia in the runners displayed the same level of activation as microglia in the dentate gyrus of the sedentary controls, based on their morphology, surface expression of activity markers and the expression level of genes reportedly involved in the regulation of neurogenesis. Although an increase in microglia proliferation was observed in running animals, this was not restricted to the dentate gyrus but was also present in other non-neurogenic sites of the hippocampus. Furthermore, in our experiments, no T cells were found to be present in the hippocampus and the surrounding tissue of both the runners and the sedentary controls.

In the dentate gyrus of adrenalectomised (ADX) rats Battista and colleagues found an increase in the number of activated microglia (activation stage 2 and 3), and a strong correlation between the number of activated microglia and number of newborn neurons (BrdU/PSA-NCAM double labeled cells) after four days of adrenalectomy. In the adrenalectomy model however, enhanced neurogenesis is accompanied by a massive increase in the level of cell death in the dentate gyrus (Krugers et al., 2007; Nichols et al., 2005), which might explain the activation of microglia. Since an elevated level of apoptosis is absent in the running wheel model (Koehl et al., 2008), this stimulus to drive microglia activation might be missing in our experiments. Clearly, microglia with altered morphology and atypical inflammatory profile, characteristic of CNS conditions with high levels of apoptotic cell death (Minghetti et al., 2005; Perry et al., 2002), were not more numerous in the runners than in the sedentary controls. Nevertheless, along with the increase in the number of BrdU positive nuclei in the subgranular zone, we found a significant increase in the number of BrdU/Iba1 double labeled microglia in the dentate gyrus of the runners, when compared to the sedentary controls. However, microglia proliferation was also

elevated in the cornu ammonis region of the hippocampus, suggesting that this proliferative response of microglial cells is most likely linked to the increased electrical activity in the hippocampus due to physical exercise (Buhl et al., 2003; Deisseroth et al., 2004; Hirase et al., 1999), rather than to increased neurogenesis (for the connection between electrical neuronal activity and microglia proliferation see Ehninger & Kempermann, 2003 and Lawson et al., 1993).

Due to our BrdU injection scheme (several hours before termination of the experiment), immunohistochemistry against BrdU and Iba1 also showed the events of microglia proliferation within a narrow time window on the last night before sacrifice. However, we did not find evidence for increase in the total number of microglia in the dentate gyri of the runners, compared to sedentary controls. It is thus rather unlikely that microglia proliferation started the first day and persisted up to the end of the experiment. It is more likely that microglia (just like neural precursors (Holmes et al., 2004) responded to the cumulative effect of the cues originating from increased physical activity and/or responded acutely to the increased hippocampal electrical activity in the active phase. The modest, but significant increase in the number of proliferating hippocampal microglia (from 2% to 5%) in the runners, together with the observation, that the total number of microglia in the different subregions of the dentate gyrus was basically the same in runners and sedentary controls, suggest the notion, that microglia proliferation most likely did not precede the increase in the level of neurogenesis in the dentate gyrus. Our data imply that microglia proliferation is not restricted to the neurogenic region of the hippocampus, and most likely does not pave the way for the onset of increase in the level of adult hippocampal neurogenesis in the running wheel model.

Ziv and colleagues described the presence of T cells and an increased number of MHCII expressing microglia in the dentate gyrus of rats after exposure to environmental enrichment for four weeks. They correlated

the presence of T cells and activated microglia with the increase in hippocampal neurogenesis, and supported their hypothesis by the observation that the basal level of subgranular zone neurogenesis was lower in SCID and nude mice when compared to wild type counterparts and it was not inducible by environmental enrichment, but was restorable by replenishment of T cells. One major interest of the present study was to investigate whether an interaction between microglia and CNS autoantigen specific T helper 2 cells would also be apparent in this model. T cell-microglia interaction is generally believed to happen through the interaction of T-cell receptor (TCR) on T cells and one of the two major histocompatibility complexes (MHC, in this case MHCII) on microglia, the two of which form a complex often referred to as the "immunological synapse" (Aloisi, 2001). This complex is the place of antigen presentation between the antigen presenting cell (APC, microglia) and the lymphocyte of the adaptive immune system (the T cells) in case of infection or under other inflammatory conditions. Generally, MHCII is almost completely absent in microglia in healthy adult mouse and rat brain (Beck et al., 2005; De Haas et al., 2008; Frank et al., 2006; Havenith, 1998; Islam et al., 1997). In agreement with this, we found almost no microglia expressing MHCII in the dentate gyrus (the number of observed MHCII positive parenchymal microglia in the dentate gyrus in the entire study was eight in total). MHCII expression was much more common in ependymal macrophages and some perivascular macrophages, both of which served as an internal control for our immunohistochemical staining. We examined the presence of T cells in the dentate gyrus and the surrounding brain structures as well. The presence of T cells in the CNS parenchyma under physiological conditions, as part of the immunological surveillance of the brain, is a debated issue. Their extravasation in postcapillary venules is possible, but under non-pathological conditions due to several factors it happens extremely rarely (Engelhardt & Ransohoff, 2005; Galea et al., 2007), if at all. In accordance with the generally accepted idea, that surveillance of

the CNS by encephalitogenic T cells is an (almost) undetectable phenomenon under physiological conditions, by the means of immunohistochemistry we did not find any CD3 positive cells in the hippocampal parenchyma of our experimental animals.

In order to exclude the possibility that we were unable to detect MHCII by immunohistochemistry, because its expression was below the detection level of this method, and also that we missed T cells because of their scarce presence, we repeated our experiment, and performed rapid isolation of microglia from the brains of our experimental animals, and subjected the isolated microglia to a more sensitive method, namely flow cytometry. These experiments confirmed our earlier findings. The microglia isolated from the hippocampus were not positive for MHCII, and there was no difference in the number of detected CD3+ positive T cells between the running mice and the control group, supporting the idea that increased (but also the basal level of) neurogenesis happens in the absence of microglia-T cell interaction - or this interaction is so rare, that it remains unobserved.

The discrepancies with the previously mentioned studies must be due to differences between the models applied. Enriched environment and voluntary physical activity are known to have distinct effects on the different aspects of both adult hippocampal neurogenesis and gliogenesis (Olson et al., 2006; Steiner et al., 2004). Microglia, as a possible factor in adult hippocampal neurogenesis, most likely behave differently in an enriched environment and upon increased voluntary physical activity.

Furthermore, voluntary physical activity affects both proliferation of precursors and survival/differentiation of the newborn cells, while exposure to an enriched environment only enhances survival/differentiation (Olson et al., 2006).

Another issue concerns the species difference. In the study by Ziv and colleagues T cells were observed in the dentate gyrus of rats only, but not in the different mouse strains. Similarly, MHCII-positive microglia

(detected by immunohistochemistry) were described solely in rats, and not in mice (Ziv et al., 2006).

Although several recent *in vitro* and *in vivo* studies have suggested a role for microglia in the regulation of different aspects of neurogenesis (Aarum et al., 2003; Butovsky et al., 2006; Cacci et al., 2008; Morgan et al., 2004; Walton et al., 2006), their precise function in respect of the regulation of adult hippocampal neurogenesis under physiological conditions remains largely unknown. A notion has developed in the field, that different modes of microglia activation are causatively linked to adult hippocampal neurogenesis under certain experimental conditions (Battista et al., 2006; Ziv et al., 2006). We provide evidence, that under physiological conditions, increased (and the basal) level of adult hippocampal neurogenesis can happen in the absence of several aspects of microglia activation in the dentate gyrus. Nonetheless, though we investigated microglia activation at multiple (transcriptional, protein and cellular) levels, with several markers, merely based on our findings however, we cannot exclude a role for microglia in adult neurogenesis. To ultimately reveal the role of microglia in the regulation of adult hippocampal neurogenesis under physiological conditions, one would have to be able to specifically inhibit microglia activity, as such. Pharmacological blockade of microglia proliferation or induction of "paralysis" of other aspects of microglia activation/function (such as cytokine or growth factor production) with the means that are available at the moment, has substantial side effects on neural cells (neurons, astrocytes and oligodendrocytes) and/or neurogenesis itself (Hailer, 2008). Thus, a model, which would enable us to specifically block microglia activity, still awaits its description. Nevertheless, based on our experimental findings we can conclude the acute increase in both aspects of adult hippocampal neurogenesis under physiological conditions is not necessarily associated with the classical signs of microglia activation. Moreover, the interaction of microglia with T cells, and subsequent neurosupportive activation is most likely not an

essential prerequisite for the increased neurogenesis due to voluntary physical activity in C57Bl/6 mice.

LIST OF ABBREVIATIONS (FIGURES AND TABLES)

IGF-1	insuline-like growth factor
BDNF	brain derived nerve growth factor
CD11b	integrin alpha-M
CD3	T-cell surface glycoprotein CD3
CD45	receptor-type tyrosine-protein phosphatase C
CD74	the invariant chain of the MHCII molecule
F4/80	EGF-like module-containing mucin-like hormone receptor-like 1
Gal1	galectin-1
GAPDH	glyceraldehyde-3-phosphate dehydrogenase
HMBS	hydroxymethylbilane synthase
HPRT1	hypoxanthine-guanine phosphoribosyltransferase
IFN-γ	interferon gamma
IL-1β	interleukin-1beta
IL-4	interleukin-4
IL-6	interleukin-6
iNOS	inducible nitric oxide synthase
LIF	leukemia inhibitory factor
MHCII	H-2 class II histocompatibility antigen
NT3	neurotrophin-3
TGF-β1	transforming growth factor-beta1
TNF-α	tumor necrosis factor alpha
β-actin	beta-actin

LIST OF REFERENCES

Aarum J, Sandberg K, Haeberlein SL, Persson MA. 2003. Migration and differentiation of neural precursor cells can be directed by microglia. Proc Natl Acad Sci U S A 100:15983-15988.

Aloisi F. 2001. Immune function of microglia. Glia 36:165-179.

Baron R, Nemirovsky A, Harpaz I, Cohen H, Owens T, Monsonego A. 2008. IFN-gamma enhances neurogenesis in wild-type mice and in a mouse model of Alzheimer's disease. FASEB J 22(8):2843-52.

Battista D, Ferrari CC, Gage FH, Pitossi FJ. 2006. Neurogenic niche modulation by activated microglia: transforming growth factor beta increases neurogenesis in the adult dentate gyrus. Eur J Neurosci 23:83-93.

Bauer S, Patterson PH. 2006. Leukemia inhibitory factor promotes neural stem cell self-renewal in the adult brain. J Neurosci. 26(46):12089-99.

Baxter AG. 2007. The origin and application of experimental autoimmune encephalomyelitis. Nat Rev Immunol 7:904-912.

Beck RD, Jr., Wasserfall C, Ha GK, Cushman JD, Huang Z, Atkinson MA, Petitto JM. 2005. Changes in hippocampal IL-15, related cytokines, and neurogenesis in IL-2 deficient mice. Brain Res 1041:223-230.

Bergami M, Rimondini R, Santi S, Blum R, Götz M, Canossa M. 2008. Deletion of TrkB in adult progenitors alters newborn neuron integration into hippocampal circuits and increases anxiety-like behavior. Proc Natl Acad Sci U S A 105(40):15570-5.

Bernardino L, Agasse F, Silva B, Ferreira R, Grade S, Malva JO. 2008. Tumor necrosis factor-alpha modulates survival, proliferation, and neuronal differentiation in neonatal subventricular zone cell cultures. Stem Cells 26(9):2361-71.

Bonde S, Ekdahl CT, Lindvall O. 2006. Long-term neuronal replacement in adult rat hippocampus after status epilepticus despite chronic inflammation. Eur J Neurosci 23: 965–974.

Buhl DL, Harris KD, Hormuzdi SG, Monyer H, Buzsaki G. 2003. Selective impairment of hippocampal gamma oscillations in connexin-36 knock-out mouse *in vivo*. J Neurosci 23:1013-1018.

Butovsky O, Ziv Y, Schwartz A, Landa G, Talpalar AE, Pluchino S, Martino G, Schwartz M. 2006. Microglia activated by IL-4 or IFN-gamma differentially induce neurogenesis

and oligodendrogenesis from adult stem/progenitor cells. Mol Cell Neurosci 31:149-160.

Cacci E, Ajmone-Cat MA, Anelli T, Biagioni S, Minghetti L. 2008. *In vitro* neuronal and glial differentiation from embryonic or adult neural precursor cells are differently affected by chronic or acute activation of microglia. Glia 56:412–425.

Cárdenas A, Moro MA, Hurtado O, Leza JC, Lizasoain I. 2005. Dual role of nitric oxide in adult neurogenesis. Brain Res Brain Res Rev 50(1):1-6.

Chen MK, Guilarte TR. 2006. Imaging the peripheral benzodiazepine receptor response in central nervous system demyelination and remyelination. Toxicol Sci 91:532-539.

Colucci-D'Amato L, di Porzio U. 2008. Neurogenesis in adult CNS: from denial to opportunities and challenges for therapy. Bioessays. 2008 Feb;30(2):135-45.

Das S, Basu A. 2008. Inflammation: A New Candidate in Modulating Adult Neurogenesis. J Neurosci Res 86:1199–1208.

De Haas AH, Boddeke HW, Brouwer N, Biber K. 2007. Optimized isolation enables *ex vivo* analysis of microglia from various central nervous system regions. Glia 55:1374-1384.

De Haas AH, Boddeke HW, Biber K. 2008. Region-specific expression of immunoregulatory proteins on microglia in the healthy CNS. Glia. 56(8):888-94.

Deisseroth K, Singla S, Toda H, Monje M, Palmer TD, Malenka RC. 2004. Excitation-neurogenesis coupling in adult neural stem/progenitor cells. Neuron 42:535-552.

Ehninger D, Kempermann G. 2003. Regional effects of wheel running and environmental enrichment on cell genesis and microglia proliferation in the adult murine neocortex. Cereb Cortex 13:845-851.

Ekdahl CT, Claasen JH, Bonde S, Kokaia Z, Lindvall O. 2003. Inflammation is detrimental for neurogenesis in adult brain. Proc Natl Acad Sci U S A 100:13632-13637.

Ekdahl CT, Kokaia Z, Lindvall O. 2008. Brain inflammation and adult neurogenesis: the dual role of microglia. (in press)

Engelhardt B, Ransohoff RM. 2005. The ins and outs of T-lymphocyte trafficking to the CNS: anatomical sites and molecular mechanisms. Trends Immunol 26:485-495.

Frank MG, Wieseler-Frank JL, Watkins LR, Maier SF. 2006. Rapid isolation of highly enriched and quiescent microglia from adult rat hippocampus: immunophenotypic and functional characteristics. J Neurosci Methods 15;151(2):121-30.

Galea I, Bechmann I, Perry VH. 2007. What is immune privilege (not)? Trends Immunol 28:12-18.
Goings GE, Kozlowski DA, Szele FG. 2006. Differential Activation of Microglia in Neurogenic Versus Non-neurogenic Regions of the Forebrain. Glia 54:329–342.

Hailer NP. 2008. Immunosuppression after traumatic or ischemic CNS damage: it is neuroprotective and illuminates the role of microglial cells. Prog Neurobiol 84(3):211-33.

Hanisch UK, Kettenmann H. 2007. Microglia: active sensor and versatile effector cells in the normal and pathologic brain. Nat Neurosci 10:1387-1394.

Havenith CE, Askew D, Walker WS. 1998. Mouse resident microglia: isolation and characterization of immunoregulatory properties with naive CD4+ and CD8+ T-cells. Glia 22:348-359.

Hirase H, Czurko A, Csicsvari J, Buzsaki G. 1999. Firing rate and theta-phase coding by hippocampal pyramidal neurons during 'space clamping'. Eur J Neurosci 11:4373-4380.

Holmes MM, Galea LA, Mistlberger RE, Kempermann G. 2004. Adult hippocampal neurogenesis and voluntary running activity: circadian and dose-dependent effects. J Neurosci Res 76:216-222.

Iosif RE, Ekdahl CT, Ahlenius H, Pronk CJ, Bonde S, Kokaia Z, Jacobsen SE, Lindvall O. 2006. Tumor necrosis factor receptor 1 is a negative regulator of progenitor proliferation in adult hippocampal neurogenesis. J Neurosci 26(38):9703-12.

Ishibashi S, Kuroiwa T, Sakaguchi M, Sun L, Kadoya T, Okano H, Mizusawa H. 2007. Galectin-1 regulates neurogenesis in the subventricular zone and promotes functional recovery after stroke. Exp Neurol 207(2):302-13.

Islam A, Mustafa M, Mustafa A, Olsson T, Winblad B, Adem A. 1997. Expression of MHC class II CD4+ and ED1 molecules in association with selective hippocampal neuronal degeneration after long-term adrenalectomy. Neuroreport 8:987-990.

Jagasia R, Song H, Gage FH, Lie DC. 2006. New regulators in adult neurogenesis and their potential role for repair. Trends Mol Med 12:400-405.

Kreutzberg GW. 1996. Microglia: a sensor for pathological events in the CNS. Trends Neurosci 19:312-318.

Koehl M, Meerlo P, Gonzales D, Rontal A, Turek FW, Abrous DN. 2008. Exercise-induced promotion of hippocampal cell proliferation requires β-endorphin. FASEB J 22(7):2253-62.

Koo JW, Duman RS. 2008. IL-1beta is an essential mediator of the antineurogenic and anhedonic effects of stress. Proc Natl Acad Sci U S A 105(2):751-6.

Krugers HJ, van der Linden S, van Olst E, Alfarez DN, Maslam S, Lucassen PJ, Joëls M. 2007. Dissociation between apoptosis, neurogenesis, and synaptic potentiation in the dentate gyrus of adrenalectomized rats. Synapse 61(4):221-30.

Lawson LJ, Perry VH, Gordon S. 1993. Microglial responses to physiological change: osmotic stress elevates DNA synthesis of neurohypophyseal microglia. Neuroscience 56(4):929-38.

Mandyam CD, Harburg GC, Eisch AJ. 2007. Determination of key aspects of precursor cell proliferation, cell cycle length and kinetics in the adult mouse subgranular zone. Neuroscience 146(1):108-22.

Matsushima GK, Morell P. 2001. The neurotoxicant, cuprizone, as a model to study demyelination and remyelination in the central nervous system. Brain Pathol 11:107-116.

Ming GL, Song H. 2005. Adult neurogenesis in the mammalian central nervous system. Annu Rev Neurosci 28:223-250.

Minghetti L, Ajmone-Cat MA, De Berardinis MA, De Simone R. 2005. Microglial activation in chronic neurodegenerative diseases: roles of apoptotic neurons and chronic stimulation. Brain Res Brain Res Rev 48(2):251-6.

Monje ML, Toda H, Palmer TD. 2003. Inflammatory blockade restores adult hippocampal neurogenesis. Science 302:1760-1765.

Morgan SC, Taylor DL, Pocock JM. 2004. Microglia release activators of neuronal proliferation mediated by activation of mitogen-activated protein kinase, phosphatidylinositol-3-kinase/Akt and delta–Notch signalling cascades. J Neurochem 90:89-101.

Nakanishi M, Niidome T, Matsuda S, Akaike A, Kihara T, Sugimoto H. 2007. Microglia-derived interleukin-6 and leukaemia inhibitory factor promote astrocytic differentiation of neural stem/progenitor cells. Eur J Neurosci 25:649-658.

Nichols NR, Agolley D, Zieba M, Bye N. 2005. Glucocorticoid regulation of glial responses during hippocampal neurodegeneration and regeneration. Brain Res Brain Res Rev 48:287-301.

Okano H, Sakaguchi M, Ohki K, Suzuki N, Sawamoto K. 2007. Regeneration of the central nervous system using endogenous repair mechanisms. J Neurochem 102:1459-1465.

Olson AK, Eadie BD, Ernst C, Christie BR. 2006. Environmental enrichment and voluntary exercise massively increase neurogenesis in the adult hippocampus via dissociable pathways. Hippocampus 16:250-260.

Perry VH, Cunningham C, Boche D. 2002. Atypical inflammation in the central nervous system in prion disease. Curr Opin Neurol 15(3):349-54.

Sakaguchi M, Shingo T, Shimazaki T, Okano HJ, Shiwa M, Ishibashi S, Oguro H, Ninomiya M, Kadoya T, Horie H, Shibuya A, Mizusawa H, Poirier F, Nakauchi H, Sawamoto K, Okano H. 2006. A carbohydrate-binding protein, Galectin-1, promotes proliferation of adult neural stem cells. Proc Natl Acad Sci U S A 103(18):7112-7.

Salam JN, FoxJM, DeTroy EM, Guignon H, Wohl DF, Falls WA. 2008. Voluntary exercise in C57 mice is anxiolytic across several measures of anxiety. Behav Brain Res (in press)

Shimazu K, Zhao M, Sakata K, Akbarian S, Bates B, Jaenisch R, Lu B. 2006. NT-3 facilitates hippocampal plasticity and learning and memory by regulating neurogenesis. Learn Mem 13(3):307-15.

Steiner B, Kronenberg G, Jessberger S, Brandt MD, Reuter K, Kempermann G. 2004. Differential regulation of gliogenesis in the context of adult hippocampal neurogenesis in mice. Glia 46:41-52.

Stranahan AM, Lee K, Mattson MP. 2008. Central Mechanisms of HPA Axis Regulation by Voluntary Exercise. Neuromol Med 10:118–127.

Taupin P. 2006. Adult neural stem cells, neurogenic niches, and cellular therapy. Stem Cell Rev 2:213-219.

Taupin P. 2007. BrdU immunohistochemistry for studying adult neurogenesis: paradigms, pitfalls, limitations, and validation. Brain Res Rev 53(1):198-214.

van der Borght K, Ferrari F, Klauke K, Roman V, Havekes R, Sgoifo A, Van der Zee EA, Meerlo P. 2006. Hippocampal cell proliferation across the day: increase by running wheel activity, but no effect of sleep and wakefulness. Behav Brain Res 167:36-41.

van Praag H. 2008. Neurogenesis and exercise: past and future directions. Neuromolecular Med 10(2):128-40.

Wachs FP, Winner B, Couillard-Despres S, Schiller T, Aigner R, Winkler J, Bogdahn U, Aigner L. 2006. Transforming growth factor-beta1 is a negative modulator of adult neurogenesis. J Neuropathol Exp Neurol 65(4):358-70.

Walton NM, Sutter BM, Laywell ED, Levkoff LH, Kearns SM, Marshall GP, Scheffler B, Steindler DA. 2006. Microglia instruct subventricular zone neurogenesis. Glia 54:815-825.

Zhao C, Deng W, Gage FH. 2008. Mechanisms and functional implications of adult neurogenesis. Cell 132:645-660.

Ziv Y, Ron N, Butovsky O, Landa G, Sudai E, Greenberg N, Cohen H, Kipnis J, Schwartz M. 2006. Immune cells contribute to the maintenance of neurogenesis and spatial learning abilities in adulthood. Nat Neurosci 9:268-275.

Ziv Y, Schwartz M. 2008. Immune-based regulation of adult neurogenesis: implications for learning and memory. Brain Behav Immun 22:167-176.

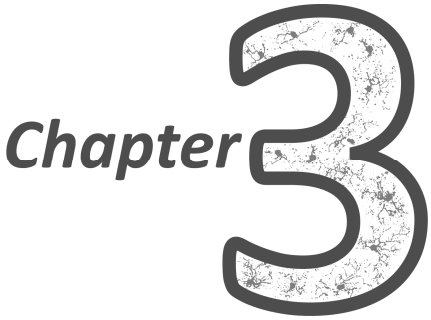

Different microglia phenotypes in white and grey matter of the central nervous system

Marta Olah[1], Stefanie Seifert[3], Divya Raj[1], Michel Meijer[1], Nieske Brouwer[1], Helmut Kettenmann[3], Knut P.H. Biber[1,2], Hendrikus W.G.M. Boddeke[1]

[1] Department of Neuroscience, Section Medical Physiology, UMCG-RuG, Groningen, The Netherlands

[2] Department of Psychiatry and Psychotherapy, Section Molecular Psychiatry, University Medical Center Freiburg, Freiburg, Germany

[3] Cellular Neuroscience, Max Delbruck Center, Berlin, Germany

manuscript in preparation

ABSTRACT

It has been suggested that microglia in different central nervous system (CNS) regions display different phenotypes. These regional differences in phenotype might contribute to the ethiology and pathophysiology of different CNS diseases and disorders. Indeed, recent studies have shown that the regional differences in microglia in different CNS compartments go beyond the morphology of these cells and can be readily detected by differences in surface expression of immunologically relevant molecules, such as CD86 and CD11b. Our aim was to investigate the anticipated regional differences in microglia phenotype in detail with the help of *ex vivo* immunophenotyping, *in vitro* functional assays and microarray gene expression analysis. We focused on microglia residing in the white- (corpus callosum) and the grey matter (cerebral cortex). Our findings suggest, that white matter microglia are phenotypically different from grey matter microglia in the adult murine brain even under physiological conditions. The genome wide gene expression analysis revealed several significantly differently expressed genes, many of which are involved in the innate and adaptive immune responses. Furthermore, in an endotoxemia model white matter microglia responded to systemic inflammation to a greater extent than their grey matter counterparts. Moreover, some of the observed differences seemed to be inherent to the cells themselves, as they were retained even in cultre, such as the differences in the intracellular calcium responses to ATP. Our results thus point to a phenotype difference between white and grey matter microglia that might have functional consequences in respect of several pathological conditions in the CNS.

INTRODUCTION

Since the seminal work of Lawson and colleagues it is known, that microglia, the resident immune cells of the central nervous system (CNS), are morphologically multifarious, displaying a wide variety of cell shapes and cellular densities in different anatomical sites of the brain (Lawson et al., 1990; Vela et al., 1995; Mittelbronn et al., 2001). Moreover, their postnatal differentiation follows a region specific time course in the developing cerebrum (Wu et al., 1993). Further research in microglia diversity have revealed, that the regional differences in microglia go far beyond their morphology and cellular density and can be readily detected as differences in the surface expression of activation markers (Wu et al., 1997; De Haas et al., 2008), neurotrophin and cytokine production (Elkabes et al., 1996; Ren et al., 1999), neurotoxicity (Kim et al., 2000) and support of neurogenesis (Goings et al., 2006). It has been suggested that these regional differences in microglia phenotype are of significant importance, since they might contribute to the etiology and pathophysiology of different CNS disease and disorders (Das et al., 1995; Garcion et al. 1997; Calingasan et al. 1998; Semmler et al., 2005; Huber et al., 2006; Carson et al., 2007).

It has been hypothesised that the described regional differences in microglia are to be attributed, at least in part, to the regional differences in the cellular environment in which the microglial cells reside. Such a cellular milieu consists of an active regulatory activity originating from neuronal cells (Biber et al., 2007), the blood-brain barrier and the extracellular matrix. Thus, not surprisingly, an increasing line of evidence suggests that the two most distinct compartments in the central nervous system, in respect of microglia phenotype, are the white and the grey matter. Based on the observation that corpus callosum microglia in mouse have a constitutively higher level of expression of co-stimulatory molecules such as B7.2, it has been suggested that microglia residing in the white matter exist at a higher

basal level of activation under physiological conditions than microglia residing in the non-myelinated regions of the CNS (Carson et al., 2007). Supporting this idea, it has been shown that the number of HLA-DR/MHCII positive microglia and/or the cellular expression level of this molecule in humans, monkeys, dogs and rats under physiological conditions is higher in the white matter (corpus callosum, capsula interna) than in the cerebral cortex (Styren et al., 1990; Sasaki et al., 1992; Gehrmann et al., 1993; Ogura et al., 1994; Ong et al., 1995; Alldinger et al. 1996; Sheffield et al., 1998). Moreover, it has been described, that microglia residing in the white matter of the forebrain, but also microglia in the spinal cord, are more affected by the aging related increase in the basal level of activation than their grey matter counterparts (Ogura et al., 1994; Seffield et al., 1998; Kullberg et al., 2001). Nonetheless, in an experimental model of chronic cerebral hypoperfusion in the rat microglia activation was mainly observed in the white matter (Wakita et al., 1994; Wakita et al., 1995; Wakita et al., 1998). Multiple sclerosis is another pathological condition of the CNS where the differences between white and grey matter microglia intriguingly manifest themselves. Grey matter lesions in MS have been described to display less pronounced inflammation, microglia activation and complement deposition, when compared to white matter lesions (Brink et al., 2005; Bo, 2009), providing further support to the above mentioned hypothesis.

Based on these evidences we formulated the hypothesis that microglia residing in the white and the grey matter of the central nervous system are phenotypically different. Our aim was to test this hypothesis. Here we report phenotype differences between two microglia populations in the healthy adult murine brain: the corpus callosum and the cerebral cortex. Our gene expression analysis sheds light on the subtantial difference that exists at the transcriptome level between these two subpopulations of microglia. Among the significantly differently expressed genes were genes involved in both the innate and adaptive

arm of immunity. Several of these differences have also been investigated at the protein level in our study. Nonetheless, acutely isolated microglia from the white and grey matter proved to be significantly different in respect of a variety of functional aspects characteristic of microglia cells: phagocytosis, migration, reactive oxigene species production, ATP evoked calcium signaling and antigen presentation. Moreover, in an endotoxemia model microglia from the white matter displayed higher levels of activation when compared to microglia isolated from gray matter. Our findings thus provide evidence for the differences existing between the microglia population of the corpus callosum and the cerebral cortex at the transcriptional, phenotype and functional level.

MATERIALS AND METHODS

Animals

All experiments were approved by the Institutional Animal Care and Use Committee of the University of Groningen (IACUC-RuG (DEC)).

Young adult (8 week old) C56Bl/6 male mice were ordered from Harlan, The Netherlands. The animals received normal chow and had access to food and water ad libitum. The animals were kept on a 12:12 hours light-dark cyle regime, with lights on at 8 AM. Animals were subjected to an experiment after at least a week of acclimatisation.

Each biological replicate (independent experiment) consisted of a pool of three animals in order to obtain a sufficient amount of microglia from the white matter (corpus callosum). For each assay at least three independent experiments were perfomed, unless mentioned otherwise. In the case of gene expression analysis, eight biological replicates were used, each consisting of a pool of three to five animals.

Morphometry

For quantitative analysis of the morphology of white and grey matter microglia we performed immunohistochemistry on the brain sections of young adult mice against Iba1, a microglia marker, following the standard immunohistochemistry protocol. In brief, animals were transcardially perfused with saline under pentobarbital anesthesia followed by perfusion with 4% PFA. Brains were postfixed for 24 hours, equilibrated in 20% sucrose solution and cryosectioned at 50 µm thickness. Free floating brain sections were blocked with 5% normal goat serum and subsequently incubated with primary antibody (rabbit anti-Iba1 antibody; Wako) for 72 hours at 4°C. Primary antibody was detected using Cy3 coupled goat anti-rabbit (Jackson Immuno Research). Sections were mounted on a glass slide and coverslipped with Mowiol (Calbiochem). Confocal images of white and grey matter microglia were made with a 63x objective on a Leica SP2 confocal laser

scanning microscope. Confocal images were deconvoluted with a Huygens Professional imaging software package (SVI). The 3D reconstruction and morphometric analysis of the cells was achieved with the help of the Filament Tracer function of the Imaris 7.0 software (Bitplane).

Endotoxemia model

Animals were injected intraperitoneally either with 50 µg of LPS dissolved in physiological salt solution/25 g body weight or with equal volume (commonly 100 µl) of saline. Eight hours after injection, the animals were sacrificed by transcardial perfusion with saline under pentobarbital (Euthasol, ASTfarma) anaesthesia. Brains were removed from the skull, white and grey matter regions were dissected and microglia were isolated from the white and grey matter tissue as described below. After isolation white and grey matter microglia were analysed by means of flow cytometry.

Acute isolation of microglia from adult murine brain

Animals were sacrificed by means of transcardial saline perfusion under pentobarbital anaesthesia. The brains were isolated and kept in ice cold dissection medium (HBSS containing 0,6 % glucose and 15 µM HEPES buffer (all from Gibco)). The forebrain was cut into three approximately 1,5 mm thick coronal sections with the help of a surgical blade. Under a dissection microscope the coronal sections were further dissected into white (corpus callosum) and grey (cerebral cortex) matter on ice. From the collected tissue microglia were isolated at high purity (> 98%) with the help of a discountinous Percoll gradient (De Haas et al., 2008). All the steps of the isolation were performed at 4°C. Briefly, the tissue was transferred to a bouncing tissue homogeniser and mechanically dissociated. The tissue homogenate was further homogenised with four flamed Pasteur pipettes of decreasing diameter until single cell suspension was attained. The cell suspension was then filtered through

a 70 µm cell strainer, washed with the dissection medium and pelleted through centrifugation. The pellet was resuspended in 75% Percoll, overlayed with 25% Percoll and finally with PBS. The density separation was achieved by centrifugation of the discontinous Percoll gradient in a swinging bucket centrifuge at a force of 800 g for 25 minutes. After centrifugation microglia were collected from the 75% - 25% Percoll interface, washed with PBS and pelleted by centrifugation. The cell pellet was resuspended in culture medium (DMEM containing 5% fetal calf serum (FCS), 1% penicillin/streptomycin and 1% sodium-pyruvate) for functional assays. In case of flow cytometric analysis of surface expression markers the pellet was resuspended in PBS. For total RNA extraction for further gene expression analysis the pellet was lysed in lysis buffer. In some cases (e.g. gene expresson analysis) before the final centrifugation a small sample of few thousand cells was taken out from the cell suspension to assess the purity of microglia isolation by the means of flow cytometry.

Functional assays

Electrophysiology and calcium-imaging

For electrophysiology and calcium imaging microglia from white and grey matter were isolated as described above and seeded on poly-L-lysine coated glass coverslips. Cells were cultured in general culture medium (DMEM (Gibco) containing 5% FCS) for at least 2-3 hours prior to commencing with the measurements. Both electrophysiological measurements and calcium imaging were perfomed at room temperature in a measurement chamber equipped with an upright microscope (Axiovert FS, Zeiss) and water immersion objectives. The measurement chamber was continuosly perfused with HEPES buffer (containing (in mM) NaCl 150,0; KCl 5,4; $MgCl_2$ 1,0; $CaCl_2$ 2,0; HEPES 10,0; glucose 10,0; pH adjusted with NaOH to 7,4) at a rate of 3-5 ml/minute. The bath solution was gassed with carbogen (5% CO_2 and

95% O_2). ATP was applied by switching the flow of the bath solution from HEPES solution to the ATP containing HEPES, and back.

The electrophysiological properties of corpus callosum and cortex resident microglia were also investigated *in situ*, in acute brain slices prepared from adult (8 weeks old) CX3CR1-GFP mice. Organotypical slices were prepared as follows: mice were decapitated, the brain was removed, washed in ice cold artificial cerebrospinal fluid (ACSF) and subsequently sectioned at 130 µm thickness with a vibratome (Leica VT1000S). During recording, acute brain slices were superfused with ACSF.

The current profile of white and grey microglia was investigated by whole cell patch clamp recording *in situ* in acute brain slices and in acutely isolated microglia on the day of isolation (3-8 hours *in vitro*) and after 22-36 hours culturing. The glass pipettes were pulled from borosilicate glass capillaries and their resistance was in the range of 5-8 MΩ. The patch pipette solution contained (in mM) KCl 130,0; $MgCl_2$ 2,0; $CaCl_2$ 0,5; EGTA 5,0 and HEPES 10. The pH was adjusted to pH 7,3 and the osmolarity was 285 mmol/l. All substances were obtained from Sigma-Aldrich (Munich, Germany). The membrane potential of microglia was clamped to a holding potential of -70 mV in the case of acute slices, and -20 mV, in the case of acutely isolated cells. Microglia were depolarised or hyperpolarised through a ramp of voltages, the steps lasting 50 ms each. To characterise the microglia current profile the membrane potential was depolarised through 10 steps of 10 mV and hyperpolarised with 15 steps of -10 mV. To investigate the effect of ATP on the microglial current profile, the cell membrane was depolarised with 5 steps of 20 mV and hyperpolarised with 7 steps of -20mV. After baseline measurements for several minutes, ATP was applied in the flow of the bathing solution for 60 seconds. Whole cell uncompensated currents were recorded with an EPC-9/10 amplifier (HEKA Electronics). The data were captured and analysed using TIDA software.

For calcium imaging after 24 hours *in vitro* cells were incubated with Fluo-4 dye (working concentration 5 µM; Invitrogen) for 30 minutes at 37°C in HEPES loading buffer and were allowed to recover for an additional 15 minutes in HEPES buffer containing glucose. After the transfer of the coverslips to the imaging chamber the cells were allowed to acclimatise for at least five minutes. Cells were imaged with a 20x water immersion objective, 300 ms exposure time at a sampling rate of 0,5 Hz. After approximately 3-5 minutes of baseline recording, ATP (at 100 µM and 1 mM concentrations) was applied to the cells for 30 minutes, after which the cells were imaged for up to 6-7 minutes. The data acquisition was done with the TIDA software. A region of interest (ROI) was placed over each cell in the field on the brightfield image. Intensity measurements were perfomed on-line for each ROI, within which the average of the brightest pixels was calculated. The intensity versus time plots were further processed in Excel and the area under the curve was determined with the use of SigmaPlot version 8.0.

Phagocytosis assay

After isolation the white and grey matter microglia cells were resuspended in culture medium and seeded in 8 well Lab-Tek™ II Chambered Coverglass (from Nunc) at a density of 5000 cells per well. Cells were allowed to attach for 20 minutes. Two hours after seeding the medium was replaced with culture medium containing 25 µg/ml of pHrodo™ E.coli BioParticles® conjugate (Invitrogen). The cell were subsequently imaged for 18 hours with a Solamere Nipkow spinning disc confocal laser scanning microscope mounted on a Leica DM IRE2 inverted microscope equipped with a Stanford Photonics XR/Mega-10I (intensified) CCD camera and an ASI MS2000 Piezo motorised stage, and a temperature (37°C) and CO_2 concentration (5%) controlled imaging chamber. For exciting the pHrodo dye the 568 nm laser line of a dynamic Krypton laser was used. During image acquisition a HC PL APO CS 10x dry objective was used. A bright field and a red channel image

was acquired every 5 minutes at each condition ("white" and "grey matter" wells). For both white and grey matter wells one field per well, which contained in both cases 20-30 cells, was imaged. Multiple cells were selected as regions of interest (ROIs) based on the bright field images. The intensity of the ROIs in the red channel images was measured in each frame of the entire image stack with the help of an ImageJ plug in (written by K. Sjollema; UMCG-UMIC, Groningen, The Netherlands). The data were plotted as a time versus intensity curve and the time needed to reach half maximum response for each cell was determined in Excel.

Gene expression analysis

In this study for each condition (white and grey matter) eight biological replicates were used, each consisting of a pool of three animals. Each sample was tested for purity of microglia preparation with flow cytometry. The microglia purity was routinly above 98%.

After the dissection of white and grey matter and isolation of microglia, the cells were lysed in lysis buffer provided with the RNA isolation kit. Total RNA isolation was performed with a Qiagen RNeasy® Micro kit. The amount of the isolated RNA was determined with the help of a NanoDrop™ 2000 spectrophotometer. 25 ng of total RNA was used from each sample. The integrity of the RNA samples was confirmed with an Agilent Bioanalyzer automated electrophoresis system using the RNA 6000 Pico LabChip® Kit. The RNA integrity was determined by visual examination of the electropherograms and by the RNA integrity number (RIN). Only samples with RIN > 8 and clear 18S and 28S ribosomal RNA peaks were included in the gene expression study. The RNA was processed for microarray analysis: copyDNA synthesis, amplification, biotin labeled copyRNA production was done with the help of an Illumina® TotalPrep™-96 RNA Amplification Kit from Ambion. Subsequently 750 ng of biotin labeled cRNA was hybridised to Illumina MouseRef-8 v2.0 bead arrays according to the protocol provided by the

manufacturer. The bead arrays were then stained with streptavidin-Cy3 and scanned with the help of iScan System from Illumina. The data were normalised in BeadStudio software from Illumina and subsequently analysed with the help of GeneSpring software. Two approaches were applied: 1) with significance testing (t-test, Benjamini correction for multiple testing) we determined the genes that were expressed at a significantly different level ($p < 0,05$, fold change > 1,5) in white and grey matter microglia; 2) with an empirically determined cut-off value (noise level) we determined the genes that were present in either white or grey matter microglia. A functional annotation chart of the differently expressed genes was generated using the DAVID Bioinformatics Resources web application (http://david.abcc.ncifcrf.gov/).

Flow cytometry

Cells resuspended in PBS were Fc blocked with 1% anti-CD16/32 (eBiosciences) for 15 minutes, stained for different surface markers for 20 minutes, washed with PBS, pelleted with centrifugation and resuspended in 200 µl of PBS for subsequent flow cytometric analysis. During the staining procedure and before analysis, cells were kept on ice. Stained cells were analysed with the help BD^{TM} LSR II multi-laser flow cytometer. The flow cytometric measurements were evaluated with the help of WinList 6.0 software. The results are presented as histograms. In the statistical analysis of the data the geometric mean fluorescent intensities (MFI) of each measurement was used.

To determine the purity of microglia preparation a small sample of the attained cell suspension was stained for CD11b and CD45 together with a live cell marker DRAQ5^{TM} (Biostatus Ltd.). For the genome wide gene expression study we determined microglia purity as the percentage of CD11bhigh/CD45low/DRAQ5+ cells (live microglia) among the DRAQ5+ cells (live cells).

For immunophenotyping of mouse microglia cells the following antibodies were used: phycoerythrin (PE) coupled rat anti-mouse CD11b

(Cat.No. 12-0112), allophycocyanin (APC)-AlexaFluor750 coupled rat anti human/mouse CD11b (Cat.No. 27-0112; discontinued), AlexaFluor700 coupled rat anti-mouse CD45 (Cat.No. 56-0451), fluorescein isothiocyanate (FITC) coupled rat anti-mouse CD45 (Cat.No. 11-0451), FITC coupled armenian hamster anti-mouse CD40 (Cat.No. 11-0402), FITC coupled armenian hamster anti-mouse CD80 (Cat.No. 11-0801), FITC coupled rat anti-mouse CD86 (Cat.No. 11-0862), FITC coupled rat anti-mouse F4/80 (Cat.No. 11-4801), PE coupled rat anti-mouse CXCR3 (from R&D, Cat.No. FAB1685P), FITC coupled rat anti-mouse MHC class II (Cat.No. 11-5321), PE coupled rat anti-mouse TLR1 (Cat.No. 12-9011), FITC coupled rat anti-mouse TLR2 (Cat.No. 11-9021), PE coupled mouse anti-mouse TLR4 (Cat.No. 12-9041). For each staining the apropriate isotype control was used in a concentration- matched manner. All anti-mouse flow cytometry antibodies (and the corresponding isotype controls) were obtained from eBiosciences, unless mentioned otherwise.

Statistics

Statistical analysis was performed in SPSS 12.0.1 software. In most cases Student's t-test was used to compare means.

In the case of microglia current profiles, data were tested for normality with the Shapiro-Wilk test. Since in most of the groups the data points were not normal distributed Kruskall-Wallis test (nonparametric) was used to compare the groups. To achieve pairwise comparison Mann-Whitney-U-Test followed by a Bonferroni-posthoc test was performed. Data are displayed as median ± the 25^{th} and the 75^{th} percentile. Groups were graphically depicted as box plots with whiskers, indicating the minimum and maximum of all the data within one group.

The statistical analysis of the gene expression data was perfomed in GeneSpring software. Unpaired t-test was perfomed with an asymptotic p value computation. As a multiple testing correction Banjamini-Hochberg method was used.

P-values in all cases were considered as significant if $p < 0,05$ (*); $p < 0,01$ (**); $p < 0,001$ (***).

RESULTS

Quantitative morphometric analysis of white and grey matter microglia in situ

Previous studies have described morphological differences between microglia residing in white and grey matter based on visual examination. We have investigated morphological differences between cortical and callosal microglia using a quantitative morphometric method. For this purpose random Iba1 immunopositive cells were chosen from both regions of the CNS. Cells were imaged by confocal laser scanning microscopy and their morphological structure was reconstructed using Imaris^{R} software. With the Filament Tracer plug in we determined objective measures of cell morphology for each cell. During the analysis we mainly focused on the dendritic arborisation of the cells, since the size, spatial arrangement and ramification of their processes are primarily affected when microglia transform from ramified/resting to activated state. Based on the objective measures, white matter microglia are morphologically different from grey matter microglia. The total dendrite length per cell was significantly higher in grey matter microglia (around 600 µm) than in white matter microglia (approximately 200 µm) (Figure 1C). Accordingly, the total dendritic volume per cell was more than three times larger in grey matter microglia (on average 300 μm^3) than in white matter microglia (less than 100 μm^3) (Figure 1D). Moreover grey matter microglia bear significantly more primary ramification points on their dendritic arborisation than their white matter counterpart. Grey matter microglia have on average five primary branching points per cell in their dendritic arborization, while white matter microglia have only two (Figure 1E). Based on their average dendrite length per cell and average dendrite diameter per cell

white and grey matter microglia also formed well-separated populations (Figure 1F).

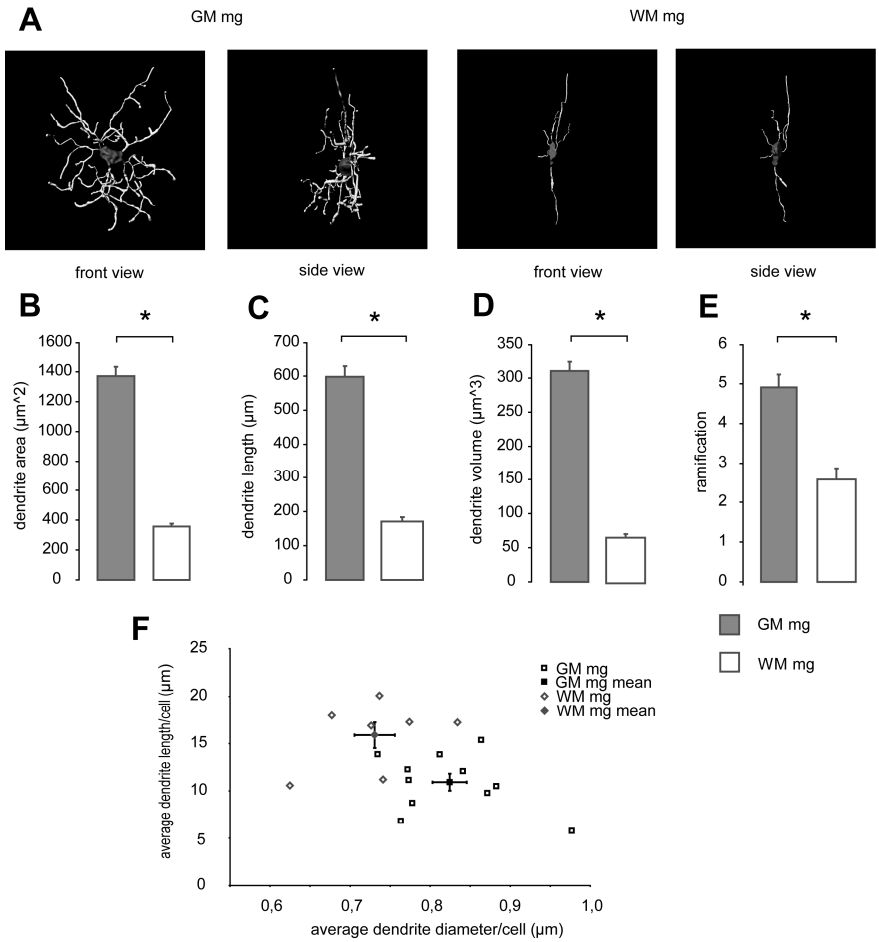

Figure 1. Microglia residing in the white matter are significantly different from microglia in the grey matter in respect of multiple measures of cell morphology. Morphometric analysis of corpus callosum (white matter) and cerebral cortex (grey matter) resident microglia with Filament Tracer function of the Imaris software package. **A** Snapshots from the 3D reconstructions of white and grey matter microglia. Front view is perpendicular to the coronal plane, while side view is perpendicular to the saggital plane. In **B**, **C**, **D** and **E** the total dendrite area per cell, the total dendrite length per cell , the total dendrite volume per cell and the total number of ramification points per cell is plotted for white and grey matter microglia, respectively. In **F** the average dendrite diameter per cell is plotted against the average dendrite length per cell. Error bars in **B**, **C**, **D**, **E** and **F** represent the standard error of the mean (SEM). N = 10 for both white matter and grey matter microglia. (* represents a p value < 0,001; GM mg grey matter microglia; WM mg white matter microglia)

Functional analysis of white and grey matter microglia

We were further interested in possible differences in the functionality of white and and grey matter microglia *ex vivo* and *in vitro*. We focused on three main functional aspects of microglia, which are believed to be representative regarding their activation state: electrophysiological properties, intracellular calcium responses and phagocytic capacity.
The electrophysiological properties of acutely isolated microglia were investigated using the whole cell patch clamp paradigm with two approaches: we determined the current profiles of white and grey matter microglia and the change in their membrane conductance properties upon stimulation with ATP. The electrophysiological characteristics of microglia were measured in acute adult brain slices *in situ*, and in acutely isolated microglia on the day of isolation (3-8 hours *in vitro*) as well as after an extended time (22-36 hours) in culture (Figure 2A''). Current responses to depolarizing and hyperpolarizing voltage steps between 50mV and -160mV were recorded with 10mV increments. Averaged current amplitudes of the -120mV step (inward currents) and of the 0mV step (outward currents) were analyzed. The average current for a particular condition is discussed below as median/75th percentile/25th percentile for the inward currents and median/25th percentile/75th percentile for the outward currents.

As shown on Figure 2A'' corpus callosum microglia *in situ* had an average inward current of -36,2/-49,5/-20,6 pA and outward current of 25,7/21,6/28,3 pA (N = 10). In acutely isolated white matter microglia both inward and outward currents were significantly reduced after 3-8 hours in culture (inward currents -14,8/-18,6/-6,4 pA and outward currents 5,5/5,0/11,1 pA) (N = 18) when compared to their currents in acute slices. After 22-36 hours in culture white matter microglia failed to recover their inward and outward currents which still significantly

differed from the ones measured in acute brain slices (inward current -18,6/-40,5-9,7 pA and outward currents 8,8/6,9/13,9 pA) (N = 68).
Cortical microglia in acute slices displayed an average inward current of -31,2/-41,4/-26,2 pA and outward current of 22,8/17,9/29,6 pA (N = 10), (Figure 2A''). Acutely isolated grey matter microglia had an average inward current (-8,4/-27,6/-6,5 pA) and an average outward current (10,1/8,3/13,9 pA) (N = 17), that were significantly reduced when compared to the relevant currents in acute slices. After 22-36 hours in culture, acutely isolated grey matter microglia still had significantly reduced outward currents (9,1/6,0/13,1 pA), but their inward currents were recovered (-22,5/-63,3/-12,3 pA) (N = 63) to the level of the inward currents of cortical microglia in acute slices.
Thus, acutely isolated white matter (corpus callosum) and grey matter (cerebral cortex) microglia were different in the induction of their inward currents in culture. However, white and grey matter microglia did not differ from each other significantly at any time point investigated in respect of the amplitudes of their inward or outward currents. (* $p < 0,05$; ** $p < 0,01$; *** $p < 0,001$). The changes in the electrophysiological membrane properties of white (N = 5) and grey (N = 9) matter microglia upon ATP stimulation were investigated 24 hours after isolation. As the representative recordings clearly demonstrate (Figure 2B'), the induction of inward current upon ATP stimulation was much stronger in white than in grey matter microglia, whereas outward currents did not differ.

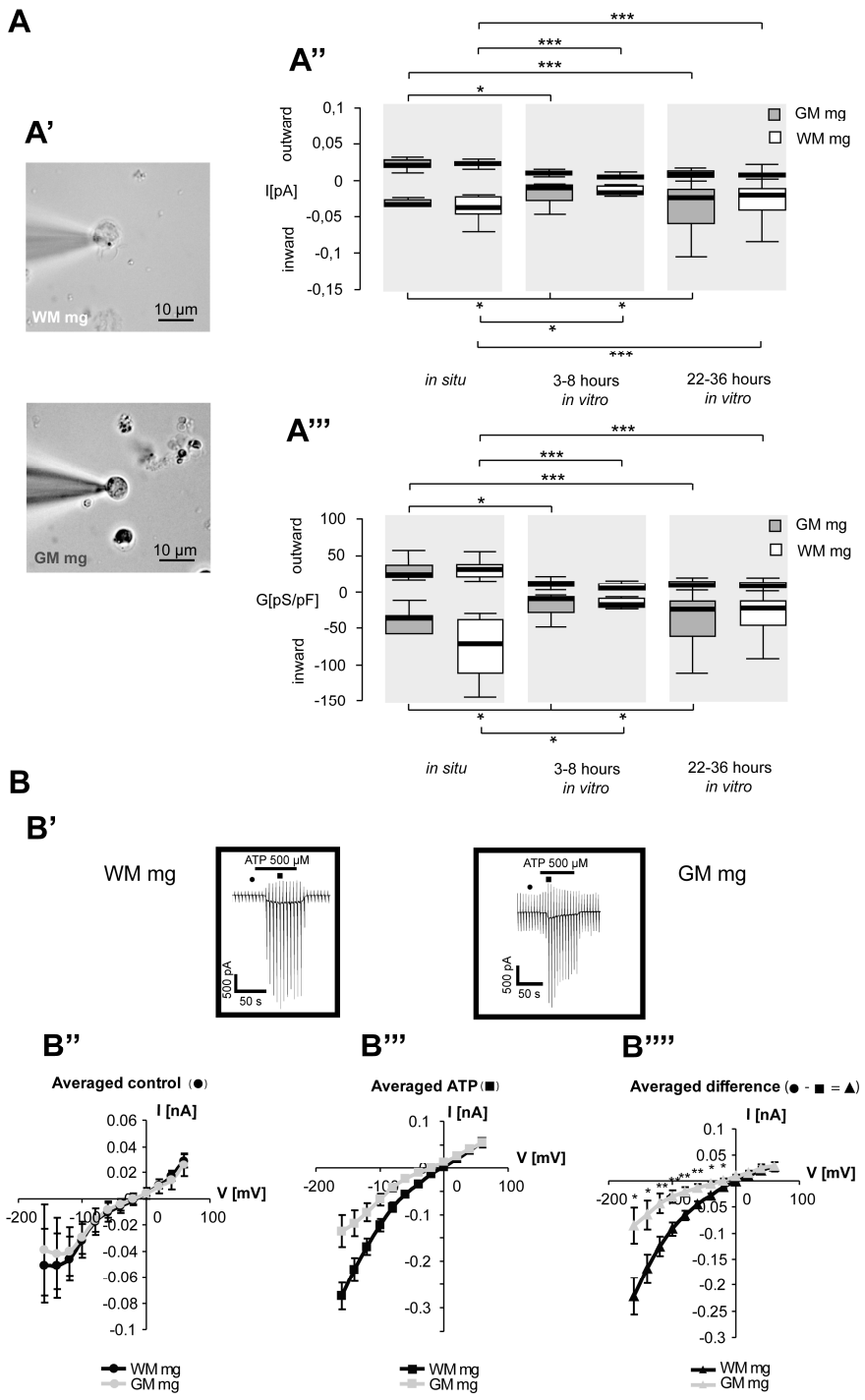

Figure 2. Functional characterisation of white and grey matter microglia. Electrophysiological properties. A The current profile of microglia was investigated by

the means of whole cell patch clamp method *in situ* and *in vitro*. **A'** Reperesentative photomicrographs of acutely isolated white and a grey matter microglia after the establishment of MΩ seal. **A''** White and grey matter microglia differed in the induction of inward currents. White and grey matter microglia average current amplitudes (I) (**A''**) and specific conductances (G) (**A'''**) were quantified in acute adult brain slices (*in situ*) and acutely isolated cells (3-8 hours *in vitro*, 22-36 hours *in vitro*). (* represents a p value < 0,05; ** represents a p value < 0,01; *** represents a p value < 0,001). **B** The induction of inward currents by application of ATP (500 µM, 60 seconds) was significantly stronger in white than in grey matter microglia. **B'** Representative measurements showing the change in the current profile of white and grey matter microglia in response to topical application of ATP (500 µM, 60 seconds). For the description of the used measurement regime please see Material and methods section. Graphs representing the currents elicited at different membrane holding potentials under control condition (**B''**) and upon ATP stimulation (**B'''**). **B''''** shows the difference between the control currents and the ATP (500 µM, 60 seconds) stimulated ones (GM mg grey matter microglia; WM mg white matter microglia; * represents a p value < 0,05; ** represents a p value < 0,01).

In the case of white matter microglia, the induced inward currents were on average five fold bigger than the inward currents present before ATP application (control), while the same induction was only three fold for grey matter microglia (Figure 2B'', B''' and B'''').

We investigated the intracellular calcium responses of white and grey matter microglia after 24-hour culturing. Two concentrations of ATP (100 µM and 1 mM) were used to elicit calcium responses in microglia cells (for 100 µM ATP N(WM mg) = 48, N(GM mg) = 65; for 1 mM ATP N(WM mg) = 7, N(GM mg) = 74). As shown in Figure 3A', depicting representative examples of calcium responses (each curve is an average of 25 individual responses), the time course of the evoked calcium responses in white and grey matter microglia was apparently different. The calcium responses seemed to persist for a longer time in white matter cells than in grey matter cells. This was particularly obvious in the case of stimulation with 100 µM ATP, where at 3 minutes (180 seconds) post-stimulation the grey matter microglia have already re-established their pre-stimulation intracellular calcium levels, while in white matter microglia the resting state calcium concentrations were only halfway restored.

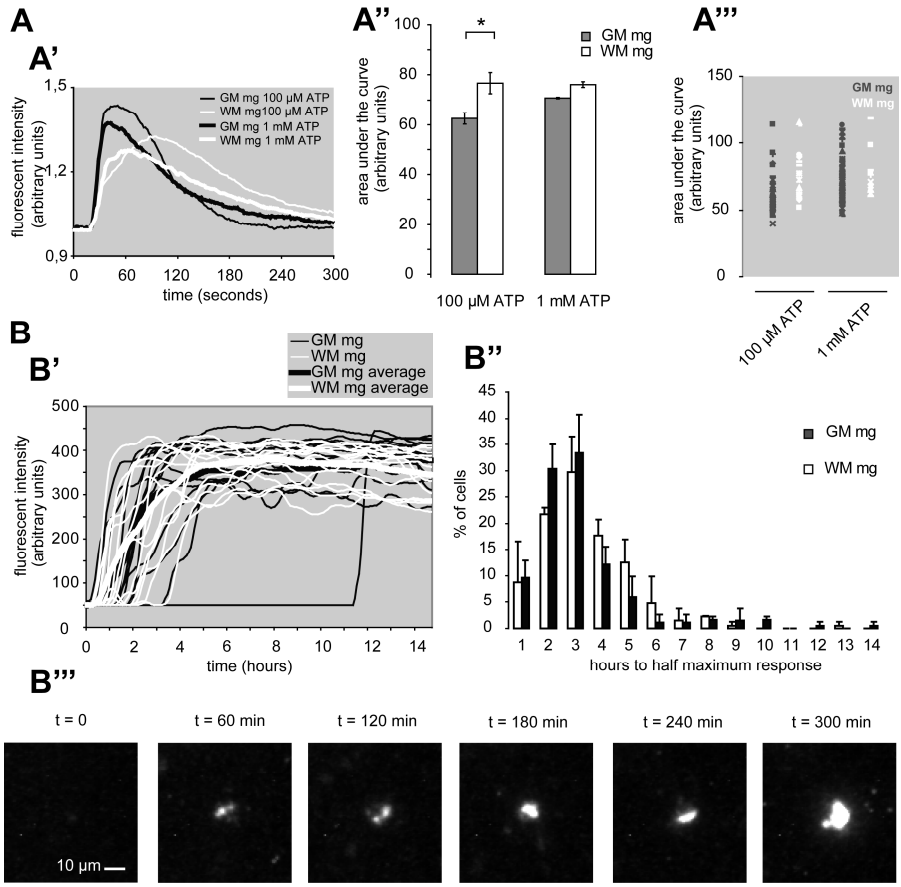

Figure 3. ***In vitro*** **functional characterisation of microglia acutely isolated from white and grey matter.** Calcium responses and phagocytosis. **A** White matter microglia have slower decaying calcium responses to topical application of ATP than grey matter microglia. **A'** Representative calcium imaging recordings of white and grey matter cells. Each graph is an average of twenty responses. **A''** The area under the curve of the white matter microglia calcium reponses to 100 µM ATP was significantly higher than that of grey matter microglia. **A'''** shows the individual measurement values (area under the curve) for each condition. **B** Acutely isolated mouse white and grey matter microglia displayed similar phagocytic capacity. **B'** Representative graphs of the time lapse measurements of pHrodo phagocytosis by white and grey matter microglia. **B''** Histogram showing the percentage of cells belonging to the given categories regarding the rate of phagocytosis. **B'''** Representative photomicrographs from the time-lapse confocal microscopic measurements showing the accumulation of the pHrodo coupled bacterial bioparticles in microglial phagolysosomes. (GM mg grey matter microglia; WM mg white matter microglia)

To quantitatively analyse the calcium responses, we measured the area under the curve for each response. As depicted on Figure 3A'', the mean

area under the curve of the calcium responses to 100 µM ATP for white matter microglia was significantly larger than that for grey matter microglia (N = 50 for both white and grey matter microglia; t-test assuming unequal variances, two tailed p value < 0,001). This was not the case for the responses to 1 mM ATP, where no significant difference could be found between white and grey matter microglia (Figure 3A'' and A'''), though there was a trend of white matter microglia having more slowly decaying calcium response. Since phagocytic capacity is one of the most important functional characteristics of microglia, we have investigated whether white and grey matter microglia inherently differ from each other in this respect. The rate of phagocytosis of pHrodo coupled bacterial particles was monitored by time-lapse microscopy in acutely isolated microglia (Figure 3B'''). The mean intensity for each cell across the image stack was measured off-line with ImageJ software for each cell and plotted against time to yield the phagocytic curves depicted in Figure 3B'. Acutely isolated white and grey matter microglia had basically the same phagocytic capacity (Figure 3B''; N = 100 for both white and grey matter microglia; three independent biological replicates). There was no significant difference between white and grey matter microglia in respect of the percentage of cells that have reached half maximum phagocytosis at any given time point (Figure 3B'').

Genome wide gene expression analysis of acutely isolated murine white and grey matter microglia

We were further interested to investigate the differences in the gene expression pattern of cortex and corpus callosum resident microglia populations. We performed a genome wide gene expression analysis using Illumina bead arrays. Eight biological replicates were used for each group (white and grey matter microglia), each of which consisted of a pool of three-five animals. After normalisation and log2 transformation, the two groups were tested for the presence of significantly differently expressed genes in GeneSpring version 10.0 We found more than 1300

genes that were expressed at a significantly higher level in grey than in white matter microglia, and around 1200 genes that were expressed at a significantly higher level in white than in grey matter microglia (Figure 4A & 4B). (Unpaired t-test; p value computation: asymptotic; multiple testing correction: Banjamini-Hochberg; corrected p value < 0,05; fold change > 1,5). The fold change difference between the expression levels of white and grey matter microglia genes was rarely above five fold, and the largest difference was less than 20 fold (Figure 4B). To investigate the identity of the significantly differently expressed genes we submitted the gene lists to gene ontology analysis using DAVID web-application (http://david.abcc.ncifcrf.gov/).

Several, neuroimmunologically relevant pathways came up to be significantly enriched (modified Fischer Exact p-value for gene enrichment analysis/EASE score threshold: 0,05; multiple testing correction: Benjamini) in significantly differently expressed genes (Figure 4C & 4D). One of the pathways that was significantly enriched in genes expressed at a significantly higher level in white matter microglia than in grey matter microglia (p = 3,0E-5; Benjamini = 4,8E-3) was the Toll-like receptor signalling pathway.

Figure 4. Genome wide gene expression analysis revealed several significantly differently expressed genes in acutely isolated white and grey matter microglia. A The scatter plot represents the normalised expression levels of the significantly (corrected p value < 0,05) differently expressed genes between white and grey matter microglia. The diagonal red lines represent the cut off value of 1,5 fold difference in expression levels. **B** Volcano plots depicting the significantly differently expressed genes between white and grey matter microglia. The fold change difference between the expression level of a given gene in white matter microglia and grey matter microglia is plotted againts the –log10 transfromed p value of the particular gene (corrected p value < 0,05; fold change > 2). The vertical red lines represent the cut off value of 1,5 fold difference in expression level. **C** and **D** show example pathways that were significantly enriched in differentelly expressed genes between white and grey matter microglia. The significantly differently expressed genes are represented in red ellipses. Pathway analysis was done using DAVID web application. Pathways reconstructed based on KEGG pathway. **C** The Toll-like receptor pathway was significantly enriched in genes that were expressed at a significantly higher level in white matter microglia. **D** The antigen processing and presentation pathway was

significantly enriched in genes that were expressed at a significantly higher level in white matter microglia. (FC fold change; p corrected p value)

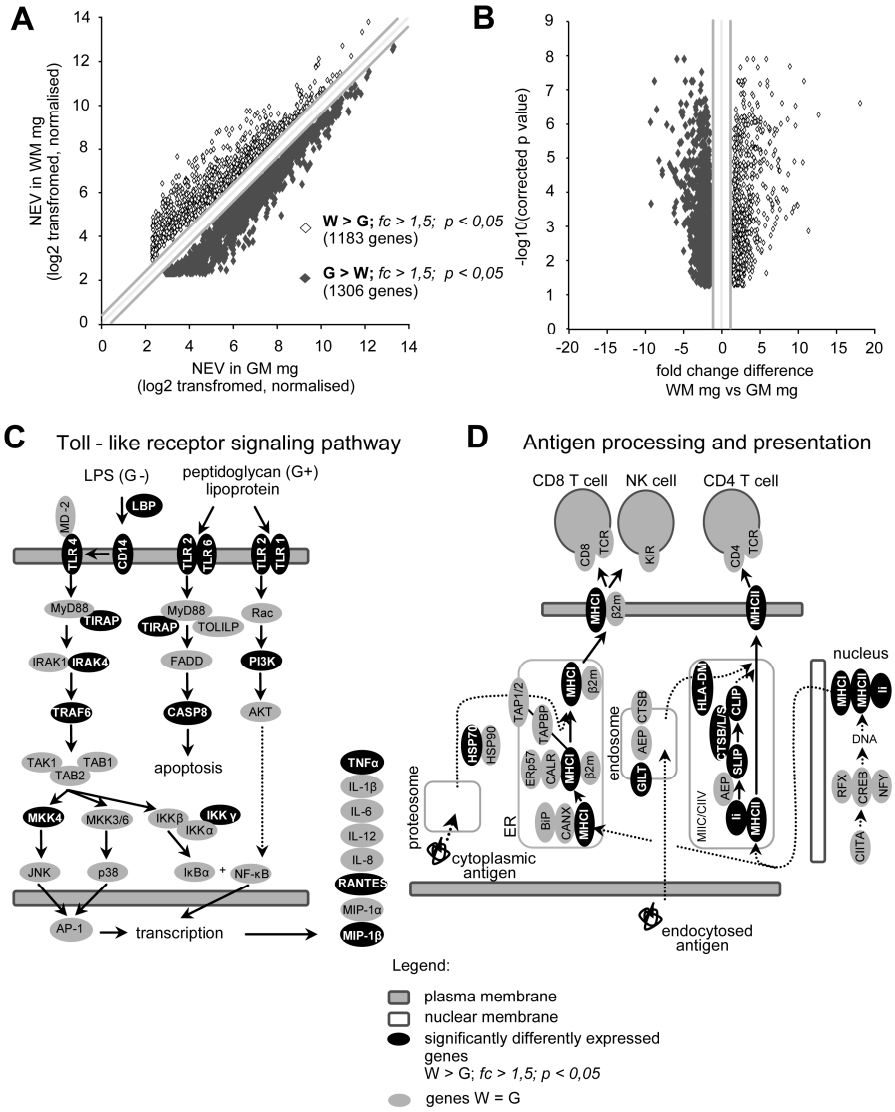

Importantly, as depicted on Figure 4C, the differently expressed genes belonging to this pathway included the receptors (*Tlr1*, *Tlr2*, *Tlr6*, *Tlr4* and *Cd14*), members of the signaling cascade (*Tirap*, *Irak4*, *Traf6*) and the effector molecules (*Tnf*, *Ccl5*, *Ccl4*). Similarly, the pathway of antigen

processing and presentation was also showing the trend of being enriched in genes expressed at a significantly higher level in white than in grey matter microglia (p = 1,8E-1; Benjaminin = 6,3E-1). Among the significantly differently expressed genes belonging to the pathway of antigen processing and presentation were genes associated with antigen processing and loading of the major histocompatibility molecules with the processed antigen (*Hsp70*, *Ifi30* (*Gilt*), *Ctsb*, *Ctsl*, *Ctss, H2-DM*. Moreover the genes associated with the major histocompatibility complex I and II and the invariant chain CD74 (*Ii*) were significantly differently expressed themselves as well.

Immunophenotyping of murine white and grey matter microglia by flow cytometry

To investigate the observed gene expression differences at the protein level, we performed immunophenotyping of white and grey matter microglia by the means of flow cytometry. We have chosen to examine the expression of the surface markers belonging to the two signaling pathways that were significantly enriched in genes expressed at a significantly higher level in white than in grey matter microglia, namely the Toll-like receptor pathway (two independent experiments) and the antigen processing and presentation pathway (three independent experiments).

Figure 5. Comparison of the expression levels of Toll-like receptors and certain microglia activation markers on white and grey matter microglia by flow cytometry. **A** Acutely isolated white and grey matter croglia showed the characteristic forward and side scatter (FSC/SSC) profile and the typical CD11b high/CD45 intermediate expression levels. The events within **R1** were used for further analysis. **B** TLR2 and TLR4 were expressed at a low level on acutely isolated white and grey matter microglia under physiological conditions, while TLR1 was not present. Representative histograms of one out of two independent experiments. **D** Induction of the expression of certain inflammatory markers on white and grey matter microglia upon systemic LPS challenge. Under physiological conditions most of the markers were expressed at a comparable level between white and grye matter microglia. In endotoxemia some markers (such as CD86, CD40 and MHCII) were induced to a greater extent in white

matter microglia than in grey matter microglia. Histograms show reperesentative measurements of one out of three independent experiments.
(MFI mean fluorescent intensity; WM mg white matter microglia; GM mg grey matter microglia; LPS lipopolysaccharide challenge; SAL saline injected; for other acronyms please see List of abbreviations)

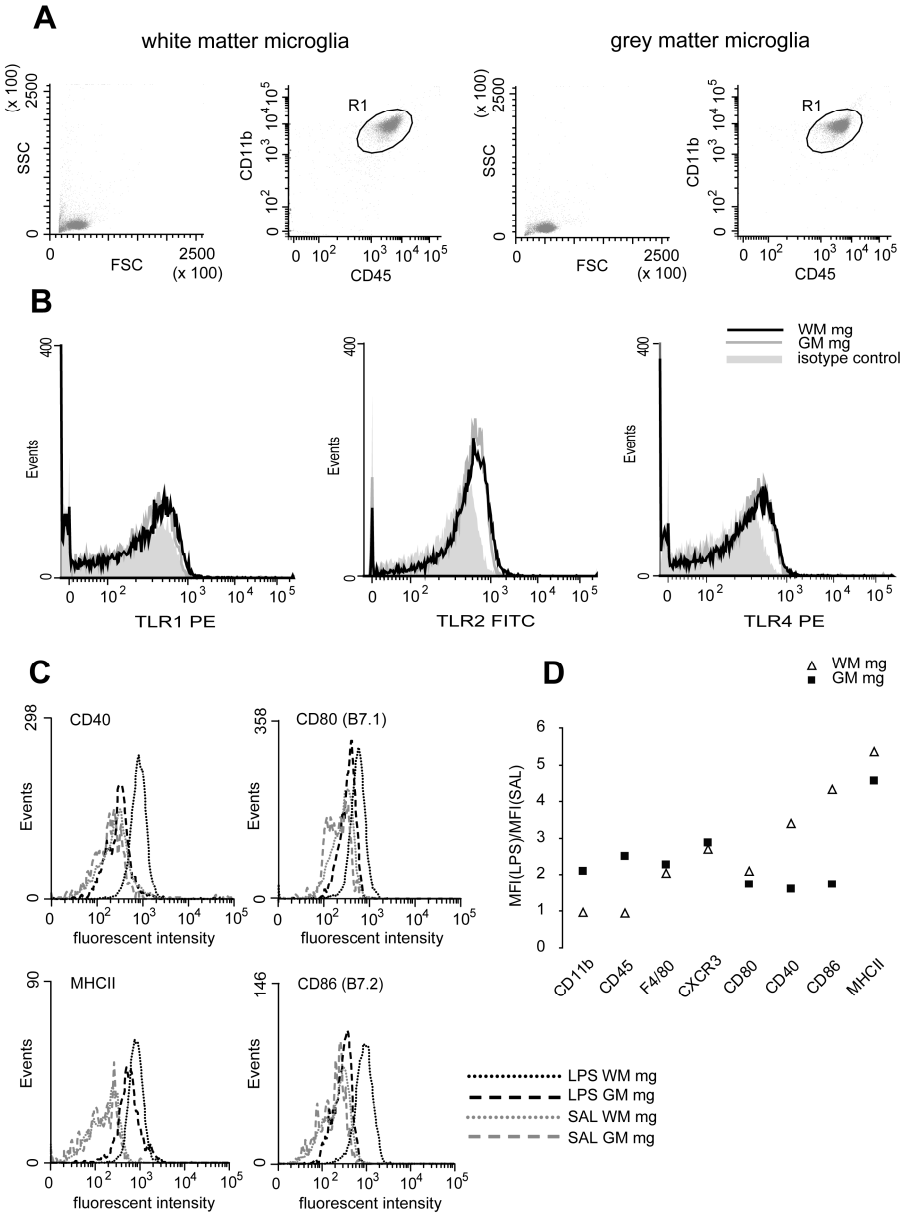

Importantly, we found no differences between white and grey matter microglia in respect of the surface expression of selected Toll-like receptors (Figure 5B), MHCII and the costimulatory molecules (SAL histograms in Figure 5C) under physiological conditions. In accordance with previous reports (Olah et al., 2009; De Haas et al., 2008), the above mentioned surface markers were either absent (e.g TLR1, MHCII) or expressed at a low level (e.g. TLR2, TLR4) on microglia in the non-inflamed murine brain. To explore whether the observed differences at the gene expression level translate into dissimilarities in the responsiveness of white and grey matter microglia upon stimulation *in vivo*, we performed flow cytometric analysis of certain selected activation markers (among others MHCII and the co-stimulatory molecules) of white and grey matter microglia in an endotoxemia model. Experimental animals were intraperitoneally injected either with LPS or with saline, and the acute isolation of microglia from white and grey matter was performed eight hours later. As depicted in Figure 5D, the induction of several activation markers was different between white and grey matter microglia. While F4/80, CXCR3 and CD80 were induced to a similar extent in white and grey matter microglia (Figure 5D), there was a three fold stronger induction of CD40 and CD86 in white matter microglia than in grey matter microglia (Figure 5C). Induction of MHCII was slightly stronger in white compared to grey matter microglia upon peripheral endotoxin challenge (Figure 5C & 5D).

DISCUSSION

The initial notion of microglia phenotype heterogeneity in the CNS (based on morphology, cellular density and poliferative capacity (Lawson et al., 1992; Lawson et al., 1990)) has been recently reinforced by a study, that has described significant regional differences in the surface expression of several, from the neuroimmunological point of view, important molecules on murine microglia (De Haas et al., 2008). Moreover, it seems likely, that at least some of the region specific phenotype traits are inherent to the microglial cells themselves (Ren at al., 1999) and that the dissimilarities existing between the distinct microglia populations might have a significant role in determining the neuropathological outcome of any disturbance to the CNS homeostasis (Kim et al., 2000).

Several lines of evidence suggests, that the most distinct differences between the microglia populations are found in the white and grey matter of the CNS - including, but not restricted to, the corpus callosum and the cerebral cortex, respectively. The level of morphological dissimilarity between these two microglia populations is second only to that found in microglia residing outside and within the circumventricular organs (Lawson et al., 1990). Next to the evident morphological disparities, white and grey matter microglia are known to be differently affected by brain aging, contribute to a different inflammatory milieu in white versus grey matter lesions in demyelinating disorders, and under physiological conditions, show differences in the cellular expression levels of several activation markers. Despite the apparent existence of dissimilarity of phenotypes and the expected relevance of regional diversity of microglia with respect to multiple pathological conditions of the CNS, the exact nature of the differences between white and grey matter microglia has not been systematically investigated yet. Thus, in this study we performed an in depth analysis of the corpus callosum and cerebral cortex resident microglia phenotype at multiple levels: cellular

morphology, surface expression of antigens, gene expression and functionality.

Despite the fact that the nature of the relationship between microglia morphology and state of activation still awaits elucidation, one of the most widely accepted signs of microglia activation is their transformation from highly ramified to rounded cells, accompanied by gradual shortening and thickening of their processes. With the help of an objective method (laser scanning microscopy, 3D reconstruction and volume analysis) we quantified multiple parameters associated with the arborisation of the processes/dendrites of microglia cells. We observed significant differences between white and grey matter microglia in respect of the length, volume and the number branching points of their dendrites, confirming the earlier subjective observations regarding their morphological differences (Lawson et al., 1990). White matter microglia had consistently fewer and less ramified processes than grey matter microglia, which might point towards a different state of activation. To investigate whether, as suggested by their morphological differences, white and grey matter microglia exist at a different state of activation, we performed genome wide mRNA expression analysis of the two microglia populations. For most of the genes, normalised gene expression levels were generally very low in both white and grey matter microglia. Nonetheless, microarray analysis of gene expression revealed more than two thousand genes that were significantly differently expressed between white and grey matter microglia. Many of the significantly differently expressed genes belong to pathways involved in neuroimmunological processes, such as the Toll-like receptor pathway and the antigen processing and presentation pathway. However, most of the differences observed at the gene expression level were small (less than five fold difference in the normalised expression levels), and were not apparent at the protein level under physiological conditions. On murine microglia cells, the surface expression of the Toll-like receptor system and the molecules associated with antigen presentation are

known to be extremely low under physiological conditions, but might be induced upon exposure to different stimuli (Trudler et al., 2010; Olah et al., 2009; De Haas et al., 2008). We therefore applied a systemic LPS challenge, to investigate whether the observed differences at the gene expression level translate to differences in the responsiveness of white and grey matter microglia in a pathological model, in this case endotoxemia. We found moderate differences between white and grey matter microglia in respect of the induction of some of the costimulatory molecules and MHCII. White matter microglia showed a more pronounced increase in the surface expression of CD86 and CD40 than grey matter microglia, while the induction of MHCII and CD80 was only modestly stronger in white matter microglia than in grey. The fact that we could, with a highly sensitive technique, detect differences at the gene expression level between corpus callosum and cortex resident microglia, that could not be identified at the protein level under physiological conditions, but were (to some extent) confirmed upon peripheral LPS challenge, might highlight the possibility that the true nature of the differences between these populations would manifest themselves under the state of compromised CNS homeostasis. Furthermore, to determine the inherent differences between white and grey matter microglia responsiveness and functionality, we resorted to in vitro approaches. We have chosen to investigate in detail three important aspects of microglia functionality: electrophysiological membrane properties, calcium responses and phagocytic capacity (Napoli & Neumann, 2009; Garden & Moller, 2006; Farber & Kettenmann, 2005). To stimulate microglia of white and grey matter origin we used ATP, which is known to be an important signaling molecule in respect of neuron-microglia and neuroglia-microglia crosstalk and regulates multiple aspects of microglia function (Inoue, 2008; Inoue et al., 2007; Davalos et al., 2005).

Despite being non-excitable cells, the state of activation and differentiation of immune cells, including microglia, is believed to be

reflected in their electrophysiological membrane properties (Eder, 2005; Farber & Kettenmann, 2005; Chandy et al., 1985). The membrane currents of microglia cells are believed to be primarily governed by different inward and outward rectifying voltage gated potassium channels, the expression pattern of which depends on the functional state of microglia (Eder, 1998). The presence of only minute outward currents and stronger inward currents is characteristic of cultured microglia from the embryonic or perinatal brain and of ameboid microglia in organotypical perinatal brain slices, pointing towards their activated state (Farber & Kettenmann, 2005). In our experiments, according to their resting state, microglia in acute adult brain slices displayed small outward currents and inward currents on the day of isolation. Both acutely isolated white and grey matter microglia after a short culturing period (3 to 8 hours) had reduced outward and inward currents in comparison to the relevant microglia currents observable in the organotypic slices. After 24 hours *in vitro* however, grey matter microglia restored their characteristic inward currents, while white matter microglia failed to do so, suggesting that they react differently to the culturing environment in respect of the surface expression of voltage gated potassium channels. On the other hand, the changes in inward currents upon ATP stimulation, which were more pronounced in white matter- than in grey matter microglia, suggest differences in the expression patterns of calcium dependent potassium channels, the purinergic receptors, or both. Many of the extracellular signaling events are translated to increase in the cytoplasmic calcium concentrations in microglia, this way linking the extracellular stimulus to a cellular effector response (Farber & Kettenmann, 2006; McLarnon, 2005; Moller, 2002). Importantly, we found differences between white and grey matter microglia in respect of the persistence of the intracellular calcium signal upon stimulation with low and high levels of ATP. Acutely isolated microglia of white matter origin had significantly more prolonged calcium responses than grey matter microglia in response to low levels

of ATP. Elevated cytoplasmic calcium concentrations upon stimulation are believed to be a sign of microglia activation (Hoffmann et al., 2003), it is thus reasonable to speculate, that differences in the time course of the intracellular calcium signals elicited by topical application of ATP point towards differences in the activation state between callosal and cortical microglia. Whether the observed differences are due to distinct expression patterns of purinergic receptors or the presence of store-operated channels (SOCs) in the two microglia populations, and whether they can be correlated with for example the extent of cytokine and chemokine release upon stimulation, needs further investigation. Another effector function of microglia cells that we have investigated in detail was phagocytosis, a prototypic function of tissue resident macrophages (Napoli & Neumann, 2009). In a time-lapse experiment white and grey matter microglia phagocytosed bacterial particles at an equal rate. There was also no difference between them regarding the total amount of ingested bacterial particles at the end of the assay. Thus, murine white and grey matter microglia proved to be equally efficient phagocytes *in vitro*.

In this study we aimed at characterising the anticipated regional difference between the phenotype and function of corpus callosum and cerebral cortex resident microglia *in situ*, *ex vivo* and *in vitro*. Acute isolation of microglia (either from mouse brain or human autopsy brain samples) and subsequent functional analysis provides us with the unique means to dissect inherent differences existing between distinct microglia populations from dissimilarities that are imposed upon them by the different cellular environments that they reside in. To our knowledge, this study is the first to investigate the intrinsic phagocytic capacity, membrane currents and calcium responses of adult microglia from different brain regions and to give a quantitative description of their morphological characteristics. With the techniques described above we were able to detect small but significant differences between white and grey matter microglia at the population level in respect of

gene expression, surface expression of markers and multiple functional aspects of both murine and human microglia. Our data further suggests, that the relevance of the intrinsic and acquired differences between these two microglia populations might truly manifest themselves upon disturbances in the CNS homeostasis and that one of the factors that possibly contribute to the development of different microglia phenotypes might be signaling from neurons.

LIST OF ABBREVIATIONS (FIGURES)

CD11b	integrin alpha-M
CD40	tumor necrosis factor receptor superfamily member 5
CD45	receptor-type tyrosine-protein phosphatase C
CD80	B7.1 antigen
CD86	B7.2 antigen
F4/80	EGF-like module-containing mucin-like hormone receptor-like 1
MHCII	H-2 class II histocompatibility antigen
TLR1	Toll-like receptor 1
TLR2	Toll-like receptor 2
TLR4	Toll-like receptor 4

REFERENCE LIST

Alldinger S, Wunschmann A, Baumgartner W, Voss C, Kremmer E. 1996. Up-regulation of major histocompatibility complex class II antigen expression in the central nervous system of dogs with spontaneous canine distemper virus encephalitis. Acta Neuropathol 92:273-280.

Biber K, Neumann H, Inoue K, Boddeke HW. 2007. Neuronal 'On' and 'Off' signals control microglia. Trends Neurosci 30:596-602.

Bo L. 2009. The histopathology of grey matter demyelination in multiple sclerosis. Acta Neurol Scand Suppl51-57.

Brink BP, Veerhuis R, Breij EC, van d, V, Dijkstra CD, Bo L. 2005. The pathology of multiple sclerosis is location-dependent: no significant complement activation is detected in purely cortical lesions. J Neuropathol Exp Neurol 64:147-155.

Calingasan NY, Park LC, Calo LL, Trifiletti RR, Gandy SE, Gibson GE. 1998. Induction of nitric oxide synthase and microglial responses precede selective cell death induced by chronic impairment of oxidative metabolism. Am J Pathol 153:599-610.

Carson MJ, Bilousova TV, Puntambekar SS, Melchior B, Doose JM, Ethell IM. 2007. A rose by any other name? The potential consequences of microglial heterogeneity during CNS health and disease. Neurotherapeutics 4:571-579.

Chandy KG, DeCoursey TE, Cahalan MD, Gupta S. 1985. Electroimmunology: the physiologic role of ion channels in the immune system. J Immunol 135:787s-791s.

Das S, Potter H. 1995. Expression of the Alzheimer amyloid-promoting factor antichymotrypsin is induced in human astrocytes by IL-1. Neuron 14:447-456.

Davalos D, Grutzendler J, Yang G, Kim JV, Zuo Y, Jung S, Littman DR, Dustin ML, Gan WB. 2005. ATP mediates rapid microglial response to local brain injury *in vivo*. Nat Neurosci 8:752-758.

De Haas AH, Boddeke HW, Biber K. 2008. Region-specific expression of immunoregulatory proteins on microglia in the healthy CNS. Glia 56:888-894.

Eder C. 1998. Ion channels in microglia (brain macrophages). Am J Physiol 275:C327-C342.

Eder C. 2005. Regulation of microglial behavior by ion channel activity. J Neurosci Res 81:314-321.

Elkabes S, Cicco-Bloom EM, Black IB. 1996. Brain microglia/macrophages express neurotrophins that selectively regulate microglial proliferation and function. J Neurosci 16:2508-2521.

Farber K, Kettenmann H. 2005. Physiology of microglial cells. Brain Res Brain Res Rev 48:133-143.

Farber K, Kettenmann H. 2006. Functional role of calcium signals for microglial function. Glia 54:656-665.

Garcion E, Nataf S, Berod A, Darcy F, Brachet P. 1997. 1,25-Dihydroxyvitamin D3 inhibits the expression of inducible nitric oxide synthase in rat central nervous system during experimental allergic encephalomyelitis. Brain Res Mol Brain Res 45:255-267.

Garden GA, Moller T. 2006. Microglia biology in health and disease. J Neuroimmune Pharmacol 1:127-137.

Gehrmann J, Banati RB, Kreutzberg GW. 1993. Microglia in the immune surveillance of the brain: human microglia constitutively express HLA-DR molecules. J Neuroimmunol 48:189-198.

Goings GE, Kozlowski DA, Szele FG. 2006. Differential activation of microglia in neurogenic versus non-neurogenic regions of the forebrain. Glia 54:329-342.

Hoffmann A, Kann O, Ohlemeyer C, Hanisch UK, Kettenmann H. 2003. Elevation of basal intracellular calcium as a central element in the activation of brain macrophages (microglia): suppression of receptor-evoked calcium signaling and control of release function. J Neurosci 23:4410-4419.

Huber JD, Campos CR, Mark KS, Davis TP. 2006. Alterations in blood-brain barrier ICAM-1 expression and brain microglial activation after lambda-carrageenan-induced inflammatory pain. Am J Physiol Heart Circ Physiol 290:H732-H740.

Inoue K, Koizumi S, Tsuda M. 2007. The role of nucleotides in the neuron--glia communication responsible for the brain functions. J Neurochem 102:1447-1458.

Inoue K. 2008. Purinergic systems in microglia. Cell Mol Life Sci 65:3074-3080.

Kim WG, Mohney RP, Wilson B, Jeohn GH, Liu B, Hong JS. 2000. Regional difference in susceptibility to lipopolysaccharide-induced neurotoxicity in the rat brain: role of microglia. J Neurosci 20:6309-6316.

Kullberg S, Aldskogius H, Ulfhake B. 2001. Microglial activation, emergence of ED1-expressing cells and clusterin upregulation in the aging rat CNS, with special reference to the spinal cord. Brain Res 899:169-186.

Lawson LJ, Perry VH, Dri P, Gordon S. 1990. Heterogeneity in the distribution and morphology of microglia in the normal adult mouse brain. Neuroscience 39:151-170.

Lawson LJ, Perry VH, Gordon S. 1992. Turnover of resident microglia in the normal adult mouse brain. Neuroscience 48:405-415.

McLarnon JG. 2005. Purinergic mediated changes in Ca2+ mobilization and functional responses in microglia: effects of low levels of ATP. J Neurosci Res 81:349-356.

Mittelbronn M, Dietz K, Schluesener HJ, Meyermann R. 2001. Local distribution of microglia in the normal adult human central nervous system differs by up to one order of magnitude. Acta Neuropathol 101:249-255.

Moller T. 2002. Calcium signaling in microglial cells. Glia 40:184-194.
Napoli I, Neumann H. 2009. Microglial clearance function in health and disease. Neuroscience 158:1030-1038.

Ogura K, Ogawa M, Yoshida M. 1994. Effects of aging on microglia in the normal rat brain: immunohistochemical observations. Neuroreport 5:1224-1226.

Olah M, Ping G, De Haas AH, Brouwer N, Meerlo P, Van Der Zee EA, Biber K, Boddeke HW. 2009. Enhanced hippocampal neurogenesis in the absence of microglia T cell interaction and microglia activation in the murine running wheel model. Glia 57:1046-1061.

Ong WY, Leong SK, Garey LJ, Tan KK, Zhang HF. 1995. A light and electron microscopic study of HLA-DR positive cells in the human cerebral cortex and subcortical white matter. J Hirnforsch 36:553-563.

Ren L, Lubrich B, Biber K, Gebicke-Haerter PJ. 1999. Differential expression of inflammatory mediators in rat microglia cultured from different brain regions. Brain Res Mol Brain Res 65:198-205.

Sasaki A, Nakazato Y. 1992. The identity of cells expressing MHC class II antigens in normal and pathological human brain. Neuropathol Appl Neurobiol 18:13-26.
Semmler A, Okulla T, Sastre M, Dumitrescu-Ozimek L, Heneka MT. 2005. Systemic inflammation induces apoptosis with variable vulnerability of different brain regions. J Chem Neuroanat 30:144-157.

Sheffield LG, Berman NE. 1998. Microglial expression of MHC class II increases in normal aging of nonhuman primates. Neurobiol Aging 19:47-55.

Styren SD, Civin WH, Rogers J. 1990. Molecular, cellular, and pathologic characterization of HLA-DR immunoreactivity in normal elderly and Alzheimer's disease brain. Exp Neurol 110:93-104.

Trudler D, Farfara D, Frenkel D. 2010. Toll-like receptors expression and signaling in glia cells in neuro-amyloidogenic diseases: towards future therapeutic application. Mediators Inflamm 2010.

Vela JM, Dalmau I, Gonzalez B, Castellano B. 1995. Morphology and distribution of microglial cells in the young and adult mouse cerebellum. J Comp Neurol 361:602-616.

Wakita H, Tomimoto H, Akiguchi I, Kimura J. 1994. Glial activation and white matter changes in the rat brain induced by chronic cerebral hypoperfusion: an immunohistochemical study. Acta Neuropathol 87:484-492.

Wakita H, Tomimoto H, Akiguchi I, Kimura J. 1995. Protective effect of cyclosporin A on white matter changes in the rat brain after chronic cerebral hypoperfusion. Stroke 26:1415-1422.

Wakita H, Tomimoto H, Akiguchi I, Kimura J. 1998. Dose-dependent, protective effect of FK506 against white matter changes in the rat brain after chronic cerebral ischemia. Brain Res 792:105-113.

Wu CH, Wen CY, Shieh JY, Ling EA. 1993. A quantitative study of the differentiation of microglial cells in the developing cerebral cortex in rats. J Anat 182 (Pt 3):403-413.

Wu CH, Chien HF, Chang CY, Ling EA. 1997. Heterogeneity of antigen expression and lectin labeling on microglial cells in the olfactory bulb of adult rats. Neurosci Res 28:67-75.

Chapter 4

Transcriptomic analysis of the remyelination supportive microglia phenotype in the murine cuprizone model

Marta Olah[1], Nieske Brouwer[1], Knut P.H. Biber[1,2], Hendrikus W.G.M. Boddeke[1]

[1] Department of Neuroscience, Section Medical Physiology, University Medical Center Groningen, Groningen, The Netherlands

[2] Department of Psychiatry and Psychotherapy, Section Molecular Psychiatry, University Medical Center Freiburg, Freiburg, Germany

manuscript in preparation

ABSTRACT

In multiple sclerosis, a demyelinating disorder of the central nervous system (CNS), attempts are made by the endogenous oligodendrocyte precursor cells (OPCs) to remyelinate the demyelinated lesions. During the disease progression, however, because of yet unknown reasons, these attempts fail. It has been suggested, that modulating the inflammatory environment of the lesion would be a promising therapeutic approach to promote endogenous remyelination. The design of any therapeutic intervention, however, aiming at modifying the cellular millieu towards a remyelination supportive function is to a great extent hindered by the lack of information on the actual phenotype of the CNS resident immune cells that promote remyelination *in vivo*. To fill up this hiatus we performed genome wide gene expression analysis of microglia cells associated with de- and remyelination in the mouse cuprizone model. We provide evidence, that microglia are involved in the phagocytosis of myelin debris and apoptotic cells during demyelination, and express the cytokine and chemokine repertoire to activate and recruit endogenous OPCs to the lesion site and deliver trophic support to them during remyelination. Moreover, in-depth analysis of the differently regulated genes and the gene expression patterns present in microglia during the course de- and remyelination in the corpus callosum revealed a single microglia phenotype associated with both processes. Thus, our study not only provides a detailed transcriptomic analysis of the remyelination supportive microglia phenotype, but also reinforces the notion, that the primary function of CNS resident microglia is the maintenance of tissue homeostasis and support of regeneration.

INTRODUCTION

Remyelination after a primary demyelinating insult is a physiological response of the central nervous system (CNS), which aims at restoring tissue homeostasis (Miller et al., 1996). In multiple sclerosis (MS), a demyelinating neurological disorder endogenous oligodendrocyte precursors do attempt to remyelinate the lesions (Patani et al., 2007; Patrikios et al., 2006). This suggests that endogenous repair mechanisms are functional and may be improved for therapeutic purposes. Given the apparent connection between inflammation and regenerative processes, it has been suggested that modulation of inflammatory events might prove to be the most effective means to enhance remyelination (Franklin & Ffrench-Constant, 2008; Franklin, 2002).

Neuroinflammation is a primary hallmark of MS (Nataf, 2009), and it was long thought to be essentially associated with tissue injury (Lassmann, 2008). Nonetheless, in contrast to the initial notion that causality only existed between inflammation and demyelination, research of the past few years has suggested a role for inflammation in the myelination and remyelination process as well (Rodriguez, 2007; Setzu et al., 2006; Foote & Blakemoore, 2005). Given the apparent connection between inflammation and regenerative processes, it has been suggested that modulation of inflammatory events might prove to be the most effective means to enhance remyelination (Franklin & Ffrench-Constant, 2008; Franklin, 2002).

As far as the immune response in the CNS is concerned, microglia, the resident immune cells of the CNS, are at the heart of it (Rivest, 2009; Hanisch & Kettenmann, 2007). However, despite expanding knowledge regarding the biology of microglia, its role in leukoencephalopathies is still somewhat obscure (Napoli and Neumann, 2009; Rodriguez, 2007). Clearly, microglia are believed to be intimately implicated in multiple aspects of the pathophysiological processes affecting the white matter. However, our understanding of their actual role in CNS de- and

remyelination is not free from contradiction. Much of the uncertainty arises from depletion studies, from which it seems, that demyelination is not complete in the absence of microglia/macrophages (Huitinga et al., 1990; Brosnan et al., 1981). On the other hand, remyelination is also seriously delayed and affected when microglia/macrophages are not present (Kotter et al., 2005; Li et al., 2005). Genetic ablation of the two classical inflammatory cytokines, TNFα and IL-1β, which after application in the CNS cause neuroinflammation and subsequent demyelination (Ferrari et al., 2004; Redford et al., 1995), had no effect on demyelination in the cuprizone model, but significantly impeded remyelination due to inadequate recruitment and differentiation of oligodendrocyte precursors (OPCs) (Arnett et al., 2001; Mason et al., 2001). This undoubtedly pointed towards the complex nature of the relationship between inflammation and remyelination. Moreover, next to microglia, other players of the immune response in the CNS (such as T cells) have proven to be indispensable for efficient myelination to occur (Bieber et al., 2003).

In this study our aim was to identify the microglia phenotypes associated with CNS de- and remyelination. We have used the cuprizone model, in which primary demyelination and the subsequent remyelination occurs with minimal contribution from peripheral immune cells (Remington et al., 2007; McMahon et al., 2002; Matsushima & Morrel, 2001), allowing us to characterise the role of microglia in particular. To our surprise, the microglia phenotype that supported multiple aspects of remyelination (such as activation, migration, proliferation and differentiation of OPCs) was identical to the phenotype that was already present during the demyelination phase. Our data suggest that the primary function of CNS resident microglia is the maintenance of tissue homeostasis and repair and points to the importance of inflammation in this respect.

MATERIALS AND METHODS

Experimental procedures involving animals and isolated cells

All the experiments conducted in this study were approved by the Institutional Animal Care and Use Committee of the University of Groningen and were thus in line with the local and international guidelines laid down for animal experiments aiming at minimising the number of animals used and the discomfort inflicted upon them.

To achieve experimental demyelination and remyelination in the corpus callosum of the brain the cuprizone mouse model was used. This model shows cuprizone-induced primary demyelination, in which demyelination and remyelination occur in the absence of significant contribution from the side of peripheral immune cells (Kipp et al., 2009; Torkildsen et al., 2008; Matsushima & Morell, 2001). Furthermore, demyelination and remyelination in the mouse cuprizone model follow a highly reproducible time course. The diet containing 0,2 % cuprizone was daily prepared freshly by thoroughly mixing bis(cyclohexanone)oxaldihydrazone (Sigma; Cat.No. C9012) and standard powder chow (ab diets; Cat.No. 2103). Animals were provided with fresh food (approximately 5g of food/mouse/day) on daily basis.

A total number of 125 C57Bl/6 male mice was used in this study. The animals were purchased from Harlan at the age of seven weeks and group housed under standard housing conditions with a 12-12 hours light-dark cycle and food ad libitum. After a week of acclimatisation they were randomly assigned to five experimental groups. Depending on the length of the cuprizone diet and of the recovery period the experimental groups were as follows: control group (standard powder chow; (subsequently referred to as C)), two weeks demyelination group (cuprizone diet for two weeks followed by sacrifice of the animals; (referred to as 2WD)), five weeks demyelination group (cuprizone diet for five weeks followed by sacrifice of the animals (referred to as 5WD)), one week remyelination group (cuprizone diet for five weeks followed

by one week of standard chow without cuprizone; (1WR)), two weeks remyelination group (cuprizone diet for five weeks followed by two weeks of standard chow without cuprizone; (2WR)). Each group consisted of twenty five animals housed five per cage.

Animals were sacrificed in groups of five per day (one cage). The order of sacrifice was 2WD, C, 5WD, 1WR and 2WR, while the age of the animals at the time of sacrifice was 10 weeks, 14 weeks, 15 weeks, 16 weeks and 17 weeks, respectively. Mice were transcardially perfused with physiological saline solution under pentobarbital anesthesia (Euthasol; ASTfarma, The Netherlands) after which the brains were removed from the scull and kept in ice cold dissection medium (HBSS (Gibco) containing 0,5 % glucose (Sigma) and 15 mM HEPES (Gibco)) till processing. Four brains per cage were cut into 2-3 mm thick coronal section from which the corpora callosa were dissected under dissection microscope in ice cold dissection medium. The dissected tissue was homogenised in dissection medium in a bouncing glass potter. The cell suspension was incubated with anti-CD11b PE (eBioscience; Cat.No. 12-0112) and anti-CD45 FITC (eBioscience; Cat.No. 11-0451) flow cytometry antibodies for 15 minutes on ice and washed in PBS. Subsequently microglia cells were sorted out by the means of Dako-Cytomation MoFlo High Performance Cell Sorter using the gate for living cells (forward scatter/side scatter) together with a gate set up for the characteristic CD11bhigh/CD45intermediate microglia profile. Between 40.000 and 100.000 microglia per sample were directly sorted into lysis buffer.

The total RNA isolation (including on column DNase digestion) was performed with RNeasy Micro kit (Qiagen) following the instructions of the manufacturer. Pure RNA was eluted from the column in RNase free water. Until further steps the RNA samples were kept at -30°C.

From each cage the brain of one randomly chosen animal was immersion fixed in 4% PFA for three days, equilibrated in 20% sucrose overnight, cryosectioned in the coronal plane at 16 µm thickness and stored at -80°C until further processing.

Genome wide gene expression analysis

The quantity of the RNA samples was determined with a NanoDrop spectrophotometer (Thermo Scientific) and the quality with an Experion RNA HighSens quality control kit (BioRad; Cat.No. 700-7105). Only samples that were having an RQI (RNA Quality Indicator) higher or equal to 9 were used for downstream applications. After adjusting the concentrations of the samples, total RNA was subjected to amplification with Illumina® TotalPrep™ RNA Amplification Kit (AppliedBiosystems; Cat.No. 4393543) according to the provided protocol. As endproduct biotinylated cRNA was attained. cRNA quality and quantity was again assessed with the NanoDrop and with an Experion RNA StdSens quality control kit (BioRad; Cat.No. 700-7111). Only samples with NanoDrop readings of the A260/A280 ratio higher than 1,9 (and lower than 2,1) were used for the gene expression analysis. A total amount of 750 ng cRNA was hybridised to the MouseRef-8 v2.0 Expression BeadChips (Illumina; Cat.No. BD-202-0202). The signal was detected with streptavidin conjugated Cy3. The expression bead chips were scanned with iScan (Illumina). The quality control of the raw data and quantile normalisation was performed with GenomeStudio software (Illumina).

The normalised gene expression data were analysed with the help of GeneSpring GX v10.0 Software (Agilent). Each experimental group (control (C), 2 weeks demyelination (2WD), 5 weeks demyelination (5WD), 1 week remyelination (1WR) and 2 weeks remyelination (2WR)) consisted of three independent biological replicates. For all the statistical analysis's probability cut-off value was 0,05 ($p < 0,05$) and fold change cut-off value was 2 ($FC > 2$). Multiple testing correction was achieved by the Benjamini-Hochberg method.

The entities that exhibited similar behavior across the experimental conditions were grouped together with the help of one of the pattern discovery tools in GeneSpring (*Find Similar Entities*), using Euclidean similarity measure and a correlation cut-off range of 0,5-1,0.

An empirically determined cut-off value was used to categorise the individual genes as expressed or not expressed in a given condition (cut-off value = 3 on the log2 transformed normalised gene expression value scale, ranging from 0 till 14).
For data interpretation and visualisation the following software packages were used: Database for Annotation, Visualisation and Integrated Discovery (DAVID) v6.7 (http://david.abcc.ncifcrf.gov/); Cytoscape BiNGO plug in (Maere et al., 2005, Bioinformatics); Genesis software (Sturn et al., 2002, Bioinformatics); Caleydo software (http://www.caleydo.org/); Venny web application (Oliveros, J.C. (2007), http://bioinfogp.cnb.csic.es/tools/venny/).

Histochemistry, immunohistochemistry and in situ hybridisation
In total the brains of 25 animals (5 animals per group, one animal from each cage) were processed for assessing the efficacy of the cuprizone treatment (the extent of de- and remyelination), to confirm the differential expression of genes at the mRNA and protein level *in situ*, and to investigate in detail the cellular events associated with de- and remyelination.
The changes in the level of myelination of the corpus callosum were detected with Luxol Fast Blue (LFB) histochemistry. The LFB working solution was prepared by dissolving 0,5 g of Solvent Blue 38 (Sigma) in 500 ml 96% ethanol (BIOSOLVE) including 10% acetic acid. During the staining procedure sections were first dehydrated in an ascending ethanol series (up to 96% ethanol), incubated in LFB working solution at 60°C for 24 hours, washed with 96% ethanol and distilled water. Differentiation was achieved in 0,125% lithium carbonate solution, after which the sections were rinsed in 70% ethanol followed by distilled water and finally counterstained with cresyl violet. After dehydration the sections were coverslipped with DePeX (Merck).
To detect the ingestion of myelin debris by microglia Oil red O staining was performed. Oil red O stains neutral lipids red and it is widely used to

visualise myelin and membrane brake down products in macrophages in demyelinating disease and their animal models (Smith, 1999; Boyle & McGeer, 1990). The stock solution was prepared by dissolving 0,5 g Oil red O (Sigma; Cat.No. O0625) in 100 ml isopropanol (BIOSOLVE). The working ORO solution was prepared freshly by diluting the stock solution 3 on 2 with water. Dehydrated sections were equilibrated in 100% isopropanol for 5 minutes then incubated in the working ORO solution for 20 minutes at room temperature. Differentiation followed in 70% isopropanol and subsequently the sections were washed with distilled water counterstained with Mayer's hematoxylin solution (Sigma-Aldrich) and coverslipped with glycerine jelly (BDH Laboratory Supplies).

Tissue sections processed for immunohistochemistry were blocked with 5% normal goat serum or fetal calf serum in phosphate buffered saline (PBS) containing 0,1% Triton-X (Fluka) for 30 minutes on room temperature. The primary antibody was applied in PBS-Triton-X containing 1% of the appropriate normal serum for overnight at 4°C. Next day the sections were washed with PBS three times for 5 minutes at room temperature and incubated with biotinylated or fluorescent dye conjugated secondary antibody at room temperature for 1,5 hour. Subsequently, in case of the fluorescent stainings, the sections were washed again three times with PBS, counterstained with Hoechst (Fluka; Cat.No. H33258) and coverslipped with Mowiol (Calbiochem). The stainings for which biotinylated secondary antibody was used, this step was followed (after extensive rinsing) by incubation of the sections with the avidin-horse radish peroxidase complex (Vector Laboratories; Cat.No. PK-6100) for 1 hour at room temperature. At the last step the staining was visualised with diaminobenzidine as a chromogen in the presence of 1,5% H_20_2 to initiate the reaction. Sections were then dehydrated and coverslipped with DePeX.

The primary antibodies used were rabbit anti-MBP (abcam, Cat.No. ab40390), rabbit anti-Iba1 (Wako, Cat.No. 019-19741), rat anti-MHCII

(eBioscience, Cat.No. 14-5321), armenian hamster anti-CD40 (eBioscience, Cat.No. 14-0402), armenian hamster anti-CD80 (eBioscience, Cat.No. 14-0801), rat anti-CD86 (eBioscience, Cat.No. 14-0862), rat anti-CD3 (eBioscience, Cat.No. 14-0032), mouse anti-TGF-β1 (Sigma, Cat.No. T0438), mouse anti-Spp1 (Novus Biologicals, Cat.No. NB110-68138), rabbit anti-Slpi (Sigma, Cat.No. PRS4249), armenian hamster anti-CD11c (eBioscience, Cat.No. 14-0114). The rabbit polyclonal antibody against galectin 3 (Gal3) was a kind gift of Wia Baron, UMCG, the Netherlands.

The secondary antibodies used were goat anti-rabbit Cy3 (JacksonImmunoResearch, Cat.No. 111-165-003), goat anti-rat FITC (JacksonImmunoResearch, Cat.No. 112-095-003), goat anti-armenian hamster Cy3 (JacksonImmunoResearch, Cat.No. 127-165-160), donkey anti-rabbit AlexaFluor488 (Invitrogen, Cat.No. A21206), donkey anti-mouse AlexaFluor488 (Invitrogen, Cat.No. A21202).

The AlexaFluor488 conjugated isolectin GS-IB4 was from Invitrogen (I21411).

In situ hybridisation was used to detect the changes in the expression level of certain selected transcripts. Polymerase chain reaction (PCR) primers were designed with PrimerExpress software. The primers used were: for ApoE (apolipoprotein E; NCBI Reference Sequence: NM_009696.2), forward: AGGTCCAGGAAGAGCTGCAG, reverse: CTCACGGATGGCACTCACAC, product: 401bp; for Lpl (lipoprotein lipase; NCBI Reference Sequence: NM_008509.2), forward: GCCTTTCTCCTGATGACGCT, reverse: TCTCGAAGGCCTGGTTGTGT, product: 501 bp. To reverse transcribe the target sequences total RNA of acutely isolated microglia (from the whole brain, isolation procedure as described in De Haas et al., 2007) and/or RNA from positive tissue controls were used. The cDNA was cloned into a pCRII vector (Invitrogen) according to the manufacturer's guidelines. The riboprobes (sense and antisense) were amplified from this vector through *in vitro* transcription with the SP6 and T7 RNA phage polymerases, in the course

of which the synthesised riboprobes were labeled with digoxigenin, by the use of DIG-UTP in the reaction buffer (DIG RNA labeling kit from Roche). The *in situ* hybridisation procedure was done according to standard protocol as described in detail elsewhere (Copray & Brouwer, 1997). Briefly, tissue sections were fixed with 4% paraformaldehyde (Merck) solution (30 minutes at 4°C), permeabilised with proteinase K solution (5 to 10 µg/ml proteinase K (Sigma), 30 minutes at 37°C), dehydrated with ascending ethanol series (50-70-96-100% ethanol) and air-dried. The freshly prepared hybridisation mix (containing the DIG-labeled riboprobe at a concentration of 500 ng/ml) was denaturated (60°C for 5 minutes) and placed on ice. Subsequently, the air-dried sections were overlaid with the hybridisation mix, coverslipped and sealed with DePeX (Merck). The riboprobe (both sense and anti-sense for each mRNA species) was allowed to hybridise overnight at 60°C. Next day the sealing was removed and the sections were first washed with 2x sodium citrate solution (2xSSC) and then treated with RNase (Sigma) for 30 minutes at 37°C. After extensive washes with SSC solutions of descending concentrations, the sections were blocked and incubated with alkaline phosphatase coupled anti-DIG antibody (Roche) for 2 hours on room temperature. In the following color reaction the *in situ* hybridisation signal was visualised with NBT/BCIT (Roche). Finally the sections were coverslipped with glycerine jelly. In some cases, after the *in situ* hybridisation procedure, immunohistochemistry was performed against Iba1 with the standard immunohistochemitry protocol described in detail above, to investigate whether the *in situ* hybridisation signal localises to microglia or not.

Image acquisition

Fluorescent images were made with a Leica SP2 AOBS confocal laser scanning microscope and Zeiss Axioskop 2 fluorescent microscope equipped with a Leica DFC300FX camera. Bright field images were

acquired with Olympus BX50 research microscope equipped with a CCD camera using the SIS software.

RESULTS

Cuprizone diet caused demyelination in the corpus callosum followed by rapid remyelination upon drug withdrawal

In order to investigate the microglia phenotypes associated with demyelination and remyelination we used the well established cuprizone model (Torkildsen et al., 2008; Matsushima & Morrell, 2001). Our experimental design is shown in Supplementary Figure 1A. As expected from the literature, five weeks of 0,2% cuprizone diet (five weeks of demyelination, 5WD) resulted in well defined demyelinated lesions in the corpus callusom.

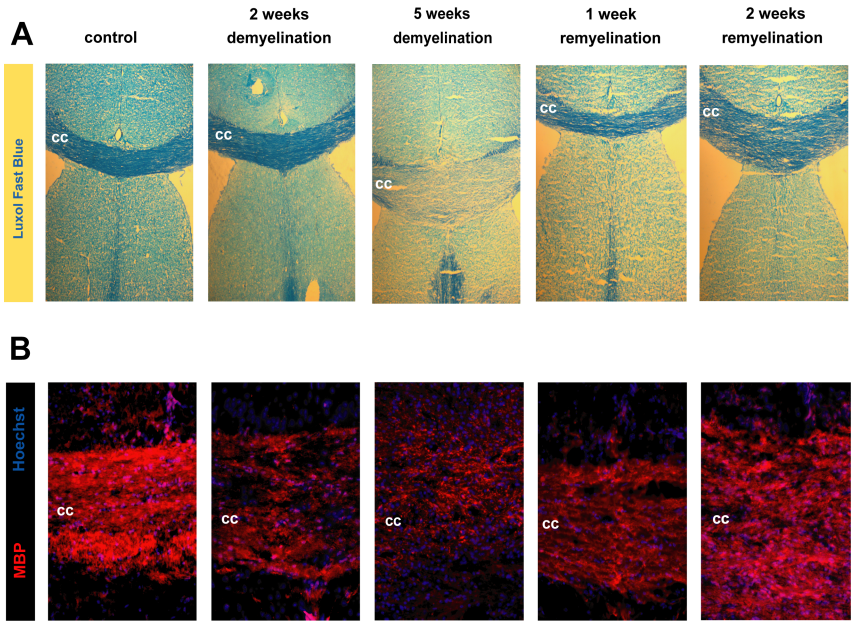

Figure 1. Cellular events during de- and remyelination. A Luxol Fast Blue (LFB) histochemistry was used to detect demyelinated lesions in the corpus callosum. Intact myelin in the control animals showed dense, strong blue staining in the white matter. The staining pattern did not change much in the 2WD group, while the 5WD group showed clear demyelinated lesions throughout the rostrocaudal extent of the corpus callosum. These lesions were characterised by the lack of myelin staining and an increase in cellularity. By the end of the first week of recovery, remyelination was almost complete. In the 1WR and the 2WR group demyelination was detectable only in patches in the corpus callosum. **B** Myelin basic protein (MBP) immunohistochemistry. Changes in the intensity and distribution of MBP immunoreactivity in the corpus

callosum showed slightly different time course than of LFB histochemistry. At 2WD MBP staining intensity was already diminished. At 5WD MBP immunopositivity was punctate at the lesion site. Recovery was seen already at 1WR, but even at 2WR the staining intensity and organisation did not reach the control levels. (cc corpus callosum)

Demyelination was detectable both by using luxol fast blue histochemistry (LFB) and by immunostaining against myelin basic protein (MBP) (Figure 1A & 1B). Upon withdrawal of cuprizone from the diet, a fast recovery was obvious both on the LFB and the MBP staining already at one week remyelination (1WR). By the end of the second week post-cuprizone-withdrawal (two weeks remyelination, 2WR), the staining intensity and the structural organisation of the affected corpus callosum was back to the control (no cuprizone diet, C) levels (Figure 1A & 1B).

Microglia activation in the coprus callosum during de- and remyelination

Microglia in the corpus callosum of 2WD animals showed no morphological sign of activation. In contrast at 5WD, microglia at the lesion sites were activated, forming a syntitium-like structure. The lesion showed a strong increase in cellularity. Immunohistochemistry against the microglia/macrophage marker Iba1 confirmed that most of the cells present at the lesion site were microglia/macrophages (Figure 5 and 7). Based on the morphology, microglia in other parts of the 5WD corpus callosum formed a mixed population, showing morphological phenotypes ranging from ramified to amoeboid. Their numbers, however, started to diminish once the toxin was withdrawn from the diet, and the decreased microglia numbers and state of activation was evident at 1WR. By 2WR the corpus callosum microglia morphologically regained their characteristic ramified morphology, though activated microglia were still peresent in patches, on sites where lesions used to be. These changes in the activation state of microglia cells were detectable both in the cellular and the RNA yield in the course of the isolation procedure (data not shown).

Microarray gene expression analysis revealed distinct gene expression patterns in microglia in the course of de- and remyelination

As a first approach, we aimed at determining the number and the identity of genes specific to the different experimental groups (control condition, demyelination and remyelination) and those which are shared among them. With an empirically determined arbitrary cut-off value (see Materials and methods section), microglia in the corpus callosum showed the expression of 7500, 9000 and 9000 genes under physiological conditions, during demyelination and in the course of remyelination, respectively - from which around 6200 genes were shared among all three conditions (Figure 2A). Genes that appeared to be characteristic of either the control condition, demyelination or remyelination, were genes associated with different metabolic pathways, cell cycle and innate immune functions, respectively. Apart from the genes that were shared by microglia from all three conditions, only few genes were shared by C and 5WD (55 genes, 0,7% of the genes expressed in C and 0,6% that of 5WD) and by C and 2WR (147 genes; 1,9% of the genes expressed in C and 1,6% that of 2WR). In contrast, the genes that were shared between 5WD and 2WR (2185 genes) represented approximately 22% of the total expressed genes in these two categories.

Detailed analysis of the microarray data revealed the existence of distinct patterns in changes occuring in the gene expression of de- and remyelination associated microglia (Figure 2B).

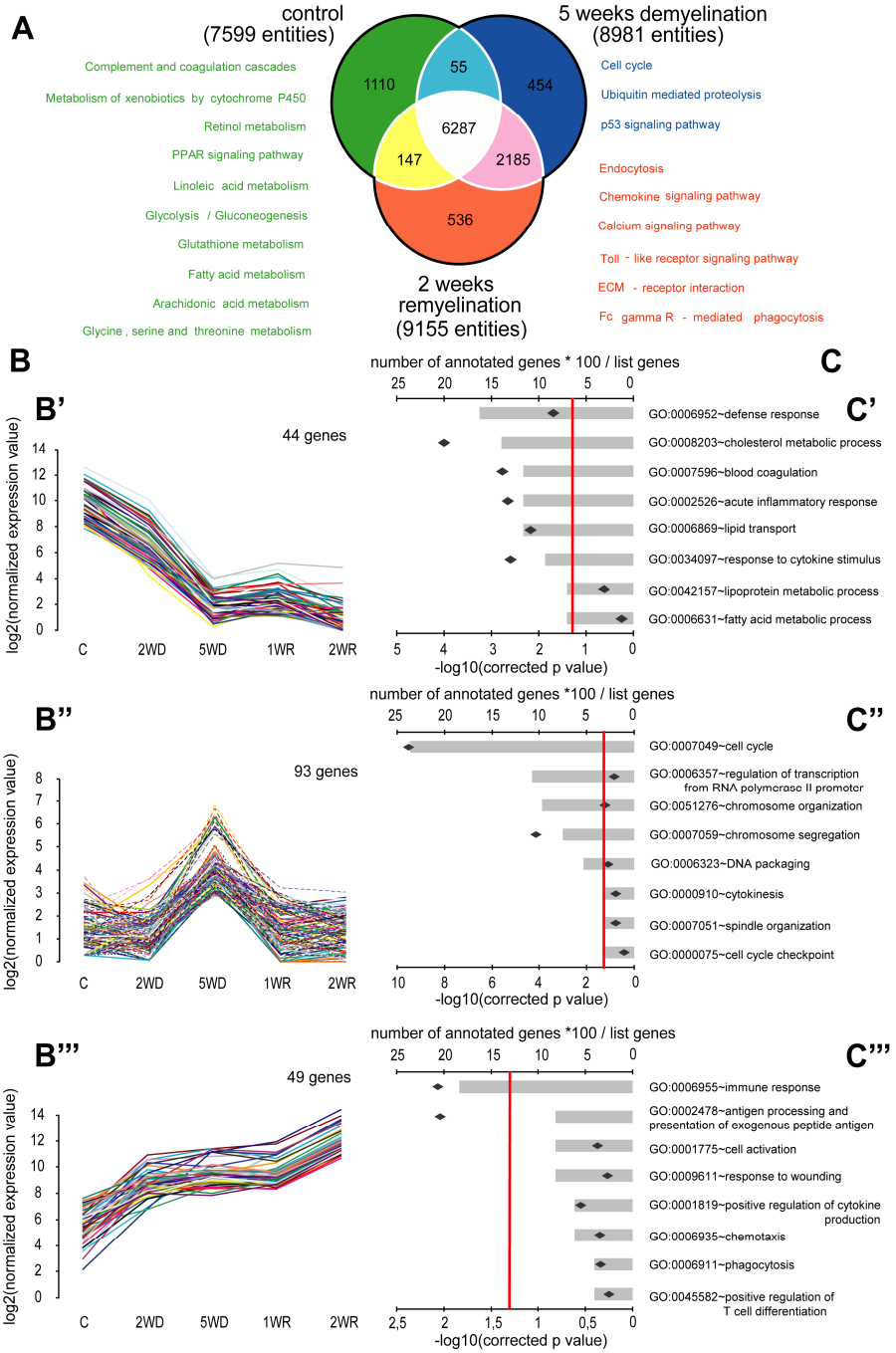

Figure 2. General overview of the gene expression analysis. A Venn diagram depicting shared and unique genes expressed by microglia at C, 5WD and 2WR conditions. Absence/presence of the gene transcripts in the different conditions was determined based on an arbitrary cut-off value (see Materials and methods and Results sections).

Major gene ontology annotations of the unique and shared genes between the C, 5WD and 2WR groups are listed (green: present only in C; blue: present only during 5WD; red: present only during 2WR). **B** Gene expression patterns across the experimental conditions. Three major groups of genes could be identified based on the pattern of the changes occuring in their expression levels during de- and remyelination. One group of genes was showing significant downregulation already at 2WD (when compared to C condition), and their expression was further downregulated at 5WD and remained downregulated during remyelination (1WR, 2WR)(**B'**). A second group of genes showed upregulation only in 5WD and during remyelination their expression returned to the levels observed in C condition (**B''**). The third group consisted of genes that were not expressed (or marginally expressed) at the control condition, but were gradually upregulated during demyelination and remained upregulated (or were further upregulated) during remyelination (**B'''**). **C** Gene ontology (GO) analysis of the genes that showed different expression patterns across the samples. Bars represent the percentage of genes from a given gene list belonging to a given gene ontology term. Diamonds represent the –log10 transformation of the p value associated with the level of enrichment of a given GO term with genes from our list genes. The red line represents the significance cut-off value (-log10 of 0,05 = 1,3). (**C'**), (**C''**) and (**C'''**) corresponds to (**B'**), (**B''**) and (**B'''**), respectively.

The existence of three dissimilar group of genes was obvious from the data: one group of genes showed rapid downregulation in the course of demyelination (already detectable at 2WD) and remained downregulated during remyelination (Figure 2B/B'). The other group of genes showed the opposite pattern – they were not expressed (or expressed at a marginal level) in the control animals, were upregulated in the course of demyelination (already noticeable at 2WD) and remained upregulated even after remyelination was complete (Figure 2B/B'''). A third group of genes was not expressed in microglia under physiological conditions, their expression was induced promptly in the 5WD group, but upon toxin withdrawal the expression of these genes returned rapidly to control levels (Figure 2B/B''). We did not find examples of genes being downregulated during demyelination and then returning to control levels, or being down- or upregulated only during the remyelination phase. To gain more insight into the identity of the three distinct groups, we performed gene ontology (GO) analysis on the lists of genes belonging to the given clusters. Around 20% of the genes that showed the expression pattern represented in Figure 2B/B' has

been annotated to the gene ontology term 'cholesterol metabolic process' (GO:0008203; Figure 2C/C'). From the same group approximately 15% of the genes belonged to the gene ontology term 'acute inflammatory response' (GO:0002526; Figure 2C/C'). Both of these gene ontology terms were significantly enriched with genes from our gene list (corrected p values 1,0E-04 and 2,2E-03, respectively). Regarding the genes that showed upregulation only during 5WD and then returned to baseline level (Figure 2 B/B''), almost one fourth of them was associated with the GO term 'cell cycle' (GO:0007049; significantly enriched, corrected p value = 3,0E-10; Figure 2C/C''). From the genes belonging to the third group (which were gradually upregulated during demyelination and remained upregulated, or were even further upregulated during remyelination (Figure 2 B/B''')) around 20% belonged to the GO term 'immune response' (GO:0006955; corrected p value = 8,7E-03; Figure 2C/C'''). In this group, another significantly enriched (partially overlapping) GO term was 'antigen processing and presentation' (GO:0002478; corrected p value = 9,2E-03), which contained more than 20% of our list genes. For the lists of the genes belonging to the different groups described above, please see Supplementary table 1.

Statistical analysis of the microarray data unveiled the significantly different expressed microglia genes during the course of de- and remyelination

To explore the genes that were significantly differently regulated in our experiment we conducted pair wise comparisons between pairs of conditions (C versus (vs) 5WD, C versus 2WR and 5WD versus 2WR). The comparisons C vs 5WD and C vs 2WR both yielded around 500 genes that were significantly upregulated and more than 200 genes that were significantly downregulated (Figure 3A). In contrast, there were only around 30 genes that were significantly upregulated and around 50 genes that were significantly downregulated from 5WD to 2WR (Figure

3A). Approximately 60% of the genes that were significantly upregulated from C to 5WD and from C to 2WR were shared among these two pair wise comparisons (Figure 3C). Similar was the percentage of shared downregulated genes (Figure 3C). In contrast, the significantly regulated genes between the conditions 5WD and 2WR were not shared with the other two comparisons.

The examples given in the volcano plots (Figure 3A) clearly demonstrate and confirm the trends in the changes of the gene-expression of microglia in the course of de- and remyelination seen already at the initial rough analysis (Figure 2). Most of the genes whose expression was significantly upregulated/downregulated from C to 5WD, remained significantly upregulated/downregulated during remyelination (for example *H2-Aa*, *Ch25h* for the upregulated genes and *Serpin1b* and *Hmgcs2* for the downregualed genes (see Figure 3A & 3B)). Some genes (such as *H2-Aa*) were further upregulated during the course of transition from the demyelination to the remyelination stage. In Figure 3D we compared the extent and directionality of the changes occuring in the expression levels of certain example genes between the three pair wise comparisons. In Figure 3D/D' and Figure 3D/D'' the genes are arranged according to the descending order of their fold change in the 5WD versus 2WR (D', first row, yellow bars) and C versus 5WD comparison (D'', third row, blue bars), respectively. From Figure 3D/D'' it is evident, that the pattern of gene expression changes occuring between C and 5WD and C and 2WR is to a great extent similar, and that for most of the genes no significant change happens from 5WD to 2WR.

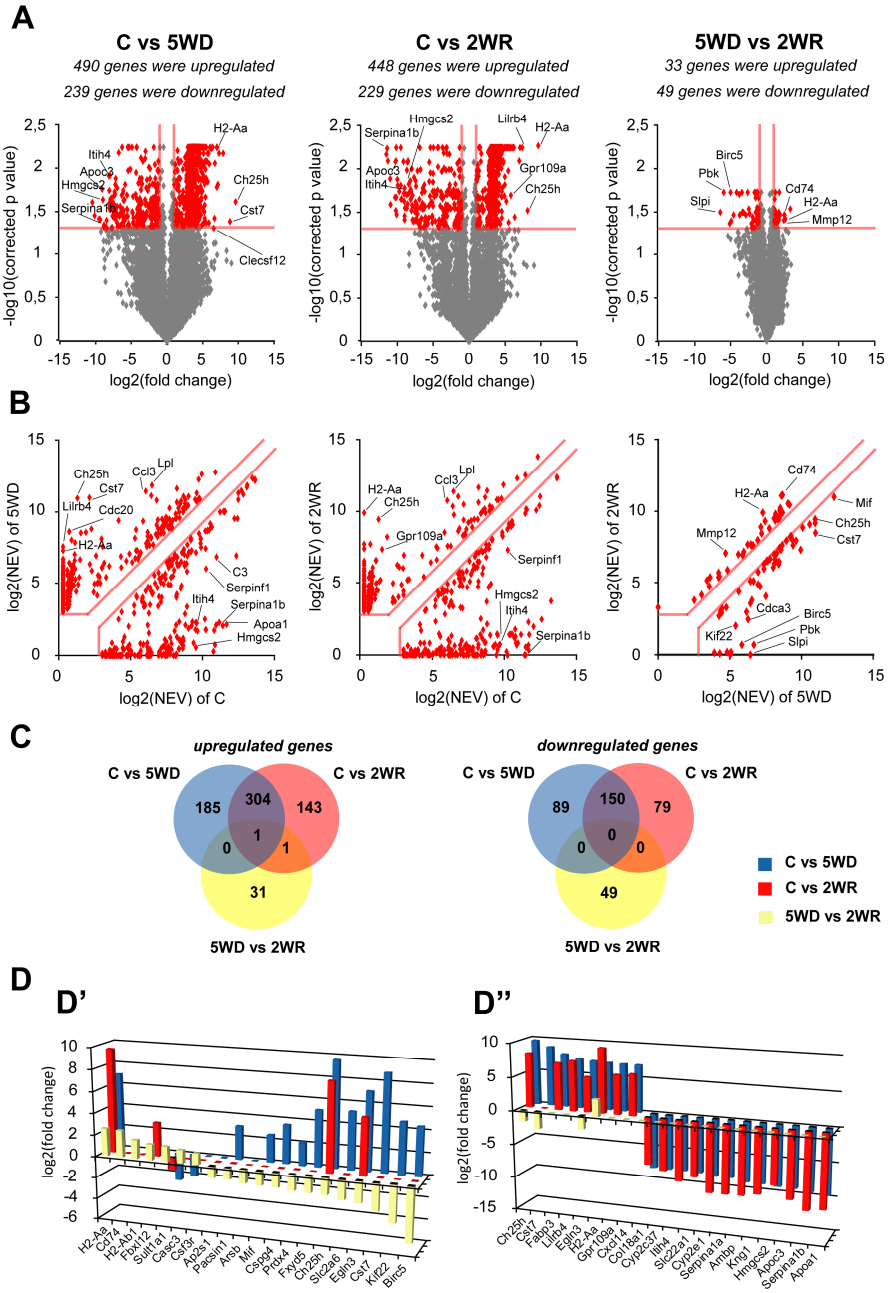

Figure 3. Significantly differently regulated microglial genes in the course of de- and remyelination in the cuprizone model. A Volcano plots showing the significantly different expressed genes between pairs of conditions (unpaired T test, $p < 0,05$, FC > 2). The abscissa represents the log2 transformed fold change in gene expression levels between pairs of conditions. Negative values indicate downregulation, while positive values represent upregulation. The ordinate represents the -log10 transformation of

the corrected p value. Red lines represent the cut off values for both the corrected p value and the fold change. Red diamonds correspond to genes that passed the significance testing, while grey diamonds symbolise the genes that did not. **B** Scatter plots displaying the log2 transformed normalised expression values (NEVs) of the significantly different expressed genes in pairs of conditions. Red lines represent the cut-off value of the fold change difference (FC > 2) and an arbitrary criterium (NEV > 3 at least at one of the conditions) aiming at excluding the marginally expressed genes. **C** Venn diagrams demonstrating the number of shared genes between the pairwise comparisons and the number of genes that were unique to them. **D** Bar graph showing the direction and the extent of changes occuring in the expression levels of selected genes between pairs of conditions. On the Y axis log2 transformation of the fold change is depicted. Negative values indicate downregulation, while positive values represent upregulation. For further details on the function of the mentioned genes see Discussion. (NEV normalised expression value; C control group; 5WD five weeks demyelination group; 2WR two weeks remyelination group)

The few significant changes that occur during the transition from demyelination to remyelination are either due to the further upregulation of some immunity associated genes (such as *H2-Aa*; Figure 3D/D') or downregulation of cell proliferation associated genes (such as *Birc5* and *Kif22*; Figure 3D/D'), that were transiently induced during the demyelination phase.

Analysis of the expression pattern of several markers of microglia/macrophage activation reveals the transcriptomic "fingerprint" of the remyelination supportive microglia phenotype

The initial analysis of the genome wide microglia gene expression in our model (gene expression patterns (Figure 2) and significance testing (Figure 3)) pointed towards the existence of a single remyelination supportive microglia phenotype, that actually develops during the course of demyelination. Next, we aimed at characterising this microglia phenotype in detail. Microglia are believed to have a suppressed immunophenotype under physiological conditions and to obtain a more macrophage like phenotype upon activation. Therefore, we assembled a list of different microglia/macrophage activation markers as well as genes associated with microglia/macrophage effector functions based on the available literature in the field. In the heatmaps of Figure 4 the

expression patterns of the genes characteristic of certain microglia/macrophage phenotypes (Figure 4A) and microglia genes associated with tissue homeostasis and regeneration (Figure 4B) are depicted. Based on the microarray data, we found that microglia in the course of de- and remyelination upregulated some (e.g. *Tlr4*, *Lyz1* and *Lyz2*, *Tnf*, *Il1a* and *Il1b*, *Mmp12*; Figure 4A), but not other (e.g. *Nos2*, *Il6*) markers of classically activated macrophages (CAMΦ). A similar pattern was found for the markers of alternatively activated macrophages (AAMΦ) (*Il13ra1*, *Il4ra*, *Il2rg* were increasingly expressed during de- and remyelination, while *Arg1* and *Msr1* were not regulated). Most prominent was the upregulation of the genes associated with the major histocompatibility complex (MHC), especially with MHCII (e.g. *Cd74*, *H2-Aa*, *H2-Ab1*), during demyelination and remyelination. The costimulatory molecules (list generated based on Viglietta and Khoury, 2007) were either not expressed (e.g. *Cd40*, *Cd80*) or not regulated (e.g. *Cd86*). Interestingly, the only costimulatory molecule that was upregulated in a similar fashion as the MHC genes, was *Cd274*. Some dendritic cell (DC) markers were also induced during demyelination and remained upregulated in the course of remyelination (*CD83*, *Clec7a*, and *Itgax*; Figure 4A). Most of the microglia markers (*Aif1* (Iba1), *Emr1* (F4/80), *Sfpi1* (PU.1)) were expressed at a relatively stable level across the samples, with only a mild downregulation of *Cx3cr1* and *P2yr12* upon activation. Moreover, based on the identity of the differently regulated genes, among the microglial effector functions in de- and remyelination are: phagocytosis of apoptotic cells and myelin debris (e.g. *Lrp1*, *Calr*, *Cd14* and *Itgb2*, *Itgam*, *Lgals3*), salvage of myelin constituents (e.g. *Hmgcs2*, *Lpl*, *Apoe*), recruitment of OPCs and trophic support for the remyelinating oligodendrocytes (e.g. *Cxcl10*, *Cxcl13* and *Igf1*, *Tgfb1*, *Pdgfa*, *Pdgfb*), and tissue remodeling (e.g. *Mmp12*, *Mmp14*).

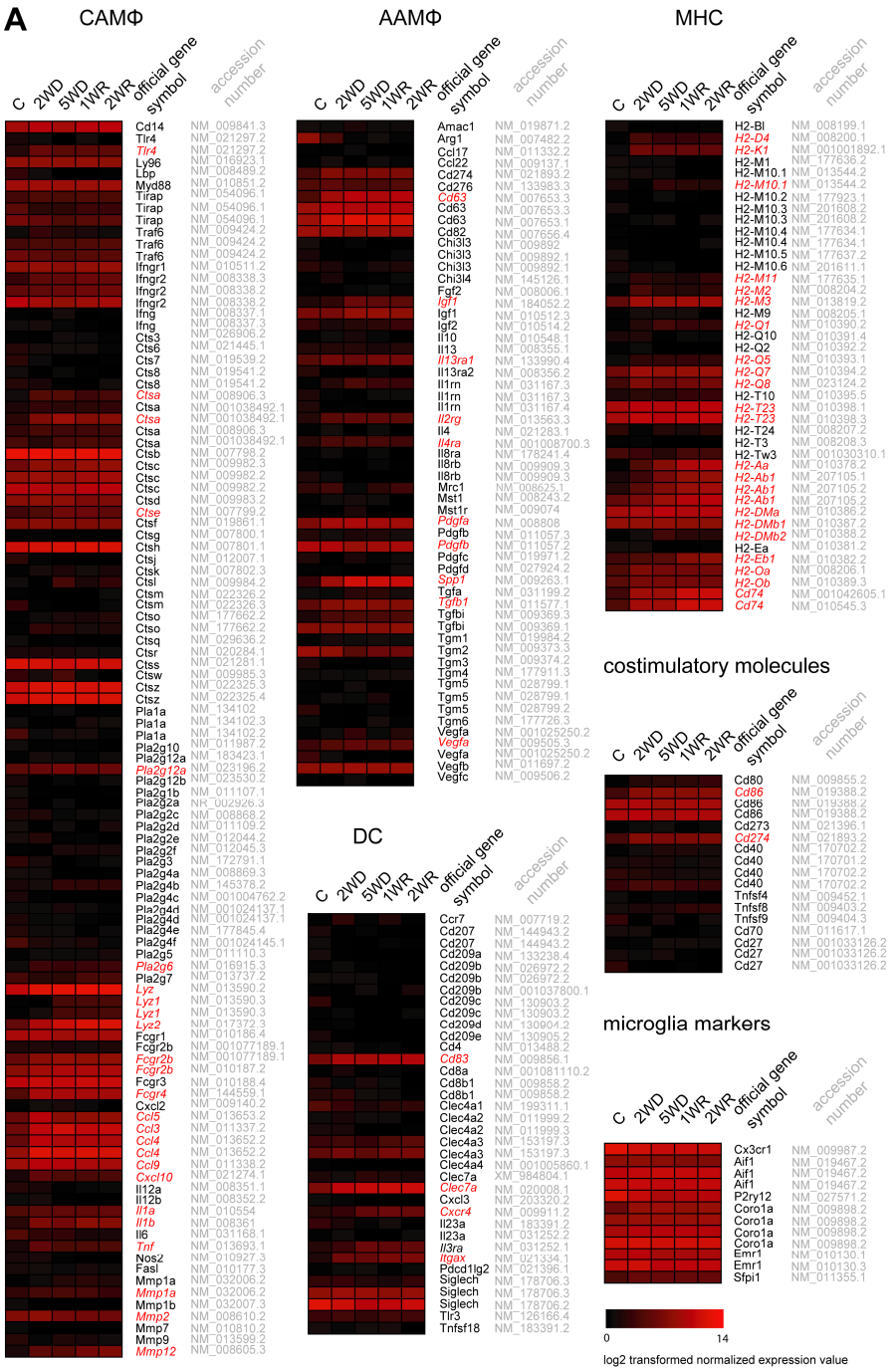
A
CAMΦ
AAMΦ
MHC
C 2WD 5WD 1WR 2WR official gene symbol accession number
Cd14 NM_009841.3
Tlr4 NM_021297.2
Tlr4 NM_021297.2
Ly96 NM_016923.1
Lbp NM_008489.2
Myd88 NM_010851.2
Tirap NM_054096.1
Tirap NM_054096.1
Tirap NM_054096.1
Traf6 NM_009424.2
Traf6 NM_009424.2
Traf6 NM_009424.2
Ifngr1 NM_010511.2
Ifngr2 NM_008338.3
Ifngr2 NM_008338.2
Ifngr2 NM_008338.2
Ifng NM_008337.1
Ifng NM_008337.3
Cts3 NM_026906.2
Cts6 NM_021445.1
Cts7 NM_019539.2
Cts8 NM_019541.2
Cts8 NM_019541.2
Ctsa NM_008906.3
Ctsa NM_001038492.1
Ctsa NM_001038492.1
Ctsa NM_008906.3
Ctsa NM_001038492.1
Ctsb NM_007798.2
Ctsc NM_009982.3
Ctsc NM_009982.2
Ctsc NM_009982.2
Ctsd NM_009983.2
Ctse NM_007799.2
Ctsf NM_019861.1
Ctsg NM_007800.1
Ctsh NM_007801.1
Ctsj NM_012007.1
Ctsk NM_007802.3
Ctsl NM_009984.2
Ctsm NM_022326.2
Ctsm NM_022326.3
Ctso NM_177662.2
Ctso NM_177662.2
Ctsq NM_029636.2
Ctsr NM_020284.1
Ctss NM_021281.1
Ctsw NM_009985.3
Ctsz NM_022325.3
Ctsz NM_022325.4
Pla1a NM_134102
Pla1a NM_134102.3
Pla1a NM_134102.2
Pla2g10 NM_011987.2
Pla2g12a NM_183423.1
Pla2g12a NM_023196.2
Pla2g12b NM_023530.2
Pla2g1b NM_011107.1
Pla2g2a NR_002926.3
Pla2g2c NM_008868.3
Pla2g2d NM_011109.2
Pla2g2e NM_012044.2
Pla2g2f NM_012045.3
Pla2g3 NM_172791.1
Pla2g4a NM_008869.3
Pla2g4b NM_145378.2
Pla2g4c NM_001004762.2
Pla2g4d NM_001024137.1
Pla2g4d NM_001024137.1
Pla2g4e NM_177845.4
Pla2g4f NM_001024145.1
Pla2g5 NM_0111110.3
Pla2g6 NM_016915.3
Pla2g7 NM_013737.2
Lyz NM_013590.2
Lyz1 NM_013590.3
Lyz1 NM_013590.3
Lyz2 NM_017372.3
Fcgr1 NM_010186.4
Fcgr2b NM_001077189.1
Fcgr2b NM_001077189.1
Fcgr2b NM_010187.2
Fcgr3 NM_010188.4
Fcgr4 NM_144559.1
Cxcl2 NM_009140.2
Ccl5 NM_013653.2
Ccl3 NM_011337.2
Ccl4 NM_013652.2
Ccl4 NM_013652.2
Ccl9 NM_011338.2
Cxcl10 NM_021274.1
Il12a NM_008351.1
Il12b NM_008352.2
Il1a NM_010554
Il1b NM_008361
Il6 NM_031168.1
Tnf NM_013693.1
Nos2 NM_010927.3
Fasl NM_010177.3
Mmp1a NM_032006.2
Mmp1a NM_032006.2
Mmp1b NM_032007.3
Mmp2 NM_008610.2
Mmp7 NM_010810.2
Mmp9 NM_013599.2
Mmp12 NM_008605.3
Amac1 NM_019871.2
Arg1 NM_007482.2
Ccl17 NM_011332.2
Ccl22 NM_009137.1
Cd274 NM_021893.2
Cd276 NM_133983.3
Cd63 NM_007653.3
Cd63 NM_007653.3
Cd63 NM_007653.1
Cd82 NM_007656.4
Chi3l3 NM_009892
Chi3l3 NM_009892.1
Chi3l3 NM_009892.1
Chi3l4 NM_145126.1
Fgf2 NM_008006.1
Igf1 NM_184052.2
Igf1 NM_010512.3
Igf2 NM_010514.2
Il10 NM_010548.1
Il13 NM_008355.1
Il13ra1 NM_133990.4
Il13ra2 NM_008356.2
Il1rn NM_031167.3
Il1rn NM_031167.3
Il1rn NM_031167.4
Il2rg NM_013563.3
Il4 NM_021283.1
Il4ra NM_001008700.3
Il8ra NM_178241.4
Il8rb NM_009909.3
Il8rb NM_009909.3
Mrc1 NM_008625.1
Mst1 NM_008243.2
Mst1r NM_009074
Pdgfa NM_008808
Pdgfb NM_011057.3
Pdgfb NM_011057.2
Pdgfc NM_019971.2
Pdgfd NM_027924.2
Spp1 NM_009263.1
Tgfa NM_031199.2
Tgfb1 NM_011577.1
Tgfbi NM_009369.3
Tgfbi NM_009369.1
Tgm1 NM_019984.2
Tgm2 NM_009373.3
Tgm3 NM_009374.2
Tgm4 NM_177911.3
Tgm5 NM_028799.1
Tgm5 NM_028799.1
Tgm5 NM_028799.2
Tgm6 NM_177726.3
Vegfa NM_001025250.2
Vegfa NM_001025250.3
Vegfa NM_001025250.2
Vegfb NM_011697.2
Vegfc NM_009506.2
H2-Bl NM_008199.1
H2-D4 NM_008200.1
H2-K1 NM_001001892.1
H2-M1 NM_177636.2
H2-M10.1 NM_013544.2
H2-M10.1 NM_013544.2
H2-M10.2 NM_177923.1
H2-M10.3 NM_201608.2
H2-M10.3 NM_201608.2
H2-M10.4 NM_177634.1
H2-M10.4 NM_177634.1
H2-M10.5 NM_177637.2
H2-M10.6 NM_201611.1
H2-M11 NM_177635.1
H2-M2 NM_008204.2
H2-M3 NM_013819.2
H2-M9 NM_008205.1
H2-Q1 NM_010390.2
H2-Q10 NM_010391.4
H2-Q2 NM_010392.2
H2-Q5 NM_010393.1
H2-Q7 NM_010394.2
H2-Q8 NM_023124.2
H2-T10 NM_010395.5
H2-T23 NM_010398.1
H2-T23 NM_010398.3
H2-T24 NM_008207.2
H2-T3 NM_008208.3
H2-Tw3 NM_001030310.1
H2-Aa NM_010378.2
H2-Ab1 NM_207105.1
H2-Ab1 NM_207105.2
H2-Ab1 NM_207105.2
H2-DMa NM_010386.2
H2-DMb1 NM_010387.2
H2-DMb2 NM_010388.2
H2-Ea NM_010381.2
H2-Eb1 NM_010382.2
H2-Oa NM_008206.1
H2-Ob NM_010389.3
Cd74 NM_001042605.1
Cd74 NM_010545.3
DC
Ccr7 NM_007719.2
Cd207 NM_144943.2
Cd207 NM_144943.2
Cd209a NM_133238.4
Cd209b NM_026972.2
Cd209b NM_026972.2
Cd209b NM_001037800.1
Cd209c NM_130903.2
Cd209c NM_130903.2
Cd209d NM_130904.2
Cd209e NM_130905.2
Cd4 NM_013488.2
Cd83 NM_009856.1
Cd8a NM_001081110.2
Cd8b1 NM_009858.2
Cd8b1 NM_009858.2
Clec4a1 NM_199311.2
Clec4a2 NM_011999.2
Clec4a2 NM_011999.3
Clec4a3 NM_153197.3
Clec4a3 NM_153197.3
Clec4a4 NM_001005860.1
Clec7a XM_984804.1
Clec7a NM_020008.1
Cxcl3 NM_203320.2
Cxcr4 NM_009911.2
Il23a NM_183391.2
Il23a NM_031252.2
Il3ra NM_031252.1
Itgax NM_021334.1
Pdcd1lg2 NM_021396.1
Siglech NM_178706.3
Siglech NM_178706.3
Siglech NM_178706.2
Tlr3 NM_126166.4
Tnfsf18 NM_183391.2
costimulatory molecules
Cd80 NM_009855.2
Cd86 NM_019388.2
Cd86 NM_019388.2
Cd86 NM_019388.2
Cd273 NM_021396.1
Cd274 NM_021893.2
Cd40 NM_170702.2
Cd40 NM_170701.2
Cd40 NM_170702.2
Cd40 NM_170702.2
Tnfsf4 NM_009452.1
Tnfsf8 NM_009403.2
Tnfsf9 NM_009404.3
Cd70 NM_011617.1
Cd27 NM_001033126.2
Cd27 NM_001033126.2
Cd27 NM_001033126.2
microglia markers
Cx3cr1 NM_009987.2
Aif1 NM_019467.2
Aif1 NM_019467.2
Aif1 NM_019467.2
P2ry12 NM_027571.2
Coro1a NM_009898.2
Coro1a NM_009898.2
Coro1a NM_009898.2
Coro1a NM_009898.2
Emr1 NM_010130.1
Emr1 NM_010130.3
Sfpi1 NM_011355.1
0
14
log2 transformed normalized expression value

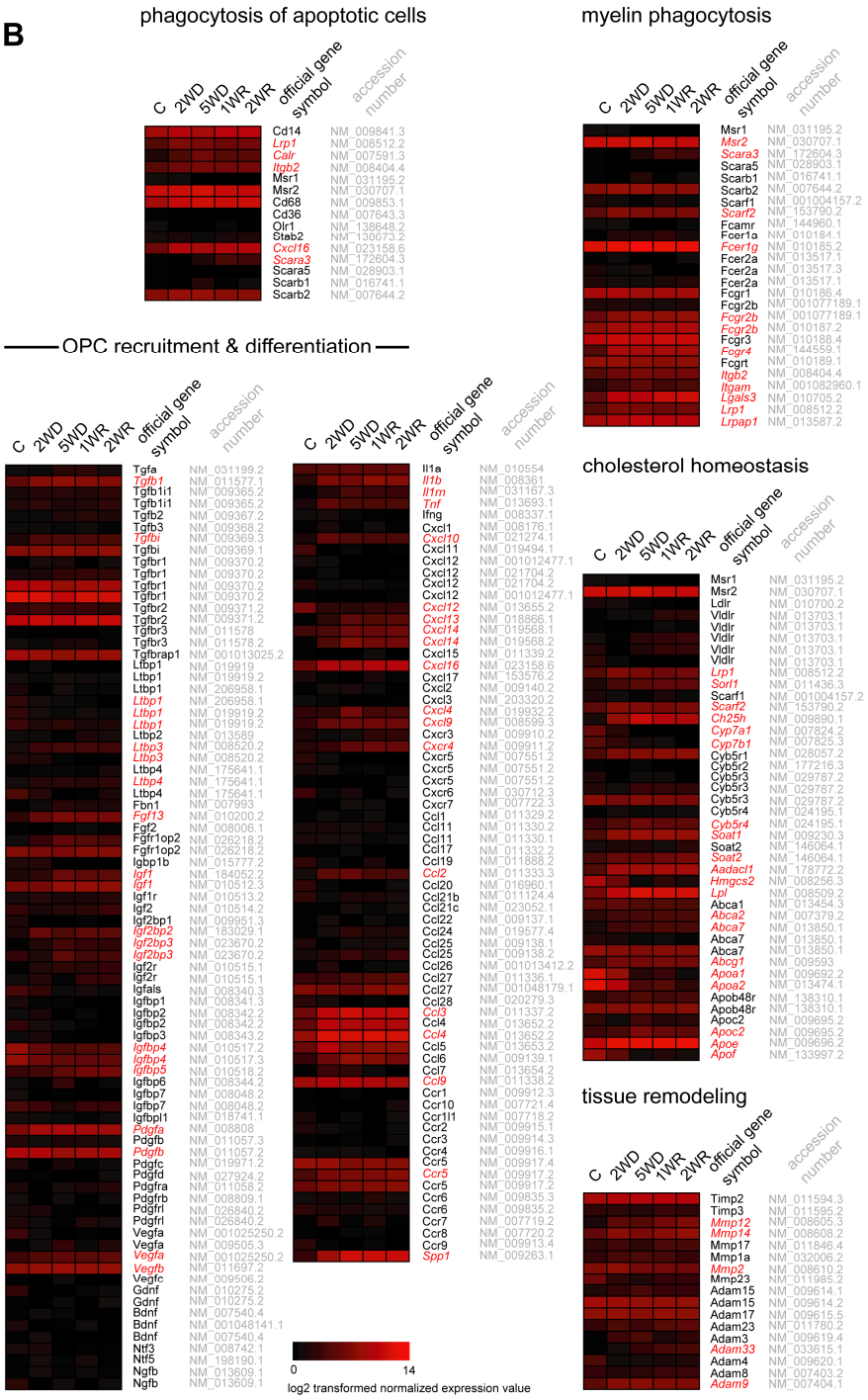
B
phagocytosis of apoptotic cells
myelin phagocytosis
OPC recruitment & differentiation
cholesterol homeostasis
tissue remodeling
C 2WD 5WD 1WR 2WR
official gene symbol
accession number
log2 transformed normalized expression value
0
14

Figure 4. Transcriptomic "fingerprint" of microglia in the course of de- and remyelination. The log2 transformed normalised expression values of the array data (an average of three independent observations for each gene) was used to produce the heatmaps. Please see the reference bar at the bottom for color coding of the expression levels. Black corresponds to absent/not expressed. **A** The microglia phenotype associated with de- and remyelination in the cuprizone model. Heatmaps showing the expression levels of marker genes attributed to classically and alternatively activated macrophages, dendritic cells and microglia. **B** The effector functions of microglia during de- and remyelination in the cuprizone model. Heatmaps showing the expression levels of genes associated with phagocytosis of apoptotic cells and myelin, tissue remodeling, cholesterol homeostasis of macrophages, secreted cytokines and chemokines relevant for the recruitment and differentiation of OPCs.

Confirmation of the genome wide gene expression analysis findings in situ at the mRNA and protein level

Taking into consideration the large number of microglia genes, that was found to be significantly differently regulated in the course of de- and remyelination, we have decided to confirm the findings of our genome wide gene expression study by investigating the expression levels of certain selected genes *in situ* at the mRNA and protein level. We focused primarily on two major aspects of the microglia phenotype and function: markers associated with the state of microglia activation (tolerance inducing, anti-inflammatory) and markers pointing towards the active involvement of microglia in the regenerative processes (trophic and metabolic support to (re)myelinating oligodendrocytes). Importantly, all the investigated markers showed an expression pattern at the protein level identical to their gene expression pattern.

The marked upregulation of mRNA of genes associated with the major histocompatibility complex prompted us to investigate the expression pattern at the protein level. At 5WD few microglia within and outside the lesions expressed MHCII in the corpus callosum. However, the number of MHCII positive microglia robustly increased during remyelination (Figure 5). Under control conditions no cells seemed to express MHCII in the CNS other than the macrophages associated with the ependymal lining of the ventricles. Since MHCII is known to be involved in cross-talk between microglia/macrophages and T cells

(Carson, 2002), we were interested whether T cells could be present in the corpus callosum in the course of de- and remyelination. To answer this question, we performed immunohistochemistry against CD3, a pan T cell marker. In the control animals, no T cells could be detected in the brain parenchyma (Figure 5). At 5WD and 2WR (in line with the previous report by Remington et al., 2007) a few CD3 positive T cells were present in the corpus callosum. However, we could not detect any difference in the cellular density of CD3 positive cells in the corpus callosum of 5WD and 2WR animals.

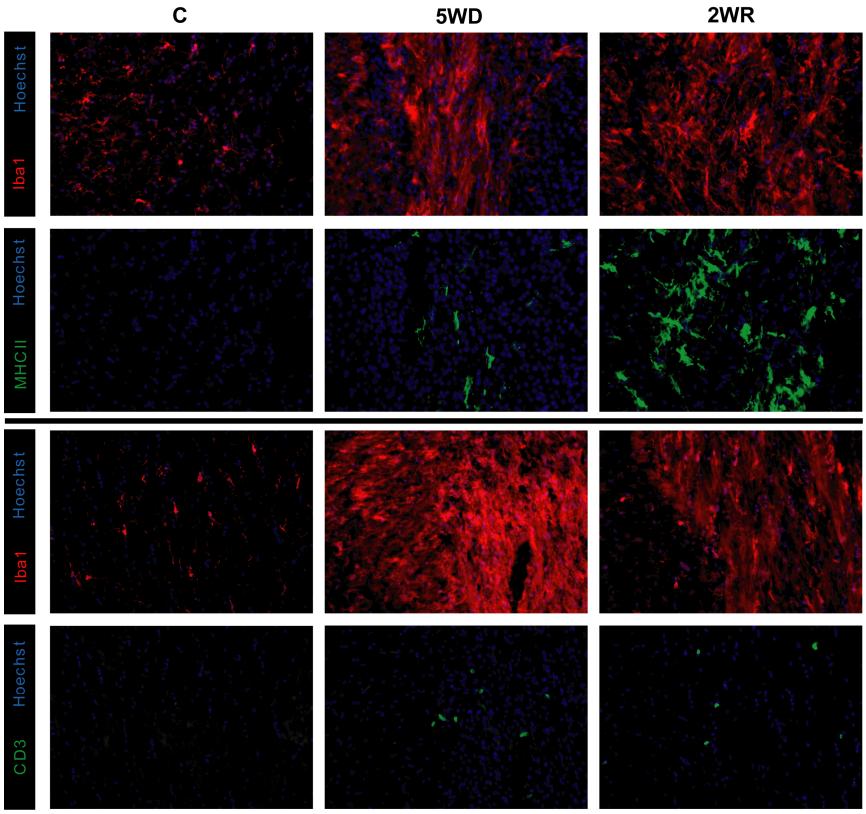

Figure 5. The presence of high levels of MHCII on microglia and the absence of costimulatory molecules point towards a tolerance inducing phenotype. Representative photomicropgraphs of immunohistochemical stainings showing the gradual upregulation of MHCII on the microglia and the presence of CD3 positive T cells in the corpus callosum parenchyma during de- and remyelination. All images depict the corpus callosum. (C control, 5WD five weeks of demyelination; 2WR two weeks of remyelination; Iba1 ionised calcium binding adaptor molecule 1, a microglia

marker; MHCII major histocompatibility complex II; CD3 a T cell marker; Hoechst a nuclear dye).

Next we investigated whether MHCII positive microglia in the demyelinating and remyelinating corpus callosum posses the necessary surface antigens to activate T cells in the course of antigen presentation. We have tested the expression of three major costimulatory molecules (CD40, CD80 and CD86) on microglia at the protein level *in situ*. In line with the findings of our array study, the expression level of none of these markers was above the detection limit of immunohistochemistry at any investigated time point (data not shown).

The data from our gene expression study suggest that microglia (similarly to the macrophages during the regeneration of peripheral nerves) have the means to salvage the cholesterol and lipids from the degenerating myelin by re-utilising it and making it available for remyelinating oligodendrocytes. To detect myelin degradation products in microglia, we performed Oil red O (ORO) histochemistry of the brain sections. At 5WD microglia seemed to be full of lipid droplets at the lesion site (Figure 6A), where the uniform pink staining pattern of the intact myelin sheets seen in C and 2WD was completely absent. At 1WR neutral lipid laden microglia could still be seen in the corpus callosum, intermingled with the developing new myelin sheets. At 2WR however, microglia in the corpus callosum was free of myelin degradation products and the organisation of the myelin sheets was back to pre-treatment level. The ORO histochemistry showed us, that microglia in the corpus callosum readily scavenge the myelin debris associated with demyelination.

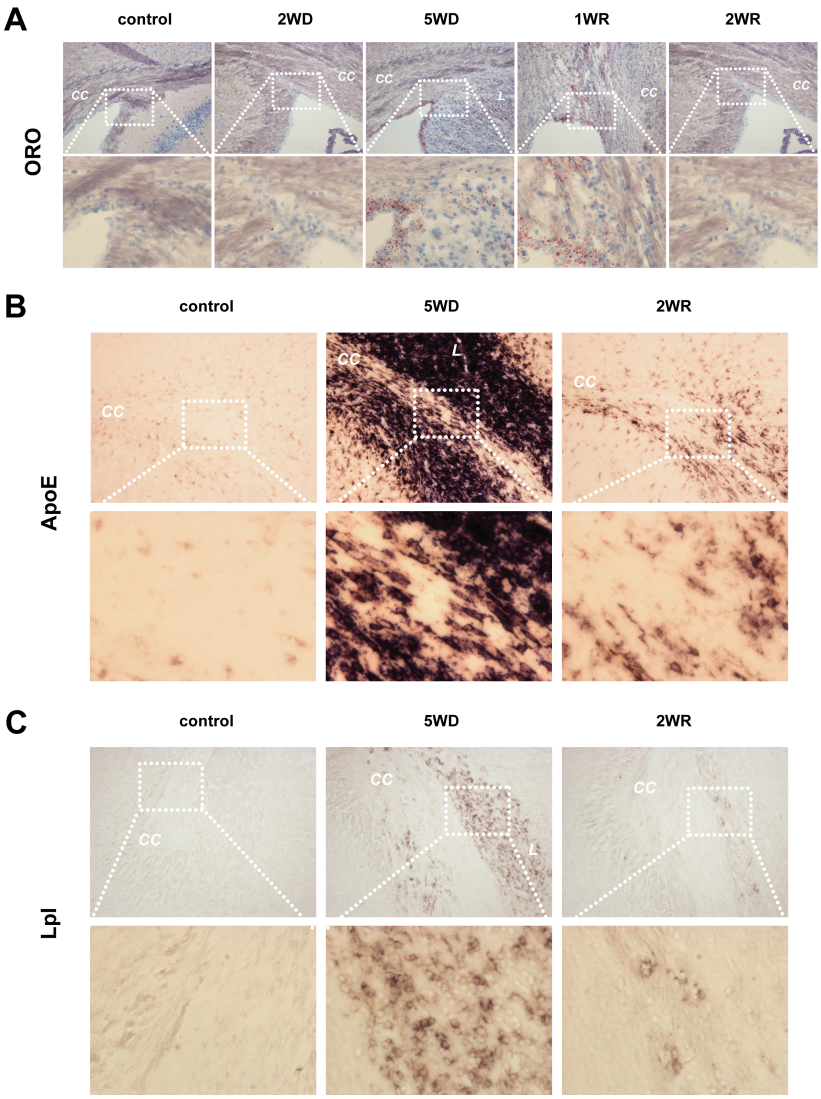

Figure 6. Myelin phagocytosis by lesion associated microglia shapes their phenotype supportive of remyelination. A Myelin degradation products (in the form of lipid droplets) were detected in microglia with the means of Oil red O histochemistry. Please note the faint pink staining of the intact myelin in the control condition and at 2WD, the accumulation of microglia that ingested myelin at the lesion site at 5WD, the persistent presence of lipid droplets in microglia at 1WR and their dissapearence at 2WR. **B** Representative photomicrographs showing the significant upregulation of Apoe mRNA in microglia associated with de- and remyelination as detected with *in situ* hybridisation. **C** Representative photomicrographs showing the significant upregulation of Lpl mRNA in microglia associated with de- and remyelination detected by the means of *in situ* hybridisation. (2WD two weeks of demyelination; 5WD five weeks of demyelination; 1WR one week of remyelination; 2WR two weeks of

remyelination; ORO Oil red O histochemistry; Apoe apolipoprotein E; Lpl lipoprotein lipase; L lesion; cc corpus callosum).

We have analysed the expression of several factors involved in this process. Apolipoprotein E (*Apoe*), is known to be associated with cholesterol efflux from macrophages. Lipoprotein lipase (*Lpl*) is an enzyme that is involved in hydrolysis of triglycerides. Both factors were among the significantly different regulated microglia transcripts during de- and remyelination in our array. We investigated their expression at the mRNA level *in situ*. ApoE mRNA was robustly upregulated in microglia in the corpus callosum at 5WD, and remained upregulated at 2WR, when compared to C (Figure 6B). In the control brains we could not detect any mRNA signal for *Lpl* with the applied technique (*in situ* hybridisation) (Figure 6C). Lesion associated microglia at 5WD however, showed strong positivity for LPL and retained the expression level of this enzyme at 2WR.

We also decided to investigate the expression pattern of certain selected genes at the protein level with immunohistochemistry. For this purpose we have chosen proteins, which have shown significant regulation across our samples and point towards the different effector functions and phenotypes of microglia including TGF-β1, osteopontin, antileukoproteinase, CD11c and galectin-3.

Transforming growth factor beta 1 has been shown to be involved in promoting OPC differentiation and myelination (Diemel et al., 2003; Bauman & Pham-Dhin, 2001; Hinks & Franklin, 1999). TGF-β1 expression was upregulated in the course of de- and remyelination in microglia both at the mRNA (Figure 4B) and the protein (Figure 7A) level. Unlike most other investigated factors, it was already expressed by some microglia in the corpus callosum under control conditions (Figure 7A).

Osteopontin (*Spp1*), which has been shown to promote myelination *in vitro* (Selvaraju et al., 2004), could be detected with immunohistochemistry in microglia associated with the lesion at 5WD as well as in microglia in the remyelinating corpus callosum (Figure 7B),

while it was absent from the white matter microglia of the control animals.

Slpi, secretory leukocyte peptidase inhibitor or antileukoproteinase (ALP), which has been implicated in the resolution of inflammation and wound healing (Doumas et al., 2005; Odaka et al., 2003; Ashcroft et al., 2000), was also among the strongly upregulated genes from C condition to 5WD, but was abruptly downregulated in microglia as early as 1WR (example entity for Figure 2B/B'' group; see Supplementary table 1). Accordingly, ALP immunoreactivity in microglia was only detectable at 5WD in the corpus callosum (Figure 7C).

Interestingly, astrocytes were intensively stained with the antibody against ALP at 5WD in brain regions other than the corpus callosum and continued its expression during remyelination (1WR and 2WR; data not shown).

Importantly, some microglia in the corpus callosum expressed the dendritic cell marker CD11c (*Itgax*; Figure 7C), which particularly became apparent during the course of remyelination (1WR and 2WR).

The expression of galectin-3 (*Lgals3*; Figure 4B), a galactose binding lectin mainly associated with microglial myelin phagocytosis (Rotshenker et al., 2008; Reichert & Rotshenker, 1999), was already detectable at 5WD on microglia in the corpus callosum and remained upregulated during remyelination (1WR and 2WR; Figure 7E).

Figure 7. Confirmation of the expression patterns of selected genes at the protein level by the means of immunohistochemistry. For all the examined markers the changes detected at the protein level were in accordance with the changes in the gene expression levels. Tgfβ (**A**) and Spp1 (**B**) were both upregulated in the course of demyelination and remained upregulated in microglia during the remyelination phase. White arrows point towards the double positive cells in the corpus callosum. **C** Antileukoproteinase (a potent anti-inflammatory secreted serine protease inhibitor) was upregulated during 5WD, but was absent from microglia at other time points. **D** Some microglia at 1WR and 2WR expressed detectable levels of the dendritic cell marker, CD11c. **E** Galectin 3 mRNA was gradually upregulated in microglia in the course of de- and remyelination, became detectable at the protein level at 5WD (data not shown) and remained upregulated up to 2WR. (5WD five weeks of demyelination;

1WR one week of remyelination; 2WR two weeks of remyelination; for other acronyms see List of abbreviations)

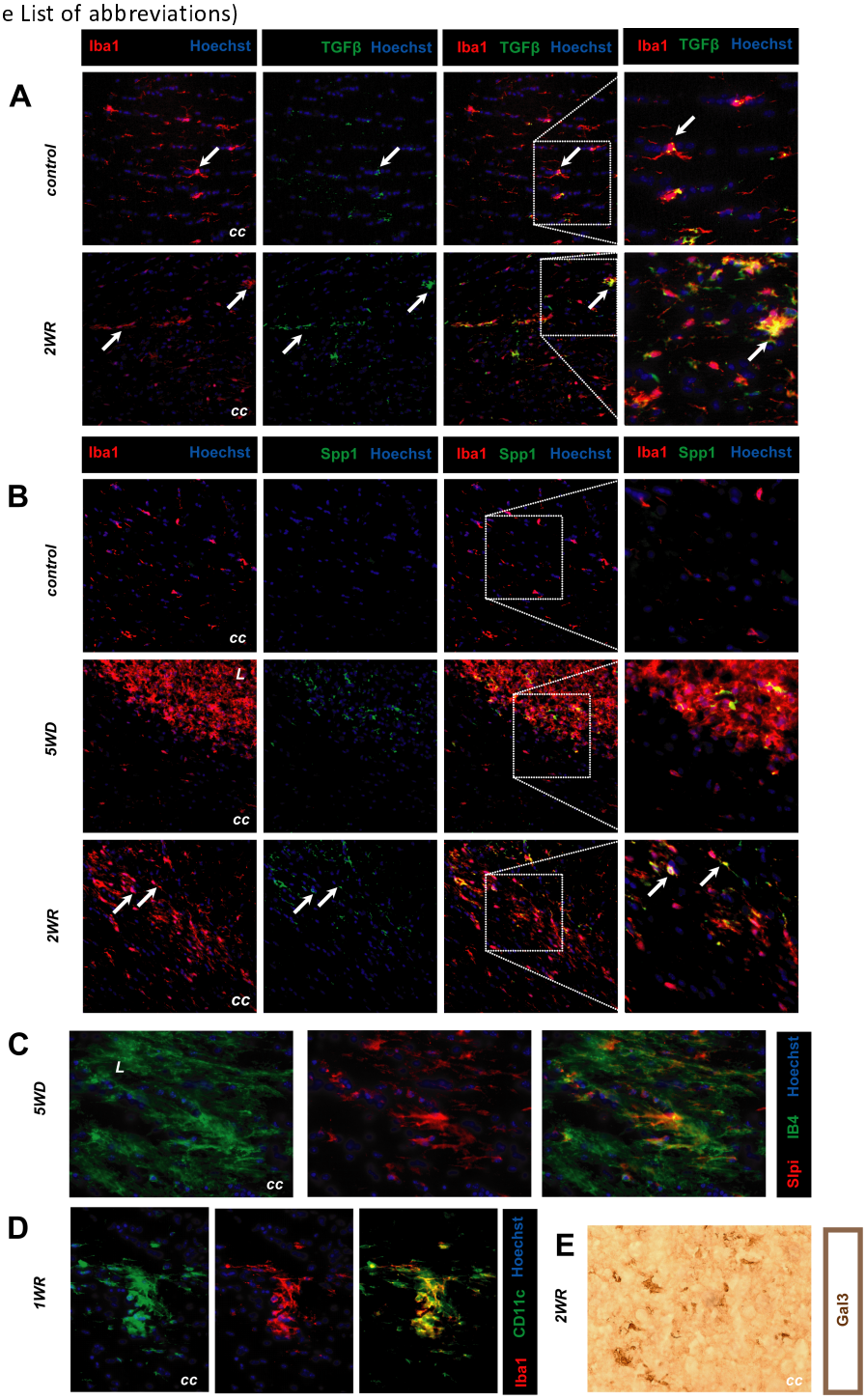

DISCUSSION

For long time it has been thought, that in multiple sclerosis remyelination doesn't occur either because of the decreased availability of oligodendrocyte precurors or their inability to colonise the lesions. With the advancement of imaging and immunohistochemical techniques however, it has become clear, that attempts to remyelinate the demyelinated lesions is much more common in MS than initially thought (Blakemore & Franklin, 2008; Blakemore & Keirstead, 1999), and the abundance of OPCs or their migratory capacity is not the limiting factor. In most cases OPCs are readily recruited to the lesion sites, but their differentiation towards a functional myelinating oligodendrocyte is halted by the lack of a supportive cellular environment (Franklin, 2002). Given the complex relationship between inflammation and remyelination (Hohlfeld, 2007; Rodriguez, 2007; Sharief et al., 1998) it has been suggested, that the modulation of the inflammatory environment of the lesion by shaping the phenotype of the resident CNS immune cells towards a remyelination supportive one would be a promising therapeutic approach (Franklin & Ffrench-Constant, 2008). Therefore, the notion arose, that it would be important to characterise the actual remyelination supportive microglia phenotype, about which the existing experimental data up till today is at least scarce (Napoli & Neumann, 2009). Only after defining this phenotype could we ask further questions such as: why does it fail to develop and why is it suppressed in MS, or which characteristics of microglia/macrophages to boost in order to create a remyelination supportive environment in the MS lesions.

We decided to approach the task by investigating the global gene expression of microglia during de- and remyelination by means of microarray analysis, followed by a detailed confirmation of our transcriptomic findings at the protein level. We used the cuprizone model, in which, due to the uncompromised blood brain barrier

(McMahon et al., 2002; Bakker & Ludwin, 1987; Kondo et al., 1987) and the relative scarcity of infiltrating blood borne cells (Remington et al., 2007; McMahon et al., 2002), peripheral immune cells do not contribute to the processes that shape the microglia phenotypes.

Moreover, demyelination and remyelination in the cuprizone model follow a highly reproducible time course (Matsushima & Morell, 2001), making it technically feasible to experimentally dissect the two processes and the microglia phenotype associated with them.

Surprisingly however, we couldn't find any evidence supporting the idea that there would be two microglia phenotypes; one associated with demyelination and another one, specifically responsible for remyelination. Despite our expectations, there was no 'switch' in phenotype from microglia present in the corpus callosum during demyelination to microglia of the remyelinating white matter. The only changes that proved to be characteristic of the demyelination phase concerned genes associated with cell cycle, proliferation and cell division. Clearly, the microglia phenotype present during remyelination developed gradually during demyelination and persisted upon remyelination. Thus, most of the genes that were significantly differently regulated among the experimental conditions showed an unidirectional change from control to demyelination and remyelination, meaning that they were upregulated/downregulated during demyelination and they remained upregulated/downregulated in the course of remyelination.

Among the genes that showed most prominently this expression pattern were the genes associated with the major histocompatibility complex (MHC), especially MHCII. The robust and sustained upregulation of the molecules belonging to the MHCII complex (such as *H2-Aa*, *H2-Ab1*, *H2-Eb1*, *Cd74*) was one of the most evident changes occuring in the gene expression of microglia in the course of de- and remyelination. Remarkable, however, was the almost complete absence of the expression of the costimulatory molecules. Next to *Cd86* (B7.2) only

Cd274 (also known as B7-H1) seemed to be peresent and upregulated in microglia during de- and remyelination. The presence of upregulated MHCII on microglia in the course of de- and remyelination together with the absence (or undetectable levels) of costimulatory molecules suggests that microglia might have acquired a tolerance inducing phenotype (Matyszak et al., 1999). Importantly, the expression of B7-H1 on antigen presenting cells (APCs) has been shown to induce T cell anergy and tolerance induction (Magnus et al., 2005; Keir et al., 2008).

We also investigated the changes in the expression of genes associated with one of the most important effector functions of microglia - clearance of tissue debris (apoptotic cells and myelin, in this case) by phagocytosis. In addition to its clearance function (Napoli & Neumann, 2009; Kotter et al., 2006), phagocytosis of apoptotic cells and myelin is also believed to direct microglial characteristics towards a regeneration supportive phenotype (Griffiths et al., 2009; Boven et al., 2006). Hence, we investigated whether microglia in the demyelinating and remyelinating corpus callosum acquired the receptor and molecular repertoire indicative of tissue support.

From the multiple receptors that have a role in the recognition and clearance of apoptotic cells by phagocytes (reviewed in Savill et al., 2002), microglia upregulated mRNA expression levels of *Cxcl16*, *Scara3* and *Cd68* in the course of de- and remyelination. CD91 (*Lrp1*), β2-integrin (*Itgb2*), and calreticulin (*Calr*) mRNAs were also upregulated, while *Cd14* was expressed at a more or less stable level across the samples. Hence, it is reasonable to speculate, that microglia in the corpus callosum during demyelination express multiple receptor systems for the recognition of apoptotic cells (such as receptors for oxydised low-density lipoproteins, cell surface phosphatidylserine, opsonic complement fragments and apoptotic cell associated molecular patterns (ACAMPs)).

Some of the scavenger receptors and molecules that are presumably associated with phagocytosis of myelin debris (Rotshenker et al., 2008;

Reichert and Rotshenker, 2003; Kuhlmann et al., 2002) seemed to be constitutively expressed in microglia (*Msr2*, *Scarb2* and some Fc receptors). Others were moderately upregulated during de- and remyelination (*Scara3*, *Scarf2*, *Itgb2*, *Itgam*, *Lgals3*, *Lrp1*; Figure 4B). Macrophages associated with the regenerating peripheral nerve have been found to scavenge and re-utilise the sequestered cholesterol, offering it to the remyelinating Schwann cells (Jurevics et al., 1998). We found several clues indicating that microglia might play a similar role in remyelination in the CNS. Some of the known lipoprotein receptor mRNAs (such as *Sorl*, *Lrp1* and *Scarf2*) were upregulated during demyelination, and remained upregulated during remyelination. Interestingly, we found a marked downregulation of the genes associated with *de novo* cholesterol synthesis (e.g. *Hmgcs2*), while others associated with hydrolysis of lipoproteins (such as *Aadacl*, *Lpl* and its cofactor *Apoc2*) were distinctly upregulated. Moreover, the marked upregulation of cholesterol 25-hydroxylase (*Ch25h*) points towards the possibility that microglia are indeed actively repressing their own cholesterol biosynthetic enzymes. On the other hand, genes associated with the cholesterol efflux system of macrophages (*Abcg1*, *Abca7* and *Apoe*) were upregulated during both de- and remyelination. The gene expression data further suggest, that microglia in the corpus callosum under de- and remyelinating conditions possess the enzyme repertoire required for tissue remodeling. Among the upregulated genes were the membrane-type matrix metalloproteinase 1 and macrophage metalloellastase (*Mmp14* and *Mmp12*, respectively), both of which are known to be involved in tissue remodeling by macrophages. Moreover, several serine protease inhibitors (e.g. alpha-1-antitrypsine) were downregulated during cuprizone treatment, while their target enzymes (e.g. urokinase-type plasminogen activator) were upregulated (data not shown), confirming the role for microglia in the tissue remodeling during demyelination.

Microglia are a major source of cytokines and chemokines in the CNS (Hanisch, 2002; Gebicke-Haerter et al., 2001). Moreover, it is widely accepted that cytokines and chemokines are involved in the recruitment, proliferation and differentiation of neural stem cells and oligodendrocyte precursors (OPCs) upon brain injury (Imitola et al., 2004; Bauer, 2009). We further investigated whether microglia during de- and remyelination expressed growth factors, cytokines and chemokines known to be involved in the regulation of OPC recruitment, proliferation and differentiation. Among the upregulated growth factors were *Pdgfa* and *Pdgfb*, *Vegfa* and *Vegfb*, which have been described to have an important role in OPC differentiation (Bradl & Lassmann, 2010; Kim et al., 2009; Woodruff et al., 2004; Frost et al., 2002). We could not detect any signal of expression of neurotrophins during cuprizone administration. Transforming growth factor beta 1 (TGF-β1) is known to have multiple functions in the CNS (Makwana et al., 2007). TGF-β1, produced by microglia, has been implicated in the regulation of adult neurogenesis (Battista et al., 2006) and it has been shown to be involved in promoting OPC differentiation and myelination (Diemel et al., 2003; Bauman & Pham-Dhin, 2001; Hinks & Franklin, 1999). In our experiments we observed a strong upregulation of TGF-β1 both at the mRNA and the protein level during de- and remyelination in microglia. The protein was detectable in corpus callosum microglia of control animals as well. Interesting is the simultaneous induction of *Mmp14*, since MMP-14 is known to be involved in the release of latent TGF-β1 from the extracellular matrix (ECM) through the proteolytic cleavage of latent-transforming growth factor beta-binding proteins (Ltbp) (Tatti et al., 2008).

Igf1, which was among the upregulated genes, has been described to instruct neural stem cell differentiation (NSCs) towards OPCs (Hsieh et al., 2004), but has also been shown to be involved in the proliferation and differentiation of OPCs (Chesik et al., 2008). It is also believed to be a survival factor for mature oligodendrocytes (Pang et al., 2007; Mason

et al., 2000). The release of IGF-1 from the extracellular matrix depends on the presence of insulin-like growth factor-binding proteins (IGFBPs) that determine the bioavailability of IGF-1 for the cells (Bunn & Fowlkes, 2003). Since some of the IGFBPs (I*gfbp4* and *Igfbp5* (the former inhibits IGF-1 action while the later protects IGF-1 from proteolytical degradation (Rechler & Clemmons, 1998)) were differently regulated in microglia during de- and remyelination, they may be promising candidates for further investigation.

The cytokines TNF-α (*Tnfa*) and IL-1β (*Il1b*) were also upregulated at the mRNA level in microglia during de- and remyelination. Both cytokines have been described to promote proliferation of OPCs and remyelination (Vela et al., 2002; Arnett et al., 2001).

Osteopontin (*Spp1* or Opn), a secreted phosphoprotein with cytokine functions, was also strongly upregulated during demyelination and remained upregulated during remyelination in microglia. Osteopontin is expressed in microglia/macrophages during demyelination in MS (Imitola et al., 2005) and is believed to be associated with the occurrence of relapses (Borsen et al., 2010). In animal models it seems to function as chemoattractant for neural stem cells (Yan et al., 2009) and it is found to enhance myelin formation *in vitro* (Selvaraju et al., 2004). We have found a strong upregulation both of the osteopontin mRNA and protein in microglia during demyelination. Moreover, (just like the gene product of *Cd74*), this mRNA species was further upregulated during the remyelination phase itself, thus the highest expression levels could be detected at 2WR

With the genome wide gene expression approach we could detect the upregulated expression of several chemokines (*Ccl2*, *Ccl3*, *Ccl4*, *Ccl5*, *Ccl6*, *Ccl27*, *Cxcl10*, *Cxcl13*, *Cxcl14* and *Cxcl16*) in the course of de- and remyelination. Many of these chemokines have been implicated in the pathophysiology of MS and it's animal model, experimental autoimmune encephalomyelitis (EAE)(Ransohoff & Bacon, 2000; Zhang et al., 2000), and have been suggested to be associated with the

recruitment of systemic immune cells to the lesion site. Since NSCs and OPCs express functional receptors for both C-C and C-X-C chemokines (Belmadani et al., 2006; Omari et al., 2005; Nguyen et al., 2003) it is reasonable to speculate that some of the regulated chemokines might be involved in the recruitment of NSCs/OPCs to the lesion site. Particularly the chemokine receptors *Cxcr4* and *Ccr5* seemed to be upregulated in microglia at the mRNA level. While *Cxcr4* is most likely involved in migration of microglia (Wang et al., 2008), the upregulation of *Ccr5* might be of particular interest, since it has been detected on microglia in early lesions in MS associated with remyelination (Trebst et al., 2008).

Based on the cytokine and chemokine gene expression profile of microglia during de- and remyelination points towards their capacity to recruit endogenous neural stem cells and OPCs, and stimulate their differentiation towards myelinating oligodendrocytes.

Microglia in the corpus callosum constitutively expressed some classically activated macrophage (CAMΦ) markers (including cathepsins, such as *Ctsb*, *Ctsh*, *Ctss* and *Ctsz*; Figure 4A), which are believed to be involved in the overall degradation and turnover of proteins in the cells. The expression of some other markers of CAMΦs were induced already during the early phases of demyelination and remained upregulated during remyelination (e.g. *Tlr4*, *Lyz1* and *Lyz2*, *Fcgr2b* and *Fcgr4*, *Tnf*, *Il1a* and *Il1b*, *Ccl3*, *Ccl4*, *Ccl5* and *Ccl9*, *Mmp12*). Despite the induction of several CAMΦ markers, the macrophage specific nitric oxide synthase (Nos2) was not induced in microglia upon demyelination and remyelination. Alternatively activated macrophage (AAMΦ) markers that were upregulated during de- and remyelination included *Cd63*, *Igf*, *Tgfb*, *Pdgfa*, *Spp1*, *Il13ra*, *Il4ra*, *Il2rg*, while *Vegfb* and *Pdgfb* were constitutively expressed in corpus callosum microglia. Importantly, two of the most characteristic markers of AAMΦs were not induced during demyelination or remyelination (*Arg1* and *Msr1*). Some dendritic cell

(DC) markers were also induced during demyelination and remained upregulated in the course of remyelination (*CD83*, *Clec7a*, and *Itgax*).
The data of the microarray analysis and the subsequent confirmation at the protein level suggest the following characteristics of a remyelination supportive microglia phenotype: I phagocytosis and degradation of myelin, II recycling of fatty acids for remyelination, III up-regulation of MHC molecules with low abundance of costimulatory molecules, IV up-regulation of genes associated with regeneration (galectin 3, osteopontin, TGFβ1,etc.) and V expression of molecules associated with OPC recruitment and differentiattion (PDGF, IGF-1).
Some questions however, remain unanswered. First of all, the clearance of tissue debris is intuitively indispensable for regeneration to occur, but whether the microglia phenotype arising from the ingestion of myelin and apoptotic cells is truly supportive of remyelination, or simply permissive in this model remains to be elucidated. One way to address this question could be to deplete microglia form the brain (by brain infusion of ganciclovir in CD11b HSV-TK transgenic mice after most of the tissue debris has been removed, but before the occurrence of the large scale remyelination. From the literature it seems likely, that the development of the microglia phenotype with repair function is strongly associated with the ingestion of myelin debris and apoptotic cells, but so far only circumstantial evidence supports the causal relationship between the two. Additionally, other factors (e.g. signaling from apoptotic oligodendrocytes, recruited neural precursors, denuded axons and/or astrocytes) may also play a considerable role in triggering the regeneration supportive microglia phenotype . It is thus of importance to investigate the effect of these factors on the microglia phenotype and the contribution of other cell types in order to get a more complete picture of the cellular environment that supports remyelination.
Several earlier studies used microarray analysis to investigate gene expression changes associated with de- and remyelination (Arnett et al., 2003; Jurevics et al., 2002; Morell et al., 1998). The findings of these

studies were, however, to a certain extent obscured by the use of whole tissue lysates for the isolation of RNA, especially because of the low abundance of microglial transcripts in relation to the total tissue mRNA content. To our knowledge, our study is the first one which investigated the gene expression changes occurring at a genome wide scale during de- and remyelination particularly in microglia. Since genome wide gene expression analysis provides us with relative gene expression levels, we considered it important to confirm our findings at the protein level (when possible) *in situ*. Clearly, the expression patterns of all the markers that have been tested at the protein level so far were similar to the expression patterns of the given genes on the microarray. Thus, we have strong confidence that our gene expression data reflects the actual microglia phenotype associated with de- and remyelination. Our study provides the scientific community working on macrophages in regeneration a useful set of data for potential target molecules and pathways. Moreover, it further supports the concept that the primary function of microglia is maintenance of tissue homeostasis in the CNS.

The unique characteristics of the cuprizone model (negligible recruitment of systemic immune cells due to uncompromised blood brain barrier, well defined remyelination phase) enabled us to describe the remyelination supportive microglia phenotype per se. The functional relevance of this specific microglia phenotype will be further investigated in EAE (experimental autoimmne encephalomyelitis, an animal model that closely mimics the pathogenesis and pathophysiology of MS), and in pre-active lesions of multiple sclerosis.

LIST OF ABBREVIATIONS (FIGURES)

ApoE	apolipoprotein E
CD11c	integrin alpha-X, a dendritic cell marker
Gal3	Gal3 galectin-3
IB4	isolectin B4
Iba1	ionised calcium binding adaptor molecule 1
Lpl	lipoprotein lipase
Slpi	antileukoproteinase
Spp1	osteopontin
Tgfβ	transforming growth factor beta;

LIST OF REFERNCES

Arnett HA, Mason J, Marino M, Suzuki K, Matsushima GK, Ting JP. 2001. TNF alpha promotes proliferation of oligodendrocyte progenitors and remyelination. Nat Neurosci 4:1116-1122.
`

Arnett HA, Wang Y, Matsushima GK, Suzuki K, Ting JP. 2003. Functional genomic analysis of remyelination reveals importance of inflammation in oligodendrocyte regeneration. J Neurosci 23:9824-9832.

Ashcroft GS, Lei K, Jin W, Longenecker G, Kulkarni AB, Greenwell-Wild T, Hale-Donze H, McGrady G, Song XY, Wahl SM. 2000. Secretory leukocyte protease inhibitor mediates non-redundant functions necessary for normal wound healing. Nat Med 6:1147-1153.

Bakker DA, Ludwin SK. 1987. Blood-brain barrier permeability during Cuprizone-induced demyelination. Implications for the pathogenesis of immune-mediated demyelinating diseases. J Neurol Sci 78:125-137.

Battista D, Ferrari CC, Gage FH, Pitossi FJ. 2006. Neurogenic niche modulation by activated microglia: transforming growth factor beta increases neurogenesis in the adult dentate gyrus. Eur J Neurosci 23:83-93.

Bauer S. 2009. Cytokine control of adult neural stem cells. Ann N Y Acad Sci 1153:48-56.

Baumann N, Pham-Dinh D. 2001. Biology of oligodendrocyte and myelin in the mammalian central nervous system. Physiol Rev 81:871-927.

Belmadani A, Tran PB, Ren D, Miller RJ. 2006. Chemokines regulate the migration of neural progenitors to sites of neuroinflammation. J Neurosci 26:3182-3191.

Bieber AJ, Kerr S, Rodriguez M. 2003. Efficient central nervous system remyelination requires T cells. Ann Neurol 53:680-684.

Blakemore WF, Keirstead HS. 1999. The origin of remyelinating cells in the central nervous system. J Neuroimmunol 98:69-76.

Blakemore WF, Franklin RJ. 2008. Remyelination in experimental models of toxin-induced demyelination. Curr Top Microbiol Immunol 318:193-212.

Bornsen L, Khademi M, Olsson T, Sorensen PS, Sellebjerg F. 2010. Osteopontin concentrations are increased in cerebrospinal fluid during attacks of multiple sclerosis. Mult Scler.

Boven LA, Van MM, Van ZM, Wierenga-Wolf A, Hintzen RQ, Boot RG, Aerts JM, Amor S, Nieuwenhuis EE, Laman JD. 2006. Myelin-laden macrophages are anti-inflammatory, consistent with foam cells in multiple sclerosis. Brain 129:517-526.

Boyle EA, McGeer PL. 1990. Cellular immune response in multiple sclerosis plaques. Am J Pathol 137:575-584.

Bradl M, Lassmann H. 2010. Oligodendrocytes: biology and pathology. Acta Neuropathol 119:37-53.

Brosnan CF, Bornstein MB, Bloom BR. 1981. The effects of macrophage depletion on the clinical and pathologic expression of experimental allergic encephalomyelitis. J Immunol 126:614-620.

Bunn RC, Fowlkes JL. 2003. Insulin-like growth factor binding protein proteolysis. Trends Endocrinol Metab 14:176-181.

Carson MJ. 2002. Microglia as liaisons between the immune and central nervous systems: functional implications for multiple sclerosis. Glia 40:218-231.

Chesik D, De KJ, Wilczak N. 2008. Insulin-like growth factor system regulates oligodendroglial cell behavior: therapeutic potential in CNS. J Mol Neurosci 35:81-90.

Diemel LT, Jackson SJ, Cuzner ML. 2003. Role for TGF-beta1, FGF-2 and PDGF-AA in a myelination of CNS aggregate cultures enriched with macrophages. J Neurosci Res 74:858-867.

Doumas S, Kolokotronis A, Stefanopoulos P. 2005. Anti-inflammatory and antimicrobial roles of secretory leukocyte protease inhibitor. Infect Immun 73:1271-1274.

Ferrari CC, Depino AM, Prada F, Muraro N, Campbell S, Podhajcer O, Perry VH, Anthony DC, Pitossi FJ. 2004. Reversible demyelination, blood-brain barrier breakdown, and pronounced neutrophil recruitment induced by chronic IL-1 expression in the brain. Am J Pathol 165:1827-1837.

Foote AK, Blakemore WF. 2005. Inflammation stimulates remyelination in areas of chronic demyelination. Brain 128:528-539.

Franklin RJ. 2002. Why does remyelination fail in multiple sclerosis? Nat Rev Neurosci 3:705-714.

Franklin RJ, Ffrench-Constant C. 2008. Remyelination in the CNS: from biology to therapy. Nat Rev Neurosci 9:839-855.

Frost EE, Nielsen JA, Le TQ, Armstrong RC. 2003. PDGF and FGF2 regulate oligodendrocyte progenitor responses to demyelination. J Neurobiol 54:457-472.

Gebicke-Haerter PJ, Spleiss O, Ren LQ, Li H, Dichmann S, Norgauer J, Boddeke HW. 2001. Microglial chemokines and chemokine receptors. Prog Brain Res 132:525-532.

Hanisch UK. 2002. Microglia as a source and target of cytokines. Glia 40:140-155.

Hanisch UK, Kettenmann H. 2007. Microglia: active sensor and versatile effector cells in the normal and pathologic brain. Nat Neurosci 10:1387-1394.

Hinks GL, Franklin RJ. 1999. Distinctive patterns of PDGF-A, FGF-2, IGF-I, and TGF-beta1 gene expression during remyelination of experimentally-induced spinal cord demyelination. Mol Cell Neurosci 14:153-168.

Hohlfeld R, Kerschensteiner M, Meinl E. 2007. Dual role of inflammation in CNS disease. Neurology 68:S58-S63.

Hohlfeld R, Kerschensteiner M, Meinl E. 2007. Dual role of inflammation in CNS disease. Neurology 68:S58-S63.

Hsieh J, Aimone JB, Kaspar BK, Kuwabara T, Nakashima K, Gage FH. 2004. IGF-I instructs multipotent adult neural progenitor cells to become oligodendrocytes. J Cell Biol 164:111-122.

Huitinga I, van RN, De Groot CJ, Uitdehaag BM, Dijkstra CD. 1990. Suppression of experimental allergic encephalomyelitis in Lewis rats after elimination of macrophages. J Exp Med 172:1025-1033.

Imitola J, Raddassi K, Park KI, Mueller FJ, Nieto M, Teng YD, Frenkel D, Li J, Sidman RL, Walsh CA, Snyder EY, Khoury SJ. 2004. Directed migration of neural stem cells to sites of CNS injury by the stromal cell-derived factor 1alpha/CXC chemokine receptor 4 pathway. Proc Natl Acad Sci U S A 101:18117-18122.

Imitola J, Chitnis T, Khoury SJ. 2005. Cytokines in multiple sclerosis: from bench to bedside. Pharmacol Ther 106:163-177.

Jurevics H, Bouldin TW, Toews AD, Morell P. 1998. Regenerating sciatic nerve does not utilize circulating cholesterol. Neurochem Res 23:401-406.

Jurevics H, Largent C, Hostettler J, Sammond DW, Matsushima GK, Kleindienst A, Toews AD, Morell P. 2002. Alterations in metabolism and gene expression in brain regions during cuprizone-induced demyelination and remyelination. J Neurochem 82:126-136.

Keir ME, Butte MJ, Freeman GJ, Sharpe AH. 2008. PD-1 and its ligands in tolerance and immunity. Annu Rev Immunol 26:677-704.

Kim HM, Hwang DH, Lee JE, Kim SU, Kim BG. 2009. *Ex vivo* VEGF delivery by neural stem cells enhances proliferation of glial progenitors, angiogenesis, and tissue sparing after spinal cord injury. PLoS One 4:e4987.

Kipp M, Clarner T, Dang J, Copray S, Beyer C. 2009. The cuprizone animal model: new insights into an old story. Acta Neuropathol 118:723-736.

Koch-Henriksen N, Sorensen PS. 2010. The changing demographic pattern of multiple sclerosis epidemiology. Lancet Neurol 9:520-532.

Kondo A, Nakano T, Suzuki K. 1987. Blood-brain barrier permeability to horseradish peroxidase in twitcher and cuprizone-intoxicated mice. Brain Res 425:186-190.

Kotter MR, Zhao C, van RN, Franklin RJ. 2005. Macrophage-depletion induced impairment of experimental CNS remyelination is associated with a reduced oligodendrocyte progenitor cell response and altered growth factor expression. Neurobiol Dis 18:166-175.

Kotter MR, Li WW, Zhao C, Franklin RJ. 2006. Myelin impairs CNS remyelination by inhibiting oligodendrocyte precursor cell differentiation. J Neurosci 26:328-332.

Kuhlmann T, Wendling U, Nolte C, Zipp F, Maruschak B, Stadelmann C, Siebert H, Bruck W. 2002. Differential regulation of myelin phagocytosis by macrophages/microglia, involvement of target myelin, Fc receptors and activation by intravenous immunoglobulins. J Neurosci Res 67:185-190.

Lassmann H. 2008. Mechanisms of inflammation induced tissue injury in multiple sclerosis. J Neurol Sci 274:45-47.

Li WW, Setzu A, Zhao C, Franklin RJ. 2005. Minocycline-mediated inhibition of microglia activation impairs oligodendrocyte progenitor cell responses and remyelination in a non-immune model of demyelination. J Neuroimmunol 158:58-66.

Maere S, Heymans K, Kuiper M. 2005. BiNGO: a Cytoscape plugin to assess overrepresentation of gene ontology categories in biological networks. Bioinformatics 21:3448-3449.

Magnus T, Schreiner B, Korn T, Jack C, Guo H, Antel J, Ifergan I, Chen L, Bischof F, Bar-Or A, Wiendl H. 2005. Microglial expression of the B7 family member B7 homolog 1 confers strong immune inhibition: implications for immune responses and autoimmunity in the CNS. J Neurosci 25:2537-2546.

Makwana M, Jones LL, Cuthill D, Heuer H, Bohatschek M, Hristova M, Friedrichsen S, Ormsby I, Bueringer D, Koppius A, Bauer K, Doetschman T, Raivich G. 2007. Endogenous transforming growth factor beta 1 suppresses inflammation and promotes survival in adult CNS. J Neurosci 27:11201-11213.

Mason JL, Ye P, Suzuki K, D'Ercole AJ, Matsushima GK. 2000. Insulin-like growth factor-1 inhibits mature oligodendrocyte apoptosis during primary demyelination. J Neurosci 20:5703-5708.

Mason JL, Suzuki K, Chaplin DD, Matsushima GK. 2001. Interleukin-1beta promotes repair of the CNS. J Neurosci 21:7046-7052.

Matsushima GK, Morell P. 2001. The neurotoxicant, cuprizone, as a model to study demyelination and remyelination in the central nervous system. Brain Pathol 11:107-116.

Matyszak MK, is-Donini S, Citterio S, Longhi R, Granucci F, Ricciardi-Castagnoli P. 1999. Microglia induce myelin basic protein-specific T cell anergy or T cell activation, according to their state of activation. Eur J Immunol 29:3063-3076.

McMahon EJ, Suzuki K, Matsushima GK. 2002. Peripheral macrophage recruitment in cuprizone-induced CNS demyelination despite an intact blood-brain barrier. J Neuroimmunol 130:32-45.

Miller DJ, Asakura K, Rodriguez M. 1996. Central nervous system remyelination clinical application of basic neuroscience principles. Brain Pathol 6:331-344.

Morell P, Barrett CV, Mason JL, Toews AD, Hostettler JD, Knapp GW, Matsushima GK. 1998. Gene expression in brain during cuprizone-induced demyelination and remyelination. Mol Cell Neurosci 12:220-227.

Napoli I, Neumann H. 2009. Microglial clearance function in health and disease. Neuroscience 158:1030-1038.

Napoli I, Neumann H. 2010. Protective effects of microglia in multiple sclerosis. Exp Neurol 225:24-28.
Nataf S. 2009. Neuroinflammation responses and neurodegeneration in multiple sclerosis. Rev Neurol (Paris) 165:1023-1028.

Nguyen D, Hopfner M, Zobel F, Henke U, Scherubl H, Stangel M. 2003. Rat oligodendroglial cell lines express a functional receptor for the chemokine CCL3 (macrophage inflammatory protein-1alpha). Neurosci Lett 351:71-74.

O'Donnell SL, Frederick TJ, Krady JK, Vannucci SJ, Wood TL. 2002. IGF-I and microglia/macrophage proliferation in the ischemic mouse brain. Glia 39:85-97.

Odaka C, Mizuochi T, Yang J, Ding A. 2003. Murine macrophages produce secretory leukocyte protease inhibitor during clearance of apoptotic cells: implications for resolution of the inflammatory response. J Immunol 171:1507-1514.

Omari KM, John GR, Sealfon SC, Raine CS. 2005. CXC chemokine receptors on human oligodendrocytes: implications for multiple sclerosis. Brain 128:1003-1015.

Paglinawan R, Malipiero U, Schlapbach R, Frei K, Reith W, Fontana A. 2003. TGFbeta directs gene expression of activated microglia to an anti-inflammatory phenotype strongly focusing on chemokine genes and cell migratory genes. Glia 44:219-231.

Pang Y, Zheng B, Fan LW, Rhodes PG, Cai Z. 2007. IGF-1 protects oligodendrocyte progenitors against TNFalpha-induced damage by activation of PI3K/Akt and interruption of the mitochondrial apoptotic pathway. Glia 55:1099-1107.

Patani R, Balaratnam M, Vora A, Reynolds R. 2007. Remyelination can be extensive in multiple sclerosis despite a long disease course. Neuropathol Appl Neurobiol 33:277-287.

Patrikios P, Stadelmann C, Kutzelnigg A, Rauschka H, Schmidbauer M, Laursen H, Sorensen PS, Bruck W, Lucchinetti C, Lassmann H. 2006. Remyelination is extensive in a subset of multiple sclerosis patients. Brain 129:3165-3172.

Ransohoff RM, Bacon KB. 2000. Chemokine receptor antagonism as a new therapy for multiple sclerosis. Expert Opin Investig Drugs 9:1079-1097.

Rechler MM, Clemmons DR. 1998. Regulatory Actions of Insulin-like Growth Factor-binding Proteins. Trends Endocrinol Metab 9:176-183.

Redford EJ, Hall SM, Smith KJ. 1995. Vascular changes and demyelination induced by the intraneural injection of tumour necrosis factor. Brain 118 (Pt 4):869-878.

Reichert F, Rotshenker S. 1999. Galectin-3/MAC-2 in experimental allergic encephalomyelitis. Exp Neurol 160:508-514.

Reichert F, Rotshenker S. 2003. Complement-receptor-3 and scavenger-receptor-AI/II mediated myelin phagocytosis in microglia and macrophages. Neurobiol Dis 12:65-72.

Remington LT, Babcock AA, Zehntner SP, Owens T. 2007. Microglial recruitment, activation, and proliferation in response to primary demyelination. Am J Pathol 170:1713-1724.

Ricort JM. 2004. Insulin-like growth factor binding protein (IGFBP) signalling. Growth Horm IGF Res 14:277-286.

Rivest S. 2009. Regulation of innate immune responses in the brain. Nat Rev Immunol 9:429-439.

Rodriguez M. 2007. Effectors of demyelination and remyelination in the CNS: implications for multiple sclerosis. Brain Pathol 17:219-229.

Rodriguez M. 2007. Effectors of demyelination and remyelination in the CNS: implications for multiple sclerosis. Brain Pathol 17:219-229.

Rotshenker S, Reichert F, Gitik M, Haklai R, Elad-Sfadia G, Kloog Y. 2008. Galectin-3/MAC-2, Ras and PI3K activate complement receptor-3 and scavenger receptor-AI/II mediated myelin phagocytosis in microglia. Glia 56:1607-1613.

Savill J, Dransfield I, Gregory C, Haslett C. 2002. A blast from the past: clearance of apoptotic cells regulates immune responses. Nat Rev Immunol 2:965-975.

Selvaraju R, Bernasconi L, Losberger C, Graber P, Kadi L, vellana-Adalid V, Picard-Riera N, Van Evercooren AB, Cirillo R, Kosco-Vilbois M, Feger G, Papoian R, Boschert U. 2004. Osteopontin is upregulated during *in vivo* demyelination and remyelination and enhances myelin formation *in vitro*. Mol Cell Neurosci 25:707-721.

Setzu A, Lathia JD, Zhao C, Wells K, Rao MS, Ffrench-Constant C, Franklin RJ. 2006. Inflammation stimulates myelination by transplanted oligodendrocyte precursor cells. Glia 54:297-303.

Sharief MK. 1998. Cytokines in multiple sclerosis: pro-inflammation or pro-remyelination? Mult Scler 4:169-173.

Sharief MK. 1998. Cytokines in multiple sclerosis: pro-inflammation or pro-remyelination? Mult Scler 4:169-173.

Smith ME. 1999. Phagocytosis of myelin in demyelinative disease: a review. Neurochem Res 24:261-268.
Sturn A, Quackenbush J, Trajanoski Z. 2002. Genesis: cluster analysis of microarray data. Bioinformatics 18:207-208.

Suzumura A, Sawada M, Yamamoto H, Marunouchi T. 1993. Transforming growth factor-beta suppresses activation and proliferation of microglia *in vitro*. J Immunol 151:2150-2158.
Tatti O, Vehvilainen P, Lehti K, Keski-Oja J. 2008. MT1-MMP releases latent TGF-beta1 from endothelial cell extracellular matrix via proteolytic processing of LTBP-1. Exp Cell Res 314:2501-2514.

Torkildsen O, Brunborg LA, Myhr KM, Bo L. 2008. The cuprizone model for demyelination. Acta Neurol Scand Suppl 188:72-76.

Trebst C, Konig F, Ransohoff R, Bruck W, Stangel M. 2008. CCR5 expression on macrophages/microglia is associated with early remyelination in multiple sclerosis lesions. Mult Scler 14:728-733.

Vela JM, Molina-Holgado E, revalo-Martin A, Almazan G, Guaza C. 2002. Interleukin-1 regulates proliferation and differentiation of oligodendrocyte progenitor cells. Mol Cell Neurosci 20:489-502.

Wang X, Li C, Chen Y, Hao Y, Zhou W, Chen C, Yu Z. 2008. Hypoxia enhances CXCR4 expression favoring microglia migration via HIF-1alpha activation. Biochem Biophys Res Commun 371:283-288.

Woodruff RH, Fruttiger M, Richardson WD, Franklin RJ. 2004. Platelet-derived growth factor regulates oligodendrocyte progenitor numbers in adult CNS and their response following CNS demyelination. Mol Cell Neurosci 25:252-262.

Xiao BG, Bai XF, Zhang GX, Link H. 1997. Transforming growth factor-beta1 induces apoptosis of rat microglia without relation to bcl-2 oncoprotein expression. Neurosci Lett 226:71-74.

Yan YP, Lang BT, Vemuganti R, Dempsey RJ. 2009. Osteopontin is a mediator of the lateral migration of neuroblasts from the subventricular zone after focal cerebral ischemia. Neurochem Int 55:826-832.

Zhang GX, Baker CM, Kolson DL, Rostami AM. 2000. Chemokines and chemokine receptors in the pathogenesis of multiple sclerosis. Mult Scler 6:3-13.

SUPPLEMENTARY MATERIAL

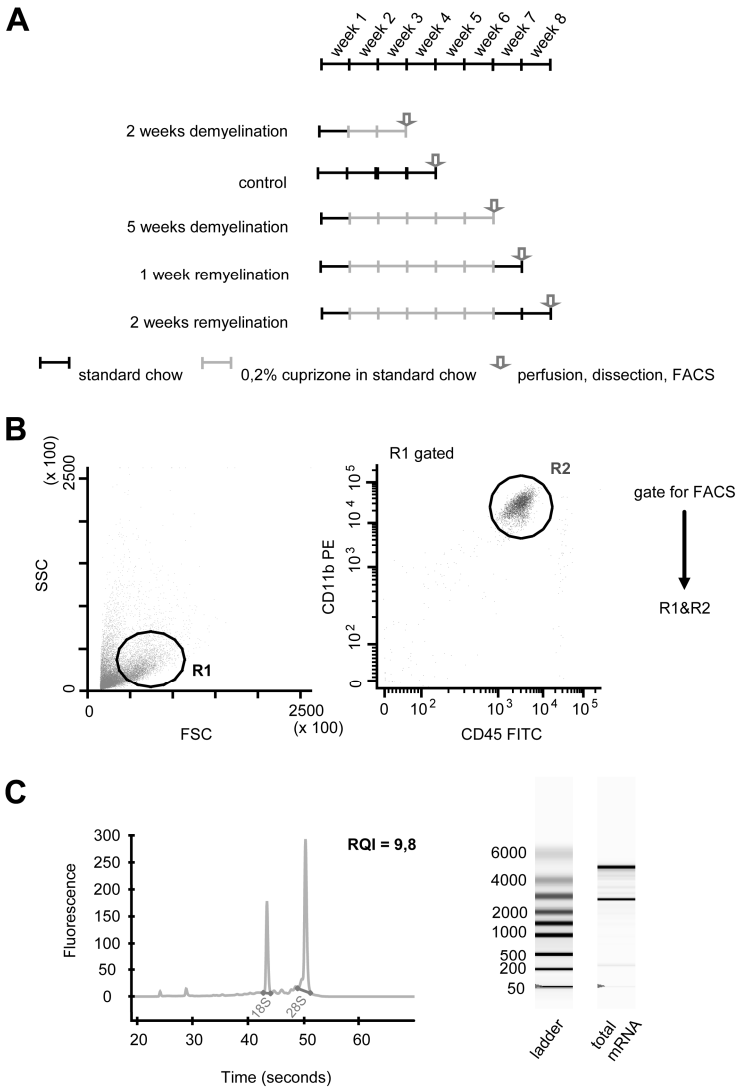

Supplementary figure 1. Overview of the experimental setup. A Schematic representation of the experimental groups with respect to the duration of the cuprizone diet, the recovery period and the time of sacrifice. After a week of acclimatisation, the animals were fed with standard powder chow containing 0,2% cuprizone (red bars) for two weeks (2 weeks demyelination, 2WD) or five weeks (five weeks demyelination, 5WD). A separate group of animals was allowed to recover after five weeks of cuprizone diet for one week (one week remyelination, 1WR) or two weeks (two weeks remyelination, 2WR) by placing them back on standard powder chow without cuprizone (black bars). The control group received only standard powder chow. Please note the time point of the sacrifice of the control group of animals. **B** The Fluorescence Activated Cell Sorting (FACS) setup. Microglia cells were sorted based on

the live cell gate on the forward/side scatter plot (region 1 (**R1**) on the FSC/SSC scatter plot) and their characteristic CD11bhigh/CD45intermediate (region 2, **R2**) expression profile. **C** Quality control of the RNA samples. RNA integrity was determined using Experion High Sense chips (BioRad). Electropherogram/gel analysis of a representative sample showing sharp peaks/bands of the 18S and 28S ribosomal RNA, characteristic of intact eukaryotic total cellular RNA. Only RNA samples with an RNA Quality Index (RQI) equal to or higher than 9 were used for subsequent analysis.

Supplementary table 1. Entities were assigned to three groups according to the pattern of changes of their expression levels across the samples (see Figure 2B).

	Official gene symbol
Genes belonging to Fig. 2B/B'	Acaa1b, Actb, Adh1, Ahsg, Ahsg, Aldob, Ambp, Apoa1, Apoa2, Apoc3, Apof, Apoh, Azgp1, Bhmt, Ces3, Crp, Cyp2a5, Cyp2e1, F2, Fga, Fga, Fgg, Gsta3, Hamp, Hmgcs2, Hp, Hpx, Itih1, Itih4, Kng1, Kng1, LOC620807, Mat1a, Mettl7b, Mgst1, Mgst1, Mup1, Mup2, Mup3, OTTMUSG00000007485, Pon1, Rbp4, Reep6, Scd1, Serpina1a, Serpina1a, Serpina1b, Serpina1b, Serpina1c, Serpina1d, Stard10, Vtn
Genes belonging to Fig. 2B/B''	1110002H13Rik, 1110049B09Rik, 1700113I22Rik, 2610510J17Rik, 2610524H06Rik, 2810417H13Rik, 3000004C01Rik, 3000004C01Rik, 3010003L21Rik, 6720460F02Rik, Adarb1, Amd2, Apitd1, Arhgdib, Asf1b, Aurka, B230317C12Rik, Baiap2l2, BC006662, Birc5, C330027C09Rik, Car13, Ccnb1, Ccnb1, Cd244, Cdc20, Cdc45l, Cdc6, Cdca2, Cdca3, Cdca5, Cenpk, Cep55, Cetn4, Cited2, Cited4, Clspn, Copg, Ctsw, D030070L09Rik, D2Ertd750e, Dynll2, E130306D19Rik, Elmo2, Epor, Fignl1, Fkbp11, Folr2, Foxm1, Fuca1, Gipc1, Golt1b, Gtse1, Hes1, Hist1h2bc, Hmbs, Id1, Impa2, Kif22, Kif23, Kif2c, Kif4, Klf1, Klf4, Kntc1, Kpna2, Lgi2, Lrrc39, Lyplal1, Mad2l1, Med1, Mns1, Ndc80, Nusap1, Olfr873, Pbk, Pfkl, Phlda3, Plk1, Plp2, Prc1, Rad51, Rbbp7, Rpl14, Rrm2, Saa3, Sacs, Scotin, Shcbp1, Slc16a3, Slc16a8, Slpi, Spag5, Spc25, Spc25, Stra13, Syce2, Thbs2, Tk1, Top2a, Tpx2, Trim72, Tsc22d1, Tyms, Uck2, Xkr7
Genes belonging to Fig. 2B/B'''	Aadacl1, Adssl1, Ank, Anxa2, Anxa5, Axl, Capg, Capzb, Ccl3, Ccl4, Cd63, Cd74, Cd74, Cd83, Clec7a, Cox7a2l, Csf2ra, Cxcl16, D10Wsu52e, Eef1b2, Egr1, Fcgr2b, Fcgr4, Gltp, Gpnmb, H2-Ab1, H2-M3, Ifi27, Ifit3, Il4i1, Lgals3, LOC100044439, LOC547343, Lpcat2, Ly9, Lyz2, Morf4l1, Oas1g, Oasl2, Pfn1, Pld3, Psme1, Rpl30, Rpl7a, Rps5, Sdc3, Sdcbp, Spcs1, Spp1, Sumo2, Tpm4, Tra2a, Tspo

Chapter 5

An optimised protocol for the acute isolation of human microglia from autopsy brain samples

Marta Olah[1], Divya Raj[1], Nieske Brouwer[1], Alexander H. De Haas[2], Wilfred F.A. den Dunnen[2] , Knut P.H. Biber[3] and Hendrikus W.G.M. Boddeke[1]

[1] Department of Neuroscience, Section Medical Physiology, UMCG-RuG, Groningen, The Netherlands

[2] Department of Pathology and Medical Biology, University Medical Center Groningen, Groningen, The Netherlands

[3] Department of Psychiatry and Psychotherapy, Section Molecular Psychiatry, University Medical Center Freiburg, Freiburg, Germany

manuscript in preparation

ABSTRACT

Microglia are increasingly recognised to be crucially involved in the maintenance of tissue homeostasis of the brain and spinal cord. Not surprisingly therefore, the growing scientific interest in the microglia phenotypes is associated with various physiological and pathological processes of the central nervous system. Nonetheless, until recently the investigation of these phenotypes was hindered by the lack of an isolation protocol that (without an extended culturing period) would offer a microglia population of high purity and yield. Thus, our objective was to establish a rapid and efficient method for the isolation of human microglia from post mortem brain samples. We tested multiple elements of already existing protocols (e.g. density separation, immunomagnetic bead separation) and combined them to minimise preparation time and maximise yield and purity. The procedure presented here enables acute isolation of human microglia from autopsy (and biopsy) samples with a purity and yield that is suitable for downstream applications, such as protein and gene expression analysis and functional assays. Moreover, the present protocol is appropriate for the isolation of microglia from autopsy samples irrespective of the neurological state of the brain or specific brain regions and (with minor modification) could be even used for the isolation of microglia from human glioma tissue.

INTRODUCTION

Microglia are the primary immune cells of the central nervous system (CNS) and contribute to innate and adaptive immune responses in the CNS (Ransohoff and Perry 2009; Bailey et al., 2006; Becher et al., 2006; Carson et al., 2006). Under physiological conditions microglia display ramified morphology and continuously monitor their direct surroundings, with their fine processes (Davalos et al., 2005; Nimmerjahn et al., 2005). Upon activation, microglia are involved in the response to CNS injury and secrete inflammatory and neurotrophic factors, phagocytose damaged cells and debris, and present antigens (Town et al., 2005; Schilling et al., 2003).

Several studies on microglia have suggested that regional differences in microglia phenotypes exist. In addition to the initial reports regarding the regional differences in microglia density (Lawson et al., 1990; Mittelbronn et al., 2001), recently a region-dependent variety in the expression levels of cell surface markers on microglial cells has also been described (De Haas et al., 2008; Jiang-Shieh et al., 2003; Wu et al., 1997). Furthermore, upon activation microglia have been shown to acquire a range of different phenotypes depending on the stimulus (Ransohoff & Perry, 2009; Hanisch & Kettenmann, 2007). Given their increasingly recognised role in physiological as well as pathological processes in the central nervous system, there is a mounting interest in microglia phenotypes associated with these different conditions. Accordingly, several human microglia isolation studies have been performed recently in order to investigate microglia phenotypes associated with various pathological states, such as glioma, Alzheimer's disease and HIV-associated dementia (Hussain et al., 2006a; Hussain et al., 2006b; De Groot et al., 2001; Lue et al., 2001; Dick et al., 1997). Most of the human microglia isolation procedures however, include extended time in culture and exposure to growth factors, such as GM-CSF (Gibbons & Dragunow, 2009), to achieve the desirable yield and purity,

that would enable the analysis of the microglia phenotype by molecular biological means. Acute isolation of human microglia from biopsy material has been described (Hussain et al., 2006a,b; Dick et al., 1997), but the purity of the obtained microglia population (percentage microglia of the live cell population) has not been discussed. Despite the fact, that acute microglia isolation procedures yielding close to 100% microglia purity have been recently established for mouse (De Haas et al., 2007; Cardona et al., 2006) and rat (Ford et al., 1995), such rapid microglia isolation protocol has not been available for human autopsy material up till now.

Thus, the aim of this study was to provide an optimal isolation method that yields a high purity microglia population from various adult human CNS regions and enables immediate downstream molecular biological and functional analysis of microglia. To circumvent the possible influence of cell culturing on the microglia phenotype, we have developed a fast (< 90 minutes) and accurate (up to 98% microglia purity) isolation protocol based on mechanical dissociation and a two step density gradient purification followed by CD11b-bead separation. This protocol allows flow cytometric analysis, assessment of microglia specific functions and gene and protein expression analysis of acutely isolated human microglia from autopsy samples with as long as 20 hours post mortem delay. Furthermore, our protocol is suitable for the isolation of microglia populations from different brain regions both from the healthy and diseased brain.

MATERIALS AND METHODS

Human brain tissue

Human brain tissue was obtained in the course of full. For the autosomal dominantly inherited neurodegenerative diseases written informed consent for brain donation for research purposes was given. For the other cases samples were anonymized according to procedures described in the National Code for the Good Use of Patient Material. Both procedures have been approved by the Medical Ethical Committee of the University Medical Center of Groningen, the Netherlands. The extracellular pH of post mortem brain tissue has been suggested to be the marker for the quality of the post mortem human brain material. We therefore determined the pH of the sampled post mortem tissues according to Monoranu et al., 2009 in certain cases. Detailed data of the autopsy samples have been summarised in Table 1.

Isolation and enrichment of microglial cells from autopsy material

Media and reagents

Microglia isolation was carried out using sterile solutions of Phosphate Buffered Saline (PBS), 1x Hank's Buffered Salt Solution (HBSS) and 10x HBSS (all: PAA Laboratories GmbH). During the microglia isolation procedure, we used a dissection medium (referred to as 'medium A'; HBSS, containing 0,5% glucose and 15 mM HEPES) for washing steps.

For the density gradient separation steps Percoll solutions with different densities have been used (GE Healthcare, 17-0891). To yield a stock isotonic Percoll solution (100%, density 1,123 g/ml), nine volume parts of Percoll (density 1,13 g/ml) were mixed with one volume part of 10x HBSS. Percoll solutions with various percentages were prepared via dilution of 100% Percoll with 1x PBS or myelin gradient buffer (Phosphate Buffer, completed with 0,8% NaCl, 0,04% KCl, and 0,2% glucose - described in detail in De Groot et al, 2000). The following

Percoll solutions in PBS have been used in this study for differential density separation of cells: 80% (density 1,098 g/ml), 75% (1,092 g/ml), 60% (1,074 g/ml), 40% (1,049 g/ml), 30% (1,037 g/ml), 25% (1,031 g/ml). The 22% Percoll solution in myelin gradient buffer had a density of 1,03 g/ml.

Enzymatic dissociation was carried out by incubation of minced autopsy tissue with collagenase and DNase I (both from Roche) for 30 minutes at 37°C. The anti-mouse/humanCD11b antibody coupled magnetic beads were obtained from Miltenyi Biotech and used according to the manufacturer's protocol.

Optimisation of the microglia isolation protocol

The described microglia isolation protocol from human autopsy brain tissue consists of two important steps, namely: tissue dissociation, to obtain a single cell suspension, and microglia enrichment through density gradient centrifugation.

In order to determine the optimal tissue dissociation method, we compared single mechanical dissociation using a glass homogeniser with mechanical dissociation followed by enzymatic dissociation using a collagenase/DNaseI solution in medium A for 30 minutes at 37^{o}C.

Microglia enrichment was achieved by Percoll density centrifugation. After separation of the myelin- and cell fraction, the cell suspension was separated on a discontinuous Percoll density gradient consisting of either 75% and 25% Percoll layers or a series of 80%, 60%, 40%, 30%, 20%, and PBS layers. All interfaces were analysed for microglia purity using flow cytometry.

The purity of the final microglia enriched cell suspension has been found to depend also on the amount of starting material. Clearly, overloading the gradient resulted in poor separation and a low yield of microglia. Therefore, volumes and tubes mentioned in the final protocol described below are based on a maximum amount of 3 grams of autopsy brain tissue/tube.

Isolation and enrichment of microglial cells from human autopsy brain tissue

The whole isolation procedure was performed on ice, using pre-cooled solutions and equipment. A swinging bucket rotor (Falcon 6/300) was used for all centrifugation steps with the settings: 4°C, slow acceleration, and no brakes, unless otherwise mentioned.

Human brain tissue was placed in a sterile Petri dish and weighed. Visible blood vessels and meninges were removed. In certain cases, brain tissue was separated under a magnifying glass into gray, white and mixed (containing the intermediate zone between cortical grey and subcortical white matter) tissue samples and processed separately to examine regional differences in microglia yield and phenotype.

Tissue (3 gram tissue/tube) was minced with sterile scalpels, mechanically disrupted in medium A in a glass homogeniser (glass Potter, Braun, Melsungen, Germany) and filtered through a pre-wetted 70-µm cell strainer (BD Biosciences 352350) in a 50 ml tube. Cell strainers were rinsed with excessive medium A and the cell suspension was centrifuged for 10 minutes at 220 g with brake. This cell pellet was resuspended in 25 ml Percoll solution with a density of 1,03 g/ml, consisting of 40 ml myelin gradient buffer, 11,7 ml Percoll, and 1,3 ml NaCl 1,5M. This solution was overlaid with 10 ml PBS and centrifuged for 20 minutes at 950 g. The first step thus separated cells from myelin and cell debris and resulted in cell suspension A (Figure 1).

The cell pellet was resuspended in 10 ml of either 75% Percoll which was overlaid with 10 ml 25% Percoll or in 80% on which 5 ml steps of 60%, 40%, 30%, 20% Percoll layers were placed. The last Percoll layer was covered by 5 ml of PBS in both cases.

Table 1. Abbreviations: m male; f female; pmd post mortem delay; n/d not determined; MSA multisystem atrophy; OPCA olivopontocerebellar atrophy; PSP progressive supranuclear palsy; SCA3 spinocerebellar ataxia ; AD Alzheimer's diesease ; DLBCL diffuse large B-cell lymphoma; MI myocardial infarction; AAA abdominal aortic aneurysm; PTLD post-transplant lymphoproliferative disorder.

Table 1. Detailed biodata of the autopsy samples used for the establishment of the protocol

ID	age	sex	PMD	pH	neurological condition	cause of death
Specimen 1	59	m	5	n/d	MSA OPCA	euthanasia
Specimen 2	65	f	9	n/d	PSP	pneumonia
Specimen 3	69	f	24	n/d	pontine myelyse	post-myocardial infarction rupture
Specimen 4	79	m	5	n/d	n/d	sudden death (post-MI)
Specimen 5	59	f	12	n/d	isolated myelitis transversa	euthanasia
Specimen 6	74	m	16	7,3	Alzheimer's disease Braak 5	ruptured AAA
Specimen 7	68	m	18	7,3	Huntington disease (mild form)	ruptured AAA
Specimen 8	55	m	18	6,9	SCA3	terminal sedation
Specimen 9	38	m	8	7,0	Progressive Multifocal Leuko-Encephalopathy	pneumonia
Specimen 10	69	f	22	6,6	AD Braak 3, multi-infarct	n/d
Specimen 11	62	f	18	6,9	MSA	n/d
Specimen 12	64	f	5	6,4	DLBCL (non-CNS)	tumorlysis
Specimen 13	49	m	20	6,2	n/d	PTLD (non-CNS), pneumonia
Specimen 14	75	m	19	7,0	AD Braak 6/vascular	pancreatic carcinoma, pneumonia
Specimen 15	70	f	10,5	7,2	Huntington disease (Vonsattel 2)	pneumonia
Specimen 16	66	m	< 10	7,1	Huntington disease (Vonsattel 3-4)	n/d
Specimen 17	19	f	9,5	7,2	n/d	car accident
Specimen 18	66	m	20	6,9	n/d	n/d
Specimen 19	28	m	19	n/d	Recklinghausen	n/d
Specimen 20	61	f	16	6,6	acute subdural hematoma	n/d
Specimen 21	79	f	10	6,2	cerebrobasal degeneration	ascesis
Specimen 22	64	m	10	6,7	bleeding aneurysm	brainstem compression

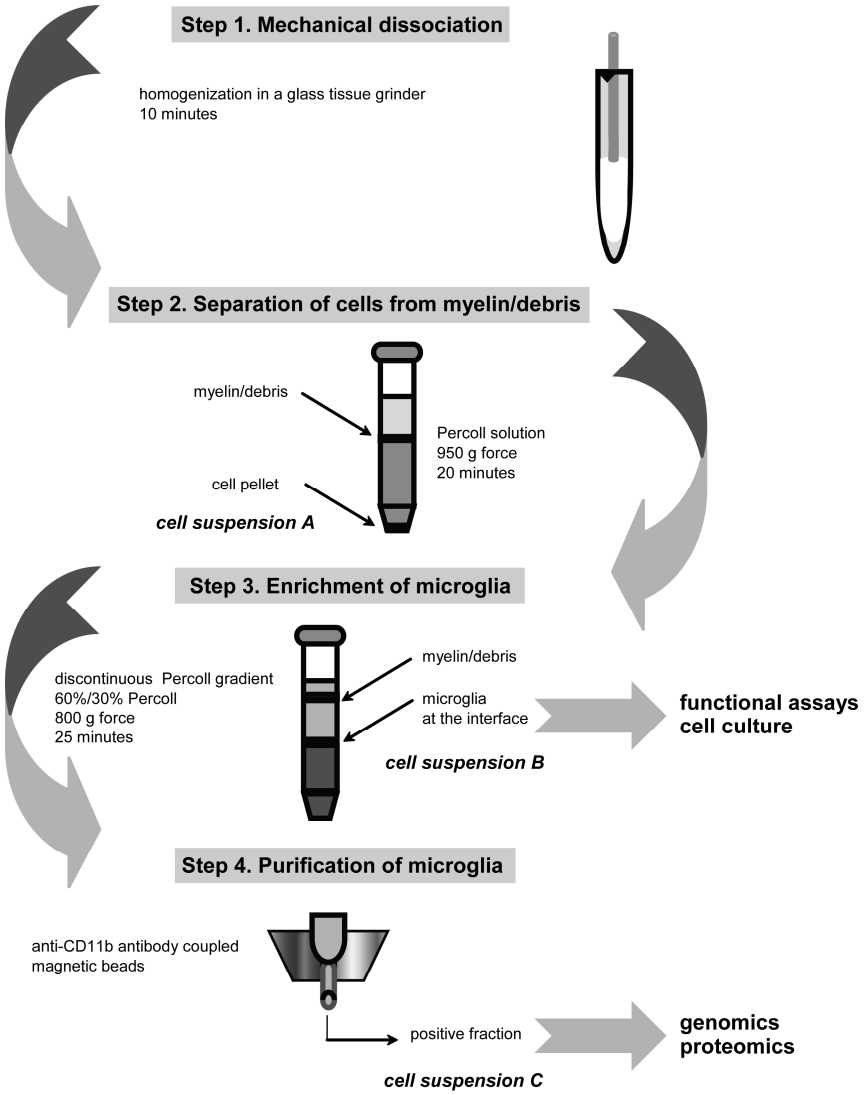

Figure 1. Microglia are purified from human brain tissue in four easy steps. Step 1 Mechanical dissociation proved to be much less time consuming and stressful for the cells, than enzymatic dissociation. Step 2 Pre-separation of cells from debris and most of the myelin content by the means of a single Percoll gradient (***cells suspension A***). Step3 Enrichment of microglia population through centrifugation on a discontinuous Percoll gradient (***cell susupension B***) consisting of a 60% and a 30% Percoll solution. Step 4 Purification of microglia with anti-CD11b antibody coupled magnetic beads (yields ***cell suspension C***).

This gradient was centrifuged for 25 minutes at 800 g. The cell layers at the interfaces between the Percoll layers were collected with a pre-wetted Pasteur pipette, washed with PBS to dilute the contaminating Percoll and centrifuged for 10 minutes at 220 g. The microglia purity of all interfaces was analysed by flow cytometry. The second purification step resulted in an enriched microglia cell suspension which we called cell suspension B (Figure 1).
After pelletting cell suspension B, the pellet was resuspended in 80 µl beads buffer (PBS, containing 2 mM EDTA) and 20 µl of anti-hm/ms CD11b microbead suspension was added. Following 15 minutes of incubation at 4°C the CD11b positive fraction was collected according to the manufacturer's protocol.
This additional purification step, using CD11b MicroBeads, resulted in a pure microglia cell suspension which we called cell suspension C (Figure 1).

Isolation of microglial cells from human glioma tissue after surgical dissection

Microglia from glioma tissue were purified using the procedure described for autopsy samples with minor modifications. Due to the low myelin content of the bulk glioma, separation of myelin and cells was not necessary. After mechanical dissociation the cell suspension was directly purified using a Percoll gradient (consisting of Percoll 60%, 40%, and PBS) was centrifuged for 20 minutes at 950 g. The interface was collected, washed, and examined for microglia purity.

Characterisation of human microglia in suspensions using protein based techniques

Specification of the used antibodies

The specifications of the used antibodies are shown in Table 2.

Flow cytometry

Cell suspensions were incubated for 15 minutes with human Fc receptor binding inhibitor (eBioscience; 14-9161) to reduce nonspecific immunofluorescence staining. After washing, cells were incubated for 20 minutes on ice with the fluorescence-labeled primary antibodies or isotype controls (see Table 2). After washing, stained cell suspensions were resuspended in 200 µl PBS and about 10 minutes before commencing with the flow cytometric measurements, an extra 100 µl DRAQ5 solution (Biostatus; 1:1000 in PBS) was added to determine cell viability.

Table 2. Antibody specifications

	antigen	species	vendor	catalogue number	isotype	conjugate
FC	CD11b	mouse	BioLegend	301306	IgG1	PE
	CD45	mouse	BioLegend	304007	IgG1	FITC
	HLA-DR	mouse	BioLegend	307603	IgG2a	FITC
	CX3CR1	rat	BioLegend	341605	IgG2b	FITC
	CXCR3	mouse	R&D	FAB160P	IgG1	PE
	CD172a	mouse	BioLegend	323805	IgG1	PE
	CD40	mouse	BioLegend	334305	IgG1	FITC
	CD14	mouse	eBioscience	11-0149	IgG1	FITC
	CD80	mouse	BioLegend	305207	IgG1	PE
	CD200R	mouse	BioLegend	329305	IgG1	PE
	ic	mouse	BioLegend	400111	IgG1	PE
	ic	mouse	BioLegend	400108	IgG1	FITC
	ic	mouse	BioLegend	400207	IgG2a	FITC
ICC & WB	Iba1	rabbit	Wako	019-19741	-	-
	GFAP	rabbit	Dako	Z 0334	-	-
	GFAP	mouse	Chemicon	MAB3402	-	-
	β-actin	mouse	Abcam	ab6276	-	-
	CD68	mouse	Dako	M0814	-	-

Abbreviations: FC flow cytometry; ICC immunocytochemistry; WB western blot; ic isotype control; for the other acronyms please see the list of abbreviations.

The surface expression of markers was measured with a FACSCalibur flow cytometer (Becton Dickinson) and the flow cytometric measurements were analysed using WinMDI 2.8 software. Microglia purity was defined as the percentage of DRAQ5 positive cells, showing CD11b high and CD45 intermediate expression.

Western blotting

Cell pellets of cell suspensions A, B, and C were lysed in RIPA solution (1% Nonidet P40, 1% SDS, 0,5% Na-deoxycholate in PBS), total protein was measured and 1 volume of 2x sample buffer (0,125M TrisHCl; pH 6,8; 20% glycerol; 4% SDS; 3% DTT; and 0,01% bromophenol blue) was added. Samples were boiled for 5 minutes at 95°C before equal amounts of total protein were loaded on a 12,5% SDS-polyacrylamide gel. After electrophoresis, proteins were transferred onto PVF membrane (Millipore) using semidry blotting. Membranes were blocked for 1 h at room temperature with Odyssey™ blocking buffer diluted 1:1 with PBS, and then probed with primary antibodies (see Table 2) in Odyssey™ blocking buffer, diluted 1:1 in PBS + 0,1% Tween-20 (PBS-T). After overnight incubation, membranes were thoroughly washed with PBS-T and incubated for 1h in the appropriate fluorescence secondary antibody solutions (1:10.000) in PBS-T. After the final washes, the membranes were scanned using the Odyssey™ Infrared Imager (LI-COR).

Immunocytochemistry

Cytospins were prepared using a Shandon cytospin centrifuge by spinning the various cell suspensions for 5 minutes at 800 rpm on poly-L-lysine coated glass slides. Preparations were dried, fixed with 4% paraformaldehyde in PBS for 10 minutes and rinsed with PBS. After blocking with 2% normal goat serum, the cytospins were incubated overnight in the primary antibodies solutions.

The next day, slides were thoroughly washed with PBS and incubated with the appropriate fluorescence conjugated secondary antibodies.

Mowiol-mounted slides were observed under a Zeiss fluorescence microscope and pictures were made using LAS AF software (Leica).
The antibodies used for Western blotting, immunocytochemistry and flow cytometry are shown in Table 2.

Functional assays in isolated human microglia

Each functional assay was performed on at least two independent samples. For functional assays cell suspension B was used.

Phagocytosis

The phagocytic capacity of acutely isolated human microglia was investigated by means of live cell imaging using pHrodo coupled to bacterial particles. This Escherichia coli bioparticle coupled dye is non-fluroescent at neutral pH but fluoresces bright red at acidic pH – making it an excellent tool to investigate the dynamics of phagocytosis with time-lapse microscopy. Therefore, acutely isolated human microglia were seeded in a Lab-Tek® 8 well chamber slide (Thermo Scientific/NUNC, Cat.No.177402) at the density of 12.000 cells per well (15.000 cells/cm^2). Cells were allowed to attach for 15 minutes. Subsequently, they were provided with fresh culture medium (Dulbecco's modified Eagle´s Medium (DMEM; PAA) substituted with 5% fetal bovine serum (FBS “Gold”; PAA), 1% penicillin/streptomycin (PAA) and 1% sodium-pyruvate (PAA)) and cultured under standard conditions (humidified chamber, 5% CO_2, 37°C). At the start of the experiment pHrodo coupled E.coli bio-particles (serotype K12; Invitrogen, Cat.No. P35361) were added to the culturing medium (final concentration 25 µg/ml). In some wells PMA (0,5 µM final concentration; Sigma, Cat.No. P1585) was also applied. Live cell imaging was performed with a Solamere Nipkow laser scanning microscope equipped with an automated stage and a temperature/CO_2 controlled cabinet. Images were captured with a CCD camera (Stanford Photonics) and InVivo software (Media Cybernetics). For pHrodo dye excitation we used the 568 nm laser line of a dynamic Kripton laser. Images were acquired

every five minutes for a period of sixteen hours. For each condition at least two non-overlapping fields were imaged. The dynamics of bacterial particle ingestion of at least twenty cells per filed were analysed. The changes over time in the amount of ingested bioparticles (increase in the fluorescent signal) was measured in ImageJ with the help of a custom made plug-in. The raw data were further processed in Excel^{R} spreadsheets, to determine the correlates of total amount of ingested bioparticle per cell and the time needed to reach half maximum phagocytosis response/cell.

Chemotaxis

Cell migration in response to ATP (100, 200, 300 µM) and C5a (50, 100, 200 ng/ml), was assessed using a 48-well chemotaxis microchamber (NeuroProbe). Serum-free DMEM without chemoattractant served as a control. 29 µl of the chemoattractant solution or control medium was applied to the lower well of the chamber. Upper and lower chambers were separated by a polyvinylpyrrolidone-free polycarbonate filter (8 µm pore size). The lower side of the filter was coated with Poly L-Lysine. In the upper wells of the chamber, 50 µl cell suspension containing 2×10^4 cells was applied. The chamber was incubated in a humidified atmosphere (5% CO_2) at 37°C for 3 hours. Measurements were done in triplicate for each group. After incubation the filter was washed, fixed in methanol and stained with toluidine blue. Migrated cells per group were counted by a double-blinded person with a scored eyepiece (3 fields ($1mm^2$) per well). Data are expressed as percentages of control migration ± SEM.

Determination of reactive oxygen species production by acutely isolated human microglia

Production of reactive oxygen species by acutely isolated human microglia was determined by detecting the conversion of H_2DCFDA (2',7'-dichlorodihydrofluorescein diacetate) into fluorescent DCF (2',7'-dichlorofluorescein) with flow cytometry. 100 µl of cell suspension containing 2×10^4 cells was incubated with 500 ng/ml Phorbol myristate acetate (PMA) or 100 mM ATP for 30 minutes and used as positive control for ROS production. Appropriate negative controls with and without H_2DCFDA addition were also included. After stimulation with PMA or ATP, 5 µM H_2DCFDA was added to the cells and incubated for 20 minutes, after which fluorescence was measured using flow cytometry.

RESULTS

Overview of the protocol

In Table 1 the details of the post mortem brain tissue samples have been listed. We have evaluated and optimised the protocol for human microglia isolation, which resulted in a four step protocol (Figure 1). The first step involved thorough dissociation of the brain tissue. Compared to enzymatic dissociation the mechanical dissociation procedure (Step 1) yielded better cell viability and proved to be less time consuming. Using a single low density Percoll separation step (Step 2) the cells were separated from debris and myelin. The resulting partially purified cell suspension was labeled cell suspension A. Centrifugation of a discontinuous Percoll gradient (Step 3) yielded further enrichment of microglia cell suspension, which was labeled cell suspension B. Finally, purification of microglia with an anti-CD11b antibody coupled to magnetic beads yielded a high purity microglia suspension labeled cell suspension C.

Determination of the optimal Percoll densities for discontinuous gradient separation

For the preparation of cell suspension B various Percoll gradients have been tested. Thus after separation of the cells from myelin and debris using a low density Percoll solution, the resulting cell pellet was subjected to a discontinuous density separation. A solution containing 9 volume parts of Percoll and 1 part of 10X HBSS mixture was defined as 100% Percoll. Different percentages of Percoll were prepared by diluting with culture grade DPBS. We started out by using a protocol established for the acute isolation of mouse microglia (De Haas et al., 2007), where the 25%/75% interface contains a purified microglia population (more than 95% of the live cells) without considerable amounts of cellular debris.

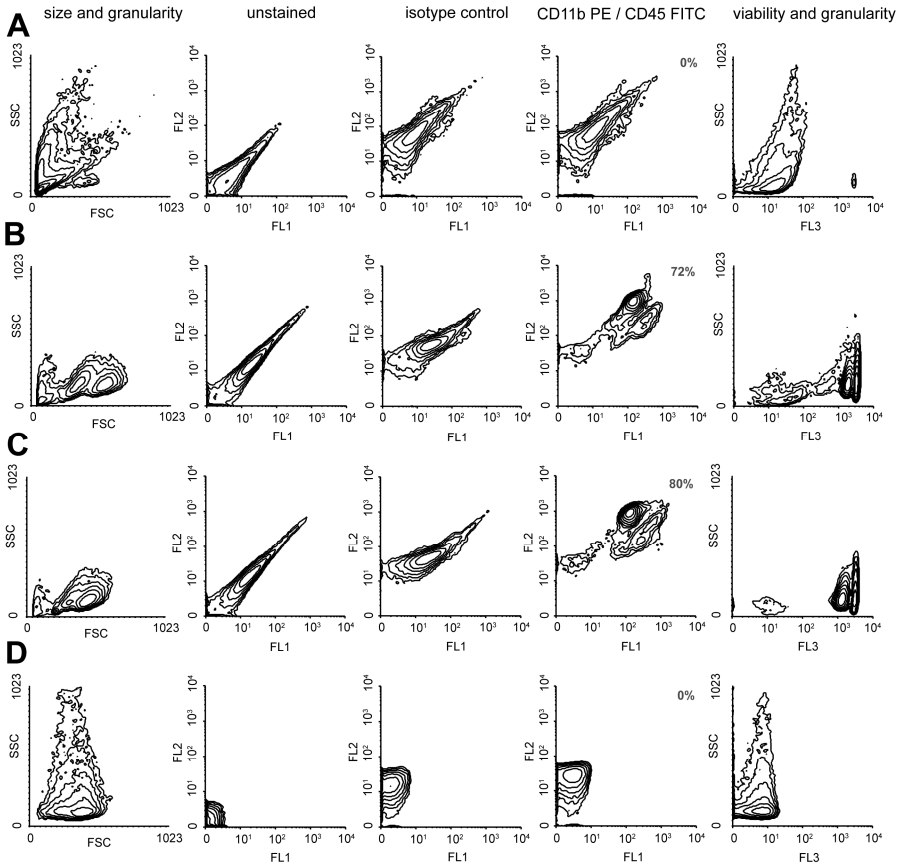

Figure 2. The optimal conditions for the enrichment of microglia through a discontinuous density separation. The discontinuous Percoll gradient consisted of 80%, 60%, 40%, 30%, 20% Percoll layers and finally a layer of PBS. To determine the optimal densities for the enrichment of microglia each interface was collected, stained for CD11b and CD45 and investigated by flow cytometric analysis. Viability was detected by the cellular retention of the DRAQ5, a far-red fluorescent DNA dye. **A** The PBS/20% interface contained hardly any live cells (DRAQ5+ events). **B** 72% of the live cells collected from the 30%/40% Percoll layer interface had the characteristic CD11bhigh/CD45intermediate microglia surface marker expression profile. **C** At 40%/60% interface 80% of the live cells were microglia. **D** The 60%/80% Percoll interface consisted almost exclusively from red blood cells. (SSC side scatter (granularity); FSC forward scatter (size); FL1, FL2, FL3 fluorescent detector channels for FITC, PE, DRAQ5 respectively)

Applying the same protocol on human post mortem brain material yielded at the 25%/75% interface a microglia population that was heavily contaminated by the presence of debris, but most importantly,

red blood cells. In order to find the density appropriate for isolation of human microglia, we prepared a more detailed Percoll gradient, wherein cells were loaded to an 80% Percoll solution and layered with equal amounts of 60, 40, 30 and 20% Percoll solutions. Flow cytometric analysis of these selected layers is shown in Figure 2. The CD11bhigh/CD45medium microglia population was generally found above the 60% Percoll layer (Figure 2C, 60%/40% interface where 80% of the live cells were microglia) and below the 30% Percoll layer (Figure 2B, 40%/30% interface, where 72% of the live cells were microglia). Red blood cells pelleted below the 60% Percoll layer (Figure 2D, 80%/60% interface) and the cellular debris and remnants of the myelin collected above the 20% layer (Figure 2A, 20%/PBS interface). Thus, we decided on the application of a discontinous Percoll separation consisting of a 60% Percoll layer (initially containing the cells), followed by a layer of 30% Percoll solution on top of which PBS is layered.

Quantification of microglia enrichment at the different steps of the protocol

After optimisation of the discontinuous Percoll gradient separation, cell suspension A, B and C were characterised by flow cytometry, Western blots and cytospins (Figure 3). Acutely isolated human microglia samples were stepwise enriched by the density gradient separation steps and subsequently purified by anti-CD11b antibody coupled magnetic bead separation. The purity of the microglia sample was expressed as the percentage of the live cells (DRAQ5+) with the characteristic CD11bhigh/CD45intermediate microglia surface expression profile. The initial separation of cells and myelin/debris (Step 2 - cell suspension A) resulted in a live cell population which contained 16% microglia (Figure 3A). Centrifugation on a discontinuous Percoll gradient (Step 3 - cell suspension B) yielded a live cell population enriched in microglia to up to 70% (Figure 3B). Immunomagnetic bead separation (Step 4 – cell

suspension C) purified microglia population up to 99% of live cells (Figure 3C).

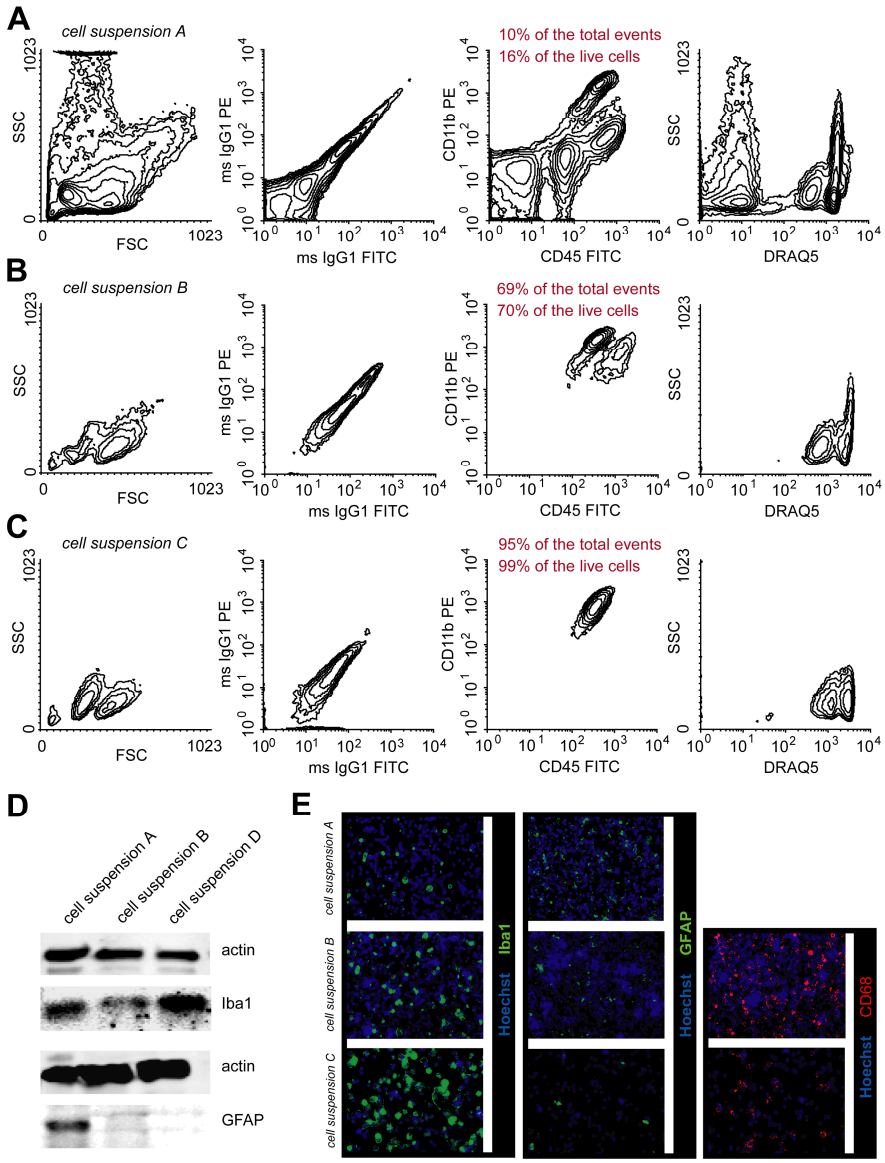

Figure 3. Microglia are gradually enriched in the course of the density gradient separation steps and finally purified by the means of immunomagnetic separation. Panels **A** till **C** – flow cytometric analysis of the cell suspensions attained in the different steps of the isolation protocol. The microglia purity was determined as the percentage of the cells bearing the characteristic CD11bhigh/CD45intermediate microglia surface expression profile. **A** The initial separation of cells and myelin/debris (step 2 – cell suspension A) resulted in a live cell population of which 16% was

microglia. **B** Centrifugation on a discontinuous Percoll gradient (step 3 – cell suspension B) yielded a live cell population enriched in microglia to up to 70%. **C** Immunomagnetic bead separation (step 4 – cell suspension C) purified microglia population to 99% of live cells. **D** Western blot analysis of the protein levels of different glial cell markers at various steps of the isolation protocol. GFAP protein is already almost absent after the discontinuous Percoll separation. After immunomagnetic bead separation with anti-CD11b coupled magnetic beads the cell suspension is highly enriched in Iba1 expression cells. **E** Immunocytochemical stainings of cytospins prepared of cell suspensions from the different isolation steps. (SSC side scatter (granularity); FSC forward scatter (size); DRAQ5 live cell marker; Hoechst nuclear counterstain; for the other acronyms please see List of abbreviations).

Western blot analysis of the protein levels of different glial cell markers at various steps of the isolation protocol showed, that GFAP protein was already almost absent after the discontinuous Percoll separation (Figure 3B). After immunomagnetic bead separation with anti-CD11b coupled magnetic beads, the cell suspension was highly enriched in Iba1 expressing cells (Figure 3B). Immunocytochemical stainings of cytospins prepared of cell suspensions from the different isolation steps (Figure 3C) showed similar pattern of enrichment in microglia along the steps of the isolation procedure.

Test of an alternative short version of the protocol

We also tested the possibility of an alternative short protocol that can be applied when time is the main constraint and the purity of the microglia preparation is not the primary concern. We performed an immunomagnetic bead separation directly after the first density separation (Figure 4), thus on cell suspension A. The positive fraction after this magnetic bead separation we named cell suspension A/C which was comparable to cell suspension B regarding microglia enrichment. An example of such a separation is shown in Figure 4.

Discontinous density separation yields different live cell populations from white and grey matter

We were interested to investigate the identity of an additional population that we observed in addition to microglia in our preparations in cell suspension B. Surprisingly, this additional population (labeled in Figure 5 with a grey arrow) was only present if the starting material contained grey matter (cortical grey matter, nucleus caudatus and putamen in Figure 5).

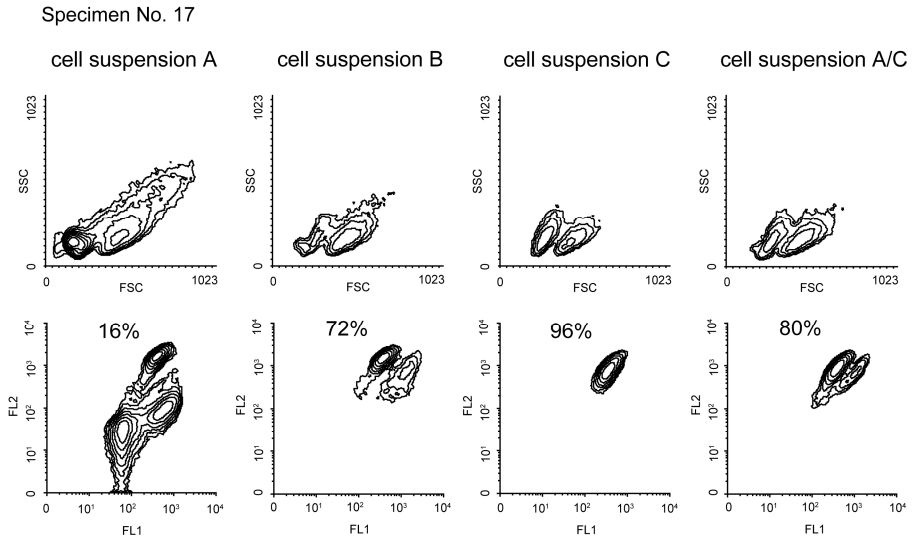

Figure 4. An immunomagnetic bead separation step after the removal of myelin/debris yields comparable purity as a discontinuous Percoll density separation step. Scatter plots of flow cytometric measurements showing the viable cell population (DRAQ5+) at each step of the protocol. Approximately 80% microglia purity can be attained by applying anti-CD11b antibody coupled magnetic bead separation to the cells suspension A. (SSC side scatter (granularity); FSC forward scatter (size); DRAQ5 live cell marker; FL1, FL2 fluorescent detector channels for FITC and PE, respectively; Specimen No. 17 case identifier, please see Table 2 for details).

The live cells in cell suspension B prepared from subcortical white matter, corpus callosum (not shown) or capsula interna consisted almost exclusively of microglia. From both white, grey and mixed tissue samples two populations of microglia could be identified after discontinuous density separation. The population that consisted of

microglia expressing CD11b/CD45 at a higher level (labeled in Figure 5 with an asteriks) are believed to be healthy microglia, while the population with somewhat lower expression levels of these markers and decreased size (labeled in Figure 5 with a white arrow) are believed to be microglia in the process of dying. The ratio between 'healthy' and compromised microglia was usually lower in white matter samples than in purely grey matter samples, which might suggest that grey matter microglia tolerate the isolation procedure better than white matter microglia.

Figure 5. White and grey matter yields different microglia purity after discontinuous Percoll separation (cell suspension B). Microglia was isolated from the subcortical white matter, cortical grey matter, capsula interna, nucleus caudatus and putamen. Microglia purity was determined by the means of flow cytometric analysis. The live cells isolated with the above described protocol from subcortical white matter and capsula interna were almost exclusively microglia, based on their CD11b/CD45 expression profile. Two populations could be observed. One with higher (labeled with an asteriks) and one with lower expression levels of CD11b/CD45 (marked with a white arrow). This later population were microglia in the process of dying. Next to these two populations, the protocol yielded an additional, non-microglial population (marked with a grey arrow) exclusively found in samples containing grey matter (cortical grey matter, nucleus caudatus, putamen). This additional population is also obvious on the forward and side scatter scatter plots. (SSC side scatter (granularity); FSC forward scatter (size); DRAQ5 live cell marker; FL1, FL2, FL3 fluorescent detector channels for FITC, PE, DRAQ5 respectively; Specimen No. 19 case identifier, please see Table 2 for details).

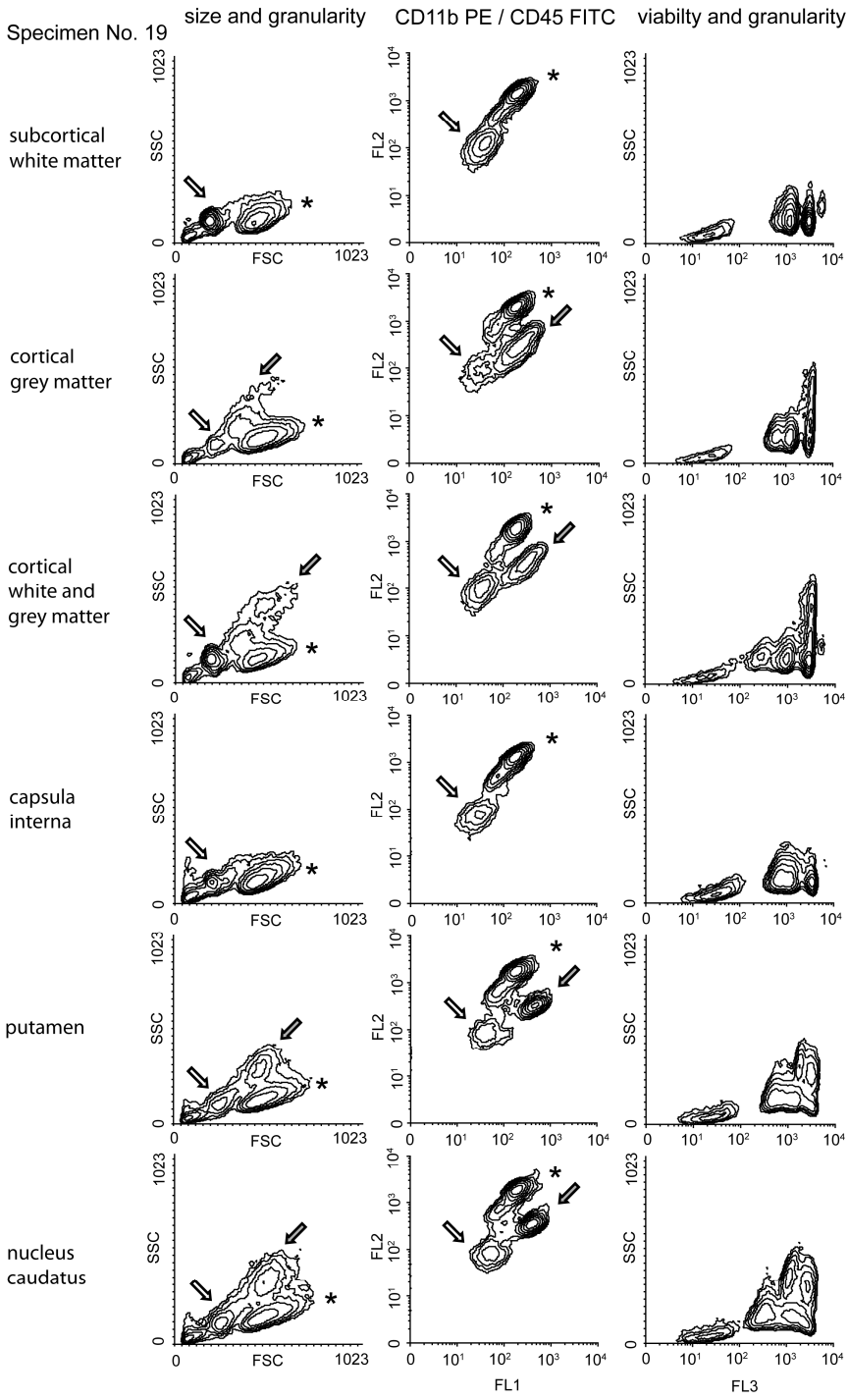
Specimen No. 19
size and granularity
CD11b PE / CD45 FITC
viabilty and granularity
subcortical white matter
cortical grey matter
cortical white and grey matter
capsula interna
putamen
nucleus caudatus
SSC
FSC
FL2
FL1
FL3
0
1023
10^1
10^2
10^3
10^4

Enzymatic dissociation has a distinct effect on the different live cell populations identifiable after discontiuous density separation

The enzymatic digestion of the brain tissue with trypsin had a drastic effect on the size and the viability of the additional population that could be identified as non-microglia in cell suspensions A and B (labeled in Figure 6 with a grey arrow) and has been seen to originate from grey matter (Figure 5). The absence of DRAQ5 (compare the FL3 channel of A' with A'', and B' with B'' in Figure 6) and the complete shift to the left on the size and granularity scatter plot (compare the FSC/SSC scatter plots of A' with A'', and B' with B'' in Figure 6) shows that this particular population was heavily affected by trypsinisation. Nonetheless, trypsin digestion did not influence the capacity of this population to bind unspecifically to anti-CD11b and anti-CD45 antibodies and their respective isotype controls. The enzymatic dissociation had a minor effect on microglia cells causing the swelling of the compromised microglia population (labeled with a white arrow in Figure 6), which could be observed both on the CD11b/CD45 staining intensity (compare the FL1/FL2 channels of C' with C'' in Figure 6), size (compare the FSC/SSC scatter plot of C' with C'' in Figure 6) and DRAQ5 retention capacity (compare the FL3 channel of C' with C'' in Figure 6).

Figure 6. The additional population in cell suspension B from grey matter and mixed samples is sensitive to trypsinisation. Mechanical dissociation was either applied alone (**A'**, **B'**, **C'**) or in combination with a trypsinisation step (**A''**, **B''**, **C''**). Cell suspensions at each step (**A**, **B** and **C** stand for cell suspension A, B and C, respectively) of the protocol were collected, stained for CD11b and CD45, and analysed by flow cytometry. Trypsinisation results in abrupt changes in the granularity and the DRAQ5 staining intensity of the additional population (in **A''** the population marked by the grey filled arrow in **A'** is missing), suggesting that the cells membrane integrity is compromised due to the trypsin treatment. The unspecific binding of the antibodies to this population is not affected by trypsinisation. The size and granularity, staining profile and viability of the microglia population (labeled with an asteriks) is only marginally affected by enzymatic dissociation with trypsin (this effect can be seen in the increase of the population marked with a white arrow in **C'** and **C''**). (SSC side scatter (granularity); FSC forward scatter (size); DRAQ5 - live cell marker; FL1, FL2, FL3 fluorescent detector channels for FITC, PE, DRAQ5 respectively; Specimen No. 19 case identifier, please see Table 2 for details).

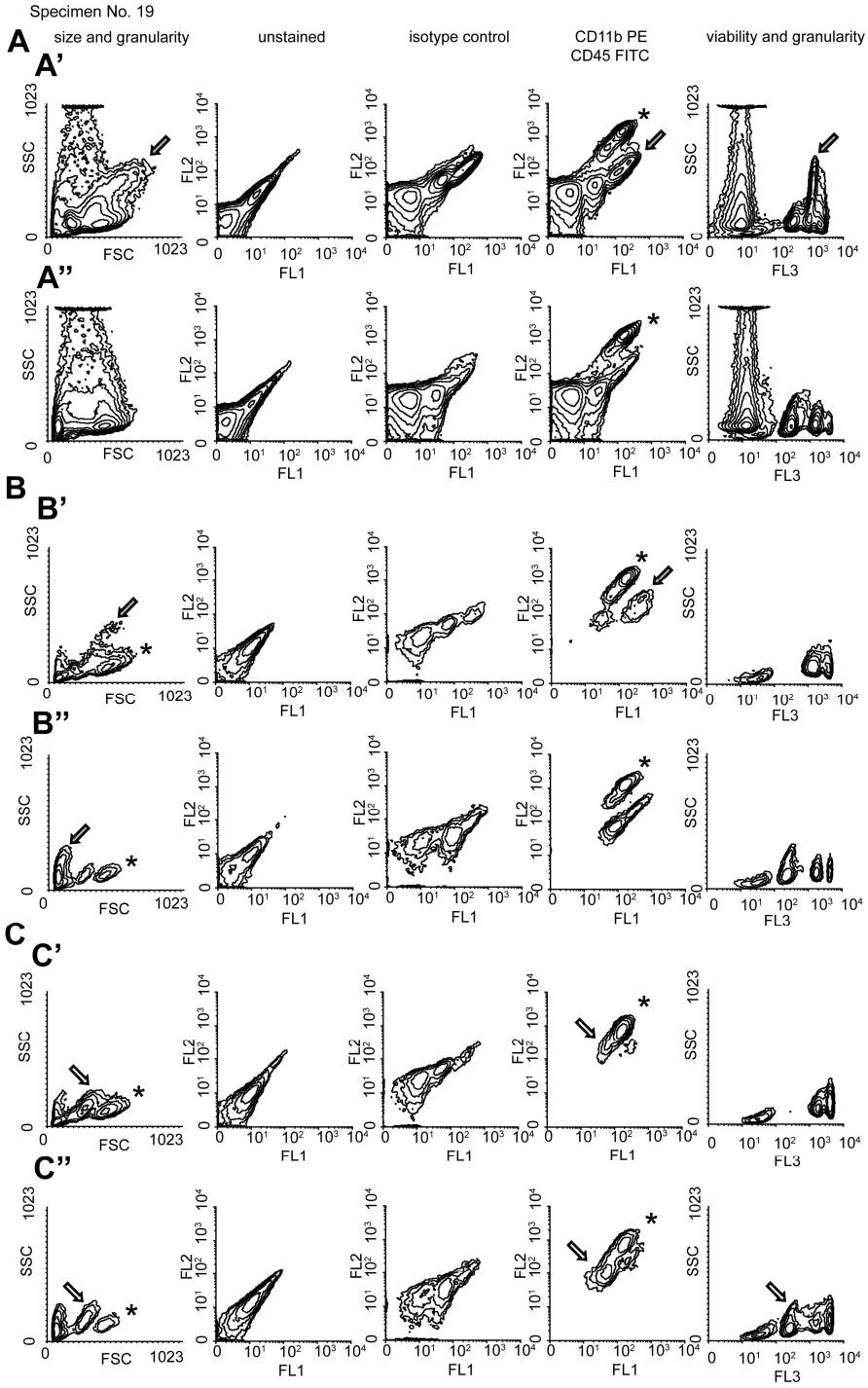
Specimen No. 19
A
size and granularity
unstained
isotype control
CD11b PE
CD45 FITC
viability and granularity
A'
A''
B
B'
B''
C
C'
C''
SSC
FSC
FL1
FL2
FL3
0
1023
10^1
10^2
10^3
10^4
*

The pH of the tissue determines the cellular yield after the enrichment step

Samples consisting of white, grey and mixed CNS tissue had a comparable cellular yield, which was around 3,5 x 10^5 cells per gram wet tissue for each condition (white matter, grey matter and mixed sample). We could not find any correlation between the cellular yield after the discontinuous density separation (cell suspension B) with the age or the neurological condition of the deceased or post mortem delay (not shown). The pH of the autopsy tissue seemed to have the most pronounced effect on the cellular yield (Figure 7B). Autopsy specimens with low pH values (pH < 7) consistently yielded low cell numbers from both white and grey matter. A pH value around and above 7 was compatible with the isolation of reasonable cell numbers from both regions.

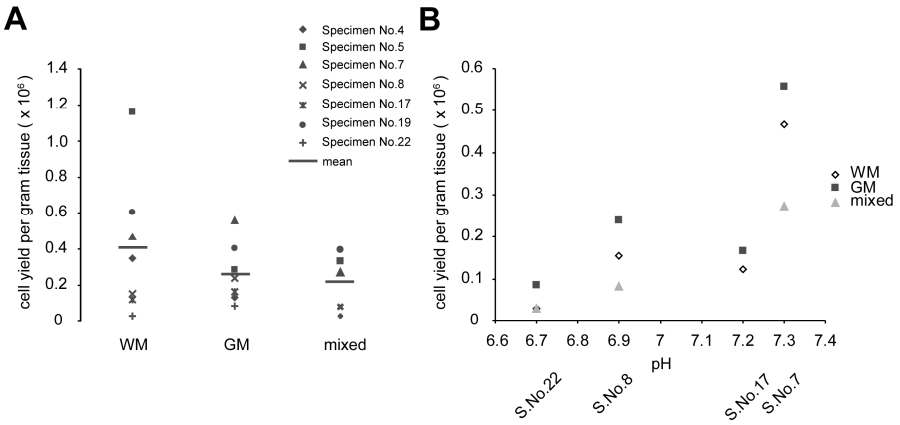

Figure 7. The cellular yield correlated with the pH of the autopsy brain material. A The yield from both white and grey matter was around 3 x 10^5 cells par gram wet tissue. **B** Lower cell yields were associated with more acidic autopsy tissues. (WM white matter; GM grey matter; mixed frontal cortex tissue containing both white and grey matter; Specimen No. and S.No. case identifiers, please see Table 2 for details).

Isolation of human microglia from glioma specimens

We also applied our protocol (with minor modifications) for the isolation of microglia from glioma samples (Figure 8). According to our

observations, the surgically dissected bulk glioma generally contained very little myelin. Hence, in order to minimise the isolation time, the myelin gradient separation was excluded. Glioma associated microglia are believed to be activated to various degrees depending on the advancement of the tumor stage. We also observed differences in the activation state of microglia isolated from different grade glioma samples, which was reflected in their forward / side scatter profile, MHCII expression and morphology. In accordance with the general assumption, that activated microglia are more prone to cell death, we were able to successfully isolate microglia from GBM samples up to grade 3, but not grade 4.

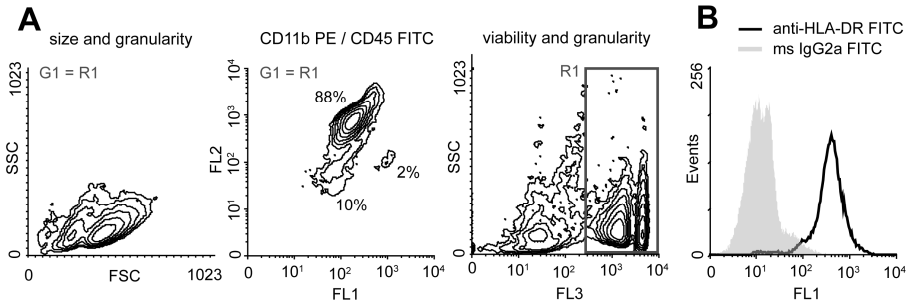

Figure 8. The protocol is suitable for isolating a pure microglia population from glioma samples. Myelin separation proved to be dispensable due to the low myelin content of the gliomas. Discontiuous Percoll separation (60%/40% Percoll solutions) directly after the mechanical dissociation yielded around 90% microglia purity as shown in **A**. **B** Microglia isolated from gliomas were HLA-DR positive. (SSC side scatter (granularity); FSC forward scatter (size); DRAQ5 live cell marker; FL1, FL2, FL3 fluorescent detector channels for FITC, PE, DRAQ5 respectively; G1 gate 1; R1 region 1, containing the DRAQ5 positive live cells)

Functionality of acutely isolated human post mortem microglia

By means of *in vitro* assays we also tested the functionality of the acutely isolated human microglia cells. For functional assays we used the cells directly from the 60%/30% discontinuous Percoll gradient interface. To achieve close to 100% purity in this case, cells were not allowed to attach for longer than 15 minutes after seeding. We investigated three of the most characteristic effector functions of

microglia – chemotaxis, reactive oxygen species (ROS) production and phagocytosis (Figure 9). We found the acutely isolated microglia to be functional and responsive to stimulation. They readily migrated to *adenosine*-5'-*triphosphate* (ATP) and the complement component C5a in a concentration-dependent manner (Figure 9A). Upon stimulation with *phorbol-myristate-acetate* (PMA), they produced reactive oxygen species as detected by the DCFDA probe and flow cytometry (Figure 9B). Moreover, acutely isolated microglia proved to be able to phagocytose bacterial particles (Figure 9C). By means of live cell imaging we followed the accumulation of the pHrodo coupled bacterial bioparticles in the lysosomes of the human microglia cells. Under control conditions 40% of the cells reached half-maximum phagocytic response within the second hour of the assay. We also tested the effect of PMA on the phagocytic capacity of microglia cells. PMA has been shown to have a biphasic effect on the phagocytic capacity of rat microglia and macrophages depending on the concentration (Smith et al., 1998). In our experiments PMA (at the concentration of 0,5 μg/ml) changed the distribution of the phagocytic capacity of acutely isolated microglia.

Differences in the phenotype and function of human white and grey matter microglia

We prepared human microglia from the frontal cortex and associated subcortical white matter of post mortem brain material.

Figure 9. Acutely isolated microglia from human autopsy brain samples are suitable for functional *in vitro* assays. A Acutely isolated human microglia migrate to ATP and C5a in a dose dependent manner. Chemotaxis of acutely isolated human microglia was determined in Boyden chambers. **A'** Quantification of the chemotactic capacity of microglia cells to increasing concentrations of ATP and C5a. Number of responsive cells for each condition is expressed as the percentage of the migrating cells in control condition (DMEM). In panel **A''** examples of the migration response to the control solution (DMEM), to 50-200 μM ATP and to 100-400 ng/ml C5a are shown. **B** Acutely isolated human microglia produce reactive oxygen species upon stimulation. Production of oxygen radicals was determined by detecting the conversion of H_2DCFDA into DCF with flow cytometry. The conversion in unstimulated microglia (control) was

compared to microglia treated with the protein kinase C activator, phorbol-myristate-acetate (5 nM) and ATP (200 µM). **C** Acutely isolated human microglia phagocytozed bacterial particles. The phagocytic capacity of acutely isolated human microglia was investigated by the means of live cell imaging using pHrodo coupled to bacterial particles. **C'** Quantification of the phagocytic response of acutely isolated human microglia. PMA treatment changed the phagocytic capacity of the cells. In **C''** representative photomicrographs are presented showing the accumulation of the fluorescent pHrodo coupled bacterial bioparticles in the lysosomes of the microglia cells. Each depicted experiment is representative of two independent experiments that yielded similar results. (DMEM Dulbecco's modified Eagle medium; ATP Adenosine-5'-triphosphat; C5a complement component 5a; FL1 fluorescent detector channel for FITC; BF bright field; calibration bars in **A''** and **C''** represent 100 and 50 µm, respectively)

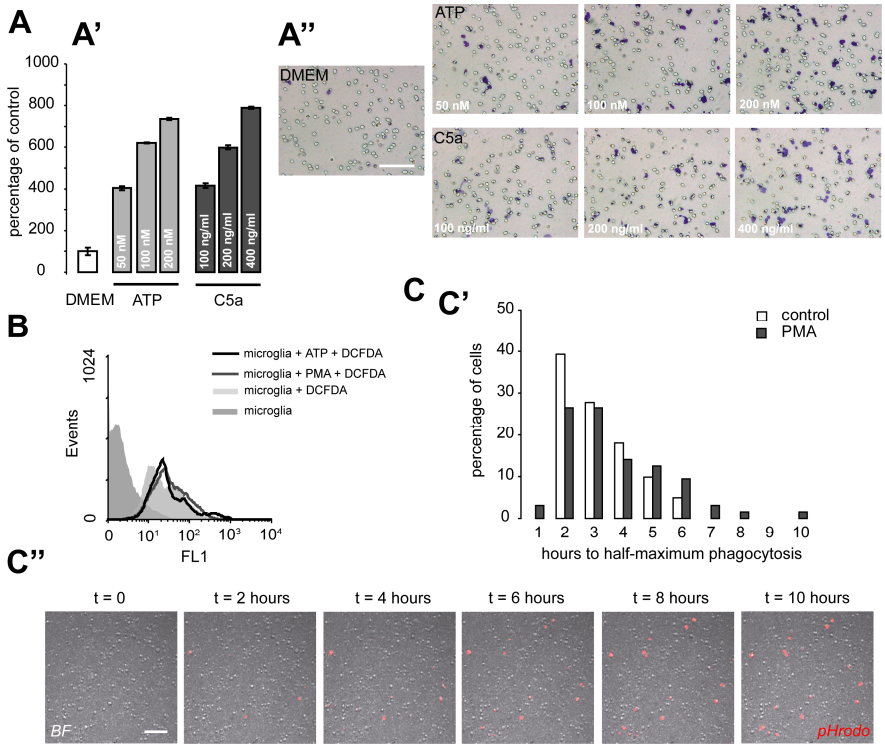

Subsequently, acutely isolated human microglia cells were submitted to immunophenotyping by flow cytometry and their phagocytic capacity was investigated with time-lapse microscopy. Interestingly, unlike murine white and grey matter microglia, acutely isolated human microglia from the subcortical white matter were having higher

phagocytic rate than their cortical counterpart (N = 2 autopsy samples; results of one representative phagocytosis assay are shown in Figure 10A).

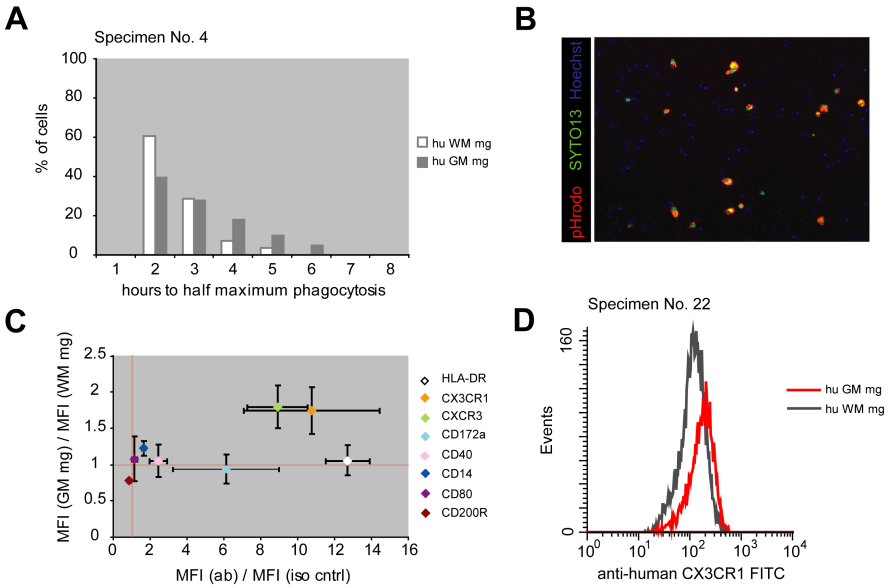

Figure 10. Functional and immunophenotype analysis of acutely isolated human white and grey matter 10croglia. Human microglia were isolated from the white and grey matter parts of frontal cortex autopsies. **A** Human microglia isolated from the white matter phagocytosed pHrodo coupled bioparticles faster than grey matter microglia. The rate of phagocytosis was measured by time lapse microscopy of pHrodo bioparticle ingestion. **B** Representative photomicrograph of a measurement field at the end of the time lapse phagocytosis assay. Live cell nuclei are labeled with Syto13, dead cell nuclei are labeled with Hoechst. The ingested pHrodo coupled bioparticles are red at the acidic pH of the lysosomes. **C** Immunophenotyping of acutely isolated white and grey matter reveals the trends in the differences of the expression levels of certain microglia and microglia activation markers between human white and grey matter microglia. **D** Representative flow cytometric measurement of acutely isolated white and grey matter microglia showing higher expression levels of CX3CR1 on the later. Error bars in **C** represent the standard error of the mean (SEM). N(phagocytosis assay) = 2, N(immunophenotyping) = 2, N(immunophenotyping CX3CR1) = 3. (MFI mean fluorescent intensity; ab specific antibody; iso cntrl isotype control; hu WM mg human white matter microglia; hu GM mg human grey matter microglia)

Within the second hour of the assay 60% of white matter microglia reached half-maximum phagocytosis, while from grey matter microglia only 40% did so. Moreover, flow cytometric analysis of the expression

levels of certain selected markers on human white and grey matter microglia revealed further differences between the two populations (N = 2 autopsy samples except for CX3CR1, where N = 3 autopsy samples). Acutely isolated human microglia displayed considerable surface expression levels of HLA-DR, CX3CR1, CXCR3, and CD172a (Figure 10C). CD40 and CD14 were marginally expressed, while CD80 and CD200R were absent (Figure 10C). Though the expression pattern of these surface markers was basically the same for white and grey matter microglia, certain trends could be observed regarding the differences in expression levels. Grey matter microglia consistently expressed higher levels of the fractalkine receptor (CX3CR1) and CXCR3. The difference between the expression levels of these two markers between grey and white matter microglia was approximately two-fold, as shown by a representative flow cytometric measurement on Figure 10D.

DISCUSSION

Various isolation protocols of microglia from human brain tissue have been practiced for more than two decades (Hussain et al., 2006; De Groot et al., 2001; Dick et al., 1997; Hayes et al., 1988). In these protocols microglia purity and yield is either determined after an extended culturing period (1-3 weeks) in the presence (De Groot et al., 2001; De Groot et al., 2000) or absence of GM-CSF (Lue et al., 2001; Lue et al., 1996) or it has not been determined at all (Hussain et al., 2006; Meeuwsen et al., 2005; Dick et al., 1997). Thus, none of these protocols allows for immediate use of microglia cells in downstream applications such as genome wide gene expression analysis or proteomic analysis. We have developed a protocol for rapid microglia isolation from different brain regions (white versus grey matter, frontal cortex versus striatum) and conditions (with and without neurological pathology (AD, HD, SCA, glioma)), which in four easy and relatively fast steps yield on average 3 x 10^5 microglia per g brain tissue at a purity of > 95%. A further advantage of the current protocol is that it removes red blood cells during the discontinuous Percoll separation, thus abolishing the need for a hypotonic lysis step. Moreover, the protocol works well even in the case of long post mortem delays (tested up till 20 hours).

Several issues have been addressed during the optimisation of the protocol. First of all we determined the optimal weight of the starting autopsy material. In our experience loading more than 3 g/tube of human post mortem brain material in the first, myelin separation step negatively influenced both the yield and the purity of the isolation procedure. We also observed region dependency in this regard, since the optimal starting amount for purely white matter samples was not more than 1-1,5 g/tube, while in the case of samples consisting of only grey matter around 2-3 g of starting material could be loaded on one tube for the myelin separation step. We also made considerable efforts to optimise the subsequent discontinuous density separation step of our

protocol. Clearly, the application of a 30-60% Percoll layers provided us with the most optimal results. In addition to a high yield, flow cytometric analysis showed a minimal presence of debris and complete absence of red blood cells at the 30-60% Percoll layer interface after centrifugation. Microglia cells collected from the 30-60% interface were functional as tested by *in vitro* experiments. From samples containing grey matter next to the CD11b+/CD45+ microglia population an additional live cell population was separated in the course of the discontinuous density separation step. Since this extra population was completely absent in white matter samples and was extremely sensitive to trypsinisation, it is possible that it represents a population of protoplasmic astrocytes with density properties similar to that of microglia cells (Chatterjee & Sarkar, 1984). Including an anti-CD11b antibody coupled magnetic beads separation step however, abolished this additional population from our isolate and yielded a final microglia purity of > 95%.

In accordance with earlier reports (Monoranu et al. 2009; Schuenke & Gelman, 2003) the factor that influenced the quality of the isolation protocol was the pH of the autopsy tissue. Microglia seemed to be extremely sensitive on the acidity of the post mortem brain material. From samples where the pH was below 7 (pH range 6,2 to 6,7) only one out of five samples gave reasonable microglia population, while in samples for which the pH was around 7 (pH range 6,9 to 7) and above (pH range 7,1-7,3) the same number was three and four out of five, respectively. Other factors such as post mortem delay or the neurological status of the deceased did not seem to have significant effect on the microglia population. The yield from white and grey matter of the frontal cortex was similar (around 300.000 cells per gram wet tissue), with a slightly higher yield from grey matter, except for certain cases with neurological conditions affecting the white matter (see S10-005, a myelitis transversa case, the outlier in Figure 7A regarding yield in the WM). Mixed tissue (containing both white and grey matter)

consistently yielded less viable cells (Figure 7A), than when the two tissue parts were separated.

Our protocol has several further advantages over previously described protocols. With the optimisation of the isolation method, the application of a hypotonic shock, culturing, differential attachment, differential trypsinisation and exposure to growth factors became dispensable. Myelin contamination in the cell suspension after the discontinuous density separation is already minimal. All of these factors have been described to influence the phenotype and function of microglia. Thus, for future studies aiming at investigating human microglia phenotypes in health and disease our isolation procedure offers a serious choice.

ACKNOWLEDGEMENTS

We would like to thank Klaas Sjollema (UMCG-UMIC, Groningen, The Netherlands) for writing ImageJ plugins for quantification of time lapse phagocytosis experiments.

LIST OF ABBREVIATIONS (FIGRES AND TABLES)

CD11b	integrin alpha-M
CD14	monocyte differentiation antigen CD14
CD172a	tyrosine-protein phosphatase non-receptor type substrate 1
CD200R	cell surface glycoprotein CD200 receptor
CD40	tumor necrosis factor receptor superfamily member 5
CD45	receptor-type tyrosine-protein phosphatase C
CD68	macrosialin, a marker of tissue macrophages
CD80	activation B7.1 antigen
CX3CR1	fractalkine receptor
CXCR3	C-X-C chemokine receptor type 3
GFAP	glial fibrillary acidic protein
HLA-DR	HLA class II histocompatibility antigen, DR
Iba1	ionised calcium-binding adapter molecule 1
β-actin	beta-actin

LIST OF REFERENCES

Bailey SL, Carpentier PA, McMahon EJ, Begolka WS, Miller SD. 2006. Innate and adaptive immune responses of the central nervous system. Crit Rev Immunol 26:149-188.

Becher B, Bechmann I, Greter M. 2006. Antigen presentation in autoimmunity and CNS inflammation: how T lymphocytes recognize the brain. J Mol Med 84:532-543.

Cardona AE, Huang D, Sasse ME, Ransohoff RM. 2006. Isolation of murine microglial cells for RNA analysis or flow cytometry. Nat Protoc 1:1947-1951.

Carson MJ, Bilousova TV, Puntambekar SS, Melchior B, Doose JM, Ethell IM. 2007. A rose by any other name? The potential consequences of microglial heterogeneity during CNS health and disease. Neurotherapeutics 4:571-579.

Chatterjee D, Sarkar PK. 1984. Isolation of protoplasmic astrocytes: a procedure based on controlled trypsin digestion. J Neurochem 42:1229-1234.

Davalos D, Grutzendler J, Yang G, Kim JV, Zuo Y, Jung S, Littman DR, Dustin ML, Gan WB. 2005. ATP mediates rapid microglial response to local brain injury *in vivo*. Nat Neurosci 8:752-758.

De Groot CJ, Montagne L, Janssen I, Ravid R, Van D, V, Veerhuis R. 2000. Isolation and characterization of adult microglial cells and oligodendrocytes derived from postmortem human brain tissue. Brain Res Brain Res Protoc 5:85-94.

De Groot CJ, Hulshof S, Hoozemans JJ, Veerhuis R. 2001. Establishment of microglial cell cultures derived from postmortem human adult brain tissue: immunophenotypical and functional characterization. Microsc Res Tech 54:34-39.

De Haas AH, Boddeke HW, Brouwer N, Biber K. 2007. Optimized isolation enables *ex vivo* analysis of microglia from various central nervous system regions. Glia 55:1374-1384.

De Haas AH, Boddeke HW, Biber K. 2008. Region-specific expression of immunoregulatory proteins on microglia in the healthy CNS. Glia 56:888-894.

Dick AD, Pell M, Brew BJ, Foulcher E, Sedgwick JD. 1997. Direct *ex vivo* flow cytometric analysis of human microglial cell CD4 expression: examination of central nervous system biopsy specimens from HIV-seropositive patients and patients with other neurological disease. AIDS 11:1699-1708.

Ford AL, Goodsall AL, Hickey WF, Sedgwick JD. 1995. Normal adult ramified microglia separated from other central nervous system macrophages by flow cytometric sorting.

Phenotypic differences defined and direct *ex vivo* antigen presentation to myelin basic protein-reactive CD4+ T cells compared. J Immunol 154:4309-4321.

Gibbons HM, Dragunow M. 2010. Adult human brain cell culture for neuroscience research. Int J Biochem Cell Biol 42:844-856.

Hanisch UK, Kettenmann H. 2007. Microglia: active sensor and versatile effector cells in the normal and pathologic brain. Nat Neurosci 10:1387-1394.

Hayes GM, Woodroofe MN, Cuzner ML. 1988. Characterisation of microglia isolated from adult human and rat brain. J Neuroimmunol 19:177-189.

Hussain SF, Yang D, Suki D, Aldape K, Grimm E, Heimberger AB. 2006. The role of human glioma-infiltrating microglia/macrophages in mediating antitumor immune responses. Neuro Oncol 8:261-279.

Hussain SF, Yang D, Suki D, Grimm E, Heimberger AB. 2006. Innate immune functions of microglia isolated from human glioma patients. J Transl Med 4:15.

Jiang-Shieh YF, Wu CH, Chang ML, Shieh JY, Wen CY. 2003. Regional heterogeneity in immunoreactive macrophages/microglia in the rat pineal gland. J Pineal Res 35:45-53.

Lawson LJ, Perry VH, Dri P, Gordon S. 1990. Heterogeneity in the distribution and morphology of microglia in the normal adult mouse brain. Neuroscience 39:151-170.

Lue LF, Brachova L, Walker DG, Rogers J. 1996. Characterization of glial cultures from rapid autopsies of Alzheimer's and control patients. Neurobiol Aging 17:421-429.

Lue LF, Walker DG, Rogers J. 2001. Modeling microglial activation in Alzheimer's disease with human postmortem microglial cultures. Neurobiol Aging 22:945-956.

Meeuwsen S, Bsibsi M, Persoon-Deen C, Ravid R, Van Noort JM. 2005. Cultured human adult microglia from different donors display stable cytokine, chemokine and growth factor gene profiles but respond differently to a pro-inflammatory stimulus. Neuroimmunomodulation 12:235-245.

Mittelbronn M, Dietz K, Schluesener HJ, Meyermann R. 2001. Local distribution of microglia in the normal adult human central nervous system differs by up to one order of magnitude. Acta Neuropathol 101:249-255.

Monoranu CM, Apfelbacher M, Grunblatt E, Puppe B, Alafuzoff I, Ferrer I, Al Saraj S, Keyvani K, Schmitt A, Falkai P, Schittenhelm J, Halliday G, Kril J, Harper C, McLean C, Riederer P, Roggendorf W. 2009. pH measurement as quality control on human post mortem brain tissue: a study of the BrainNet Europe consortium. Neuropathol Appl Neurobiol 35:329-337.

Nimmerjahn A, Kirchhoff F, Helmchen F. 2005. Resting microglial cells are highly dynamic surveillants of brain parenchyma *in vivo*. Science 308:1314-1318.

Ransohoff RM, Perry VH. 2009. Microglial physiology: unique stimuli, specialized responses. Annu Rev Immunol 27:119-145.

Schilling M, Besselmann M, Leonhard C, Mueller M, Ringelstein EB, Kiefer R. 2003. Microglial activation precedes and predominates over macrophage infiltration in transient focal cerebral ischemia: a study in green fluorescent protein transgenic bone marrow chimeric mice. Exp Neurol 183:25-33.

Schuenke K, Gelman BB. 2003. Human microglial cell isolation from adult autopsy brain: brain pH, regional variation, and infection with human immunodeficiency virus type 1. J Neurovirol 9:346-357.

Smith ME, van der MK, Somera FP, Sobel RA. 1998. Effects of phorbol myristate acetate (PMA) on functions of macrophages and microglia *in vitro*. Neurochem Res 23:427-434.

Town T, Nikolic V, Tan J. 2005. The microglial "activation" continuum: from innate to adaptive responses. J Neuroinflammation 2:24.

Williams K, Dooley N, Ulvestad E, Becher B, Antel JP. 1996. IL-10 production by adult human derived microglial cells. Neurochem Int 29:55-64.

Wu CH, Chien HF, Chang CY, Ling EA. 1997. Heterogeneity of antigen expression and lectin labeling on microglial cells in the olfactory bulb of adult rats. Neurosci Res 28:67-75.

Chapter 6

General discussion

Nederlandse samenvatting

Összefoglaló magyar nyelven

Ackowledgements

GENERAL DISCUSSION

The present doctoral dissertation gives an account of the scientific investigation performed in the course of the PhD project aimed to characterise microglia phenotypes associated with maintenance of central nervous system tissue homeostasis. In this respect three major aspects of microglia phenotype and function have been addressed: differences in the microglia phenotypes residing in distinct brain regions of the healthy brain, microglia phenotypes associated with hippocampal functional and anatomical plasticity and the microglia phenotype involved in regenerative processes in the CNS. In **Chapter 1** we have given an overview of the literature regarding the phenotype heterogeneity of microglia cells in the CNS and the causes and functional consequences thereof (Olah et al., 2010).

Chapter 2 discusses the role of microglia in the regulation of adult neurogenesis under physiological conditions. In our study we used the mouse running wheel model, in which voluntary physical exercise elevates the level of hippocampal neurogenesis without inflicting stress upon the animals (Salam et al., 2009). Of our particular interest was a microglia phenotype, that has been suggested to arise from the interaction of microglia with encephalitogenic IL-4 producing T cells of Th2 type (Butovsky et al., 2006). This specific microglia phenotype is characterised by detectable levels of MHCII (pointing towards their interaction with T cells) and IGF-1 expression, and has been implicated to be involved in the regulation of adult hippocampal neurogenesis in other models (Ziv et al., 2006). Thus, we investigated multiple aspects of the microglia phenotype associated with basal (sedentary control) and physiologically elevated levels (“runners”) of adult hippocampal neurogenesis, including morphology, gene expression and surface expression of activation markers. In accordance with the literature (van Praag et al., 1999), ten days of voluntary physical exercise robustly

enhanced both the proliferation of neural precursors and the survival of newborn neurons in the subgranular zone of the hippocampal dentate gyrus. Regarding the microglia phenotype however, we found no evidence of MHCII expression on hippocampal microglia in the control group or in the voluntary physical exercise group. Moreover, T cells were generally absent from the dentate gyrus parenchyma. The microglia phenotype that was associated with both the basal and elevated levels of adult hippocampal neurogenesis in our model lacked any morphological or immunological (cytokine profile, among other IGF-1 expression) sign of activation. Nonetheless, we found a moderate induction of the expression of CD45 at the protein level, which is generally believed to be an activation marker of microglia. However, since the ligand for CD45 is unknown (Saunders & Johnson, 2010), it is difficult to speculate about the functional significance of the observed increase in the surface expression of this molecule. On the other hand, CD45 has been shown to be a negative regulator of microglia activation under certain conditions (Penninger et al., 2001; Tan et al., 2000), thus it might serve autoregulatory functions and the modest upregulation of this receptor-type tyrosine-protein phosphatase on microglia cells in this model might point towards their attempt to limit their own activation. Interestingly, the number of proliferating hippocampal microglia was also significantly increased in the runners compared to the sedentary controls. However, this increase could be detected in both the neurogenic (dentate gyurs) and the non-neurogenic (cornu ammonis) region of the hippocampus, suggesting that it might not be directly involved in the enhancement of adult hippocamapal neurogenesis in this model. Based on our experimental findings we concluded that the microglia phenotype associated with the hippocampal neurogenic niche in the adult and with physiological scale changes in the level of hippocampal neurogenesis, does not bear any signs of possible interactions with T cells (Olah et al., 2009). Thus, our data supports the notion, that adult hippocampal neurogenesis can occur in the absence

of microglia T cell interactions or microglia activation in general. Moreover, since this particular microglia phenotype has been suggested to be causally linked to the increased neurogenesis in rat hippocampus upon exposure to enriched environment (Ziv et al., 2006) our study also highlights the importance of considering model and species differences in respect of the regulation of adult hippocampal neurogenesis.

In **Chapter 3** our aim was to investigate the phenotype differences between corpus callosum and cerebral cortex resident microglia in the healthy brain. It has been suggested that the regional heterogeneity of microglia cells might reflect (inherent and/or acquired) differences in their activation state and thus have functional consequences in respect of CNS immunity (Carson et al., 2007). The two most distinct microglia phenotypes of the CNS parenchyma based on their morphology reside in the white and the grey matter of the forebrain. Accordingly, the inflammatory environments that have been found at these two anatomical sites differ considerably. The differences between the multiple sclerosis lesions located in the white and the grey matter of the brain may serve as an ideal example, where cortical lesions witness far less complement deposition, microglia activation, disruption of blood brain barrier and perivascular lymphocyte infiltration than their callosal counterparts (Stadelmann et al., 2008; Bo et al., 2006). Thus, we investigated the phenotype of acutely isolated white and grey matter microglia at multiple levels: cellular morphology, gene and protein expression and functionality. Our results suggest, that the corpus callosum resident microglia are phenotypically distinct from the ones residing in the cortex in respect of multiple measures of microglia function and phenotype *in vivo* and *in vitro*. We found significant differences between microglia of grey and white matter origin with respect to their cellular morphology, time course of intracellular calcium responses to ATP, electrophysiological membrane properties in culture and responsiveness to endotoxemia *in vivo*. Furthermore, genome wide

gene expression analysis revealed significant differences of several inflammatory pathways at the gene expression level as well. However, it is important to mention, that the observed differences were quantitative rather than qualitative. We could not reject, nor confirm earlier suggestions, that white matter microglia would exist at a higher level of basal activation under physiological conditions than grey matter microglia (Carson et al., 2007). Rather, our data suggest a complex relationship between the difference between phenotypes and the functional dissimilarities between white and grey matter microglia populations that needs further investigation.

In **Chapter 4** the characteristics of the microglia phenotype associated with central nervous system de- and remyelination are discussed. Remyelination, an endogenous regenerative process aiming at restoring the myelin sheets along the denuded axons after a demyelinating insult, has a complex and yet not clearly clarified relationship with inflammation (Hohlfeld, 2007, Ruffini, 2004). Since in multiple sclerosis (MS) the recruitment of endogenous oligodendrocyte precursors (OPCs) to the demyelinated lesion does not seem to be the limiting factor in respect of remyelination (Wolswijk, 2000; Scolding et al., 1998), it has been suggested that the failure of regenerative processes in MS might be attributable (at least in part) to the lack of support for the differentiation of OPCs from the side of the local inflammatory environment (Franklin, 2002). However, the actual cell types and factors that support remyelination haven't been described yet. Microglia are the gatekeepers of CNS immunity and are at the epicenter of any inflammatory response in the brain and spinal cord (Tambuyzer et al., 2009; Streit et al., 2005). Thus we investigated the microglia phenotype associated with de- and remyelination in the murine cuprizone model by means of genome wide gene expression analysis in acutely isolated microglia. The choice of model aimed at minimising the contribution of systemic immune cells to our study (Remington et al., 2007; Matsushima

& Morrel, 2001), thus enabling us to investigate the phenotype of microglia in particular. Surprisingly, there was no phenotype switch between microglia present in the corpus callosum during demyelination and remyelination. Rather, a single phenotype could be observed that gradually developed in the course of demyelination and persisted during remyelination. Based on the functional (gene ontology) analysis of the differently expressed genes in the course of de- and remyelination, the most robust characteristics of this phenotype were the altered lipid metabolism and the upregulation of MHCII expression in the absence of costimulatory molecules. Moreover, the observed microglia phenotype was in possession of the necessary molecular repertoire for performing several effector functions, such as phagocytosis of apoptotic cells and myelin, recruitment of oligodendrocyte precursors and support of their differentiation towards myelinating oligodendrocytes. Whether this microglia phenotype is indeed supportive of remyelination, or merely permissive, still has to be determined. Nonetheless, our data clearly demonstrates that, in contrast to the earlier views in the field (Gebicke-Haerter, 2001; Pocock & Liddle, 2001; Banati et al., 1993), microglia activation per se and maintenance of tissue homeostasis in the CNS are not mutually exclusive phenomena. Even more, our findings point towards the significant involvement of microglia in various aspects of remyelination, such as clearance of tissue debris, tissue remodeling, mobilisation of endogenous neural precursors, trophic and metabolic support of OPC differentiation and possibly tolerance induction.

Chapter 5 describes a fast and efficient method for microglia isolation from human central nervous system autopsy and biopsy samples. Microglia, the resident immune cells of the brain and spinal cord, are known to be crucially involved in not only in the maintenance of tissue homeostasis but also several (if not all) pathophysiological conditions affecting the CNS (Graeber, 2010; Hanisch & Kettenmann, 2007). Not surprisingly thus, there is a growing interest in dissecting the specific contribution of microglia to the above mentioned processes. Up till now

however, these efforts were largely hindered by the lack of an isolation procedure that would allow the attainment of a purified microglia population from both non-diseased and diseased human brain samples with a significant yield. Previous protocols employed extended culturing periods to increase purity and yield of microglia, during which exposure to growth factors and serum has undoubtedly influenced their phenotype.

Our aim was to set up an optimised acute isolation protocol for human microglia. The four step isolation procedure (mechanical dissociation, myelin separation, enrichment and purification) described in this chapter enables us to investigate the microglia phenotypes in the healthy and diseased brain by the means of immunophenotyping, protein and gene expression analysis and functional assays. Moreover, since the yield and the purity of microglia preparation was not significantly affected by differences in post mortem delay or the neurological status of the CNS tissue, and could be even successfully used to isolate pure microglia population from glioma samples, the protocol presented in this dissertation is not only fast and efficient, but has a broad spectrum of potential applications as well.

LIST OF REFERENCES

Banati RB, Gehrmann J, Schubert P, Kreutzberg GW (1993) Cytotoxicity of microglia. Glia 7: 111-118.

Bo L, Geurts JJ, Mork SJ, van d, V (2006) Grey matter pathology in multiple sclerosis. Acta Neurol Scand Suppl 183: 48-50.

Butovsky O, Ziv Y, Schwartz A, Landa G, Talpalar AE, Pluchino S, Martino G, Schwartz M (2006) Microglia activated by IL-4 or IFN-gamma differentially induce neurogenesis and oligodendrogenesis from adult stem/progenitor cells. Mol Cell Neurosci 31: 149-160.

Carson MJ, Bilousova TV, Puntambekar SS, Melchior B, Doose JM, Ethell IM (2007) A rose by any other name? The potential consequences of microglial heterogeneity during CNS health and disease. Neurotherapeutics 4: 571-579.

Franklin RJ (2002) Why does remyelination fail in multiple sclerosis? Nat Rev Neurosci 3: 705-714.

Gebicke-Haerter PJ (2001) Microglia in neurodegeneration: molecular aspects. Microsc Res Tech 54: 47-58.

Graeber MB (2010) Changing face of microglia. Science 330: 783-788.

Matsushima GK, Morell P (2001) The neurotoxicant, cuprizone, as a model to study demyelination and remyelination in the central nervous system. Brain Pathol 11: 107-116.

Olah M, Ping G, De Haas AH, Brouwer N, Meerlo P, Van Der Zee EA, Biber K, Boddeke HW (2009) Enhanced hippocampal neurogenesis in the absence of microglia T cell interaction and microglia activation in the murine running wheel model. Glia 57: 1046-1061.

Olah M, Biber K, Vinet J, Boddeke HW (2010) Microglia Phenotype Diversity. CNS Neurol Disord Drug Targets.

Penninger JM, Irie-Sasaki J, Sasaki T, Oliveira-dos-Santos AJ (2001) CD45: new jobs for an old acquaintance. Nat Immunol 2: 389-396.

Pocock JM, Liddle AC (2001) Microglial signalling cascades in neurodegenerative disease. Prog Brain Res 132: 555-565.

Remington LT, Babcock AA, Zehntner SP, Owens T (2007) Microglial recruitment, activation, and proliferation in response to primary demyelination. Am J Pathol 170: 1713-1724.

Ruffini F, Kennedy TE, Antel JP (2004) Inflammation and remyelination in the central nervous system: a tale of two systems. Am J Pathol 164: 1519-1522.

Salam JN, Fox JH, Detroy EM, Guignon MH, Wohl DF, Falls WA (2009) Voluntary exercise in C57 mice is anxiolytic across several measures of anxiety. Behav Brain Res 197: 31-40.

Saunders AE, Johnson P (2010) Modulation of immune cell signalling by the leukocyte common tyrosine phosphatase, CD45. Cell Signal 22: 339-348.

Scolding N, Franklin R, Stevens S, Heldin CH, Compston A, Newcombe J (1998) Oligodendrocyte progenitors are present in the normal adult human CNS and in the lesions of multiple sclerosis. Brain 121 (Pt 12): 2221-2228.

Stadelmann C, Albert M, Wegner C, Bruck W (2008) Cortical pathology in multiple sclerosis. Curr Opin Neurol 21: 229-234.

Streit WJ, Conde JR, Fendrick SE, Flanary BE, Mariani CL (2005) Role of microglia in the central nervous system's immune response. Neurol Res 27: 685-691.

Tambuyzer BR, Ponsaerts P, Nouwen EJ (2009) Microglia: gatekeepers of central nervous system immunology. J Leukoc Biol 85: 352-370.

Tan J, Town T, Mori T, Wu Y, Saxe M, Crawford F, Mullan M (2000) CD45 opposes beta-amyloid peptide-induced microglial activation via inhibition of p44/42 mitogen-activated protein kinase. J Neurosci 20: 7587-7594.

van Praag H, Kempermann G, Gage FH (1999) Running increases cell proliferation and neurogenesis in the adult mouse dentate gyrus. Nat Neurosci 2: 266-270.

Wolswijk G (2000) Oligodendrocyte survival, loss and birth in lesions of chronic-stage multiple sclerosis. Brain 123 (Pt 1): 105-115.

Ziv Y, Ron N, Butovsky O, Landa G, Sudai E, Greenberg N, Cohen H, Kipnis J, Schwartz M (2006) Immune cells contribute to the maintenance of neurogenesis and spatial learning abilities in adulthood. Nat Neurosci 9: 268-275.

NEDERLANDSE SAMENVATTING

In dit proefschrift wordt onderzoek naar microglia fenotypes die een rol spelen bij de homeostase van het central zenuwstelsel beschreven. Drie aspecten van het microglia fenotype en functie zijn onderzocht: de microglia fenotype diversiteit in verschillende hersengebieden, het microglia fenotype dat betrokken is bij neurogenese in de hippocampus en het microglia fenotype dat betrokken is bij regeneratieve processen in de hersenen.

In **Hoofdstuk 1** wordt een overzicht gegeven van de literatuur betreffend de fenotype diversiteit van microglia cellen in het central zenuwstelsel en de functionele betekenis hiervan (Olah et al., 2010).

In **Hoofdstuk 2** wordt de rol van microglia bij de regulatie van adulte neurogenese in de muis besproken. In deze studie is gebruik gemaakt van een tredmolen. Het is bekend dat fysieke inspanning de neurogenese in de hippocampus versterkt (Salam et al., 2009). Het onderzoek was gericht op de identificatie van een microglia fenotype dat geinduceerd wordt door interactive met Th2 type T cellen die interleukine-4 produceren (Butovsky et al., 2006). Dit specifike microglia fenotype, dat wordt gekarakteriseerd door expressie van MHCII en van IGF-1, lijkt betrokken te zijn bij de regulatie van hippocampale neurogenese in de muis (Ziv et al., 2006). Verschiilende aspecten van het microglia fenotype zoals hun morfologie en expressie van specifieke membraan eiwitten zijn onderzocht in muizen met een basale neurogenese (controle) en muizen die door de beschikbaarheid van een tredmolen veel fysieke inspanning leverden en hierdoor een versterkte neurogenese hadden. Zoals reeds in de literatuur beschreven (van Praag et al., 1999) versterkte een 10-daagse fysieke inspanning de proliferatie van neurale voorlopercellen in de subgranulaire zone van de dentate gyrus in de hippocampus. In de hippocampale microglia werd echter noch in controle muizen noch na fysieke inspanning expressie van MHCII en IGF-1 gevonden. Verder werden er in de dentate gyrus van

beide groepen muizen bijna geen T cellen aangetroffen. We werd er in microglia van controle muizen en na 10-daagse fysieke inspanning expressie van CD45 eiwit (receptor-type tyrosine-proteine fosfatase) aangetroffen, hetgeen een indicatie is voor een milde activatie van de microglia onder beide omstandigheden. Omdat het ligand voor CD45 nog niet bekend is (Saunders & Johnson, 2010), is het moeilijk om over de functionele betekenis van deze CD45 expressie te speculeren. Wel is bekend dat CD45 de activatie van microglia remt (Penninger et al., 2001; Tan et al., 2000). Het is denkbaar dat de microglia, als een vorm van autoregulatie, door expressie van CD45 hun eigen activatie beperken.

In vergelijking met controle muizen was na 10-daagse fysieke inspanning het aantal proliferende microglia significant toegenomen. Deze toename werd echter niet alleen in de dentate gyrus, maar ook in het niet neurogene deel van de hippocampus (cornu ammonis) waargenomen, wat suggereert dat dit fenomeen niets met adulte neurogenese te maken heeft.

Op grond van onze experimenten hebben we geconcludeerd dat het microglia fenotype in de neurogene zone van de hippocampus bij zowel basale- als versterkte neurogenese geen aanwijzingen geeft voor interactive met T cellen (Olah et al., 2009). Het is duidelijk dat onze gegevens geen aanwijzingen geven voor de betrokkenheid van interactie tussen microglia en T cellen bij adulte neurogenese. Deze conclusie is belangrijk omdat verondersteld werd dat het bovengenoemde specifieke microglia fenotype een cruciale rol lijkt te spelen bij neurogenese die veroorzaakt wordt door blootstelling aan een verrijkte omgeving (Ziv et al., 2006). Onze studie benadrukt hiermee het belang van het verschil tussen experimentele diermodellen voor het bestuderen van adulte neurogenese.

In **Hoofdstuk 3** wordt onderzoek naar het microglia fenotype dat aangetroffen wordt bij de- en remyelinisering besproken. Remyelinisering, een regeneratief proces dat bedoeld is de aanleg van myeline rond beschadigde axonen te bevorderen, heft een complexe en

nog niet volledig begrepen relatie met neuroinflammatie (Hohlfeld, 2007, Ruffini, 2004). Omdat bij multiple sclerosis (MS) the recrutering van endogene oligodendrocyt voorlopercellen naar de beschadigde gebieden geen beperkende factor lijkt te zijn (Wolswijk, 2000; Scolding et al., 1998), wordt gesuggereerd dat het gebrek aan herstel van MS lesies te wijten is aan gebrek aan ondersteuning van de differentiatie van deze voorlopercellen (Franklin, 2002). Echter de relevante cel- types en factoren die remyelisatie ondersteunen zijn nog niet bekend. Microglia zijn de bewakers van de homeostase van het central zenuwstelsel en staan centraal bij iedere denkbare ontstekingsreactie van het brein en het ruggenmerg (Tambuyzer et al., 2009; Streit et al., 2005). Wij hebben in het cuprizon model in de muis het microglia fenotype onderzocht dat gevonden wordt bij de- en remyelinisatie. Hierbij zijn acuut geisoleerde microglia onderzocht op gen-expressie. Het cuprizon demyelinisatie model is hiervoor optimaal omdat de bijdrage van perifere immuuncellen in dit proefdiermodel minimaal is (Remington et al., 2007; Matsushima & Morrel, 2001). Hierdoor kan het microglia fenotype goed onderzocht worden. Tot onze verrassing vond er in het cuprizon model het corpus callosum tijdens het demyelinisatie en remyelinisatie proces geen verandering van het fenotype plaats in microglia. Er ontwikkelde zich gedurende het demyelinisatie process één fenotype dat zich tijdens het remyelinisatie process handhaafde. Op grond van analyse van het gen-expressie profiel van dit fenotype werden diverse processen zoals veranderingen in het lipide metabolisme, verhoogde expressie van het MHCII complex en afwezigheid van expressie van co-stimulatoire molecule vastgesteld. Verder bleekt het bovengenoemde microglia fenotype in staat tot fagocytose van apoptotische cellen en myeline, en tot recrutering van oligodendrocyt voorlopercellen waarvan ze differentiate ondersteunden. Er moet nog vastgesteld worden of dit microglia fenotype het remyelinisatie process inderdaad actief ondersteunt. Onze gegevens later echter zien dat in tegenstelling tot een vroegere

opvatting (Gebicke-Haerter, 2001; Pocock & Liddle, 2001; Banati et al., 1993), microglia activatie en handhaving van weefselhomeostase in het brein kunnen samengaan. Verder duiden onze bevindingen op de betrokkenheid van microglia bij deelaspecten van het remyelinisatie process zoals de inductie van immuuntolerantie, het opruimen van weefsel debris, weefselherstel, recrutering van endogene neurale voorlopercellen en ondersteuning van de differentiatie van oligodendrocyt voorlopercellen.

In **Hoofdstuk 4** is gezocht naar de verschillen in fenotypen van microglia in het corpus callosum (witte stof) en de cerebrale cortex (grijze stof) in het gezonde brein. Er wordt gesuggereerd dat mogelijke regionale verschillen tussen microglia verantwoordelijk zijn voor verschillende vormen van microglia activatie, hetgeen consequenties zou kunnen hebben voor de immuunrespons van het central zenuwstelsel (Carson et al., 2007). De twee meest diverse microglia fenotypen zijn gebaseerd op hun morfologie en bevinden zich in witte- en grijze stof. Het neuroinflammatie proces in witte- en grijze stof verschilt aanzienlijk. Zo vertonen MS lesies in grijze stof veel minder microglia activatie, complement vorming, beschadiging van de bloed-hersenbarriere en infiltratie van perivasculaire lymfocyten dan in witte stof (Stadelmann et al., 2008; Bo et al., 2006). We hebben om deze reden het fenotype van acuut geisoleerde microglia uit witte- en grijze stof nauwkeurig geanalyseerd, waarbij gekeken is naar cellulaire morfologie, gen- en proteine expressive en microglia functie. De resultaten suggereren dat het fenotype van microglia uit het corpus callosum verschilt van het fenotype in de cortex. Duidelijke verschillen werden waargenomen in cellulaire morfologie, ATP-geinduceerde calcium fluxen, electrofysiologische membraaneigenschappen en de respons op bacteriele lipopolysacchariden. Verder werden, na analyse van gen-expressie verschillen gevonden in de expressive van genen die betrokken zijn bij het inflammatie proces. Hierbij moet wel opgemerkt worden dat waargenomen verschillen in gen –expressie meer gebaseerd

zijn op quantitieve dan op kwalitatieve verschillen. We konden vroegere suggesties dat witte stof microglia in vergelijking met grijze stof microglia een grotere mate van activatie hebben noch bevestigen noch afwijzen (Carson et al., 2007). Wel suggereren onze data een complexe relatie tussen de microglia fenotypes in witte en grijze stof en verschillen in functie tussen deze fenotypes.

In **Hoofdstuk 5** wordt een snelle en efficiente method voor de isolatie van microglia uit menselijk weefsel van het central zenuwstelsel verkregen door autopsie of biopsie. Microglia zijn de primaire immuun cellen van het centrale zenuwstelsel en ze zijn betrokken bij zowel handhaving van de homeostase van het centrale zenuwstelsel als bij de immuunrespons bij neuropathologische aandoeningen (Graeber, 2010; Hanisch & Kettenmann, 2007). Er bestaat daarom een toenemende belanstelling voor de eigenschappen en functies van microglia. Tot nu toe bleek het moeilijk om een zuivere populatie microglia uit human hersenweefsel te isoleren. Bij conventionele protocollen moeten uitgebreide celkweek procedures uitgevoerd worden om de zuiverheid de de opbrengst van de geisoleerde microglia te verhogen. Hierbij wordt het microglia fenotype onvermijdelijk beinvloed door het serum en de groeifactoren die gebruikt worden tijdens de celkweek. Het was daarom onze doelstelling om een verbeterd protocol voor acute isolatie van humane microglia uit hersenweefsel te maken. De vier stappen tellende isolatie procedure (mechanische weefsel dissociatie, verwijdering van myeline, verrijking en verhoging van de zuiverheid) die in dit hoofdstuk beschreven wordt stelt ons in staat om fenotypes van microglia uit zowel gezond hersenweefsel als hersenweefsel met neurologische aandoeningen te onderzoeken. Opvallend hierbij is dat opbrengst en de zuiverheid van de microglia preparatie nauwelijks beinvloed wordt door de mate van ‘post mortem delay’ en neurologische status. Het protocol kon met succes toegepast worden op glioma biopsie weefsel. Hiermee is het nieuwe isolatie protocol niet allen snel en eenvoudig maar heeft ook een breed spectrum aan mogelijke applicaties.

ÖSSZEFOGLALÓ MAGYAR NYELVEN

Mikroglia, az immunrendszer központi idegrendszeri nagykövete, hosszú évtizedekig, mint afféle titokzatos sejtféleség volt ismeretes tudományos körökben. A mikroglia elősejtek (primitív makrofágok) az embrionális fejlődés kései szakaszában kolonizálják a központi idegrendszert (Ginhoux et al., 2010), és a születés utáni időszakban sejtenként, egy egymáséval át nem fedő, szférikus területen belül telepednek le. Mikroglia a klasszikus (hisztokémiai és immunohisztokémiai) módszerekkel láthatóvá téve az egészséges felnőtt agyszövetben látszólag nyugalmi állapotban van, melyre vékony, többszörösen elágazó sejtnyúlványrendszer és a többi szöveti makrofág marker repertoárjának majdnem teljes hiánya jellemző. Bármely zavar az agyszövet sejtközötti állományának összetételében, illetve az idegsejtek működésében mikroglia aktivációhoz vezet, mely során a mikroglia sejtalkata megváltozik, a sejt legömbölyödik, osztódik és a sérelem helyére vándorolva ellátja a kiváltó okhoz szabott effektor funkciót. Mivel mikroglia aktivació jellemző velejárója majdnem minden, a központi idegrendszert érintő fizikai traumának illetve betegségnek, kézenfekvőnek tűnt, hogy a kettő között ok-okozati összefüggés áll fenn. Az a tudományos álláspont, mely szerint mikroglia aktiváció idegrendszeri károsodáshoz vezet, majdnem egy évszázadig tartotta magát. Az elmúlt néhány év során azonban, a technológiai újítások és fejlesztések nyomán lehetővé vált kisérleteknek köszönhetően, mikrogliáról alkotott véleményünk gyökeres változáson ment keresztül. A legújabb kutatási eredmények fényében úgy tűnik, hogy egyes neurodegeneratív betegségek esetén a mikroglia aktivació csupán másodlagos jelenség, a kórfolyamatokhoz nem járul aktivan hozzá (Grathwohl et al., 2009). Továbbá, egyértelművé vált az is, hogy a mikroglia nyugalmi állapota az egészséges agyszövetben valóban csupán látszólagos. Mint ahogy arra a mikroglia sejtjeiben zöld fluoreszcens fehérjet kifejező genetikailag módosított egéren végzett 2-foton

mikroszkópos kisérletek rámutattak (Nimmerjahn et al., 2005), mikroglia sejtek állandó megfigyelés alatt tartják a közvetlen környezetüket. Finom nyúlványaikkal folyamatosan mintavételezik a sejtközötti teret és zavar vagy sérülés esetén percek alatt képesek reagálni (Davalos et al., 2005). Mint a központi idegrendszer hivatásos falósejtjei részt vesznek a sejttörmelék eltávolításában, és ezáltal, valamint citokinek és növekedési/túlélési faktorok termelése es felszabadítása által, lehetővé teszik a sérülést követő szöveti átrendeződést és megújulási folyamatokat. Mindamelett, az idegrendszer felnőttkori, fiziológiás plaszticitásához is hozzájárulnak, úgy struktúrális, mint szinaptikus szinten. Sierra és munkatársai bemutatták (Sierra et al., 2010), hogy a felnőttkori hippokampális idegsejtképződés során a mikrogliának központi szerepe van a be nem illeszkedett granuláris sejtek eltávolításában, ezzel fenntartva a fogazott tekervény (gyrus dentatus) összeköttetésrendszerének dinamikus egyensúlyát. Továbbá, Tremblay es kollegái összefüggést tártak fel az elsődleges látokéregben vizuális depriváció során a mikroglia fagocitotikus tevékenysége és a dendritek eltávolítása között, ezzel valószínűsítve a mikroglia szerepét a szenzoros tapasztalattól függő szinaptikus átrendeződésben (Tremblay et al., 2010). A fent említett tudományos eredmények rámutattak arra hogy, a kezdeti feltevésekkel ellentétben, mikroglia elsődleges feladata a központi idegrendszer homeosztázisának fenntartása. Amennyiben a mikroglia (az öregedés során jelentkező funkcióvesztés következtében (Streit, 2006), vagy pedig meg nem szűnő ingerlés nyomán kialakuló krónikus aktiváció miatt (van Rossum & Hanisch, 2004)) ezen támogató és szöveti egyensúlyt fenntartó feladatát nem tudja teljeskörűen ellátni, az az idegszövetre ártalmas következményekkel járhat.

Mindezen új tudományos kutatási eredmények fényében nélkülözhetetlenné vált a különböző mikroglia fenotípusok (a mikroglia különböző funkcionális állapotainak) részletes leírása és tanulmányozása. A közelmúltig a mikroglia kutatás embrionális vagy újszülött eredetű mikroglia tenyészeteken végzett kísérletekre

korlátozódott. Mivel azonban a mikroglia, funkciójából kifolyólag, rendkívül érzékeny környezetének összetételére, az in vitro végzett kísérletek a felnőtt központi idegrendszer mikroglia fenotípusainak mibenlétére nézve kevés információval szolgálnak. Nemrégiben a tanszékünkön kifejlesztett mikroglia elkülönítési eljárásnak köszönhetően azonban lehetővé vált a mikroglia fenotípusok *ex vivo* vizsgálata úgy fehérje, mint génexpresszió szintjén (de Haas et al., 2007).

A fent említett új izolációs módszer előnyeit kihasználva a jelen PhD projekt a központi idegrenszer plaszticitásához és regenerációjához kapcsolódó mikroglia fenotípusok vizsgálatát tűzte ki célul.
A doktori értekezés első fejezete általános áttekintést nyújt a mikroglia fenotípusos sokféleségével kapcsolatban rendelkezésünkre álló tudományos eredményekről (Olah et al., 2010), valamint felvázolja a mikroglia kutatás még feltáratlan területeit, megválaszolatlan kérdéseit. A második fejezet a mikroglia felnőttkori hippokampális idegsejtképződésben betöltött szerepét tárgyalja. Kisérleti eredményeink rámutattak arra, hogy a felnőttkori hippokampális neurogenezis (a közismerettel ellentétben) mikroglia aktiváció, pontosabban mikroglia T sejt kölcsönhatás nélkül is végbe mehet (Olah et al., 2009). A harmadik fejezetben bemutattuk, hogy az agy fehér és szürkeállományának mikroglia populációja fiziológiás körülmények között génexpresszió szintjén és funkcionálisan szignifikánsan különbözik egymástól. A feltárt különbségek neuroimmunológiai szempontból jelentékeny szignalizációs útvonalakat és funkciókat érintettek. A negyedik fejezet a demielinizációért és remielinizációért felelős mikroglia fenotípus génexpressziós tájképét térképezi fel. Ezen tanulmány során fény derült arra, hogy a remielinizációért felelős mikroglia fenotípusa a demielinizáció során a kérges test területén jelen lévő mikroglia fenotípusából ered. Az ötödik fejezet egy új izolációs módszert ir le, melynek segítségével magas sejthozamú és nagy tisztaságú mikrogliapopulácio különíthető el *post mortem* emberi

agyszövetből. A hatodik fejezetben pedig az angol, holland es magyar nyelvű összefoglalók találhatók.

IRODALOM

Davalos D, Grutzendler J, Yang G, Kim JV, Zuo Y, Jung S, Littman DR, Dustin ML, Gan WB (2005) ATP mediates rapid microglial response to local brain injury in vivo. Nat Neurosci 8: 752-758.

De Haas AH, Boddeke HW, Brouwer N, Biber K (2007) Optimized isolation enables ex vivo analysis of microglia from various central nervous system regions. Glia 55: 1374-1384.

Ginhoux F, Greter M, Leboeuf M, Nandi S, See P, Gokhan S, Mehler MF, Conway SJ, Ng LG, Stanley ER, Samokhvalov IM, Merad M (2010) Fate mapping analysis reveals that adult microglia derive from primitive macrophages. Science 330: 841-845.

Grathwohl SA, Kalin RE, Bolmont T, Prokop S, Winkelmann G, Kaeser SA, Odenthal J, Radde R, Eldh T, Gandy S, Aguzzi A, Staufenbiel M, Mathews PM, Wolburg H, Heppner FL, Jucker M (2009) Formation and maintenance of Alzheimer's disease beta-amyloid plaques in the absence of microglia. Nat Neurosci 12: 1361-1363.

Nimmerjahn A, Kirchhoff F, Helmchen F (2005) Resting microglial cells are highly dynamic surveillants of brain parenchyma in vivo. Science 308: 1314-1318.

Olah M, Ping G, de Haas AH, Brouwer N, Meerlo P, Van Der Zee EA, Biber K, Boddeke HW (2009) Enhanced hippocampal neurogenesis in the absence of microglia T cell interaction and microglia activation in the murine running wheel model. Glia 57: 1046-1061.

Olah M, Biber K, Vinet J, Boddeke HW (2010) Microglia Phenotype Diversity. CNS Neurol Disord Drug Targets.

Sierra A, Encinas JM, Deudero JJ, Chancey JH, Enikolopov G, Overstreet-Wadiche LS, Tsirka SE, Maletic-Savatic M (2010) Microglia shape adult hippocampal neurogenesis through apoptosis-coupled phagocytosis. Cell Stem Cell 7: 483-495.

Streit WJ (2006) Microglial senescence: does the brain's immune system have an expiration date? Trends Neurosci 29: 506-510.

Tremblay ME, Lowery RL, Majewska AK (2010) Microglial interactions with synapses are modulated by visual experience. PLoS Biol 8: e1000527.

van Rossum D, Hanisch UK (2004) Microglia. Metab Brain Dis 19: 393-411.

ACKNOWLEDGEMENTS

I would like to express my sincere gratitude to…

…my promoter and supervisor, Erik Boddeke for his faith in me, for handling my introverted and eccentric nature with patience, for channeling all my uncertainties, skepticism, erratic moods and aspirations into one stream, the result of which is the book at hand.

…Knut Biber, for being instrumental in the projects presented in this dissertation, for all the scientific discussions that we had regarding microglia biology and neurosciences in general, for his comments and suggestions which made my manuscripts more unambiguous, without disturbing my personal writing style.

…the members of the reading committee, Christine Dijkstra, Paul Luiten and Tibor Harkány, for their fast responses and valuable comments on the manuscript.

…the members of BCN staff, Britta Küst, Diana Koopmans, Janine Wieringa, Rob Visser, for helping me with starting up in Groningen, for organising graduate courses and master classes.

…Mieke Kapteyn at the Graduate School of Medical Sciences, for arranging the paperwork related to the defense.

…Sjef Copray, for all the discussions we had regarding culture, politics and neurosciences, and for being our guide in Paris.

…Bart Eggen, for the useful discussions and hints regarding PostDoc life and moving to the US.

…Gábor Juhász and Magor Lőrincz, who were my supervisors during my startup as a scientist in Budapest and István Ábrahám, for suggesting me to come for PhD to Groningen, from where he also received his degree.

…Evelyn Wesseling, Marjolein Hensens, Ietje Mantingh-Otter, Loes Drenth and Nieske Brouwer for keeping all the labs well organised, to

Marjolein in particular, for the cheerful hours spent culturing cells under the hood.

…Trix van der Sluis-Rozema and Gerry Hoogenberg for helping us with so-so many paper-work.

...Wieb Patberg, for his willingness to share his experiences with us.

…Inge Zijdewind and Rob Bakels for keeping up the electrophysiology spirit at the department.

…the PostDocs, Vesna Stanulović, Marloes van Zwam, Veerakumar Balasubramaniyam, Jonathan Vinet for sharing their knowledge with us.

…Michel Meijer, for his help around the confocal microscope and Tjalling Nijboer, for his help with SigmaPlot.

…the collaborators in the Kettenmann lab in Berlin, Steffanie Seifert and Grietje Tessmann for their welcome and enthusiasm, and Birgit Jarchow, for arranging my stay at the MDC.

…Katrin Kierdorf in the Prinz lab in Freiburg, with whom we tried to implant acutely isolated white matter microglia into the cortex.

…collaborators Peter Meerlo and Eddy van der Zee, for introducing me to the running wheel model and immunohistochemistry.

…collaborators at the UMCG Genetics department, Pieter van der Vlies, Bahram Sanjabi and Marcel Bruinenberg, for their courage to work with the tiny RNA amounts of tiny cells.

…Klaas Sjollema at the UMIC-UMCG, for teaching me live cell imaging.

…my students, Gao Ping, Bart Lubbers, Soesma Medema-Jankipersadsing and Fiona Katoen, for their contribution to the respective projects.

…and to all others, with whom I had less interaction, for just contributing to the MedFys (8^{th} floor) experience…Marije Zomerdijk, Jaap Muntinga, Henk Schuil.

…the past and present PhD students ((in order of appearance): Eiko de Jong, Hiske van Duinen, Veerakumar Balasubramaniyan, Hilmar van

Weering, Alexander de Haas, Marijn Post, Ming San Ma, Annebet van der Meulen, Anneke Steens, Reinhard Rößler, Shamsudheen Moidunny, Divya Raj, Vishnu Kannan, Marcin Czepiel, Xin Dai, Ria Wolkorte, Fabrizio Bianchi, Wandert Schaafsma, Raaj Thurmann, Inge Holtman) for making the working environment at the department friendly and encouraging.
…to Marloes van Zwam for introducing me to the analysis of flow cytometry data, to Alexander de Haas, for teaching me his microglia isolation protocol, which I made use of throughout my studies, to Anneloes Bohte, who showed me cryostat sectioning and immunohistochemistry, during my first weeks at the department.
…the fellow microglia isolators, Nieske Brouwer and Divya Raj, for the long but "gezellig" isolation sessions extending deep into the night, for helping me deal with my initial aversion from human post mortem brain material, and in particular to Nieske, for helping me with plenty of perfusions and proof reading my manuscript.

…Falak Sher, without whom I would have long given up, for giving me strength, protecting and encouraging me, for always being there for me.
…my parents, György and Celesztina, and my sister, Magdolna without whose altruistic love my whole education wouldn't have been possible.